British Geological Survey

DFID Department for International Development

TECHNICAL REPORT WC/00/20
Overseas Geology Series

DFID Project No. R5563

Volcanic hazard mapping for development planning

P N Dunkley and S R Young

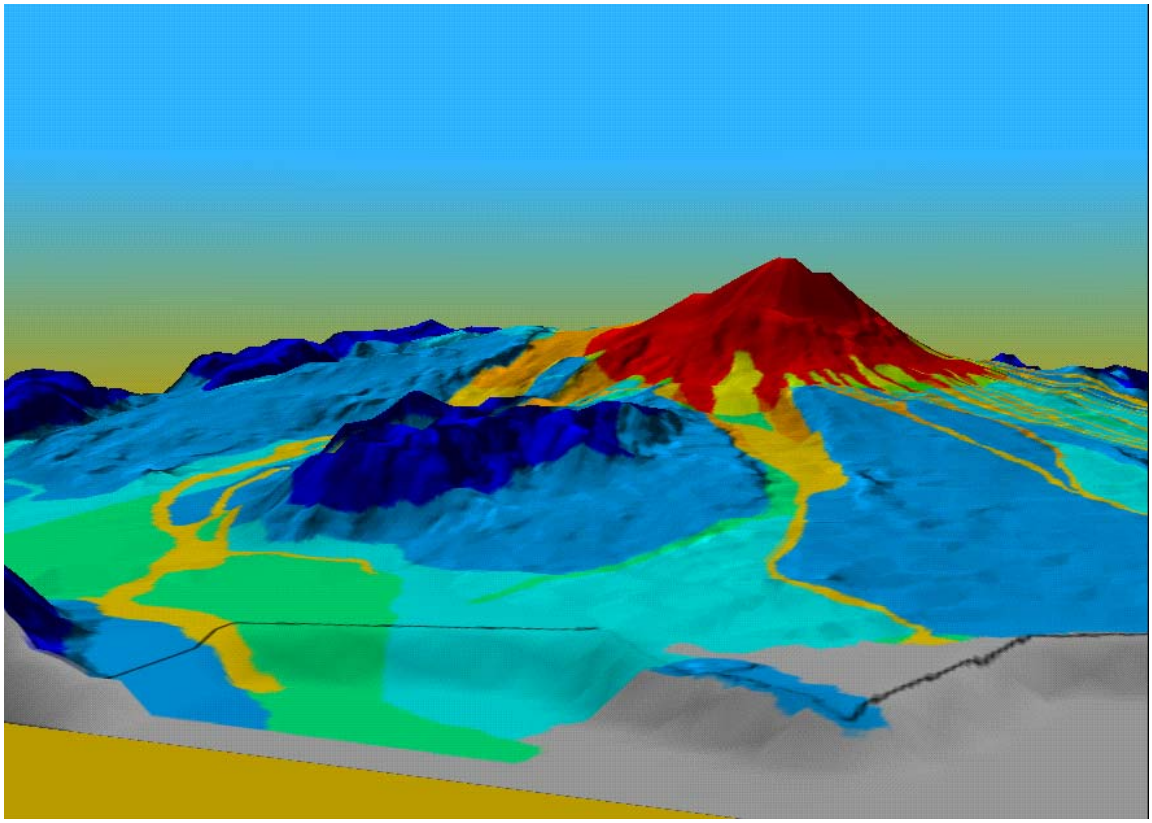

Natural Environment Research Council

BGS International®
British Geological Survey
Keyworth
Nottingham NG12 5GG
United Kingdom

TECHNICAL REPORT WC/00/20
Overseas Geology Series

DFID Project No. R5563

Volcanic hazard mapping for development planning

P N Dunkley and S R Young
With contributions by R A Nicholson

A report prepared for the Department for International Development (DFID) under the Knowledge and Research Programme as part of the UK provision of technical assistance to developing countries. The views expressed are not necessarily those of DFID.

DFID classification :
Subsector: Geoscience
Theme: G2 - Improve geological, geochemical and geotechnical hazard avoidance strategies in development planning
Project title: Volcanic hazard mapping for development planning
Project reference: R5563

Bibliographic reference:
Dunkley, P N and Young, S R. 2000 Volcanic hazard mapping for development planning.
BGS Technical Report WC/00/20

Keywords: volcanic hazards, risk mitigation, hazard mapping

Front cover illustration: Perspective view of a digital terrain model of volcán Villarrica draped with volcanic hazard zones

Keyworth, Nottingham, British Geological Survey, 2000

EXECUTIVE SUMMARY

It is estimated that more than 500 million people are at risk from the hazards posed by volcanoes. The potential therefore exists for major loss of life and damage to property in a number of regions, especially where large urban areas occur in proximity to dangerous volcanoes. As population pressures intensify, hazardous areas are likely to become increasingly developed, so raising the level of risk.

In the case of major eruptions, losses to property, infrastructure and economic activity can run into hundreds of millions or even billions of dollars and high casualty rates may be inflicted, although even relatively minor activity can have adverse impacts through the disruption of economic activity, lack of investor confidence and harm to health. Eruptions may therefore seriously disrupt development plans by causing burdensome economic setbacks that divert precious resources into relief and reconstruction, which would otherwise be destined for development. This can be severe in developing nations with small, poorly diversified economies.

Because disasters are inextricably linked to human and economic development, the most efficient way to prevent them or reduce their impact is to take natural hazards into routine consideration when formulating development plans. An integrated approach to hazard management and development planning will also result in more realistic cost-benefit analyses of potential development projects, by taking into account the estimated costs and benefits of hazard reduction measures.

Although numerous volcanoes pose a high level of risk in many developing countries, relatively few have been the subject of hazard assessments. The main objective of the project has therefore been the development and evaluation of rapid and cost-effective methods for volcanic hazard mapping in developing countries.

Volcanic hazard mapping methods are described and the role that these have to play within the broader framework of risk reduction is discussed. With respect to this framework, the recurring problem of the failure of uptake and utilization of volcanic hazard information is examined within the context of the communications interface between civil authorities and volcanologists, and recommendations are made for improving the efficiency of the process through a number of measures.

Two volcanic hazard assessment case studies were undertaken by the project on the Chilean volcanoes of Nevados de Chillán and Villarrica. A detailed assessment of Nevados de Chillán was carried out over several years by a team of specialists using a conventional approach, whilst a much more rapid and less expensive methodology was applied by a single geologist at Villarrica. These two studies, together with a pre-existing detailed assessment of Villarrica, allow the merits of rapid volcanic hazard assessment methods and conventional methods to be compared. Both case studies used reconnaissance survey techniques based upon the interpretation of aerial photographs and satellite images, and developed simple geographical information systems and digital cartographic methods for the production and presentation of hazard maps in forms which should be more easily visualised and understood by civil authorities and decision makers involved in the downstream processes of volcanic risk reduction.

The project has shown that it is possible to produce simple but effective hazard maps using techniques that are considerably more rapid and less expensive than conventional methods. The level of detail of hazard mapping is only slightly compromised using these methods compared with conventional assessments, and is certainly sufficiently accurate and informative to be fit for the purpose of development planning and disaster preparedness. The benefits of using hazard maps of this kind to reduce volcanic risk within the framework of development planning and civil protection are potentially very large, when compared with the disastrous impacts that volcanic activity can have on the vulnerable infrastructure of developing countries.

A third case study was undertaken on volcán Irazú, situated close to the Costa Rican capital of San José. Various aspects of the 1963-65 eruption of Irazú were investigated, including the economic impact of the eruption and the vulnerability of the human population, buildings and infrastructure to the effects of volcanic ash and mudflows. Proposals were made by the sub-project for reducing the risks during future eruptions at Irazú through better community preparedness.

The Montserrat eruption has provided a test bed for a number of aspects of volcano hazard and risk assessment addressed by the project. Experience gained through the project has been applied to the Montserrat crisis, leading to successful hazard and risk assessment and the provision of pertinent and timely advice to civil authorities.

Whilst the project has demonstrated that the methods exist for producing effective and cost-beneficial hazard and risk assessments by rapid methods, the problem remains of convincing civil authorities that such assessments are necessary in the first place, bearing in mind the reluctance to implement risk-reduction policies under dormant volcanic conditions which normally prevail at most volcanoes.

LIST OF CONTENTS

LIST OF TABLES

LIST OF FIGURES

1. INTRODUCTION

This report provides a synthesis of the work of the Volcanic Hazard Mapping for Development Planning Project (R5563), which was undertaken on behalf of the Department for International Development (DFID).

The project was administered under the auspices of the Knowledge and Research (KAR) Programme (formerly the Technology Development Research Programme) of the Engineering Division of DFID, but was funded by the Emergency Aid Department as part of the United Kingdom's contribution to the United Nations' International Decade For Natural Disaster Reduction (IDNDR).

The project began in the latter half of 1993 and was originally due to be completed in March 1996. However, with the inception of the volcanic eruption of Montserrat in July 1995, members of the project team became increasingly engaged in the management of the volcanic emergency that ensued. As a result, the work of the volcanic hazard mapping project was seriously disrupted and its completion postponed for several years.

It should be stressed that whilst the Montserrat eruption has had a disruptive effect upon the schedule of the volcanic hazard mapping project, there have also been positive effects of mutual benefit to both the project and the management of the Montserrat crisis. Firstly, through the work of the volcanic hazard mapping project a group of scientists was already functioning under the influence of BGS/DFID at the onset of the Montserrat eruption, and this facilitated the rapid deployment of suitable personnel to help manage the crisis. Secondly, the work undertaken at Montserrat has provided an extra case study for the hazard mapping project, allowing methodologies to be tested and extended into the area of risk assessment for planning and civil protection purposes.

1.1 Objectives of the project

The main objectives of the project have been to examine the role of volcanic hazard maps in development planning, and to develop rapid and cost-effective methods for the assessment of volcanic hazards and the production of hazard maps that can be utilised by authorities without specialist geological knowledge.

The work has been multifaceted and has endeavoured to demonstrate the severe impacts that volcanic activity can have, especially upon developing countries which may not have sufficient financial nor technical resources to mitigate the effects of such hazards.

The project has shown that it is possible to produce simple but effective hazard maps using techniques that are considerably more rapid and cost-effective than traditional methods, and that such assessments can be used effectively in planning and civil protection measures to mitigate the impacts of volcanic hazards. The benefits of using hazard maps of this kind to reduce volcanic risk within the framework of development planning and civil protection are potentially enormous, when compared with the disastrous impacts that volcanic activity can have on the vulnerable infrastructure of developing countries.

1.2 Structure of the report

The report covers a number of topics related to volcanic hazards and the role that hazard maps have to play in disaster reduction.

Section 2 briefly analyses the impacts of natural hazards, with particular reference to developing countries, and discusses the basic concepts of *hazard*, *vulnerability* and *risk* assessment and the part these should play in disaster reduction through development planning and civil protection measures.

Section 3 provides an introduction to volcanic hazards. The size and frequency of eruptions and the impacts of volcanic disasters are examined. A broad framework for volcanic risk reduction is outlined, and the role that volcanic hazard assessments and volcanic hazard maps have to play within this framework is discussed. The problems of uptake and utilisation of volcanic hazard information are examined in the context of the interface between planners and civil protection authorities on the one hand and vulcanologists on the other. The importance is stressed of using volcanic hazard information within the broader framework of risk reduction, rather than viewing it as a means to an end in itself, and several examples of volcanic risk assessments are described in Section 4.

Section 5 describes each of the main volcanic hazard types in detail. The impacts of each hazard type are illustrated with examples of volcanic disasters from the historical record, and the methodologies that have been used for mapping hazard zones for each type of hazard are reviewed.

Section 6 summarises the salient features and conclusions of four case studies of volcanic hazard assessments which were undertaken either directly by the project, or in the case of Montserrat in association with it. Details of each case study are provided in a series of separate reports. The four case studies are as follows.

The active volcano of Nevados de Chillán in southern-central Chile was surveyed in detail by a team from the BGS, the University of Bristol, the University of Lancaster and the Chilean Servicio Nacional de Geología y Minería (SERNAGEOMIN). This survey was directed by Bristol University and employed a full range of modern geological techniques to elucidate the evolution and eruptive history of the volcano in order to assess its hazards (Dixon *et al.* 1995; Gilbert and Young, 1998).

The active volcano of Villarrica, situated in southern Chile, was assessed by a single member of BGS (Young, 1998), using a considerably more rapid and less expensive methodology to produce volcanic hazard maps and present them in a form that is more useful to non-geoscientists. The primary objective of this study was to examine the feasibility of using rapid techniques, and to compare the results in terms of quality, utility and cost with more conventional volcanic hazard assessments, as for example that of Nevados de Chillán.

The third case study consisted of a hazard assessment and community preparedness study of Irazú in Costa Rica (Young *et al*. 1998). Various aspects of the 1963-65 eruption of Irazú were investigated, including the economic impact of the eruption and the vulnerability of the human population, buildings and infrastructure to the effects of volcanic ash and mudflows.

Proposals were made for reducing the risks during future eruptions at Irazú through better community preparedness.

The Montserrat eruption has provided an intense test bed for a number of aspects of volcano hazard and risk assessment addressed by the project. Experience gained through the project has been applied to the Montserrat crisis, leading to successful hazard and risk assessment and provision of pertinent and timely advice to management authorities. The lack of action on an earlier hazard assessment of Montserrat which highlighted the dangers of the volcano (Wadge and Isaaks, 1987; 1988), exemplifies the problem of the uptake and utilization of volcanic hazard information by planners and other authorities, and the necessity of using such information in the process of development planning to reduce risk in the longer term.

2 NATURAL HAZARD ASSESSMENT IN DEVELOPMENT PLANNING

Volcanic hazards are one of a number of natural hazard types which affect developing and developed countries alike. Although each type of natural hazard produces its own particular set of problems, the broad approach to hazard mitigation in terms of procedures and policies is similar for all. Indeed, many regions are subject to a complex interplay of natural hazards which exacerbate one another and call for an integrated approach to mitigation.

The impact of natural hazards on developing countries is considered in this section, and the role of hazard assessment and hazard mapping is described in general terms within the wider context of risk assessment, development planning and risk reduction.

2.1 Natural hazards and disasters in developing countries

Natural hazards are potentially damaging natural events. They include droughts, floods, windstorms, earthquakes, landslides, volcanic events, wildfires and tsunamis.

Natural disasters occur when natural hazards seriously disrupt communities, causing widespread human, material and environmental losses and damage.

It has been estimated that 3 million people were killed by natural disasters in the 1970's and 1980's, and that in the 1980's alone more than 1.6 billion people were affected by them (UNESCO, 1993). Natural disasters affect all regions, but have greatest impacts on the most vulnerable and poor communities of the developing world, where it is estimated that about 95% of all natural disasters occur (Press, 1993). Furthermore, the scale, complexity and frequency of disasters appear to be accelerating as population pressures force vulnerable communities to become increasingly concentrated in urban settlements in hazard-prone areas. The cost of disasters, in constant (1990) dollars increased dramatically in the latter half of the twentieth century. Natural disasters in the 1960's are estimated to have cost $40 billion, increasing to $70 billion in the 1970's and to $120 billion in the 1980's. Furthermore it was estimated that without disaster reduction measures the cost would rise to at least $280 billion in the 1990's (Boutros-Ghali, 1994). In hindsight this last estimate is likely to have been exceeded significantly, considering for example that damage by the El Niño phenomena in 1998 alone was estimated at $90 billion (IDNDR, 1999) and the cost of property damage caused by the 1995 Kobe Earthquake was estimated at between $95 and $147 billion (EQE International, 1995).

Population pressures themselves also modify the environment in adverse ways, by causing such effects as deforestation and over-grazing, which heighten vulnerability to hazards. Disasters, too, can also increase vulnerability to natural hazards: Inadequate post-disaster assistance and rehabilitation can lead to what has been termed the 'ratchet wheel effect' (Davis, 1994), whereby the vulnerable become progressively more vulnerable as they are pushed into greater poverty and exposure to successive disasters. The risks imposed by natural hazards are therefore in effect created by human activity. This point is well-illustrated by volcanic activity, which in remote and unpopulated areas usually poses little threat, but in developed areas can have disastrous effects.

It is widely recognised that natural disasters in developing countries seriously disrupt development plans. Disasters usually cause burdensome economic setbacks by diverting precious resources into relief and reconstruction, which would otherwise be destined for development. Additionally, income from production and export declines because of the disruption caused by disasters, and this can be severe in nations with small, poorly diversified economies based upon a limited range of activities. Furthermore, because natural disasters recur with frequency in many developing countries they not only cause major economic setbacks, but they strain the social fabric, resulting in unrest which can contribute significantly to regional and global political instability. Disaster reduction is therefore not just of national or domestic concern, but calls for a global approach.

Relief has traditionally been the main approach used in disaster management and was estimated by UNESCO (1993) to have accounted for 96% of all resources spent on disaster-related activities. This is despite the fact that long-term disaster reduction programmes based upon prevention and preparedness measures are much more cost-effective than short-term relief and reconstruction.

Because disasters are inextricably linked to human and economic development, the most efficient way to prevent them or reduce their impact is to take natural hazards into routine consideration when formulating development plans. Disaster reduction measures embodied within a development project from the outset will undoubtedly be less expensive and are likely to be more effective. An integrated approach to hazard management and development planning will also result in more realistic cost-benefit analyses of potential development projects, by taking into account the estimated costs and benefits of hazard reduction measures.

2.2 Disaster reduction measures: prevention, preparedness and emergency response

Disaster reduction activities fall into three broad categories, namely **prevention**, **preparedness** and **emergency response**.

Prevention measures include land-use planning, which limits or prohibits the development of hazardous areas, and engineering techniques which make buildings and other structures more resistant to hazards. Legislation and regulation are required to ensure that building and planning codes are adhered to, but these can only be effective if they are enforced. Building codes may be ineffective if they are not sufficiently detailed, or if engineers and builders have not been trained to implement them. Land-use planning on the other hand requires less technical knowledge and may be implemented more easily, particularly at the local level. Economic inducements also have a part to play in disaster prevention and may be more effective than legislation in regulating building codes and land-use planning. Governments may offer financial incentives in the form of grants, subsidies or tax relief to encourage good practices. Similarly, the insurance industry can foster the design and construction of hazard resistant buildings and encourage development in hazard free areas by offering reduced premiums.

Preparedness measures include the installation of monitoring, prediction and warning systems, and the establishment of emergency response plans for warning and evacuation, search and rescue, rehabilitation and reconstruction. Public education programmes, which include simulations and drills, are vitally important, so that the authorities and public are aware of the nature of the hazards concerned and are conversant with procedures to be implemented during emergencies. Prediction and warning systems can greatly reduce the loss of life, but they may also lull the public into a false sense of security to the detriment of other more effective disaster reduction measures. It is therefore necessary that warning systems are implemented and maintained in conjunction with public awareness programmes.

When a natural hazard crisis occurs, emergency response plans are implemented to minimise impact. In the first instance such response tends to concentrate on search and rescue to reduce casualties, and on medical treatment, temporary housing and feeding. In the longer term response measures include such activities as reparation, redevelopment and resettlement.

Prevention activities are more cost effective than preparedness measures, because they reduce vulnerability on a long-term basis. This is particularly so when prevention is taken into account in the planning phase of development. A balance should, however, be maintained between prevention, preparedness and emergency response measures, so that the cost of risk reduction is spread across a range of activities and damage is limited if certain measures fail.

The benefits of disaster reduction measures are difficult to quantify. Potential reductions in damage to property may be estimated for certain types of disasters, but the benefits of reductions in fatalities, injuries, emotional stress, loss of natural resources and general disruption, together with maintenance of political stability cannot be readily equated in monetary terms. Despite the difficulties in equating the costs incurred in the short-term with the long-term gains of disaster planning, cost-benefit analysis is probably the only effective method for justifying disaster mitigation plans. This consists of measuring the net economic loss associated with a natural disaster and estimating the losses that could be avoided or reduced with the implementation of mitigation measures.

2.3 Hazard, vulnerability and risk assessment

To weigh the benefits and costs of disaster reduction measures it is necessary to evaluate the potential losses or *risk* that a community or region faces over time due to natural hazards. Three main steps are involved in this process. These are **hazard assessment**, **vulnerability analysis** and **risk assessment**.

2.3.1 Hazard assessment

At the beginning of Section 2.1 natural hazards were simply defined as potentially damaging natural events. However, to evaluate the risks fully, it is necessary to estimate the frequency of hazards and delimit the areas that are likely to be affected by them. A more precise and meaningful definition of natural hazard is therefore required for risk assessment purposes. A suitable definition given by UNDRO (1990) is:

> **Natural hazard:** the probability of occurrence, within a specific period of time in a given area, of a potentially damaging natural phenomenon.

Hazard assessments form the basis of risk assessment and are also essential for civil protection planning.

The first step in the process of hazard assessment involves the identification of the specific hazards affecting a region (e.g. floods, landslides, volcanic eruptions). Hazard zones are then mapped according to the location, intensity, frequency and probability of future hazardous events.

Preliminary hazard identification is usually undertaken using existing information, such as geological maps, climatic and hydrological records, and historical and published reports on past disasters.

2.3.2 Vulnerability analysis

When a hazard has been identified and assessed, its potential impact may be estimated using vulnerability analysis. This considers the vulnerability of population, man-made structures and other facilities, infrastructure, and economic activity at risk in hazard prone areas.

The concept of vulnerability, as applied to risk analysis, is defined by UNDRO (1990) as:

> **Vulnerability:** the degree of loss to a given element at risk, or set of such elements, resulting from the occurrence of a natural phenomenon of a given magnitude, and expressed on a scale from 0 (no damage) to 1 (total loss).

In this definition **elements** at risk include population, buildings and the component parts of infrastructure such as transport and communication systems, public services and utilities, as well as economic activities. Economic vulnerability not only includes potential direct losses due to a disaster, such as the destruction of a factory or a plantation, but also potential indirect losses incurred during the recovery period, for example, due to loss of production while a factory is rebuilt or a plantation is replanted and matures. Vulnerability analysis has traditionally concentrated upon the physical and economic aspects of vulnerability, but Davis (1994) argues that the less tangible social aspects of communities, termed **community vulnerability**, must also be taken into account.

Vulnerability may be assessed analytically or empirically, or by a combination of the two. The vulnerability of buildings and other civil engineering structures may, for example, be assessed theoretically using calculations and laboratory tests, or empirically on the basis of damage records of similar structures from past disasters. Much of the data required for vulnerability analysis on the performance and losses of structures during past disasters are available in historical records. An example of a vulnerability assessment was undertaken by the present project for the hazard of volcanic ash from volcán Irazú on the Costa Rican capital of San José (Young *et al.*, 1998).

Vulnerability assessments must be updated periodically. A community's vulnerability changes continuously with population fluctuations and the construction of new buildings, roads, industry and other infrastructure. In addition, information obtained after natural disasters should be used to update vulnerability assessments.

2.3.3 Risk assessment

Taken together, hazard assessments and vulnerability analyses can be used to estimate the likely losses or risks due to natural hazards over time. Once losses have been estimated, the benefits of the various disaster prevention, preparedness and emergency response measures can be evaluated.

The full value of risk assessments has not often been realised because they have been used primarily as a tool for developing emergency response plans. They should, however, form a critical basis for planning long-term prevention activities that will reduce a community's vulnerability on a more permanent basis.

It is not possible to reduce risks completely, especially in hazardous areas where significant development has already taken place. Nevertheless, where possible a balance should be struck between population growth, urban development, infrastructure and land use, and the risk posed by natural hazards. When these factors can be balanced and a favourable cost-benefit relationship can be found, a level of **acceptable risk** is said to have been attained.

The loss due to a particular type of natural hazard on a specific category of elements at risk, for example the population, or the bridges in a given hazard zone, is known as **specific risk**, and is the product of vulnerability and hazard. The overall level of risk can be evaluated for a given area by summation of the specific risks for each category of elements at risk.

The definitions of specific risk and risk given by UNDRO (1990) are:

> **Specific risk:** the expected degree of loss due to a particular natural phenomenon as a function of both natural hazard and vulnerability.
>
> **Risk:** the expected number of lives lost, persons injured, damage to property and disruption of economic activity due to a particular natural phenomenon, and consequently, the product of specific risk and elements at risk.

The reason for referring to specific risks, is simply that different parts of the man-made environment behave differently and cannot be systematically compared. For example, the behaviour of buildings and their resistance to hazards varies according to design and construction materials. Thus, different types of buildings must be analyzed in separate groups for each type of hazard. Similarly, roads must be assessed in a different manner from buildings: roads are linear features and the level of hazard, and consequently vulnerability, may vary significantly along a given length, whereas buildings are located at points where the level of hazard is constant for the entire structure.

Risk may be calculated as:

Risk = Value × Vulnerability × Hazard

Where hazard is expressed as the probability of a damaging event within a specified time, vulnerability is expressed in terms of expected damage on a scale of 0 (no damage) to 1 (complete destruction), and value is expressed as either the number of lives lost or casualties, or the monetary value of structures, material goods and economic activity at risk.

The foregoing description of risk assessment only addresses the direct losses caused by hazards. For a complete analysis, **secondary** and **consequential losses** must also be taken into account. Secondary losses are due to events or chains of events triggered by the primary hazard. In the case of volcanic activity these might include such effects as urban fires, dam failures and flooding. Consequential losses are those resulting from the loss or disruption of essential services, industry and commerce. The consequential losses from damage to buildings or to elements of infrastructure are determined by their contents or functions, otherwise known as their **sensitivity** and these may greatly exceed the material value of the elements themselves. It is therefore important to classify buildings and other installations into categories of sensitivity according to their function, so that the siting and vulnerability of sensitive elements are given special attention in the planning of hazardous areas.

Examples of risk assessments related to volcanic hazards are rare, but several are described in Section 4.

2.4 Planners and the interface between hazard mapping and risk assessment

Risk assessment and mapping is normally the responsibility of urban and physical planning bodies. It is a complex multi-disciplinary process which in addition to planners, requires specialist inputs from geoscientists, engineers, civil defense authorities, public works departments and economists. Given the complexity of the process, an organizational framework should be adopted from the outset to conform with routine planning procedures.

When considering risk in physical planning, planners need to be able to:

- Identify areas at risk in terms of their degree of exposure to hazard.
- Assess the specific risk (probable percentage loss per unit time) to existing elements within a given region.
- Assess and compare the levels of risk involved in locating a given structure in one of several possible sites with different levels of hazard.
- Implement planning measures to control or reduce risk.

To be able to achieve these tasks planners require the following information from geoscientists and engineers:

> Hazard maps at the appropriate scale showing the distribution of hazard zones, with indications of the expected hazard intensities and probability of occurrence within given time periods.
>
> Vulnerability coefficients which relate the degree of expected loss to hazard intensity for each element at risk for a given area.

Geohazard maps are produced by scientists and the information they contain is often presented in a form not fully understood by planners. Good communications are therefore required between scientist and planners if hazard maps are to be used successfully for risk analysis. Planners should therefore be involved with all stages of hazard and risk assessment and should instigate and take the co-ordinating role in the overall process. By doing so, they are likely to become more conversant with the nature of the hazard, and the resultant hazard maps will be better tailored to their requirements. This calls for close co-operation and mutual understanding between planners and geoscientists.

Hazard maps need to be clear and instructive, and should be accompanied by written descriptions, aimed at non-scientists, which provide information on the nature and effects, the likely duration, and speed of onset of the hazard. An over abundance of technicalities can slow down and confuse the decision maker or planner, and therefore the number of documents should be limited to a usable level. Volcanic hazard maps are a special case, because eruptions often produce a number of different hazards which have different effects and intensities, but need to be presented in a combined form. Maps showing a combination of hazards have the advantage of reducing the number of documents, but when compiling maps of this type the overriding requirement of clarity must not be compromised.

The scale of hazard maps needs to be decided upon at the outset of an assessment. Geologists in developing countries usually map large areas at large scales (mostly at scales of 1:250,000 or 1:100,000), whereas planners are accustomed to small-scale maps covering small areas. Planners and geoscientists are usually able to match their work at scales of 1:50,000 or 1:100,000. Volcanic hazard maps are generally produced at scales ranging from 1:50,000 to 1:200,000 depending on the size of the volcano, although maps at a regional or national scale may be required to portray the hazard of ash dispersed downwind from large eruptions.

2.5 Digital cartography and geographical information systems

Rapid developments in digital technology over the past decade have enabled the simplification of digital cartographic techniques and have led to the growth of powerful but easy-to-run Geographical Information Systems (GIS). Such systems are increasingly used for emergency planning in developing countries, and the application of GIS to hazard and risk assessment has developed rapidly. They allow diverse types of information to be superimposed and displayed as customised maps. They also facilitate the integration and

analysis of spatially related data to produce derived information, such as, for example, the derivation of risk maps from the integration and analysis of primary spatial information on the distribution of population density, hazard zones and estimates of vulnerability.

The problems related to the matching and integration of maps of various scales, as described in the previous section, are reduced to some extent or obviated by geographical information systems, which readily allow spatial information of any scale to be integrated. However, there are limitations which need to be taken into account when interpreting information derived from the integration of primary layers of data that were originally mapped at widely different scales and levels of precision. Derived information will be limited to some extent by the least precise layer of information within the system.

2.5.1 Digital mapping techniques used in the case studies of this project

State-of-the-art digital cartographic and remote sensing techniques have been used in the case studies to produce volcanic hazard maps of the present project (e.g. Figures 6.3 – 6.4). Aerial photographs and satellite images of the volcanoes were interpreted during the planning stage and photo-geological maps produced for use in the field. These were checked and modified during the course of fieldwork, and revised geological and hazard maps were prepared in digital form on return to the office. A simple GIS was developed for each case study, and was populated with information such as topography (contours, drainage, roads and settlements), population distribution, geological maps, volcanic hazard zones and satellite images.

Digital terrain models and shaded relief maps were also derived using digital techniques. The GIS allowed various levels of information to be superimposed and displayed with ease. Hazard maps have been presented using three different methods, which include hazard zones superimposed on conventional topographic maps, on shaded relief maps and upon digital terrain models, examples of which are shown in Section 6. Such techniques greatly enhance the presentation of hazard information over conventional methods of using “flat” maps. In particular, the distribution of hazard zones in relation to topography is much easier to visualize and can readily be understood by authorities and decision makers who are not generally conversant with using maps.

At the beginning of the project many of these digital techniques were at the development stage, but over the past five years they have become increasingly easier to apply. Thus for example, early in the project (1994) digital terrain models (DTM’s) were derived from topographic maps using semi-automated methods which were relatively time consuming, and the resulting DTM’s were only used as a means to display final hazard maps (e.g. Figure 6.5). In contrast, at the time of compiling this report it has been possible to produce very detailed DTM’s in a matter of hours from aerial photographs. Distortion free aerial photographs (orthophotographs) can also be produced digitally and can be draped over DTM’s, allowing volcanoes to be viewed in real time from any angle in three dimensions and at a detailed scale. Such products facilitate detailed interpretations of volcanic features prior to undertaking fieldwork. As a result, fieldwork can be better planned and undertaken more efficiently, and information may be recorded on orthophotographs in the field and can be easily transferred digitally to geographical information systems in the office, so speeding up the final analysis and production of hazard maps.

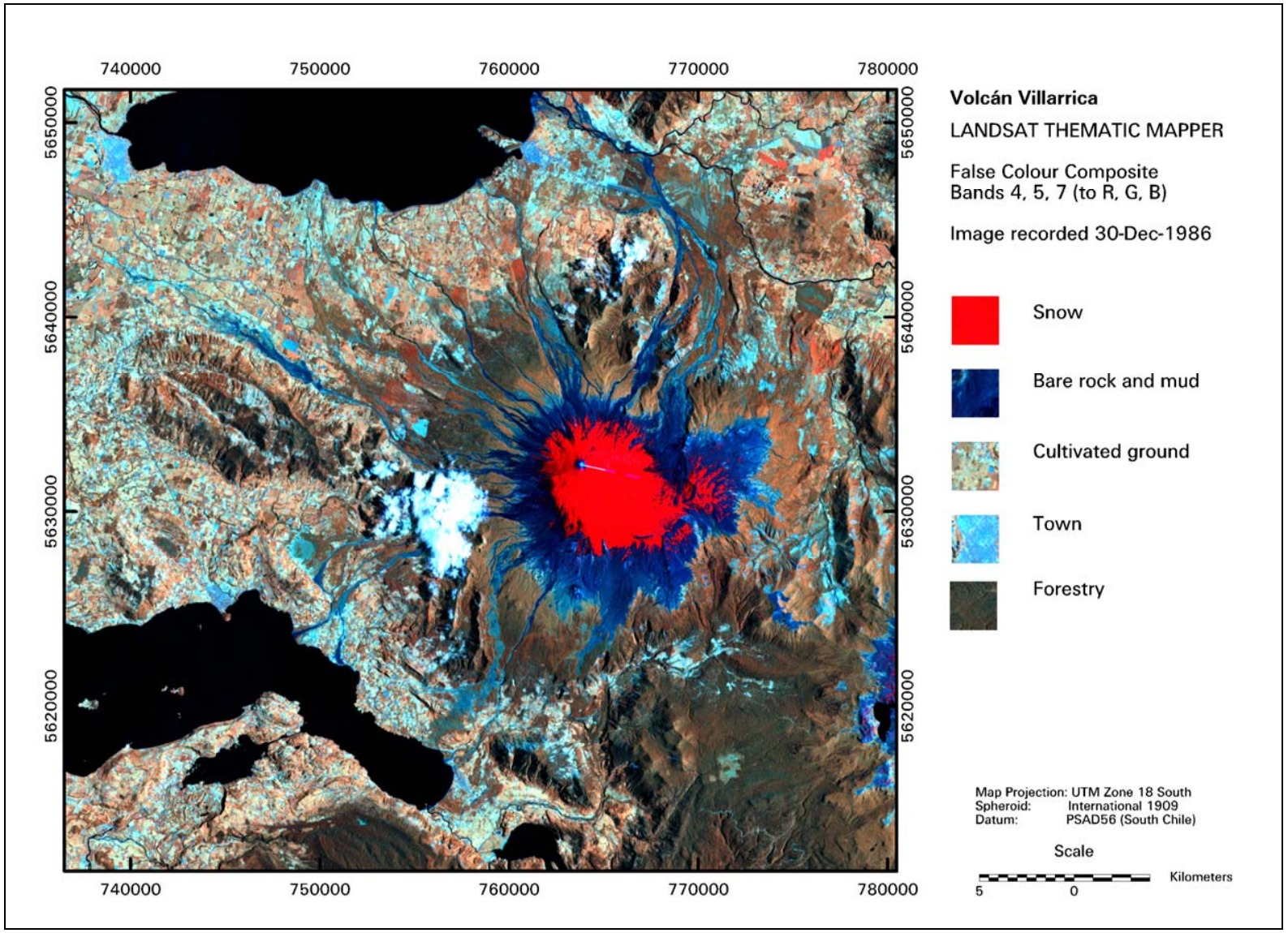

Figure 2.1: False colour Landsat Thematic Mapper image of Villarrica volcano, Chile, draped over a shaded relief map, showing land use and pathways of mudflows (deep blue). Black areas are lakes

3 GENERAL CONSIDERATIONS OF VOLCANIC HAZARDS AND HAZARD ASSESSMENTS

The purpose of this section is to describe in general terms the impacts of volcanic hazards and the broad strategies used for reducing volcanic risks through hazard assessment and hazard mapping.

It is estimated that more than 500 million people are at risk from the hazards posed by volcanoes (Tilling and Lipman, 1993), the majority of whom live in the developing world. The potential therefore exists for major loss of life and damage to property in a number of regions, especially where large urban areas occur in proximity to dangerous volcanoes. As population pressures intensify, hazardous areas are likely to become increasingly developed, so raising the level of risk.

As with natural hazards in general, the level of volcanic risk may be reduced by disaster prevention, preparedness, and emergency response measures. Hazard assessment underpins all of these activities and is fundamental to sound land-use planning, which ultimately offers the most effective means of reducing risk in the long-term.

3.1 Size and frequency of volcanic eruptions

A fundamental premise that underpins all volcanic hazard assessment is that the eruptive history of a volcano provides a general indication of its future activity.

At volcanoes where detailed records of historical activity are known, and where geological information is available on prehistorical activity, an analysis of the frequency, size and style of eruptions over time may allow predictions to be made about the nature of future eruptions. By way of example, detailed analyses of this kind undertaken by Petit-Breuilh (1995) and Dixon *et al*. (1995) during the course of the present project proved to be very useful in the hazard assessment of the Chilean volcano of Nevados de Chillán (Section 6.2; Gilbert and Young, 1998).

A general analysis of the global volcanic record also provides useful background information which should be born in mind in volcanic hazard assessment, particularly for volcanoes for which detailed eruption histories are not available. Simkin (1994) reported that at least 1,300 volcanoes have erupted over the past 10,000 years, and because the lifetimes of volcanoes are very long, many of these are likely to erupt again in the future. Within any given year between 60 and 70 volcanoes are typically active.

The size of eruptions may be gauged by a number of different criteria, but a widely used scheme is the **Volcanic Explosivity Index** (VEI) developed by Newhall and Self (1982). This semiquantitative scheme is based primarily upon the total volume of explosively erupted products, but also takes into account the eruption column height and the duration of the eruption, as well as a number of other more qualitative indicators including eruption style. Together these yield an index of increasing explosivity on a scale from 0 to 8 (Table 3.1). Passing up the scale, each VEI increment signifies an approximate tenfold increase in volume. Non-explosive eruptions of lava flows are assigned an index of 0, even though they may

involve large outpourings.

The historical record of eruptions is not comprehensive. Although a fairly complete record of larger eruptions is available, smaller eruptions have not been fully reported, particularly further back in history. Despite this bias in reporting, smaller eruptions are still nevertheless far more frequent than large ones. Simkin (1994) estimated that eruptions with VEI≥2 occur every few weeks whilst those with VEI≥3 take place several times per year. Eruptions with VEI≥5, such as the 1980 eruption of Mount St Helens, occur perhaps once per decade, and those of VEI 6, such as Krakatau (1883) and Mount Pinatubo (1991), only occur about once every century. Only one known historic eruption, that of Tambora in 1815, has been assigned a VEI of 7 (≥100 km^3 of tephra), and on average thousands of years may pass between eruptions of this magnitude.

The long intervals between eruptions at many volcanoes have a dual effect on human perception. The danger may be exaggerated at volcanoes which have had large-scale eruptions much closer to the present time than their mean eruption interval. On the other hand, volcanoes that have remained dormant for very long periods may be wrongly regarded as extinct and of no threat.

Long intervals between volcanic activity commonly precede unusually violent eruptions. An analysis of the Smithsonian Institution's Volcano Reference by Simkin and Siebert (1984) indicates a median repose period of 865 years for the 25 most explosive eruptions for which the preceding interval of inactivity is known. Of the historical eruptions in this group, half caused fatalities. Of the 16 largest explosive eruptions in the 19th and 20th centuries, all but four occurred at volcanoes with no known historic eruptions (Simkin, 1994).

The long repose periods of many volcanoes should therefore be considered more as a cause for concern than for reassurance (Simkin and Siebert, 1994). For the purpose of hazard and risk assessment, no volcano should be assumed to be extinct, simply because it has not erupted within historical times. This important point is emphasised by several disasters in recent years. The 1991 eruption of Mt Pinatubo was the second largest of the century (VEI 6), but prior to this event Pinatubo had lain dormant for more than four centuries and was therefore not even considered within the Philippines volcano surveillance programme. Similarly, Mount Lamington in Papua New Guinea was not recognised as a volcano until it suddenly erupted catastrophically in 1951 (VEI 4), killing almost 3,000 people.

Volcanic Explosivity Index	0	1	2	3	4	5	6	7	8
General description	Non-Explosive	Small	Moderate	Moderate - Large	Large	Very Large			
Volume of Tephra (m^3)		$<10^4$	$<10^6$	$<10^7$	$<10^8$	$<10^9$	$<10^{10}$	$<10^{11}$	$<10^{12}$
Height Eruption Column (km) Above crater Above sea level	<0.1	0.1-1	1-5	3-15	10-25	>25			
Qualitative Description	Gentle	Effusive	Explosive		Cataclysmic		Paroxysmal		Colossal
Eruption Type	Hawaiian	Strombolian		Vulcanian	Plinian			Ultra-Plinian	
Tropospheric Injection	Negligible	Minor	Moderate	Substantial					
Stratospheric Injection	None	None	None	Possible	Definite	Significant			
Number of Eruptions	699	845	3477	869	278	84	39	4	0

Table 3.1: Summary of criteria for Volcanic Explosivity Index (VEI) after Simkin and Siebert (1994) and Newhall and Self (1982).

3.2 The impact of volcanic disasters

3.2.1 Casualties

Historically the casualties caused by volcanic eruptions have been significantly lower than for other types of natural hazard such as droughts and floods. This is because large volcanic eruptions are relatively infrequent compared with other natural hazards and the areas affected tend to be more restricted. However, when volcanic eruptions do occur they can be highly destructive and can inflict very high losses to property and life in restricted areas. Furthermore, unlike other natural disasters, such areas may be so devastated by volcanic disasters that they may never be redeveloped.

Tilling (1989) estimated that during the last millennium approximately 290,000 people were killed by volcanic eruptions, although more recently Tanguy *et al*. (1998) published a slightly lower estimate, largely as a result of revising downwards the previously accepted death toll caused by the eruption of Tambora. Of the total, slightly less than 60% of the casualties may be attributed to four eruptions only, namely Tambora in 1815 (60,000), Krakatau in 1883 (36,420), Mont Pelée in 1902 (29,000) and Nevado del Ruiz in 1985 (23,000). According to Tanguy *et al.* (*op. cit.*) most fatalities can be attributed to post-eruption famine and epidemics (30.3%), pyroclastic flows and surges (26.8%), mudflows (17.1%) and volcanogenic tsunamis (16.9%).

The fact that post-eruptive famine and disease has been the largest single cause of fatalities suggests that in the modern world much can be done to reduce mortality by disaster relief measures, although the most effective means must lie in long-term land-use planning and disaster preparedness measures based on sound hazard and risk assessments.

3.2.2 Economic impact

Volcanic eruptions affect economic activity in numerous ways, some of which are not obvious. Blong (1984, section 8.1) lists some of the diverse effects that have been produced by various types of volcanic hazards, although firm and reliable information on the actual costs of disasters is scarce.

Information is available on the economic impact of three well-documented volcanic eruptions of recent years. These are the 1980 eruption of Mount St Helens, USA, the 1989-90 eruption of Redoubt volcano in Alaska, and the 1991 eruption of Mount Pinatubo in the Philippines. Even in these examples the quoted figures vary significantly from one source to another, but they do provide a general indication of the economic losses incurred as a result of major eruptions. In addition to these three eruptions, the present project has also assessed the economic impact of the 1963-65 eruption of Irazú in Costa Rica (Young *et al.* 1998, and Section 6.4.7 of this report).

The eruption of Mount St. Helens destroyed about 380 km^2 of commercial forest containing timber valued at $400 million. More than 4,800 km of streams and 169 lakes were either moderately damaged or destroyed. Total damage to crops and property was estimated to be more than $1.8 billion, in addition to short-term economic losses of more than $860 million (Perry and Hirose, 1991, page 44).

The eruption of Redoubt volcano in a rural area of Alaska in 1989-90 is reported to have caused losses of $160 million (Miller and Chouet, 1994 - based upon an unpublished report by Tuck *et al.*, 1992). Much of this loss was incurred by damage to an airliner which flew into the eruption plume. Truck and Huskey (1994) provide a brief but informative description of the methodology of cost-benefit analysis used to assess the economic disruption caused by the eruption, exemplifying it with losses incurred by the aviation industry due to damage and disruption, which alone amounted to $101 million.

The eruption of Mount Pinatubo was one of the largest of the century. It had disastrous effects on the economy of central Luzon, which prior to the eruption had been one of the most affluent regions in the Philippines and the country's largest agricultural producer. About 3,855 km^2 of forest and agricultural land were badly damaged by ash and mudflows (ADB, 1991a). Damage to crops, infrastructure and personal property during 1991 and 1992 was estimated to be US$443 million, and additional losses due to forgone business was estimated at US$18.4 million (Mercado *et al.*, 1996). During the same period a total of 8,260 houses were destroyed and 73,395 partially damaged, and the cost of caring for evacuees was estimated at US$93 million. An additional US$154 million was expended during this period on dykes and dams to control lahars (Mercado *et al.*, *op. cit.*). Losses in agricultural production for the five year period following the eruption were expected to amount to $890 million (ADB, 1991b). Previously the region had enjoyed a high rate of employment (89% in 1990), but in the year following the eruption a total of 28% of the workforce lost employment. Not only did the disaster have a major impact on the Philippines, but it also inflicted immediate and direct losses of over $1 billion to United States' military installations and precipitated a change in U.S. strategic military presence in the western Pacific that will have implications for decades (United States National Science and Technology Council, 1996).

Considering the size of the Pinatubo eruption and the population of the area, the loss of life was relatively low, because of timely warning and evacuation. About 5.7 million people were affected to some degree or other and at least 1,200 people perished. Many of the casualties resulted from the collapse of buildings under the weight of ash, although a significant proportion of the deaths occurred in refugee camps due to disease and stress related ailments.

The 1963-65 eruption of Irazú was prolonged but not catastrophic, but it did adversely affect the Costa Rican economy (Young *et al.* 1998: Section 6.4.7 this report). The GDP for the period 1961-70 averaged 6.1%, but in 1963 slowed to 4.8% and in 1964 to 4.1%. The impact could have been more severe but was offset by high commodity prices for the main exports during this period, although the construction industry was hard hit due to eruption-related uncertainty. There is also evidence to suggest that the uncertainty over the destructive capability of the eruption significantly influenced long-term investment in the country.

Even the secondary effects of eruptions can have severe impact. In the 1783 eruption of the

Laki fissure in Iceland, voluminous outpourings of lava were accompanied by the emission of large amounts of sulphur gases together with some ash which affected global climate and caused widespread acid rain over northwest Europe. Most of Iceland's crops were destroyed and grazing was stunted, resulting in the death of 79% of the country's sheep and 50% of its cattle, and in the ensuing famine 24% of the country's population perished (Thorarinsson, 1969).

The main impacts of eruptions on economic activity are usually felt close to source. An exception worthy of note is that of the 1991 eruption of Hudson volcano, which is situated in a remote part of southern Chile. Ash was dispersed downwind to cover 150,000 km^2 of Argentine Patagonia. Over much of this area the thickness of the ash was only a few millimeters or less, but this was sufficient to severely affect water supplies and grazing and so cause heavy losses of sheep. Breeding stocks never recovered from these losses and many ranches were therefore forced to close, resulting in devastating consequences for the economy of a region which was already in long-term decline (Financial Times, 17 September 1993).

3.3 Reduction of volcanic risk

In keeping with the general definition of risk given in Section 2, **volcanic risk** may be defined as the expected number of lives lost, persons injured, damage to property and disruption of economic activity due to volcanic hazards.

Although the intensity of volcanic hazards is generally related to the size and proximity of an eruption, other factors related to human settlement also determine the level of risk. In many volcanic areas risks are accentuated by population pressures which have resulted in the haphazard settlement and cultivation of volcanoes and their environs. This point is poignantly illustrated by the relatively small eruption (VEI 3) of Nevado del Ruíz in Colombia in 1985, which generated mudflows that destroyed the city of Armero, killing 23,000 people (Section 5.7.3). Although Armero was located more than 50 km from the summit region of the volcano, it was built within a river valley, upon a site that was known to have been overrun by large-scale lahars on at least two other occasions within historic times.

Two geoscientific strategies may be used to help reduce the level of volcanic risk. These are **volcano surveillance** and **volcanic hazard assessment**. Ideally, both approaches should be applied at high risk volcanoes.

The routine surveillance of high risk volcanoes can provide advance warning of eruptions and so facilitate the timely and orderly implementation of civil protection plans. In particular, the forewarning and evacuation of populations at risk can greatly reduce casualties and loss of life.

A number of different techniques are used to monitor volcanoes. These principally include visual monitoring, seismic monitoring, ground deformation studies using surveying techniques, and the monitoring of volcanic gas compositions. In addition, thermal measurements, microgravity surveys, and the monitoring of physical and chemical changes in fumaroles, hot springs and crater lakes have application. Volcano surveillance is not a subject of this report, but for a comprehensive and practical account of volcano monitoring

techniques the reader is referred to USGS Bulletin 1966, which is available in English and in Spanish (Ewart and Swanson, 1992; 1993) and to McGuire *et al*. (1995).

Hazard assessments may be used to delimit hazard zones for use in risk assessment and long-term land-use planning, with the objective of preventing or regulating the development of hazardous areas. This offers the most effective method of reducing risk in the long term. In addition, hazard assessment information is also required for the formulation of civil protection measures and can play a vital role in reducing risk during eruptions, as exemplified by the case study of Montserrat (Section 6.5 of this report; Montserrat Volcano Observatory, 1997; 1998).

In volcanic regions that are already densely populated and development is too far advanced, it is unlikely that hazard maps can influence land-use planning effectively for risk reduction. Tilling and Lipman (1993) suggest that the only practical means of reducing volcanic risk in such areas is to improve volcano monitoring and eruption prediction. Whilst this may be largely true, a balanced approach to disaster reduction should nevertheless be maintained by applying a range of prevention and preparedness measures. Even in established urban areas the planning of new developments should be regulated and if possible existing installations of a sensitive or strategic nature should be relocated into less hazardous areas over the longer term.

3.4 Volcanic hazard zone maps

Hazard maps may be used as a basis for sound land-use planning in volcanic areas, with the objective of regulating the development of hazardous areas and reducing the level of risk posed by future eruptions. In addition to land use planning, the information provided by hazard maps is needed for the formulation of civil defense plans. Volcanic hazard maps should therefore not be considered as an end product in their own right, but should be viewed as a component or tool within the broader process of risk reduction. Consequently it is important that hazard maps contain relevant information presented in a form that may be understood and utilised by others involved with the downstream activities of planning and risk reduction.

3.4.1 Problems regarding the communication and use of volcanic hazard information

It has often been alleged that the utilization of volcanic hazard information is seriously hampered by failures in communication between geoscientists and authorities responsible for risk reduction and planning. This is a complicated issue in which the reasons for failure to use hazard information effectively are manifold, as illustrated by several volcanic emergencies and disasters described in the following paragraphs.

A clear example of failure to act upon hazard information in the context of development planning is illustrated by an assessment undertaken on the island of Montserrat in the 1980's by Wadge and Isaacs (1987; 1988). At the time of publication this assessment had little or no impact and was not integrated into any disaster preparedness planning (Davis *et al*., 1998), despite the fact that it gave clear warning that the volcano was active and would erupt again, and that the capital of Plymouth was vulnerable. Following the damage caused by Hurricane Hugo in 1989, major investments were made in redevelopment on the island without taking the volcanic hazard assessment into account. Within six years the volcano erupted and largely destroyed Plymouth, including a newly constructed hospital which was never opened.

Problems have also arisen where volcanic hazard and risk information has not been used effectively for managing volcanic crises. Although this may not be of primary interest in the context of long-term development planning, it is of relevance because hazard maps and hazard information compiled for this purpose (i.e. long-term planning) also form a basis for civil defense planning during volcanic emergencies. The failure to act effectively on hazard information during an eruption is well-illustrated by the 1985 catastrophe that befell the city of Armero when 23,000 people perished in mudflows generated by the melting of snow and ice during the eruption of Nevado del Ruiz. The issues surrounding this disaster are summarised by Voight (1990). The hazard of mudflows had been accurately foreseen and mapped, although the timing of such an event could not be predicted precisely for reliable warning to be given, and government was not willing to bear the economic or political cost of an early evacuation or false alarm. Had a system of warning been in place and activated when the volcano erupted the catastrophe would probably have been averted. Voight (*op cit*.) concluded that "the catastrophe was not caused by technological ineffectiveness or defectiveness, nor by an overwhelming eruption, or by an improbable run of bad luck, but rather by cumulative human error – by misjudgment, indecision and bureaucratic shortsightedness.

A small eruption in 1976 of La Soufrière volcano on Guadaloupe precipitated a large-scale and expensive evacuation of 72,000 residents, because of the fear that the eruption would enter a catastrophic phase. In reality no major eruption took place and volcanologists were blamed for the false alarm. Decker and Decker (1981) cite the "cry wolf forecast" during the Guadaloupe crisis to illustrate the point that volcanologist and governing officials are faced with a no-win situation. They pose the question, "what does one cry when there *may* be a wolf?"

In an analysis of this dilemma Voight (*op cit*.) summarised the problem as one in which the volcanologist has to state the probabilisitic chance of error in the forecasting and delineation of hazards, but at the same time has to be sufficiently specific to encourage the authorities to take action, and the public to respond. Unfortunately, because of the nature of volcanoes, which in general appear to be dormant for prolonged periods, a window of opportunity for meaningful communication opens infrequently between volcanologists who foresee disaster on a crude probabilistic scale, and authorities that have to make pragmatic decisions. As a result authorities may choose not to implement risk-reduction policies under dormant volcanic conditions, and may only be galvanized into action when confronted with a volcanic event which is perceived to be dangerous.

Communication and utilisation of volcanic hazard information for long-term development planning is also impeded by a fundamental lack of understanding by decision makers and planners of the nature and effects of the hazards themselves. There is a great need therefore, for all those involved in volcanic disaster mitigation to be educated in the nature of volcanic hazards. This may be accomplished through lectures, seminars, literature and films. Another impediment to the communication of information appears to be that non-geoscientists have difficulties in understanding hazard maps. This issue is more complicated than appears at first sight and is not simply due to the specialised nature of such maps, although this is a contributing factor. Whilst some volcanic hazard maps may appear complicated to non-geoscientists, there is an added complication that many people involved in decision making and risk reduction are not sufficiently conversant with using maps in general, and therefore have difficulties in understanding spatial information presented in map form. Volcanic hazard zone maps therefore need to be clear and simple, and alternative methods of presentation should be considered which make hazard information more easy to visualise. Such methods could include the presentation of hazard zones on three dimensional terrain models, shaded relief maps or oblique aerial photographs, in addition to more conventional maps. As part of the present project such presentation techniques were used in the case study of volcán Villarrica (Young, 1998; Section 6.3 of this report).

In order to overcome the impediments to the uptake of volcanic hazard information and ensure that it is used effectively, closer co-operation and mutual understanding is essential between planners and volcanologists. Planners should be involved with all stages of hazard and risk assessment and should instigate and take the coordinating role in the overall process. By doing so, they are likely to become more conversant with the nature of the hazards, and the resultant maps will be better tailored to their requirements. Ideally, hazard assessments should be carried out at the request and under the direction of planners or national emergency bodies, so that a sense of ownership of the resultant hazard maps is engendered. This is probably the single most effective measure for ensuring that the information presented on hazard maps is pertinent and is taken heed of and utilised by planners and civil protection authorities.

3.4.2 The salient features of volcanic hazard zone maps

In conclusion to the foregoing paragraphs it is very important that hazard zone maps are presented in a format that can be understood by non-geoscientists, and that they contain information pertinent to planning, risk assessment and civil protection.

Volcanic hazard zone maps should convey the following basic information:

The areas or zones under threat from each type of volcanic hazard.

The probability (frequency) of a hazardous event occurring within a given period of time in each hazard zone.

The expected intensity of a hazardous event in each hazard zone.

Hazard maps need to be clear and instructive. An over abundance of technicalities can slow down and confuse the decision maker or planner, and therefore the number of documents should be limited to a usable level.

The maps should also be accompanied by descriptions, written for non-scientists, which provide information on the nature and effects of the hazards, and on their likely speed of onset and duration. Although this information can be provided in reports, it is important that it should also be presented as marginal notes on the hazard maps themselves.

3.4.3 The basic principles of volcanic hazard assessments

Volcanic hazard assessments are usually based upon the premise that future activity of a volcano will be similar to past activity, in terms of style, size and frequency of eruption. Such information on past activity may be obtained from records of historical eruptions, if available, and from the examination, interpretation and dating of ancient deposits which permit a reconstruction of volcanic history. However, another factor that should not be discounted is that future eruptions may occur of a size and style unprecedented in a volcano's history, but comparable to events that have occurred at similar volcanoes elsewhere. Such events might, for example, include very large eruptions or large-scale debris avalanches.

Another basic assumption made in volcanic hazard assessments is that the hazardous effects of eruptions decrease in severity with distance from source. Although this is generally the case, the actual extent of the hazard also depends upon the magnitude and explosivity of an eruption, as well as on the type of hazard. The size of an eruption therefore needs to be considered when delimiting hazard zones. For example, relatively local flowage hazards (pyroclastic flows, lava flows and mudflows) may be portrayed on small-scale maps, whereas the more widespread hazard of ash-fall may need to be presented on regional or national-scale maps. At some volcanoes separate hazard zonation schemes have been made for small, relatively frequent eruptions, and for moderate to large infrequent eruptions. An example of such a dual scheme is described in section 5.2.3 for the hazard of air-fall at Rabaul volcano (McKee *et al*., 1985).

Flowage hazards of different types often occur during the course of single eruption, and invariably follow similar pathways. It is therefore a common practice to map zones for the combined hazard of pyroclastic flows, mudflows and lava flows. This practice has been adopted by the United States Geological Survey on hazard maps of several volcanoes in the USA, as for example Redoubt volcano in Alaska (Till *et al*., 1993) and Mount Shasta (Miller, 1980).

The reliability of volcanic hazard assessments depends upon the level of understanding of a volcano's past eruptive activity. The more that is known about a volcano's geological history, the more reliable will be the hazard assessment. Most high risk volcanoes in the developed world have been studied in detail, and the style, magnitude and frequency of past eruptions is therefore usually well-known. For such volcanoes it is possible to map hazard zones with reasonable precision and usually obtain estimates of the probability of eruptions.

In contrast, only a small proportion of the hundreds of volcanoes in developing countries have

been studied in detail, and few have been the subject of hazard assessments. Given the need for integrating hazard and risk assessments within development and civil protection plans, and bearing in mind the large number of volcanoes that need to be assessed, there is a requirement for cost-effective techniques that facilitate the rapid mapping of volcanic hazards. The case study of volcán Villarrica undertaken by the present project (Young, 1998; Section 6.4 of this report) demonstrates that this can be achieved by using rapid mapping methods which involve the interpretation of aerial photographs and satellite images, followed by fieldwork in selected areas, in a manner similar to any other type of reconnaissance geological survey. When rapid assessments are required, as for example during volcanic emergencies, and little or nothing is known of a volcano's history, much can be achieved from the examination of aerial photographs and topography, and by drawing analogies with known eruptions at similar volcanoes elsewhere.

In the case of well-studied volcanoes where deposits have been radiometrically dated or there is a long history of recorded activity, it may be possible to estimate the frequency of hazardous events with reasonable confidence. In practice however, reliable historical records are not available for many volcanoes, and radiometric dating is expensive and time consuming, typically taking months to several years to complete depending on the techniques employed. Consequently it may not be possible to quantify frequency during the course of rapid hazard assessments. For this reason the majority of volcanic hazard maps produced do not provide quantitative estimates of hazard probability. Exceptions which do quantify hazard frequency are shown in Figure 5.13 for the hazard of pyroclastic flows and lahars at Mount Shasta, and in Figure 5.3 for the hazard of lavas on Hawaii.

In the majority of volcanic hazard maps, only relative terms are used to convey an idea of hazard frequency and intensity. In the Philippines for example, hazard zones are expressed as *high*, *moderate* and *low-danger zones*. Similarly, Indonesian hazard zone maps show *forbidden zones* and *first* and *second danger zones*. Some hazard maps from the USA use terms for decreasing probability such as; *area most likely to be affected, area less likely to be affected, area that could be affected* and *area that may be affected* (e.g. Redoubt volcano, Till *et al.*, 1993). While such terms provide a measure of the relative frequency of a hazardous event taking place, they are not precise and cannot be utilized in the quantitative assessment of risk.

There is, therefore, a real need to obtain historical and geochronological data during hazard assessments so that estimates of eruption frequency can be made. However, in rapid hazard assessments this may not be possible, and 'first pass' hazard maps based on rapid mapping methods may therefore not be suitable for detailed risk assessment, other than for making general statements. Even for well-studied volcanoes it may not be possible to estimate eruption frequency with confidence. For the majority of volcanoes it may therefore only be possible to assess risk in a qualitative rather than quantitative manner.

In section 3.1 it was shown that small eruptions are much more frequent than large eruptions, whilst very large eruptions are rare on the historical scale. Hazard maps for many volcanoes commonly reflect this size - frequency relationship, with separate zonation schemes being prepared for eruptions of different sizes and frequency. This is exemplified by the hazard zonation schemes produced by the case studies of this project for volcán Villarrica (Young, 1998) and Nevados de Chillán (Gilbert *et al*., 1998). In the case of Villarrica, separate hazard

zone maps have been compiled for small 10-year eruptions, moderate-size 100-year eruptions and large events with a periodicity of thousands of years. For Nevados de Chillán, zonation schemes were produced for *small normal* or *decadal eruptions*, which in effect are most likely to represent the "next eruption", *moderate-size eruptions* which occur every few hundred to a thousand years, and *large eruptions* that are related to caldera forming events associated with large pyroclastic flows which are a regional hazard every few tens of thousands of years.

A balance is necessary when utilizing hazard information and hazard maps for potential eruptions of different sizes and frequencies. Ideally, hazard maps for small and moderate size eruptions should underpin development plans, with hazardous areas being avoided for the construction of buildings, settlements and infrastructure. On the other hand it is not realistic nor prudent to enforce land-use planning regulations over very large areas in anticipation of rare large-scale eruptions, or for rare events such as large-scale debris avalanches, except possibly for installations of a sensitive or strategic nature. However, hazard maps for very large and rare eruptions should form the basis of civil protection plans for use in the event that such a crisis were to arise.

4 VOLCANIC RISK ASSESSMENT

In the previous section it was stated that volcanic hazard maps should not be considered as an end product in their own right, but should be viewed as a component or tool within the broader process of risk assessment and risk reduction. This section briefly describes some of the methods that have been used at selected volcanoes to combine volcanic hazard maps with data on population, economic development and vulnerability to produce volcanic risk assessments.

Volcanic risk assessments and risk maps offer distinct advantages over hazard maps by providing tangible indications of the losses that may arise as a consequence of volcanic activity. Such losses may be expressed in economic terms or as human casualties, and are useful in demonstrating the need for, and the advantages of mitigation, including long-term planning, volcano monitoring, and civil defense measures. Volcanic risk assessments therefore have an important role to play, by conveying the dangers of volcanic hazards in a quantitative form which is more meaningful to those involved in the "downstream" aspects of disaster mitigation, such as planners, civil defense authorities, economists and politicians.

Despite their utility, very few volcanic risk assessments have been undertaken. Examples are described below for the four volcanoes of Vesuvius, Santa María, Furnas and Monserrat. These follow the same broad process of assessing risk as the product of **hazard** (probability), **vulnerability** and **value**. Each assessment however, varies according to whether the risk is estimated in terms of economic losses, damage to buildings or as human casualties. Furthermore, at Vesuvius, Santa María and Furnas risk has been assessed in a form suitable for long-term planning and mitigation, whereas the assessment at Montserrat estimates the risk to the human population posed by the current eruption for the purpose of emergency planning and mitigation in the short-term.

4.1 Assessment of vulnerability with respect to volcanic hazards

In order to assess volcanic risk using the information contained in hazard maps, it is also necessary to assess vulnerability, since risk is the product of hazard and vulnerability.

Little has been published on vulnerability with respect to volcanic hazards, although Blong (1984) provides a considerable amount of general information. Section 5 of this report also briefly describes the hazardous effects of the main types of volcanic hazards.

Vulnerability may be assessed empirically or analytically. The empirical approach assesses vulnerability by examining the adverse impacts and effects of hazardous volcanic phenomena during previous disasters. The analytical approach is particularly applicable to assessing the built environment, by looking at the materials and designs used in construction and calculating the effects and failure rates of structures in response to physical conditions likely to be experienced during eruptions. Both of these approaches have been used to assess vulnerability in the case study of volcán Irazú (Section 6.4; Young *et al.*, 1998) and the methodologies developed were later applied to risk assessment at Montserrat (Montserrat Volcano Observatory, 1998a).

At Irazú the vulnerability of buildings with respect to loading by ash and impact from lahars was investigated as well as the vulnerability of the health of the population with respect to ash. The methodologies employed during these investigations are described in detail by Young *et al.* (1998) who used the information to make recommendations for reducing the risk during future eruptions. At Montserrat the vulnerability of buildings was assessed with respect to impact by ballistic bombs and roof collapse due to loading by ash, and the vulnerability of the population was examined in terms of casualties caused by collapsing roofs and adverse effects on health due to ash within the environment. The information was used to assess the risk posed by the on-going eruption and to formulate civil protection measures for reducing this risk.

4.2 Risk assessments at Vesuvius

Barberi *et al.* (1990) describe a risk assessment for the hazard of collapsing roofs due to loading by tephra fall in the area surrounding Vesuvius. From the history of past volcanic activity it was concluded that the most likely eruption in future would be a subplinian event. Based on the size of past eruptions and repose periods, predictions were made as to the mass of material likely to be erupted, the mass eruption rate (kg/s) and the height of the eruption column. Taking wind directions into account (from meteorological records) the fallout of tephra was modelled and hazard maps generated which defined contours of equal probability of having tephra blankets heavier than 100 kg/m^2 and 200 kg/m^2 . To illustrate the application of the hazard maps, a roof-collapse risk map was generated using the criteria that a loading of tephra greater than 200 kg/m^2 would cause collapse of 100% of roofs (vulnerability = 1). The probability of such an eruption taking place within a given time period appears not to have been addressed.

In a more comprehensive study Scadone *et al*. (1993) evaluated the risk at Vesuvius in terms of loss of human life for a range of hazards.

The risk was calculated using the standard formula:

$$\text{Risk} = \text{Hazard} \times \text{Vulnerability} \times \text{Value}.$$

Based on the history of past activity and repose periods it was considered that future eruptions most likely to produce risk to human life at Vesuvius would be in the size range VEI 3 to VEI 5, and from a statistical analysis of the periodicity of past activity the probability of such eruptions occurring within a ten year period were calculated as:

VEI 3 = 0.0989, VEI 4 = 0.0175, VEI 5 = 0.0030

Hazard was then calculated as the probability of occurrence of each class of eruption multiplied by the relative probability that an area would be affected by a given hazardous volcanic phenomena. Relative probabilities were estimated separately for the hazards of lava, pyroclastic fall, and the combined hazard of pyroclastic flow, surge and lahar (particulate flows). For VEI 3 eruptions the region was divided up into zones and the relative probabilities of each zone being affected by lavas and by particulate flows was estimated by counting the

number of times these areas had been affected by these phenomena during the period 1631 - 1944. For VEI 4 eruptions a probability of 0.5 was arbitrarily assigned to the occurrence of lavas. Insufficient historical information exists for a statistical analysis of the areas affected by particulate flows produced by VEI 4 and VEI 5 eruptions. For each of these sizes of eruption the region was therefore divided into two zones, one of which was assigned a relative probability of 1 and the other 0.5. The size and extent of the zones were based on the maximum distance travelled by particulate flows, being more extensive for VEI 5 eruptions than for VEI 4 eruptions. For the hazard of pyroclastic falls the dispersal patterns of tephra for the three sizes of eruptions were modelled using the annual distribution of wind directions between 5,500 and 12,000 metres at Rome airport.

Each hazard type was assigned a separate value of *vulnerability*. Lavas, being viscous and slow moving, were not considered to pose a serious threat to human life and were accordingly assigned a low vulnerability value of 0.01. Pyroclastic fall deposits 1 m thick were considered likely to produce extensive collapse of flat roofs, whereas a thickness of 0.5 m might only produce a few collapses. Vulnerability values of 0.1 and 0.05 were therefore assigned to areas likely to be covered by fall deposits of thickness $\leq$ 1 m and $\leq$ 0.5 m respectively. Particulate flows are very dangerous and were assigned vulnerability values according to size of eruption and distance from source as follows: Vulnerability for VEI 3 eruptions was assigned a value of 0.3 to a distance of 4 km in areas where flows might be expected: For VEI 4 eruptions a vulnerability of 0.6 was assigned to a distance of 4 km, and a value of 0.3 from 4 km to a distance of 10 km: Vulnerability for VEI 5 eruptions was assigned a value of 0.6 to a distance of 10 km.

Value was taken as the number of inhabitants living in each town around Vesuvius.

The towns within the environs of Vesuvius were ranked according to their risk coefficients on a logarithmic scale, and divided into four groups according to their risk. A risk map was also produced dividing the region into three zones of very high, high and medium risk. The towns with the highest risk occur along the coast on the southern flanks of the volcano, within the area most devastated by historical eruptions. Although the coefficient of risk is high for this area, the probability of a disastrous event is low; the high coefficient of risk partly reflects the high population density in this area.

The risk assessment estimated that the total number of casualties would range between 15,000 and 20,000 for eruptions of size VEI 3 to 5, assuming no action were taken to reduce the effects of an impending eruption.

The classification of the settlements into four classes of risk provides a useful basis for mitigation measures. It was recommended that urban planning should aim to reduce the population density of towns within the highest risk category and that these towns should be the first to be evacuated in the case of an impending eruption. The towns graded as high risk should be evacuated only when a sufficiently high certainty of an eruption exists. The towns graded at medium risk should take measures to reduce the risk, such as the removal of ash from roofs, and evacuation should be considered depending on the size of the eruption and the location of the town.

4.3 Risk assessment of Santa María volcano

Santa María volcano in Guatemala is one of the few volcanoes for which a risk map has been produced. The dome complex of Santiaguito on the southwest flank of the volcano has been in continuous eruption since 1922, principally producing pyroclastic flows and mudflows. Green and Rose (1998) produced a risk map of the volcano using a geographical information system in which they were able to combine a hazard zone map with four layers of economic and population data comprising:

Standard of living (adjusted to GDP per capita)
Population Density (persons/hectare)
Infrastructure (kilometres of highway and power lines)
Land use - economic activity contributing to GDP

From the four layers of economic data the value was computed in terms of dollars per hectare:

$$\text{Value} = (\text{Standard of living} \times \text{Population Density}) + \text{Infrastructure} + \text{Land use}$$

Volcanic Risk was then calculated using the standard formula:

$$\text{Volcanic Risk} = \text{Value} \times \text{Vulnerability} \times \text{Hazard}$$

Hazard was defined as the probability of a given area being affected by a potentially destructive process within a given period of time, and vulnerability by the proportion of value likely to be lost in a given event. The probabilities for volcanic events were estimated from historical information.

The resultant risk map shows the expected loss expressed in terms of dollars per year for each hazard zone. From the map it is readily apparent which hazard zones carry the highest risk. The total expected loss due to the volcano for all the hazard zones was calculated to be between US$3,323,301 and US$8,363,082 per year.

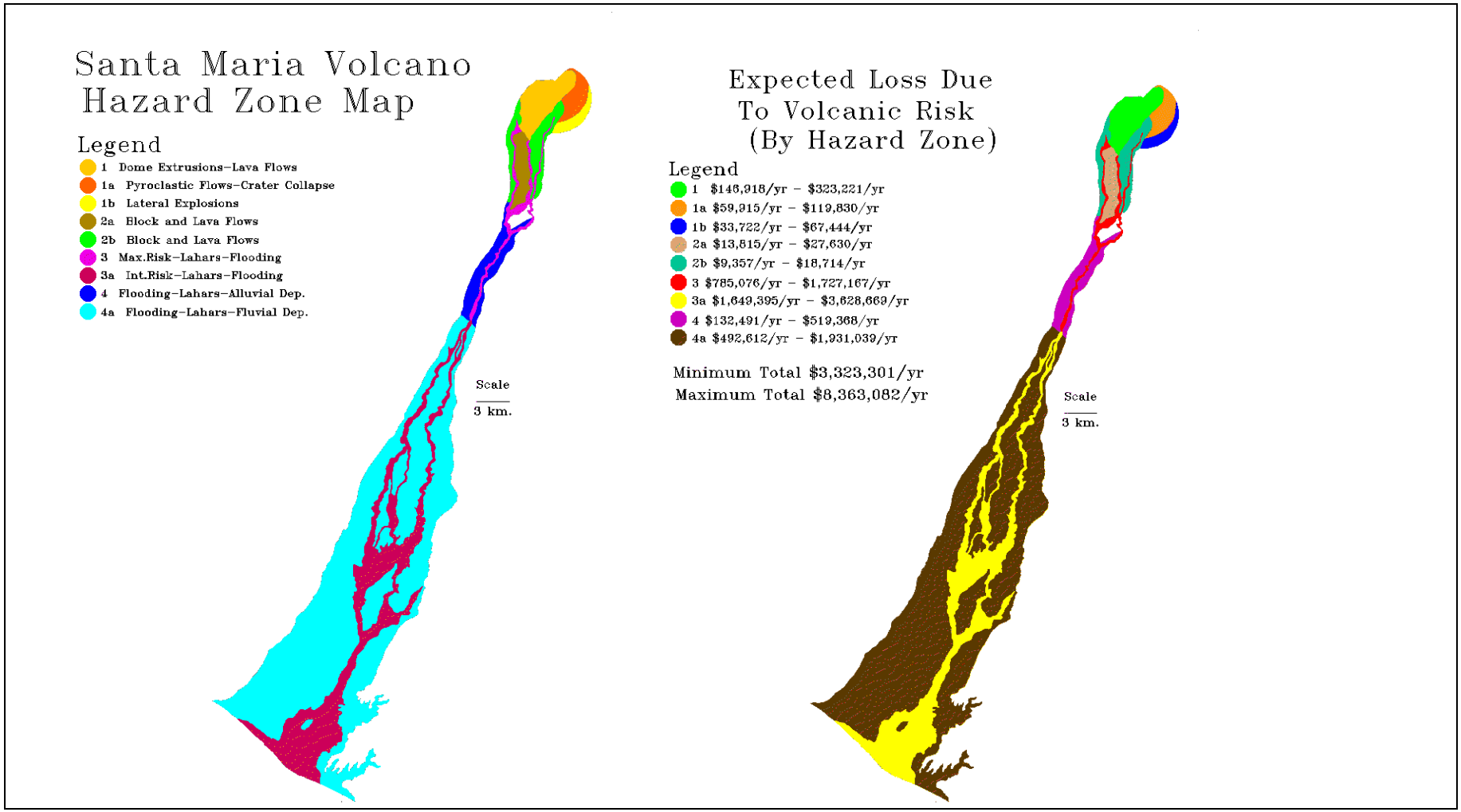

Figure 4.1: Example of hazard and risk maps for Santa María volcano, Nicaragua (Green and Rose, 1998)

4.4 Risk assessment at Furnas

Pomonis *et al*. (1999) assessed the risk to residential buildings and human beings at the caldera volcano of Furnas in the Azores, which has experienced 10 explosive eruptions over the past 5,000 years, the last having occurred in 1630 when more than 190 lives were lost. The study evaluated the risk posed in the event of a sub-Plinian eruption similar to, or stronger than the event of 1630. The purpose of this was to develop methods for assessing the vulnerability of buildings to damage from volcanic hazards, and to assist in defining improved preparedness measures.

The study covered all the buildings in two settlements within and near the caldera, and parts of two other settlements located around the volcano. External surveys were undertaken on a total of 1911 buildings, and a further 15 representative houses were surveyed in detail at the settlement of Furnas, situated within the caldera. These were surveyed in terms of structural type, design, building materials and condition, and building vulnerability was assessed with respect to several types of hazard that could be expected, including pyroclastic flows and surges, volcanic earthquakes, ground deformation, tephra fall and impact of pyroclastic bombs.

It was concluded that most houses within the paths of pyroclastic flows and surges would not be able to withstand the dynamic pressure likely to be exerted and would be destroyed. Furthermore, little can be done to design domestic buildings to resist pyroclastic flows. It was therefore concluded that the only method of reducing the risk would be to avoid building in the areas prone to pyroclastic flows by taking hazard maps into account in future planning.

Volcanic earthquakes occur as precursors to eruptions. It was stated that although these do not have the shock characteristics of tectonic earthquakes, they can cause strong shaking of the ground because of their shallow focus. The old rubble stone masonry houses of the area were considered to be vulnerable to such ground shaking: This point is illustrated by damage caused on the Azorean island of Faial in 1958 when more than 500 houses were destroyed during a 2-day earthquake swarm occurring near Capelinhos, the site of a volcanic eruption 9 months earlier (Blong, 1984).

Pomonis *et al*. (*op. cit*.) assessed earthquake damage on the basis of structural and earthquake engineering and knowledge of the seismic vulnerability of Azorean buildings. A map was constructed of the Modified Mercalli seismic intensity distribution expected from volcanic earthquakes during a 1630-type eruption , and from this the numbers of houses within each isoseismal interval were estimated. Assessment of damage for three main types of building was made for earthquake intensities of 6, 7 and 8 on the modified Mercalli scale. It was concluded that for earthquakes of intensity 6 no buildings would collapse, but for intensity 7 and 8 there would be a significant number of total collapses. The estimate of the number of collapsed houses was combined with statistical information on human vulnerability in buildings during earthquakes (Coburn *et al*., 1992), in order to calculate the number of casualties shown in Table 4.1. The estimates take into account two different levels of occupancy during the day and night.

Recommendations were made for decreasing vulnerability from volcanic earthquakes. The most cost-effective involved the maintenance of masonry, and the fitting of metal anchors and straps to connect masonry to floors. More expensive intrusive strengthening techniques are available if the benefits can be shown to justify the costs. Recommendations were also made for improving construction standards for new buildings.

	Nighttime	Daytime
Number of totally collapsed masonry buildings	209	209
Average building occupancy	2.35	1.29
People inside totally collapsed buildings	491	270
People trapped under debris	164	60
People killed instantly	41	22
Entrapped people seriously injured	57	32
Entrapped people lightly injured	66	36
Entrapped people eventually dying	18	10
Total seriously injured	39	22
Total lightly injured	66	36
Total fatalities	59	32

Table 4.1: Summary of expected casualties due to building collapse caused by volcanic earthquakes at Furnas (from Pamonis *et al*., 1999)

A detailed analysis was undertaken of the effects of tephra loading for four different categories of roof design. Based on isopachytes of tephra for a 1630-type eruption an assessment of the failure of roofs was made for different thicknesses of wet tephra and a chart was compiled for the probability of failure against thickness of wet tephra for each of the four roof types.

Estimation of human casualties due to roof collapse were made for the area expected to receive tephra fall in excess of 25 cm. Using population and building statistics it was possible to calculate the average occupancy for houses with each type of roof. The number of roof collapses for each of the four roof types was estimated, based upon design and expected loading. Information on the vulnerability of people during roof collapse due to tephra loading is very scarce, but based on experience from the eruption of Mount Pinatubo, the authors made tentative conclusions regarding the likely entrapment rate and the likely occurrence of injury or fatality. In single storey buildings it was estimated that a third of occupants would be entrapped, of which half would be injured and half killed due to suffocation or impact by falling debris. For two- or three-storey buildings it was estimated that 10% of the occupants would be entrapped, of which half would be injured and half killed due to suffocation or impact by falling debris. On this basis it was possible to estimate the total number of casualties expected for each roof type in the area with greater than 25 cm ash.

	Roof type				Total
	A	B	C	D	
Number of buildings	2350	1170	705	470	4695
Estimated number of collapsed or buried one-storey buildings	1010	525	315	210	2060
Estimated number of collapsed or buried buildings with two or more storeys	1230	645	390	260	2525
People killed in collapsed or buried one-storey buildings	543	282	169	113	1107
People killed in collapsed or buried buildings with two or more storeys	200	105	64	42	411
Total possible fatalities	743	387	233	155	1518
People injured in collapsed or buried one-storey buildings	543	282	169	113	1107
People injured in collapsed or buried buildings with two or more storeys	200	105	64	42	411
Total possible injuries	743	387	233	155	1518

Table 4.2: Estimates of casualties due to roof collapse caused by tephra loading during a 1630-type eruption at Furnas (from Pomonis *et al.*, 1999).

4.5 Risk assessment at Montserrat

At Monserrat a series of risk assessment have been undertaken during the course of the eruption in order to assess potential loss of life within specific areas for various hazard scenarios, for the purpose of emergency planning and hazard mitigation (e.g. Montserrat Volcano Observatory, 1998a). The assessments have been repeated at approximately six month intervals and updated to take into account new information and changes in style of eruption over the interim period. These assessments are thought to be the first examples of detailed risk assessment undertaken during the course of an eruption.

The probabilities of hazardous events have been calculated using a method of expert elicitation, based upon the aggregated weighted opinions of a group of volcanologists as to the future behaviour of the volcano (Montserrat Volcano Observatory, 1998a). The use of expert judgement is standard practice in quantitative risk assessment pertaining to geological hazards, such as exposure to landslides or earthquakes, but had not previously been used in volcanic hazard assessment.

As part of the elicitation process all the relevant scientific data on the eruption is thoroughly debated and a series of questions posed regarding possible future eruptive events. To facilitate this process a number of eruptive events that have occurred earlier in the eruption are used as standards against which future activity may be gauged. For each question each expert expresses an opinion in terms of probability, including an upper and lower limit, that the conditions of the question might be met: A typical question for example might be, "what is the probability of a dome collapse of a specified size occurring within a given period of time"? The responses to the questions are analysed using specialist software based upon algorithms rooted in the formal mathematical theory of scoring rules. The opinions of each expert are weighted against those of other experts and the mean result of the elicitation weighted in favour of those who demonstrate the greatest depth of knowledge and those who provide accurate opinions.

This information is used to assemble all plausible volcanic scenarios for the volcano on a logic-tree framework with branching to accommodate a hierarchy of related hazards (Figure 4.2). A Monte Carlo simulation is used to sample the probability distributions of each branch of the logic-tree. Conditional probabilities, that is probabilities that given events would impact on given areas, are also estimated. The product of the probability of the initiating event with that of the conditional probability define the likelihood of a hazard occurring in a particular place.

The population distribution is taken from a population zone map of the island. In attempting to assess the impact of a specific volcanic hazard type on a particular area, additional factors have been introduced to take account of vulnerability under varying circumstances, such as whether an event occurs in daytime or at night-time, and whether any alert or warning lead-time might be possible.

Two types of risk have been estimated for Montserrat. **Individual risk** is defined as the probability with which an individual may be expected to sustain a given degree of harm from a specific hazard. **Societal risk** is the probability with which specified numbers of people in a given population, or population as a whole, sustain a specified level of harm from a specific hazard. Annualised individual risk has been computed for a number of different areas: In the 1997 assessment individual risk ranged between 1:100 for the highest risk area to 1:200,000 for the lowest risk area farthest from the volcano in the north of the island. Societal risk is quoted in terms of numbers of fatalities expected for exceedance of given probability levels of 1:100, 1:1,000 and 1:10,000. Tables of hazard scenarios have also been compiled during each assessment, showing the probabilites of specified hazardous events within the following six months and the expected number of fatalities assuming no change in the population distribution.

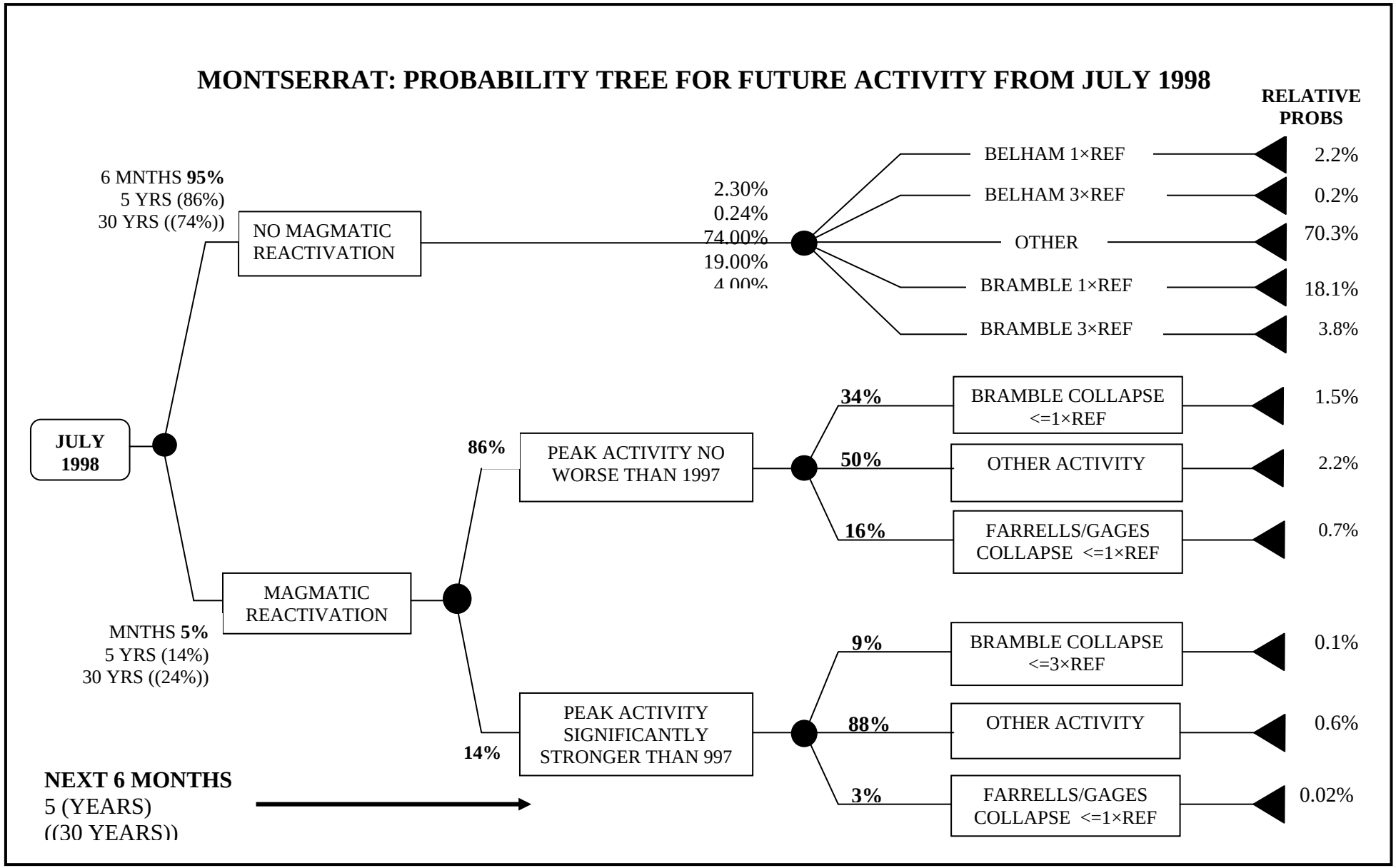

Figure 4.2: Probability tree for future volcanic hazards on Montserrat obtained from expert elicitation in July 1998.

The risks from volcanic bomb impacts were also assessed (Montserrat Volcano Observatory, 1998a). Impacts upon various construction materials were modelled, based upon the physics of projectiles, and used to assess the vulnerability of buildings. The construction materials of five different types of roofs were assessed, and it was predicted that clasts with a density of $1g/m^3$ and diameter of 10 cm falling with terminal-fall velocities from a sub-Plinian eruption would penetrate some roofs, and that clasts with diameters of 20 cm would have a 100% penetration rate. The assessment also examined human vulnerability with respect to the impact of falling clasts. It was predicted that serious skull injuries would be inflicted on people struck by clasts of 10 cm diameter ($1g/m^3$) falling with terminal velocities. A conservative clast diameter of 5cm was therefore used for preparing a risk map of Montserrat, based upon modelling of tephra fall using the method of Carey and Sparks (1986) for a sub-Plinian eruption of similar size to that which had occurred on the island in September 1996.

The health risks of ash was assessed and has been regularly monitored and re-assessed during the course of the eruption. The original assessment (MVO, 1998a) looked at the risk of silicosis in communities exposed to ashfalls. Test showed that the respirable fraction of ash in the air (<10 microns) contained 10-24% cristobalite, a mineral considered to be more toxic than quartz (Baxter *et al*. 1999). The high concentrations occurred in ash produced by pyroclastic flows generated by lava dome collapses. The cristobalite was thought to have been produced by vapour phase crystallisation in the lava dome, and due to milling effects in the pyroclastic flows was preferential concentration within the very fine (respirable) fraction of associated ash clouds. Monitoring of ambient dust levels in the air suggested that levels of respirable ash, and thus cristobalite, were comparable to levels in metal mines where miners have developed silicosis: In some communities the average levels of cristobalite in the air over 24 hours exceeded the occupational standard adopted for the USA. Although the toxicity of cristobalite is not fully understood, it was felt that silicosis could develop in the population if exposure to the measured ambient levels continued for a number of years.

Risk maps of Montserrat have been compiled on the basis of these risk calculations and used for hazard mitigation by defining exclusion zones from which the population has been evacuated.

5 VOLCANIC HAZARD TYPES

This section provides information on each of the main types of volcanic hazard and is written as a guide to geologists with little or no knowledge of volcanology. It does not address the methodology of identification and mapping of volcanic deposits in the field. For further information on the mapping and elucidation of volcanic stratigraphy and volcanic evolution the reader is referred to the case studies of the hazard assessments of Nevados de Chillán and Volcán Villarrica, which were undertaken as part of this project (Dixon *et al.*, 1995; Gilbert *et al.*, 1998; Young, 1998).

The following hazards are described:

- Lava flows
- Pyroclastic falls
- Pyroclastic flows
- Hot pyroclastic surges
- Cold pyroclastic surges
- Lateral blasts
- Debris avalanches
- Lahars and floods
- Tsunamis
- Volcanic gases
- Volcanic earthquakes

Descriptions are given of each of these phenomena, and their hazardous effects are illustrated with examples of historical disasters. Methods that have been used for the assessment and mapping of each type of hazard are also described and illustrated with examples of hazard maps from various volcanoes around the world.

5.1 Lava Flows

Lavas are flows of magma extruded onto the surface by essentially non-explosive eruptions. In general it is rare for lavas to cause the direct loss of life, because they usually flow slowly, allowing sufficient time for people to be evacuated. They do however destroy everything in their paths by a combination of burial, crushing and heat.

—

5.1.1 Characteristics of lava flows

Lava flows of different compositions vary considerably in their mode of eruption, flowage behaviour and form. The main features of concern in the hazard assessment of lava flows are size, morphology and rate of movement, which are determined by complexly interrelated factors, including slope-angle and surface roughness, the rate of effusion, and the intrinsic physical properties of the magma, such as yield strength and viscosity, which are in turn functions of temperature, chemical composition, volatile content and the degree of crystallization of the magma.

The viscosity of lava flows generally increases with silica content and decreases with temperature and volatile (water) content. Basalts are the most fluid of the common lava types and are typically erupted at temperatures of 1100°–1200°C. With increasing silica content and decreasing temperature there is a general increase in viscosity through andesite and dacite to rhyolites which are erupted at temperatures of approximately 700°–900°C.

The most voluminous lavas are flood lavas which are erupted from fissures and cover vast areas. They are predominantly basaltic, but also include unusual flood phonolites and trachytes, such as those found adjacent to the East African Rift. An example which illustrates the exceptional scale of flood lavas is given by the mid-Miocene Columbia River basalts of western USA, which have a total volume of about 170,000 km^3 and include individual lavas tens of metres thick that flowed for distances of up to 300 km. Flood lavas have not been experienced in historic times and are confined to the geological record where their vast outpourings have been related to major tectonic events such as the rise of mantle plumes and rifting of continents. Flood lava events are rare when taken in the context of geological time, and although they would undoubtedly pose a severe hazard and cause serious changes to world climate if they were to occur it would be unrealistic to consider them for the purpose of hazard ***zoning*** and land-use planning.

Lavas erupted in historical times from point sources or fissures on central volcanoes are several orders of magnitude smaller than flood lavas, but they are of common occurrence and pose a threat to communities living close to volcanoes.

A useful parameter for describing the gross morphology and dimensions of lavas is that of *aspect ratio* (Walker, 1973). This is the ratio of the horizontal extent (H) to thickness (V), where H is taken as the diameter of a circle with the same area as that of the flow (Figure 5.1). Walker collated data on the dimensions of a large number of Quaternary lavas and distinguished two main groups (Figure 5.2). These are low-viscosity, low-aspect ratio lavas comprising basalts and feldspathoidal-bearing types, and high-viscosity, high-aspect ratio lavas consisting of trachytes, andesites, dacites and rhyolites. A third but minor group consisting of basaltic andesites and phonolites overlaps the field of the other two groups.

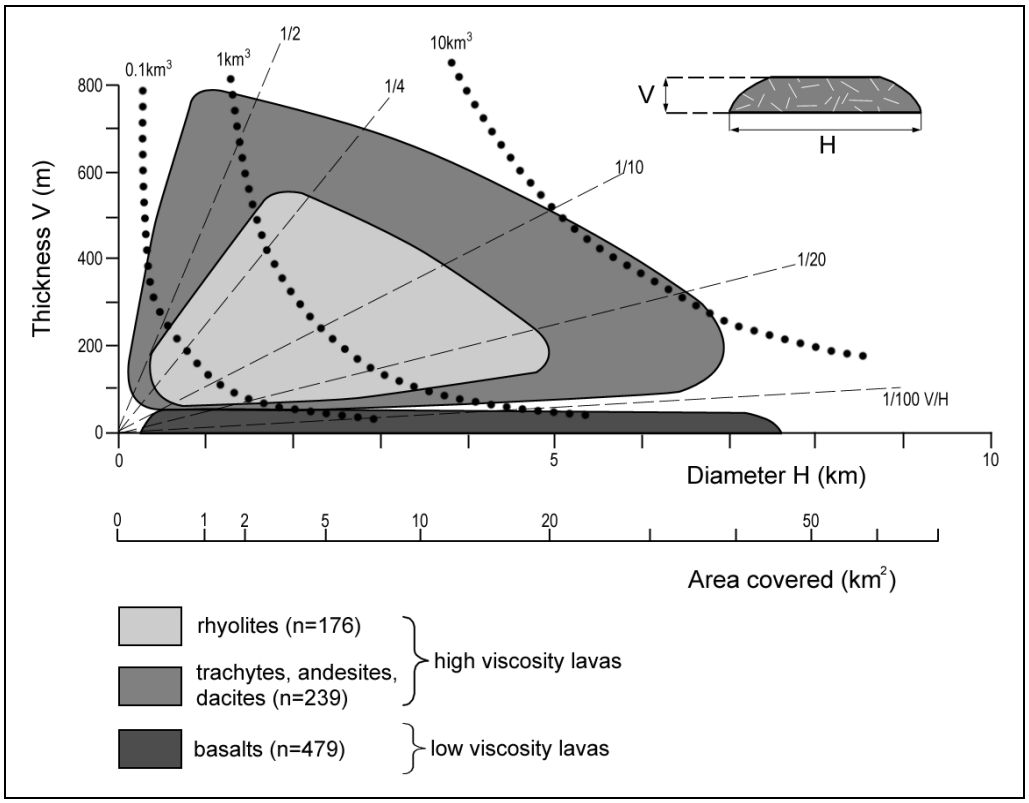

Figure 5.1: Aspect ratios of lavas of different compositions. The dashed lines denote aspect ratios (V/H) and the dotted lines give the volumes of circular disk-like bodies as a guide to the volumes of lavas. (Based on the dimensions of Quaternary lavas, after Walker 1973).

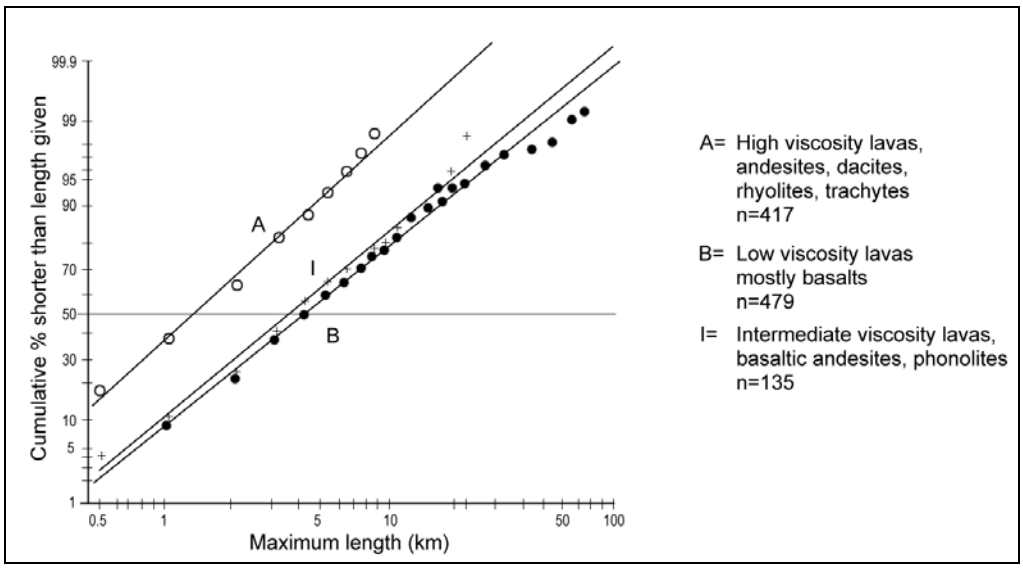

Figure 5.2: Logarithmic probability plot of the length of Quaternary lavas of different compositions. (Based on the dimensions of Quaternary lavas, after Walker 1973).

Walker (1973) concluded that effusion rate is the most important single factor in determining the morphology and length of lava flows. He believed that this is related to cooling, with lavas erupted at high rates tending to travel farther before cooling reduces their viscosity sufficiently to stop movement.

Basaltic magmas with high rates of effusion produce simple sheet-like lavas which flow relatively long distances, whilst low rates of effusion result in many small flows that pile up near the vent. Basalts are usually erupted from fissures or from parasitic scoria cones. The most fluid are alkali basalts which are commonly erupted by 'fire fountaining' along fissure zones on the flanks of shield volcanoes. The largest basaltic eruption of historic times was that of the Laki fissure of Iceland in 1783, which extruded 12.3km^3 of magma at a rate of about 5000m^3/sec, producing lavas that spread over 565km^2 and flowed for distances of up to 65 km (Thorarinsson, 1969). Even larger Quaternary basalt lavas have been reported with lengths of up to about 160km (Stephenson and Griffin, 1976). It should be stressed however, that basalts of these magnitudes are exceptional, as can be seen from the data of Walker (1973) presented in figure 5:2. The data of walker (*op. cit.*) indicates that the frequency distributions of flow lengths for each of the main lava groups are log-normally distributed, and that for basaltic lavas the median length of the measured flows is 4.1km, whilst 80% have lengths less than about 10km and 95% less than about 25km.

In contrast, high viscosity lavas, including andesites, dacites and rhyolites, are typically erupted at low rates and form short, thick flows or steep-sided domes of limited extent. Magmas of intermediate to silicic composition usually contain high volatile contents, and in order for them to erupt non-explosively as lavas they need to degas before reaching the surface to avoid a build up of gas pressure. This may be achieved by the escape of exsolved volatiles through vents or hydrothermal systems, or by explosive release during pyroclastic eruptions, which may explain why lavas of intermediate to silicic compositions are commonly extruded during the final phases of many explosive eruptions. The maximum length reported by Walker for a silicic lava is 18 km (for the Ring Creek dacite), although the present study has discovered andesites and dacites at Nevados de Chillán which have lengths exceeding 30 km and 20 km respectively (Dixon *et al.*, 1995). These examples are, however, exceptional, as indicated by Walker's data which show that 95% of silicic lavas are shorter than about 4.5 km whilst the median flow length for the silicic lava group as a whole is only 1.3 km.

The rate of movement of lavas typically ranges from a few metres per hour for silicic compositions to several kilometres per hour for fluid basalts. In extreme cases rates may be higher, as exemplified by the 1977 eruption of Nyrangongo in Zaire. During this eruption a very fluid basalt lava lake situated in the summit crater drained rapidly through fissures on the flanks, producing several thin but rapidly flowing lavas. Flow rates are estimated to have ranged between 30 and 100 km/hr, and one flow advanced 20 km during the half hour of the eruption and is reported to have engulfed and killed between 60 and 300 people. Elsewhere, similar flow rates have been measured within specific parts of alkali basalt lava fields, although the overall rate of advance of the lava fronts themselves is invariably very much lower. This point is exemplified by the 1885 eruption on Hawaii, where rates of up to 64 km/hr were recorded within flow channels but the front of the lava only advanced 1.5 km in a week.

Apart from exceptions like that of Nyrangongo, lavas rarely cause loss of life, although they

do destroy everything in their paths. Secondary hazards associated with lavas are generally more life-threatening than the flows themselves. The most hazardous effects are pyroclastic flows and lateral blasts associated with the growth and collapse of steep-sided silicic lava domes and flow-fronts on steep-sided volcanoes (see sections 5.3.3 and 5.5.1). Bush fires caused by the ignition of vegetation can also be a problem, whilst floods and lahars may be generated when lavas are erupted onto or beneath snow and ice (Section 5.7.3). Large-scale lava eruptions may also be accompanied by gas hazards. In the Laki eruption of 1783 large amounts of sulphur gases and some ash were emitted which affected global climate and caused widespread acid rain in northwest Europe (Sigurdsson, 1982). Most of Iceland's crops were destroyed and grass became stunted, resulting in the death of 79% of the country's sheep and 50% of its cattle, and in the ensuing famine 24% of the human population perished (Thorarinsson, 1969).

5.1.2 Hazard zoning for lava flows

As discussed in the previous section, the length of lava flows and the areas they cover is a function of composition, temperature and rate of effusion, with basalts generally flowing farther and covering larger areas than andesites and more silicic lavas. The hazard generally decreases with distance from source, and valleys and depressions extending off the flanks of volcanoes generally have higher hazard rankings than positive ground because lavas are channelled by topography.

Lava hazard zones for land-use planning purposes are usually based simply upon the distribution of earlier flows, with topography also being taken into account to help delimit or refine the positions of zone boundaries. On volcanoes where lavas form only part of the stratigraphy and where other types of activity are prevalent, hazard maps often portray the hazard of lavas as a single generalized zone based upon the mapped extent of previous flows.

On volcanoes where a significant proportion of individual lavas can be distinguished and mapped, and where information is available on their ages, it is possible to delimit hazard zones based upon the relative frequencies of lava eruptions. Probabilities can be assigned which provide estimates of the likely frequency of flows occurring within these zones in the future. Information on the age of lavas may be obtained from historical reports and from radiometric dating and other techniques (e.g. ^{14}C dating of charcoal or other carbonaceous material underlying flows). Where data on absolute age is not available, relative ages are still of great use and can be ascertained by mapping and examination of field relationships between flows and groups of flows.

A good example of hazard zoning based upon the relative frequencies of lava flows is that adopted for the island of Hawaii (Figure 5.3, after Wright and Pierson, 1992). The island comprises five volcanic centres of varying age, each composed predominantly of basaltic lavas. These lavas are characteristically very fluid when erupted and often travel large distances. Based upon the ages of lavas and considerations of topography the island is divided into a number of zones, ranked 9 to 1 in order of increasing hazard. The zone of least hazard (9) covers the slopes of Kohala volcano which has not erupted for at least 10,000 years. Mauna Kea erupted during the recent prehistoric past, but not within historic times, and is covered by zones ranked 8 and 7, with the zone of greatest hazard (i.e. 7) being located over

the summit area. The volcanic centre of Hualalai has only erupted twice in historic times (1800 and 1801 AD) and is given a hazard zone ranking of 4. In contrast, the axial rift zones which cut across the summit regions of Kilauea and Mauna Loa have been the sources of numerous lavas within the recent past and continue to be active up to the present day. These are thus given hazard rankings of 1, whilst the flanks that slope away from the rift zones have rankings of 2 and 3.

A similar approach to lava hazard zoning has also been used by Crandell (1983) for the Hawaiian island of Maui (Figure 5.4). The western part of the island is composed of an old basaltic shield volcano which is deeply dissected and inferred to have been inactive for at least 20,000 years. To the east lies the large basaltic shield of Haleakala which last erupted lavas in 1790. The highest potential hazard exists in Zone I which comprises the crater and southwest rift zone of Haleakala, where lavas have been erupted with an average rate of one per 100-200 years over the past 1,000 years. In Zone II, lavas are known or inferred to have erupted with a frequency of at least one per 500 years and the latest flows have an age of less than 1,000 years. In Zone III, lavas are inferred to have been erupted at an average rate of at least one per 2,000 years and the last flow occurred within the last 10,000 years. Zone IV includes the ground in which lavas have been erupted with an average rate of once every 20,000 years, with the latest flow being older than 10,000 years, whilst Zone V covers areas that have not been affected by lavas over the last 20,000 years.

Once an eruption is underway and source vents have been identified it is possible to delimit more precise hazard zones by considering topography and predicting the paths that flows are likely to take. However, even when eruptions of lava are taking place it is notoriously difficult to make predictions, other than general ones, regarding the final length of the flows. In general, higher rates of effusion will produce more extensive flows, although it should also be born in mind that effusion rates are usually highest at the beginning of an eruption and decrease with time as pressure drops within the magma reservoir. Nevertheless, on active flows which are threatening communities it is important to monitor rates of effusion, rates of movement and temperature, because these can help to build up an understanding of the overall behaviour of the flow, which is useful for assessing the scale of the hazard and for defining and re-defining hazard zones with more precision as the eruption progresses.

The examples of the hazard zoning schemes for the Hawaiian islands are for very fluid basaltic lavas. Lavas of intermediate composition tend to be much less fluid, although when erupted at high rates can flow for considerable distances, as exemplified by andesite and dacite lavas at Nevados de Chillán (Dixon *et al.*, 1995). Where viscous andesitic and silicic lavas and domes are erupted on steep-sided volcanoes the nature of the hazard is completely different and there is a greater danger of block-and-ash pyroclastic flows produced by the gravitational or explosive collapse of lava flow-fronts or the flanks of domes (see Section 5.3.3). Such pyroclastic flows move at high velocities and are highly destructive, and are a serious hazard in valleys down slope from silicic lava domes and steep-sided lava flows.

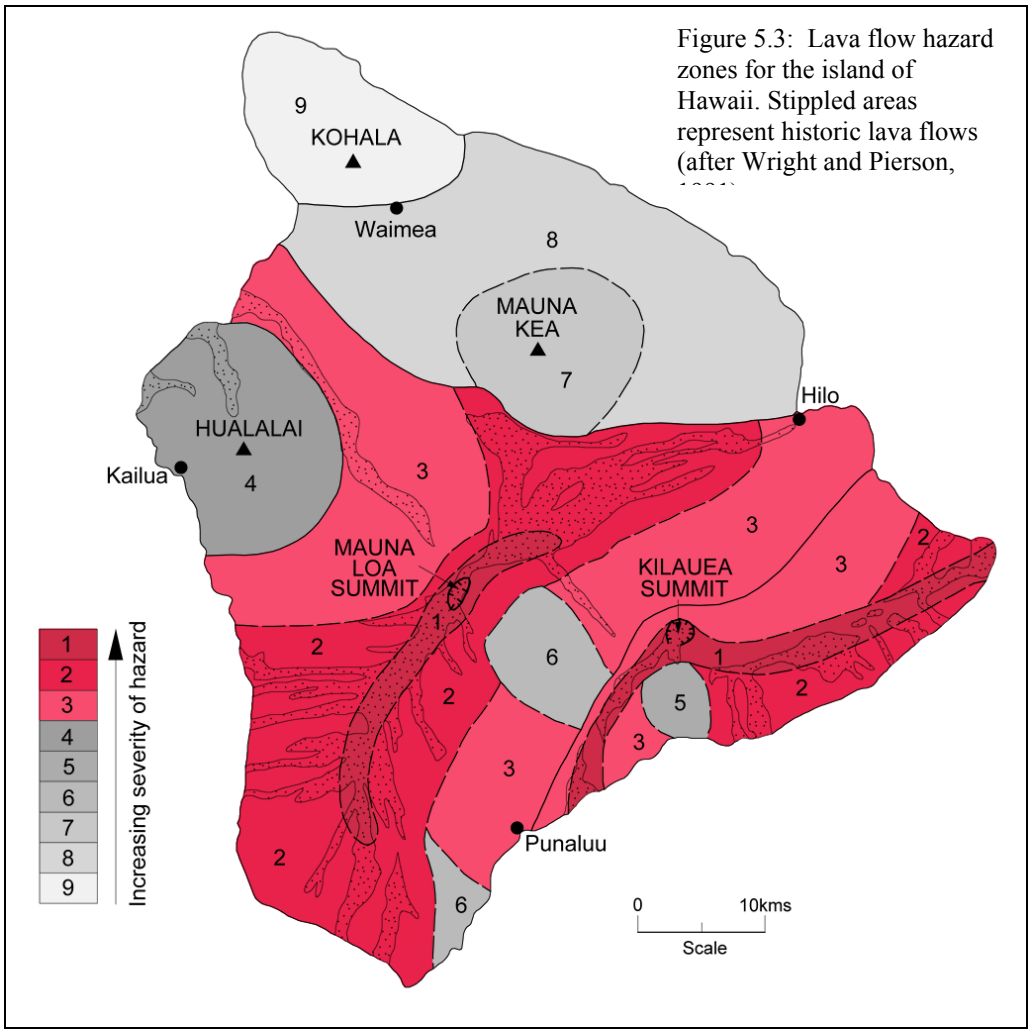

Figure 5.3: Lava flow hazard zones for the island of Hawaii. Stippled areas represent historic lava flows (after Wright and Pierson,

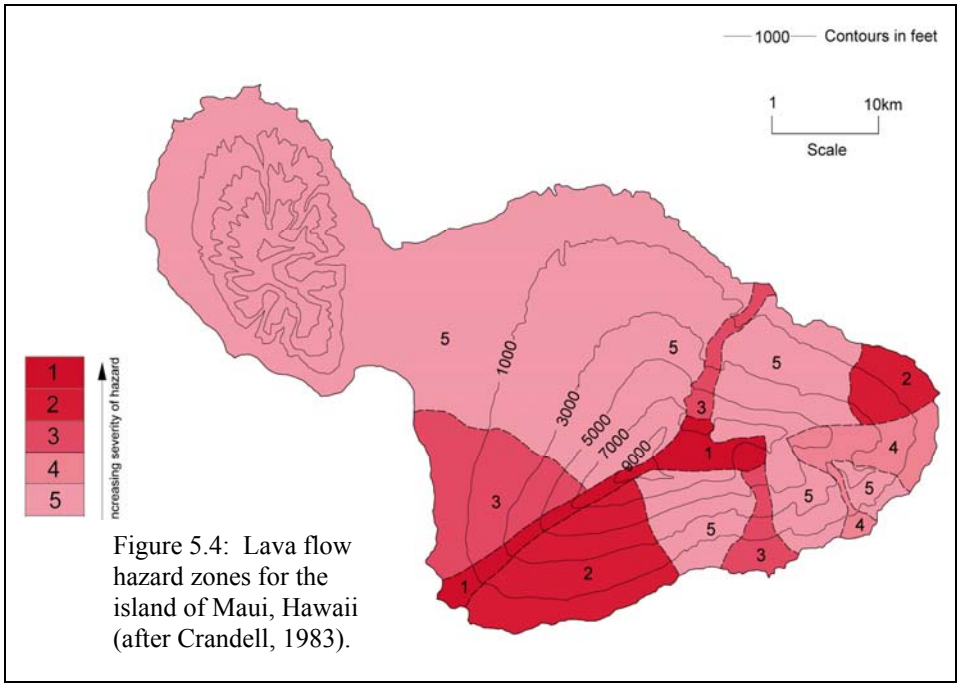

Figure 5.4: Lava flow hazard zones for the island of Maui, Hawaii (after Crandell, 1983).

5.2 Pyroclastic Falls

Explosive eruptions eject fragments into the atmosphere, which consist of magma, crystals and rock. Such fragments produced by explosive activity are termed **pyroclasts** and include the finest dust and ash as well as coarse blocks. On falling back to the ground pyroclastic material accumulates as pyroclastic fall deposits or **tephra** deposits. The ejection of tephra into the atmosphere and its subsequent fall back to the ground gives rise to a range of hazards depending upon the style and scale of eruption and on proximity to the eruptive source. Relatively local problems may be associated with small-scale eruptions whilst at the other extreme whole regions may be affected down-wind of large-scale explosive eruptions on stratovolcanoes of intermediate to silicic composition.

5.2.1 General characteristics of eruption columns and tephra dispersal

Tephra is classified according to pyroclast size into ash (<2mm), lapilli (2-64mm) and blocks and bombs (>64mm) which may reach several metres in diameter. It varies in character from low-density vesicular pumice or scoria, through to dense rock fragments and crystals. Pyroclasts derived from the magma causing the eruption are said to be **juvenile** in origin, whilst those incorporated from pre-existing rocks during the course of eruption are termed **lithic** or **accidental**.

Tephra is carried upwards by eruption columns which can range in height from a few tens of metres to more than 50 km in extreme cases. Material is initially blasted upwards by gas thrusting from within the vent, typically propelling it to heights ranging from a few hundred metres to a few kilometres in the largest eruptions. Above the gas thrust region particles are buoyed upwards by convection within a hot turbulent column which usually accounts for most of the vertical height of the eruption plume. Eventually a situation is reached where the overall density of the eruption column is equal to that of the surrounding atmosphere, at which point the column expands laterally and spreads radially outwards, although the central part also continues to rise because of its momentum: The combined effect of these two processes produces an umbrella-shaped cloud. The general features of volcanic eruption columns are illustrated in Figure 5.5.

The height of an eruption plume is principally governed by the mass discharge rate and the temperature of the material erupted, with higher rates of discharge generally producing higher eruption columns. Vertical convective velocities are greatest within the axial cores of eruption columns and decrease towards the margins. Therefore larger and denser clasts can be buoyed upwards along the core of a column than at its margins. Carey and Sparks (1986) consider that, except for the weakest eruptions, the upward convection velocities in the axial regions of eruption columns are sufficiently large to carry fist-sized lithic clasts almost to the tops of the columns, although the velocities towards the margins of columns would generally not be sufficient to support such clasts. Clasts that move laterally from the axial regions towards the margins of columns may therefore be too heavy to be supported and fall out.

Although most tephra becomes entrained in upward convecting eruption columns, the largest clasts in the lower parts of columns are not affected by these dynamics. Initially large clasts are propelled by gas thrusting and then follow ballistic trajectories which can carry them out of the vertical eruption column altogether. Such **ballistic clasts** need to be taken into account in hazard assessment. Their range is determined by initial velocity, size, density and ejection angle, but they are generally confined to the vicinity of source vents, usually within a distance of 5 km, but in exceptional cases they may be propelled more than 10 km.

Eruption plumes are affected by winds, the direction and strength of which can vary considerably from one level of the atmosphere to the next, and in some cases show complete reversal in direction. The effects are complex, but in general the strongest eruption columns, which rise to the greatest heights, are deflected least, whilst weaker and smaller columns may be substantially displaced or bent over in a downwind direction. Carey and Sparks (1986) predicted that, in general, columns that are powerful enough to reach the tropopause (10 to 17 km depending on latitude) will not to be significantly bent over; this conclusion is supported by observation.

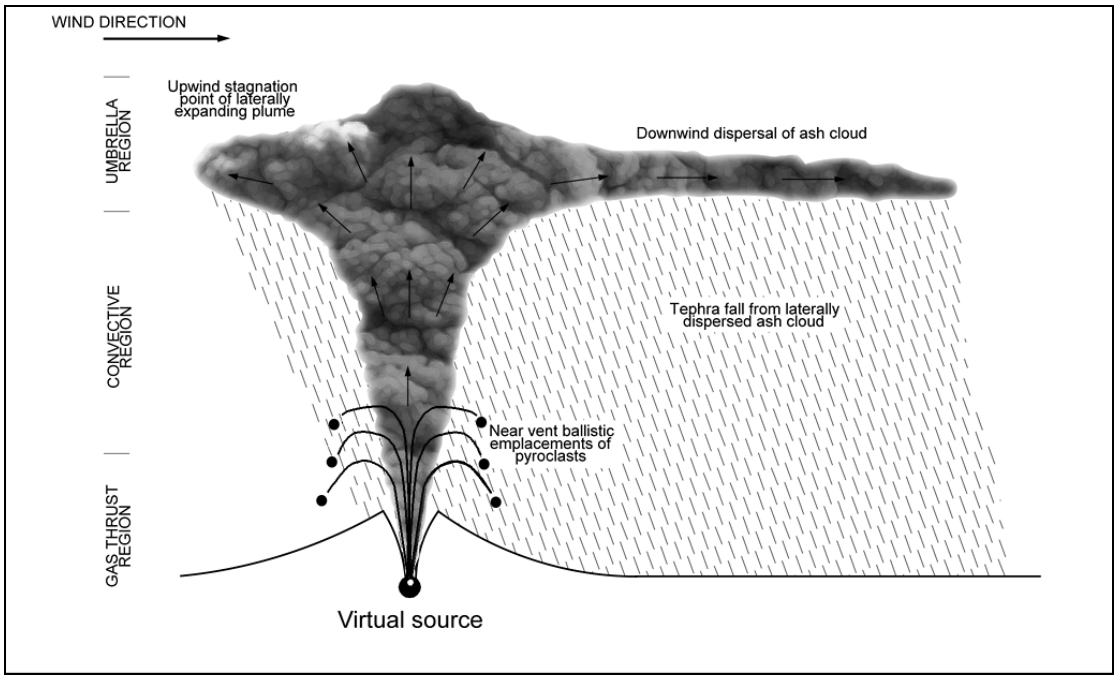

Figure 5.5: Sketch of main features of an eruption column and dispersion of tephra downwind (modified after Sparks, 1986). See text for explanation.

Tephra is dispersed in the umbrella regions of volcanic plumes by winds which in the upper parts of the atmosphere travel at high speeds. For example, during the 1980 cataclysmic eruption of Mount St Helens the plume front expanded downwind initially at a velocity of about 250 km/h and at an average velocity of 100 km/h over the first 1,000 km. In the largest plumes it is possible for the umbrella cloud to spread laterally against the prevailing wind for some distance before reaching a point where it is eventually counteracted and stagnates.

Higher eruption columns disperse clasts of a given size more widely than smaller columns. Tephra gradually falls out of volcanic plumes as they spread laterally away from their source. Coarser and denser clasts fall out first and finer material is carried to greater distances, whilst the very finest dust reaching the upper atmosphere during large eruptions may remain in suspension and be borne around the globe for prolonged periods.

Pyroclastic fall deposits typically accumulate in beds that uniformly mantle the pre-existing surface. The deposits are usually well to moderately well-sorted and in general show gradual decreases in thickness and grain size away from source. In classic examples the isopachytes (contours of equal thickness) of tephra fall deposits show ellipsoidal patterns that are elongated downwind from source. The fall deposits associated with stronger winds or weaker eruption columns tend to be restricted to narrower zones parallel with the wind direction, and so produce more elongated dispersion patterns. However, rainfall and variations in winds as well as other factors can result in thickness and grainsize variations which depart from the classic dispersal pattern.

5.2.2 Hazardous effects of pyroclastic falls

Of all the primary volcanic hazards, tephra falls produce the most widespread and diverse effects. Areas of thousands or even tens of thousands of square kilometres can be affected to varying degrees downwind of the largest eruptions.

The primary hazards associated with tephra falls include:

- Impact and heat from falling pyroclasts
- Burial
- The effects of ash suspension in the air and in water
- Toxic and corrosional effects of volcanic gases and salts transported with the tephra

Secondary hazards associated with tephra falls include lahars (volcanic mudflows) which are common and can be considerably more hazardous than the primary hazard (see Section 5.7).

Impact from falling pyroclasts and ballistic projectiles is a hazard close to an eruption but decreases with distance from the vent. Blong (1984) noted that volcanic explosions rarely throw ballistic projectiles more than 5 km, although more exceptional examples are cited in the literature. Hot bombs were hurled 8 km during the 1963 eruption of Angung on Bali (Zen and Hadikusomo, 1964) and hot pumiceous bombs reached distances of up to 11 km during the 1783 eruption of Asama (Aramaki, 1976). During the initial phase of the eruption of Fuji in 1707 hot rocks the size of footballs are reported to have fallen on the village of Shubashiri situated about 12 km from the summit (Tsuya, 1955). People may survive the impact of small bombs if they seek shelter, but larger bombs can cause substantial damage to buildings.

Descriptions of the damage caused to buildings by impact are provided by Blong (1984). A risk assessment of Montserrat also modelled the effects of volcanic bomb impact upon various construction materials, based upon the physics of projectiles, and used this to assess the vulnerability of buildings. The methodology used in this risk assessment is described in detail in a report of the Montserrat Volcano Observatory (1998a). The construction materials of five different types of roofs were assessed, and it was predicted that spherical clasts with a density of 1g/m^3 and diameter of 10 cm falling with terminal-fall velocities from a sub-Plinian eruption would penetrate some roofs, and that clasts with diameters of 20 cm would have a 100% penetration rate. The assessment also examined the vulnerability of humans to the impact of falling clasts. It was predicted that serious skull injuries would be inflicted on people struck by clasts of 10 cm diameter (1g/m^3) falling with terminal velocities. A conservative clast diameter of 5cm was therefore used for preparing a risk map of Montserrat, based upon the modelling of tephra fall using the method of Carey and Sparks (1986) for a sub-Plinian eruption of similar size to that which had occurred on the island in September 1996.

Falling juvenile magmatic clasts can cause fires. To do so they must be sufficiently hot when ejected and large enough to retain their heat during passage through the air. This hazard is therefore greatest close to the site of eruption. During the 1973 eruption on Heimaey, buildings in the settlement situated 1.5 km from the vent were struck by blocks between 0.1 and 1.2 m in diameter which penetrated roofs and unprotected windows and caused fires (Blong, 1984). Extreme examples are the 1707 eruption of Fuji in which pumice fragments 20-30 cm diameter started fires on wooden roofs up to 10km from the vent, and the 1883 eruption of Krakatau where large pumice lapilli were still hot enough to burn holes in clothing 70-80 km from the vent.

Burial and loading is the most common and widespread hazard associated with tephra falls. It causes the collapse of roofs, the breakage of electrical power and telephone lines, and blocks drainage systems. During the eruption of Mount Pinatubo approximately 300 people were killed by roofs collapsing under the weight of tephra. The densities of tephra range from about 0.4-0.7 g/cm^3 for dry unconsolidated material to about 1 g/cm^3 for wet tephra (Blong, 1981a), although values of up to 1.25 g/cm^3 have been reported for moist tephra (Sarna-Wojcicki *et al.*, 1981). These densities equate with loads of between 40 and 125 kg/m^2 for every 10 cm depth of tephra depending upon the degree of compaction and moisture content. Flat roofs are more vulnerable to collapse than steeply pitched roofs which tend to shed their tephra loads. Wind may keep roofs clear of tephra, or alternatively produce drifts which cause uneven loading and asymmetrical stresses which result in structural damage. Rainfall aggravates the hazard by increasing the bulk density of the tephra. Rainfall also frequently occurs during pyroclastic eruptions and this can produce wet tephra fall or mud rain which is much more cohesive than dry tephra and can stick more easily to pitched roofs and be more difficult to remove.

Based upon the structural design of buildings and the strength of construction materials, it is possible to calculate the loading capacity of roofs and estimate the thickness of tephra likely to cause collapse. An engineering evaluation of this type was undertaken as part of the present study of Volcán Irazú (Section 6.4.5) and is described in detail by Young *et al.* (1998). The information from the evaluation was used to assess the vulnerability of the building stock and

to make recommendations for community preparedness. The same strategy was later applied in the risk assessment of Montserrat (Montserrat Volcano Observatory, 1998a) and has also been applied to Furnas volcano in the Azores by Pomonis *et al.* (1999) (see Section 4.4 of this report). Engineering approaches of this kind not only provide estimates of the weight or thickness of ash likely to cause collapse, but can also give indications of the manner in which structures might fail, so that roofs may be strengthened to withstand such effects. In the case of the Irazú study it was found that roof purlins were the most likely structural element to fail, and that tephra thicknesses of 40 to 80 cm could cause roof collapse.

In addition to loading factors, toxic ash can also weaken roofs by rapid corrosion due to adsorbed acid compounds, as documented for corrugated iron roofs in the vicinity of Irazú during the 1963-65 eruption (Young *et al*., 1998).

Heavy tephra falls can drastically affect drainage and irrigation systems. Thick deposits of permeable coarse ash and pumice can result in increased infiltration of rainfall into the ground and so reduce surface runoff, whereas fine impermeable ash promotes increased surface run-off, causing erosion, floods and lahars. River and irrigation channels usually become clogged by increased sediment loads produced by tephra falls and are no longer able to cope with floods and lahars which overtop their banks, often with devastating effects for adjacent areas.

Thick falls of tephra kill vegetation and even thin coatings can damage crops. Ingestion of ash can severely effect the health of animals, causing abrasion of teeth, gastrointestinal problems and poisoning (e.g. fluorosis). Burial of grazing land or the stunting of plant growth also results in the starvation of animals. The effect on pasture and animal health is illustrated by the 1991 eruption of Hudson volcano in southern Chile. Ash and pumice were dispersed downwind (to the east) to cover an area of 150,000km^2 of Argentine Patagonia, severely affecting water supplies and grazing which resulted in heavy sheep losses with devastating consequences for a region already in long-term economic decline (Financial Times, 17/9/93).

A striking example of the toxic effect of ash is that related to the eruption of Hekla in 1970 (Thorarinsson and Sigvaldson, 1972). The tephra contained very high fluorine contents reaching up to 2000 ppm, which caused acute fluorosis and deaths in thousands of sheep. It was found that tephra thicknesses of about 1 mm or less were sufficient to cause death in grazing sheep within a few days. The fluorine was believed to be in the form of HF which adhered to the tephra grains. There was thus more fluorine in fine grained tephra, and in addition the fine grained tephra adhered more efficiently to grass and was thus easily ingested by grazing animals. The fluorine was rapidly leached by rainfall and within about a month most areas were considered fairly safe for livestock.

Ash suspensions can severely affect health, particularly amongst people with pre-existing respiratory problems. This problem is aggravated in dry climates where secondary dispersion by wind may continue for prolonged periods after eruption. The health impacts of volcanic ash during the 1963-65 eruption of Irazú were investigated during the course of this project (Young *et al*., 1998). Effects included acute conjunctivitis and throat irritation which affected almost everyone, except those that protected themselves with masks and goggles, although these effects cleared up quickly once exposure ceased. Some people developed severe bronchitic symptoms, but most of these had pre-existing chest disease. The risk to health of

ash was also assessed for Montserrat (MVO, 1998a). This study looked at the risk of silicosis in communities exposed to ashfalls. Test showed that the respirable fraction of ash in the air (<10 microns) contained 10-24% cristobalite, a mineral considered to be several times more toxic than quartz (Baxter *et al*. 1999). The high concentrations occurred in ash produced by pyroclastic flows generated by lava dome collapses. The cristobalite was thought to have been produced by vapour phase crystallisation in the lava dome, and due to milling effects in the pyroclastic flows was preferential concentration within the very fine (respirable) fraction of associated ash clouds. Monitoring of ambient dust levels in the air suggested that levels of respirable ash, and thus cristobolite, were comparable to levels in metal mines where miners have developed silicosis, and in some communities the average levels of cristobalite in the air over 24 hours exceeded the occupational standard adopted for the USA. Although the toxicity of cristobolite is not fully understood, it was felt that silicosis could develop in the population if exposure to the measured ambient levels continued for a number of years.

Fine ash may also pollute supplies of drinking water and cause mechanical problems for pumping stations. Tephra suspensions in the atmosphere also reduce visibility and in large eruptions darkness may occur during daylight hours, causing fear and disorientation in people which may add to general confusion during evacuations.

Ash suspension can effect electrical supply systems in many ways by causing short circuits, and electrical storms that usually accompany tephra falls also result in lighting strikes to transmission systems. Lightning strikes are also a real hazard for people. The build-up of static electricity also disrupts radio communication and this can have serious consequences for the transmission of warnings and evacuation instructions to communities at risk. This latter point needs to be stressed, because the upper flanks of many volcanoes overlooking nearby cities are the sites of numerous radio and telecommunications antennae: In the event of even small eruptions, these telecommunication systems can become inoperable.

Fine particles suspended in the air also damages electrical equipment, machinery and vehicle engines, causing abrasion of moving parts and blocking filters. Heavy tephra falls can wreak havoc with transport by blocking roads and airports, and even relatively minor amounts of fine ash suspended in the air can disable vehicle engines. The potential disruption of communications and transport by tephra fall is therefore a factor that must be taken into account in devising evacuation and contingency plans.

Tephra in the atmosphere poses a serious hazard to air transport. Casadevall (1994a) indicated that more than 80 jet aircraft had been damaged by unplanned encounters with volcanic ash in the 15 years preceding 1994. In seven of these cases this caused in-flight loss of jet engine power, which almost resulted in crashes, putting more than 1,500 passengers at severe risk. Two of the worst encounters occurred over Java in 1982 when on separate occasions Boeing 747 airliners flew into ash plumes from Galunggung volcano, resulting in the complete failure of all four engines, which were only re-started after the planes had descended more than 20,000 feet. A similar incident occurred when a Boeing 747 airliner approaching Anchorage in Alaska flew into an ash plume downwind of the eruption of Redoubt volcano in 1989. This also caused failure of all four engines and the damage to the aircraft was estimated to have been US$80 million. For a detailed appraisal of the hazard of volcanic ash and aviation safety the reader is referred to a comprehensive volume on the subject by Casadevall (1994b).

Although tephra falls pose the most widespread of volcanic hazards, their detrimental effects can be mitigated quite effectively by planning and preparation. Buildings may be designed or strengthened to withstand the loads imposed by tephra, and during eruptions deposits may be cleared from roofs and from roads as they accumulate. Tephra may be removed from the ground or stabilized to reduce the hazardous effects of reworking by wind or by floods and lahars. Vehicles and other machinery may be protected by the design and installation of more efficient filters, and the inhalation of fine ash and gases by people can be reduced by wearing respirators, masks or damp cloths over mouths and noses.

In the case of air safety, much is now done to avoid the hazard of ash. Aviation authorities should be informed of explosive eruptions, so that air traffic can be re-routed to avoid potential problems. In many regions, systems have been set-up by volcano observatories, meteorologists and air traffic controllers to provide timely warnings for the aviation industry of volcanic eruptions and the movement of hazardous ash clouds. Details of wind directions and speeds may be used to predict the migration of ash clouds and weather satellites can be used to track their actual progress, so providing valuable information for air traffic controllers. The satellite surveillance of ash clouds is undertaken by a number of Volcanic Ash Advisory centres distributed around the globe, coordinated under the National Oceanic and Atmospheric Administration (NOAA) of the United States Department of Commerce (see internet site: http://hpssd1en.wwb.noaa.gov/VAAC/).

5.2.3 Hazard zoning for pyroclastic falls

Hazard assessment for tephra falls are applied on two different time scales. The majority of assessments are for long-term planning purposes, but when an eruption is imminent or in progress, more refined short-term assessments or forecasts may be made which take into account the actual wind regime, size of the eruption and height of the eruption column. Simple models exist (e.g. Hurst, 1994) and more complex models are being developed for near real time prediction of ash cloud dispersal and tephra fallout, as for example in the case study of Volcán Irazú (Young *et al*., 1998) undertaken as part of the present project. The following account however is concerned only with methods of hazard zoning for long-term planning purposes.

The hazards and risks associated with tephra are proportional to the amount of material that falls and they decrease downwind, away from the volcano. Tephra fall hazard ***zoning*** schemes are usually based upon the thickness distribution of older deposits. The choice of thickness values for delimiting hazard zones should ideally be related to the physical effects of tephra on buildings, crops, health and other elements. In reality this is difficult to achieve because each element of the environment and infrastructure has a different tolerance for ash, making it impossible to equate the specific risks posed to each by given amounts of tephra: For example, tephra falls that may be insufficient to damage buildings could destroy crops and livestock and have serious effects on human health. Tephra hazard zones therefore usually portray decreasing relative risk with distance from source, but do not specify the degree of risk applicable to specific elements of the infrastructure. If, however, hazard zones need to be delimited for a single purpose (e.g. building vulnerability) this can be achieved by using tephra thickness values that have known significance to the specific risk being assessed.

The thickness of tephra falls is governed by the volume of material erupted, the height of the eruption column, and on wind direction and strength. Hazard assessments for tephra fall are therefore usually based upon the extent and thickness distribution of previous fall deposits considered in relation to regional wind patterns obtained from meteorological records.

As a first step to the hazard assessment of tephra fall it is important to recognise and map the extent and thickness of existing deposits. On volcanoes that have produced numerous tephra falls, detailed investigations of the deposits combined with information on their age (obtained from historical records and radiometric dates) can be used to place probability constraints on the thickness and frequency of tephra falls. In assessing older deposits the effects of erosion and compaction should be born in mind, but even then the magnitude of a past eruption may be underestimated by failure to recognise the true extent of a deposit. This latter point is illustrated by numerical modelling of the distribution of tephra fall from the 1982 eruption of El Chichon, Mexico (Carey and Sigurdsson, 1986), which indicated that the observed volume of tephra fall only represented about half of the volume that was actually erupted, leading to the conclusion that up to one half of the erupted mass was deposited elsewhere as highly dispersed tephra.

Hazard assessments based upon the distribution and thickness of older tephra deposits combined with data on wind direction and wind strength are exemplified by hazard zoning schemes for Mount St Helens (Crandell and Mullineaux, 1978) and for Rabaul in New Britain (McKee *et al.*, 1985). The salient features of these two schemes are as follows.

At Mount St Helens, tephra fall hazard zones (Figure 5.6) were based upon the extent of three older tephra deposits combined with information on the regional wind regime. The three deposits have volumes of about 0.01, 0.1 and 1 km^3 and were chosen as being representative of small, moderate and large tephra eruptions from Mount St Helens. From records of the volcano's eruptive history it was estimated that small eruptions occur at an average rate of one per 100 years, moderate eruptions one per 500-1,000 years and large eruptions once every 2,000-3,000 years. To the east of the volcano the boundaries of three hazard zones were placed at 30, 100, and 200 km from source. These intervals were chosen because the thicknesses of the three selected tephra deposits at these distances are relatively well-known (Figure 5.6c); the thicknesses at these distances do not however have any special significance with respect to vulnerability.

Meteorological data for the Mount St Helens region indicate that strong winds blow towards the east and northeast for about 50% of the year, and generally eastwards for more than 80% of the time. Fallout patterns from past eruptions reflect this, with more than 90% of all known tephra deposits from Mount St Helens lying to the east of the volcano. Because strong winds rarely blow towards the west, and because the older tephra deposits are of limited extent on this side of the volcano, the hazard zone boundaries on the western side were arbitrarily delimited at 25% of the distances of the boundaries to the east.

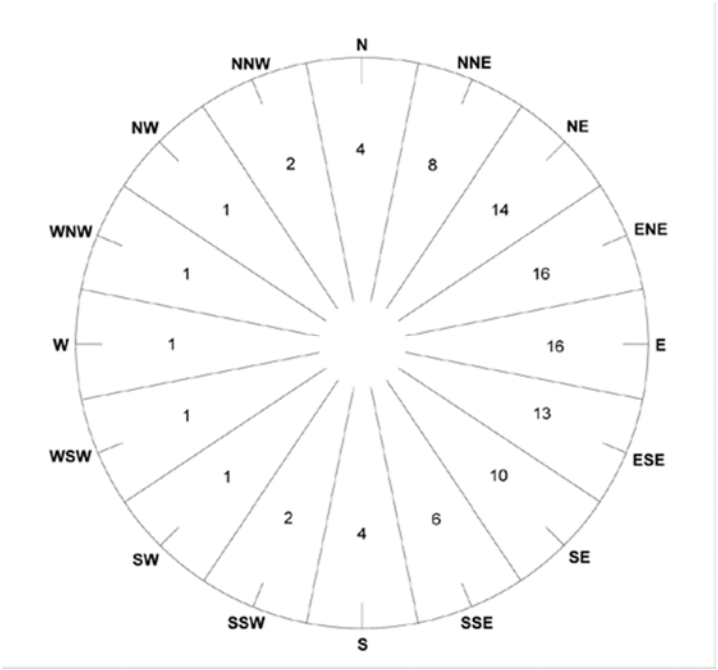

Figure 5.6a: Approximate percentage of time, annually, that the wind blows toward various sectors in western Washington. Percentages are rounded averages of frequencies determined at various altitudes between 3000 and 16000m at Salem, Oregon., and Quillayute, Washington. (After Crandell and Mullineaux, 1978).

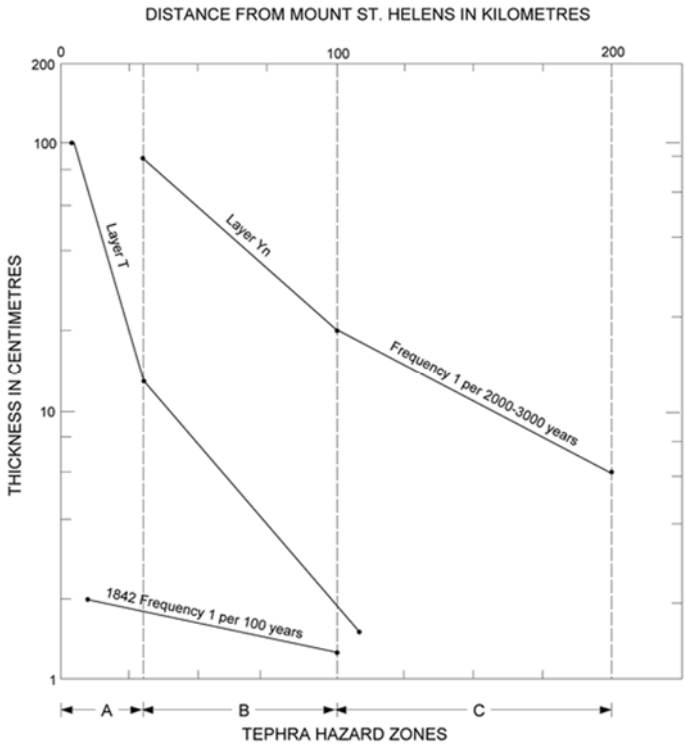

Figure 5.6b: Relationship between distance downwind from Mount St Helens and estimated average present thickness of tephra along the thickest parts of the lobes. The tephra layers may have been as much as twice as thick as shown here when they were deposited. The lines represent three tephra deposits of different volumes: layer Yn, layer T and an unnamed layer formed in 1842. These are estimated to have volumes, respectively, on the order of 1km, 0.1km and 0.01km. The expectable frequencies of similar eruptions in the future are based on the eruptive behaviour of Mount St Helens during the last 4500 years. (After Crandell and Mullineaux, 1978).

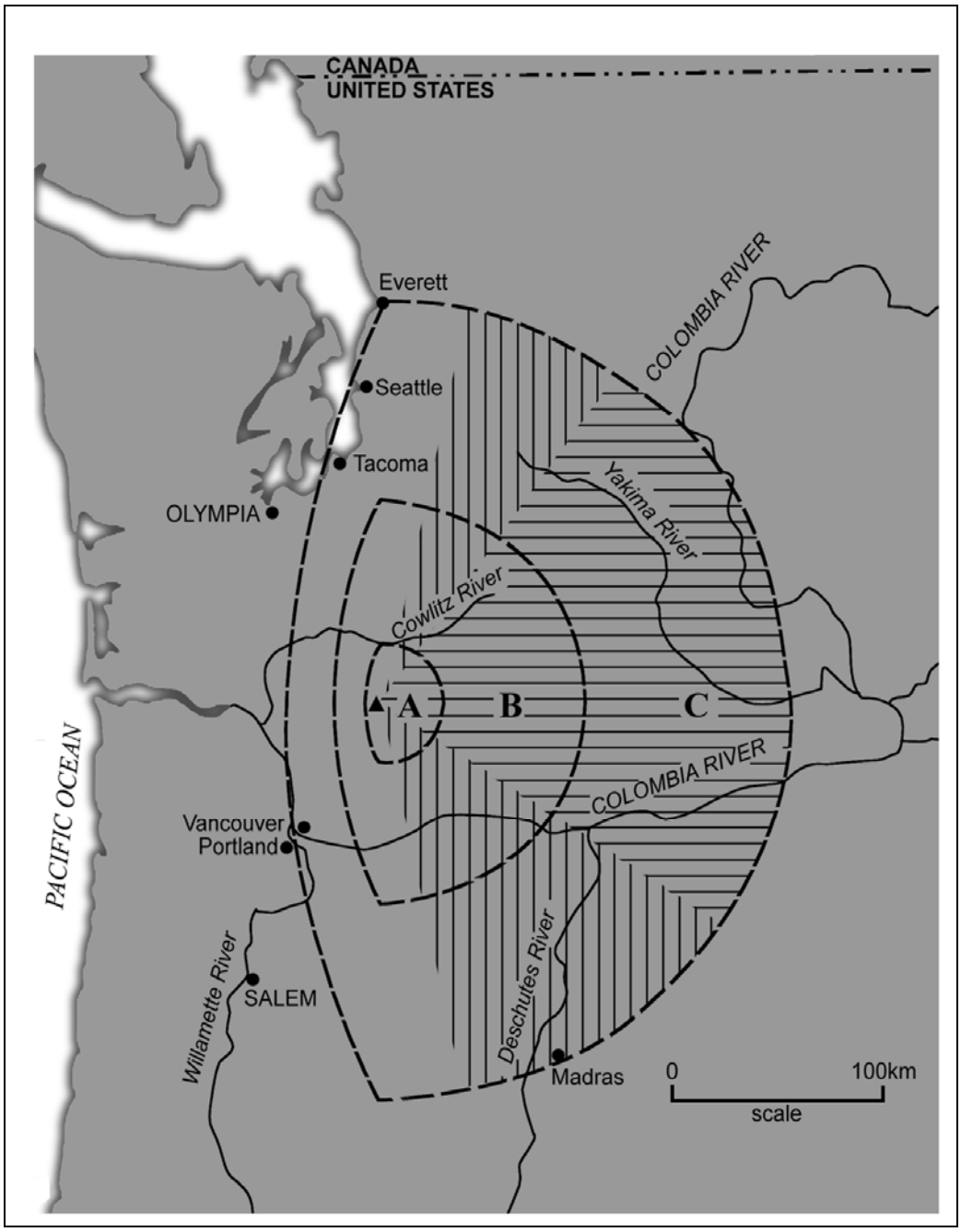

Figure 5.6c: Tephra hazard zones for Mount St Helens (after Crandell and Mullineaux, 1978). Potential thickness is greatest in zone A, and progressively less in zones B and C, (compare Fig. 5.6a,b). In each zone, potential thickness decreases outward with distance from the volcano. Winds blow from the volcano to the sectors shown by horizontal lines about 80 percent of the time, and toward the vertically lined sector about 50 percent of the time. These sectors therefore include the areas in which tephra will fall most frequently during future eruptions.

At Rabaul volcano airfall tephra hazard zones have also been based upon the analysis of wind data and the thickness distributions of older tephra deposits, but in addition take cognisance of computer models of idealised tephra fall distributions (McKee *et al.*, 1985). Two deposits were selected to represent the products of eruptions of contrasting size and frequency. These are the tephra fall deposit of the 1937 eruption (Figure 5.7) which was of small to moderate size, and the deposit of a moderate to large size eruption that occurred about 1,400 years BP (Figure 5.8). Separate hazard maps were produced for each scale of eruption and these have strikingly different hazard zone patterns which reflect contrasting wind directions at different levels in the atmosphere.

Small to moderate size eruptions at Rabaul are presumed to be relatively frequent. Four hazard zones were delimited for eruptions of this size (Figure 5.7). An innermost zone (A) includes an elliptical area in which eruptions are likely to take place, augmented by a 2 km wide marginal zone subject to the impact of ballistic pyroclasts. Three outer zones (A_s, B_s and C_s) take into account the dispersal effect of prevailing winds at low altitudes shown in the wind rose of Figure 5.7. These zones have double fan-shaped segments, whose radial axes are parallel to the two dominant seasonal wind directions. The radial boundaries of zone A_s include 95% of the wind directions in the season of the southeast trade winds and 87% of the wind directions during the monsoon season. The radial boundaries of zones B_s and C_s diverge by an additional 15° and 30° respectively from those of zone A_s to account for lateral wind shear. The outer arcuate boundaries of the three zones were set at distances of 9, 15 and 60 km downwind, corresponding to thicknesses of 20, 10 and 1 cm of tephra fall from the 1937 eruption. These thicknesses do not have any specific risk implications, although McKee *et al.* (1985) indicate that a thickness exceeding 20 cm is likely to cause widespread collapse of buildings.

For moderate to large eruptions three hazard zones (A_L, B_L and C_L) were delimited at Rabaul (Figure 5.8). These are mainly located to the west of the volcano, reflecting the overwhelming predominance of easterly winds at high altitudes in the region (see wind rose of figure 5.8). These zones are based upon mapping of the 1,400 BP fall deposit, but also take into consideration the results of computer modelling of idealised tephra fall patterns for 10 and 20 km high eruption columns. These idealised distributions were computed using three different physical models which take into account the effects of lateral wind shear as outlined by Blong (1981b). The outer limits of the three hazard zones were delimited at distances of 40 km (A_L), corresponding to a thickness of 20 cm for the 1,400 BP deposit, at 60 km (B_L) corresponding to 10 cm of ash, and at 100 km (C_L). Upwind spreading was estimated by arbitrarily taking the eastern limits of each zone at 25% of the distance of the western limits, as used in the hazard zoning scheme at Mount St Helens (see above).

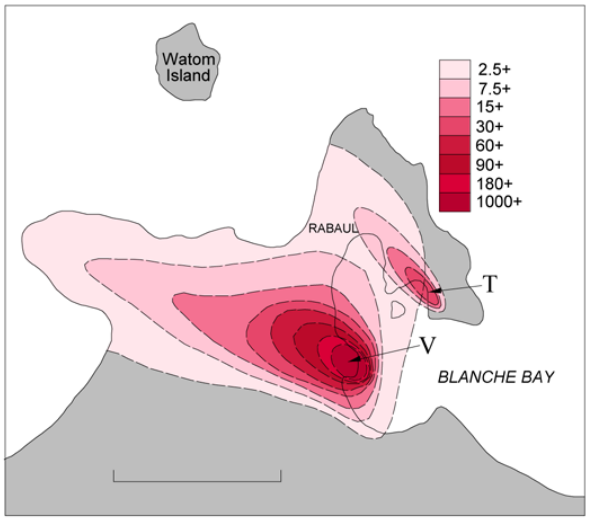

Isopachytes (in cms) showing the thickness distribution of tephra from the small-moderate 1937 eruption of Rabaul, from the vents of Vulcan (V) and Tavurvur (T) .(After McKee et al., 1985)

Rose diagram for low-level Rabaul winds from the surface to an altitude of 3.1kms, showing the percentages of time each year that the wind blows towards 16 sectors of the compass. Numbers in each sector are maximum wind velocities in knots, followed by average velocities in brackets. (After McKee et al., 1985)

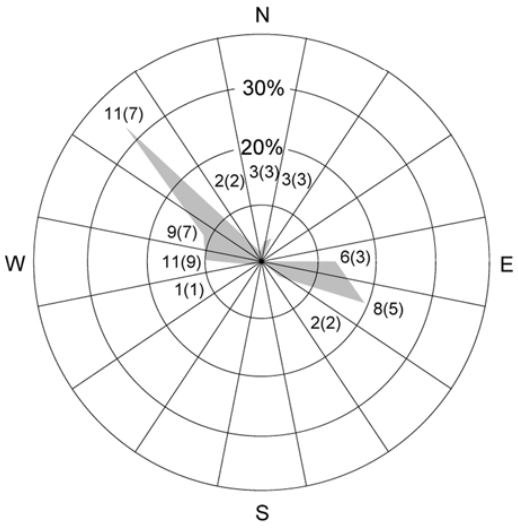

Tephra fall hazard zones for small-moderate size eruptions at Rabaul. (See text for explanation). (After McKee et al., 1985)

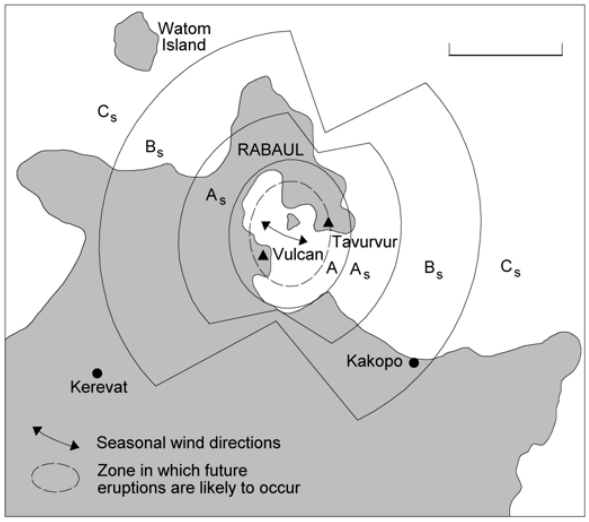

Figure 5.7: The hazard of tephra fall at Rabaul from small to moderate size eruptions.

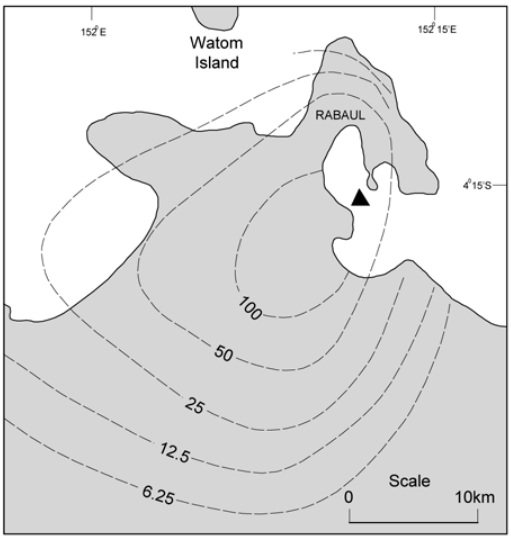

Isopachytes of tephra produced from the moderate-large eruption of Rabaul approximately 1400y B.P. (thickness in cms). (After Walker et al., 1981)

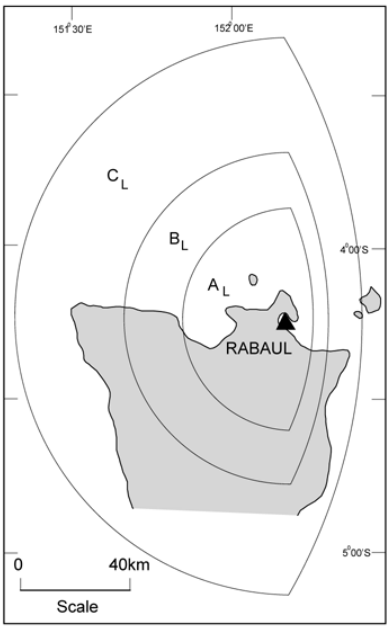

Tephra fall hazard zones for moderate-large size eruptions at Rabaul (see text for explanation). (After McKee et al., 1985)

Rose diagram for high-level winds at Rabaul, between 4.4 and 17.8kms above sea level, showing the percentages of time each year that the wind blows towards 16 sectors of the compass. Numbers in each sector are maximum wind velocities in knots, followed by average velocities in brackets. (After McKee et al., 1985)

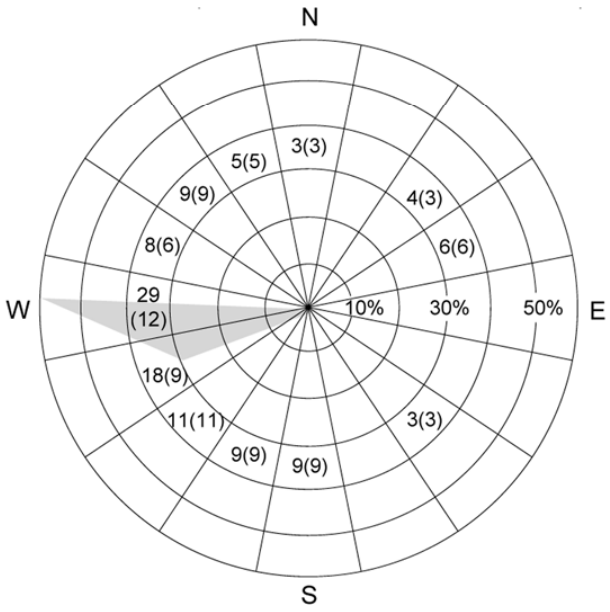

Figure 5.8: The hazard of tephra fall at Rabaul from moderate to large size eruptions.

Hazard maps for airfall tephra from volcanoes which do not produce high eruption columns nor large volumes of fine ash tend to concentrate on the proximal effects of impact and loading damage. An example from Volcán Villarrica in Chile (Young, 1998) provides a methodology for producing a conservative hazard map, based upon the maximum thickness and maximum clast size recorded from tephra units from a number of localities around the volcano; the two measurements do not need to be from the same deposit at a given location. Isopach and isopleth maps drawn from these data record the event which produced the thickest and coarsest deposit at any single location, and thus can be regarded as maxima for future eruptions.

In addition to the more usual 'empirical' approach to tephra fall hazard assessment described above, theoretical numerical modelling has also been used to predict tephra fall distributions. For example, Armienti *et al.* (1988) computed tephra fall patterns for the 1980 eruption of Mount St Helens and Macedino *et al.* (1988) for the 79 AD eruption of Vesuvius, both of which closely conformed with the distribution of the actual deposits.

Given the success of their numerical model, Macedonio *et al.* (1990) applied the technique to a potential future eruption at Vesuvius. From an analysis of the size and style of past eruptions and of the repose time between eruptions at Vesuvius it was estimated that the next eruption is likely to be of ultrastrombolian or subplinian style with an estimated maximum mass discharge of about 2×10^{11} kg and mass discharge rate of between 0.4 and 0.2×10^{7} kg/s. Numerical modelling based upon this mass discharge rate, but also taking additional assumptions into account on gas content, lithic clast content and column diameter, predicted a maximum height of 11-16 km for the eruptive column. Further numerical modelling, taking into account seasonal wind velocity profiles and assuming pyroclast properties similar to those of ancient vesuvian tephra deposits, was used to compute tephra fall distribution patterns. This resulted in a series of maps showing predicted tephra fall distribution patterns for eruption columns varying in height between 11 and 16 km under different seasonal wind regimes. The computed distributions were presented using lines of isomass (kg/m^2), which have direct application in assessing the loading effects of tephra on buildings. In an extension to this numerical modelling study, Barberi *et al*. (1990) combined the fallout model for Vesuvius with a statistical analysis of wind patterns and the density of urban settlement to obtain a quantitative assessment of the risk of building collapse in the vicinity of the volcano (see Section 4.2).

The reliability of the results of numerical modelling are strongly dependent upon a number of input values and assumptions, the most crucial of which are mass discharge, mass discharge rate and gas content. Macedonio *et al.* (1990) acknowledge that the prediction of these values is strongly dependent upon a knowledge of the eruptive history of the volcano and of the nature and distribution of its deposits, which in the case of Vesuvius are relatively well understood. Nevertheless, because of uncertainties in volcano behaviour and eruption dynamics in general, such models should not be applied to hazard and risk assessment in a too deterministic or restrictive manner.

5.3 Pyroclastic Flows and Surges

Pyroclastic flows are hot density currents consisting of mixtures of rock debris and gas which flow along the ground at high speed under the influence of gravity. They are generally controlled by topography and tend to flow down topographic gradients along valleys and depressions, although examples are known of prehistoric flows that were sufficiently energetic to flow across topography and surmount obstacles such as ridges or mountain ranges.

Pyroclastic surges are turbulent, low-density mixtures of gases and solid particles which flow close to the surface at high velocity, but differ from pyroclastic flows by containing a much lower proportion of solid particles and by being less dense. They are generally grouped into hot surges and cold surges, reflecting two contrasting modes of formation. Hot surges, which are also referred to as dry surges, are closely associated with pyroclastic flows and form by similar mechanisms. Cold surges, also known as wet surges, are associated with hydrovolcanic activity and are described separately in section 5.4.

Pyroclastic flows and hot surges are common during explosive eruptions of andesitic, dacitic and rhyolitic volcanoes, and they also occur at trachytic and phonolitic centres. They are the most dangerous of the more common volcanic hazards, because of their high temperature, high velocity and high mobility.

5.3.1 General characteristics of pyroclastic flows

Pyroclastic flows are made up of two main components. The main body consists of a dense basal part composed of fluidised rock fragments and ash which travels along the ground. This is overlain and also preceded by a turbulent ash cloud elutriated from the basal flow. Pyroclastic surges may also develop as a third component from the overriding ash cloud and also at the margins of pyroclastic flows. Flow is largely maintained by the process of fluidisation, caused by expanding and escaping gases which originate from several sources. These include magmatic gases released from pyroclasts, air entrapped during the formation and advance of the flow which expands on heating, volatiles produced by the incineration of vegetation incorporated into the flow, and the vaporisation of surface water, snow and ice.

Small pyroclastic flows have been observed to travel for distances of up to 20 km from source at speeds of over 200 km/hr. Studies of prehistoric deposits on the other hand indicate that some large pyroclastic flows have travelled distances exceeding 100 km, and theoretical analysis based on the heights of topographical barriers surmounted by such flows indicate that velocities may exceed 100 m/sec and in extreme examples may even exceed 200 m/sec (720 km/hr) (e.g. Wilson, 1985).

Temperatures measured directly or estimated indirectly by various methods indicate that the deposits of pyroclastic flows are generally emplaced at temperatures ranging between 200 and 800°C.

Pyroclastic flows are generated by two main mechanisms. These are the gravitational collapse of vertical eruption columns (Figure 5.9) and the structural or explosive collapse of lava domes or lava flow fronts on the steep slopes of volcanoes (Figure 5.10). Secondary pyroclastic flows may also be produced on steep slopes when primary pyroclastic deposits that are still hot are destabilised and remobilised by phreatic explosions caused by the infiltration of groundwater. After large pyroclastic eruptions in wet climates this process may continue for some time, as for example at Mt. Pinatubo in the Philippines, where secondary pyroclastic flows were a hazard for several years following the eruption in 1991.

5.3.2 Pyroclastic flows formed by the collapse of eruption columns

Pumice-rich pyroclastic flows, or pumice flows as they are also known, consist of hot fluidised mixtures of pumice lapilli and ash which form during the vigorous eruption of gas-rich magmas from volcanic vents. They are commonly produced when substantial quantities of pumiceous pyroclastic material fall out of the overloaded parts of continuous or semi-continuos eruption columns sustained by gas streaming (Sparks and Wilson, 1976). Small-scale collapses also occur when short explosions eject dense slugs of pyroclastic material to altitudes of a few hundred metres, which then fall back to the ground.

As pyroclastic material falls back to the ground its potential energy gained during ascent is converted into kinetic energy, and through the entrainment of hot gases and air it becomes fluidised and produces pyroclastic flows which move radially away from source as density currents. The mobility or energy of such pyroclastic flows is therefore a function of the height of the eruption column from which the material falls: Large eruptions with sustained and high discharge rates tend to produce high eruption columns and hence larger and more energetic pyroclastic flows.

Large volume pumiceous pyroclastic flows produced by the collapse of high and sustained eruption columns can travel at very high velocities and surmount major topographical barriers. Fortunately events of this magnitude appear to be relatively uncommon and have not occurred historically, although many examples are known from the geological past. Such pyroclastic flows can affect hundreds or even thousands of square kilometres, and would be very difficult to mitigate against, except by the evacuation of large areas, assuming sufficient warning could be given.

Small pyroclastic flows generated by the collapse of eruption columns are quite common at volcanoes of intermediate and silicic compositions. Because they are less energetic their passage is controlled by topography and they become channelled into valleys and depressions as they flow down the volcano's flanks. Pyroclastic flows of this kind are sometimes termed **Soufrière type** after the volcano on the island of St Vincent in the West Indies where 2,000 people were killed in 1902 by such a flow. Pyroclastic flows of this type have accompanied the current eruption of Montserrat, where as many as 85 column-collapse events were recorded between August and October 1997. Mt. Mayon in the Philippines is another volcano where pyroclastic flows of this type are prevalent and hazardous in historic times, and from where good eye witness descriptions have been provided by Moore and Melson (1969).

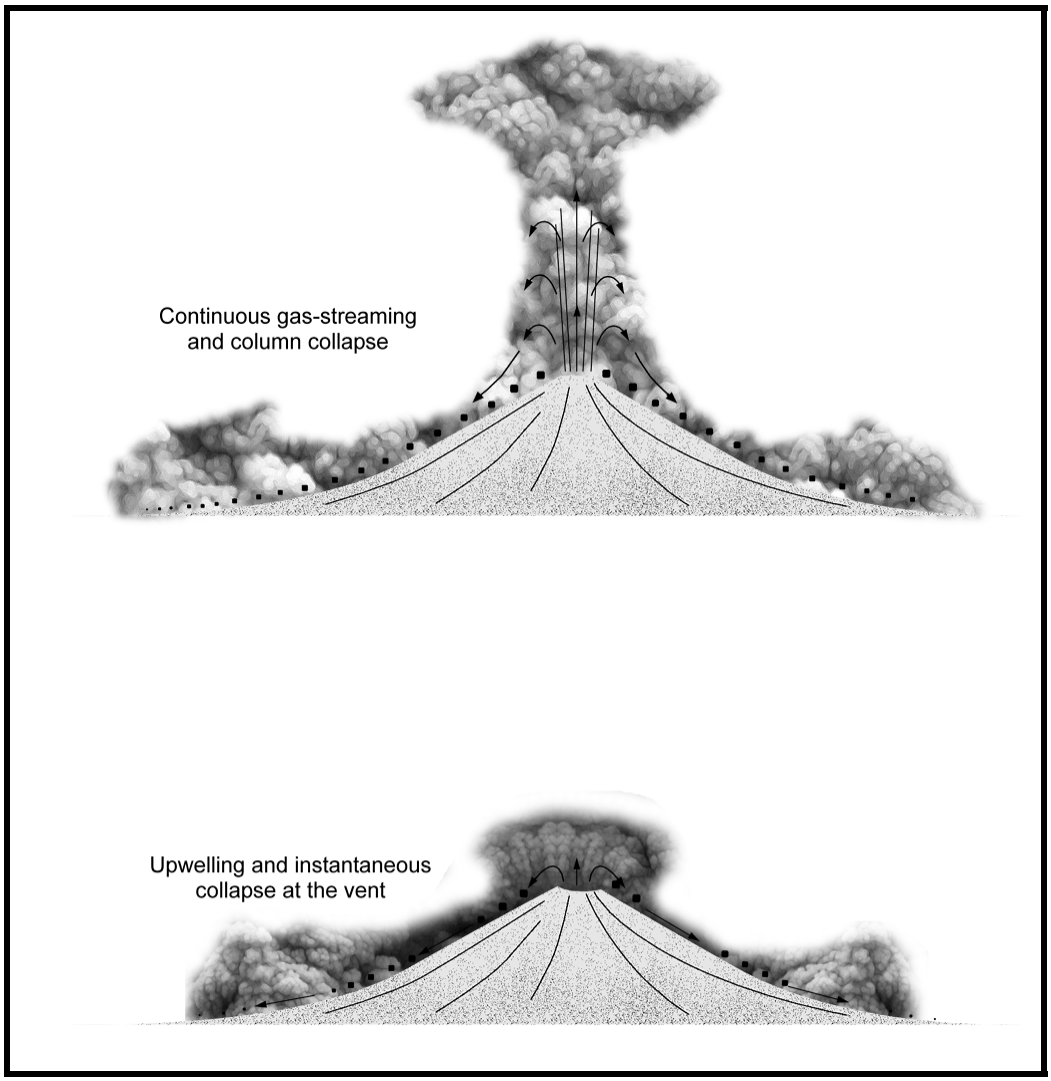

Figure 5.9: Generation of pyroclastic flows by the collapse of eruption columns.

At the lowest end of the energy spectrum eruptive columns may collapse almost immediately without gaining significant height, generating low energy pyroclastic flows which spill over the margins of the vent. The 1877 eruption of Cotopaxi exemplifies this type of eruption and has been likened to the spilling-over of a pan of boiling rice.

5.3.3 Pyroclastic flows formed by the collapse of lava domes or lava flow fronts

Pyroclastic flows composed of lava fragments form when actively growing lava domes or lava flows extruded high on the flanks or summit areas of steep-sided volcanoes become unstable and collapse. Collapse may be triggered simply by gravitational instability, or by blasts caused by the explosive release of gases. The rapid unloading and release of pressure within a lava dome due to an initial gravitational collapse can also lead to explosive collapse, so that both processes may operate almost simultaneously. As the hot rock debris avalanches down slope it breaks up and becomes fluidised to produce pyroclastic flows, which are usually channelled into valleys.

Pyroclastic flows generated in this way are termed **block-and-ash flows** because they form deposits composed mainly of lava blocks mixed with finer dust or ash. They are also referred to as **glowing avalanches** or **nuée ardentes**. These typically produce deposits of small volume, sometimes only consisting of a veneer of blocks strewn on the flanks of the volcano; even numerous separate flows accumulated from the same eruption typically have volumes of much less than 1km^2. They are nevertheless very hazardous on account of their high temperature and the speed at which they travel, as illustrated by the following examples.

Pyroclastic flows produced by the **gravitational collapse** of lava domes or lava flow fronts on steep-flanked andesite-dacite volcanoes are often called **Merapi-type pyroclastic flows** after the Javanese volcano where this type of activity is prevalent (Figure 5.10). Pyroclastic flows of this kind are well-documented from Unzen volcano in Japan (Nakada and Fujii, 1993) and from the recent activity at Montserrat (Cole *et al*., 1998).

Unzen had lain dormant for almost two hundred years when seismic activity began late in 1989. Minor ash emissions started at the end of 1990 and in May 1991 a high-silica dacite dome began to be extruded into one of the summit craters on the steep-sided cone of Fugen-dake. The dome grew rapidly and within a few days extended several tens of metres above the crater rim when material began to spall off its unstable margins and avalanche down the steep flanks of the cone. Over the ensuing months several domes grew and collapsed, so generating many hundreds of pyroclastic flows which were channelled along valleys to the east and northeast for distances of up to 5.5 km (Figure 5.11). This activity combined with heavy rainfall also generated mudflows which extended to distances of 7.5 km along the valleys. Damage to property within the Mizunashi valley on the east flank was significant, but loss of life was kept to a minimum by the prompt evacuation of the population. However, on 3 June a large mass of lava (about 0.5 million m^3) collapsed from the dome and generated a pyroclastic flow that moved down the Mizunashi valley into the settlement of Kita-Kamikoba, killing 42 people, including journalists and several volcanologists who had entered the evacuated zone. The main body of the pyroclastic flow travelled for a distance of 3.2 km through a vertical drop of 1,000 m, and from this flow an ash-cloud surge detached itself and travelled an additional 0.8 km, knocking down trees and burning houses but leaving a deposit only 30 cm thick. It was this surge that was responsible for the casualties, many of whom died of burns. In the weeks that followed similar surges were associated with other large pyroclastic flows, which produced zones of searing of vegetation along the margins of the flows.

Pyroclastic flows generated by the explosive collapse of lava domes are sometimes called **Peléean-type**, after the volcano of Mont Pelée on the island of Martinique where numerous pyroclastic flows or nuée ardentes were produced in 1902-03 and 1929-32.

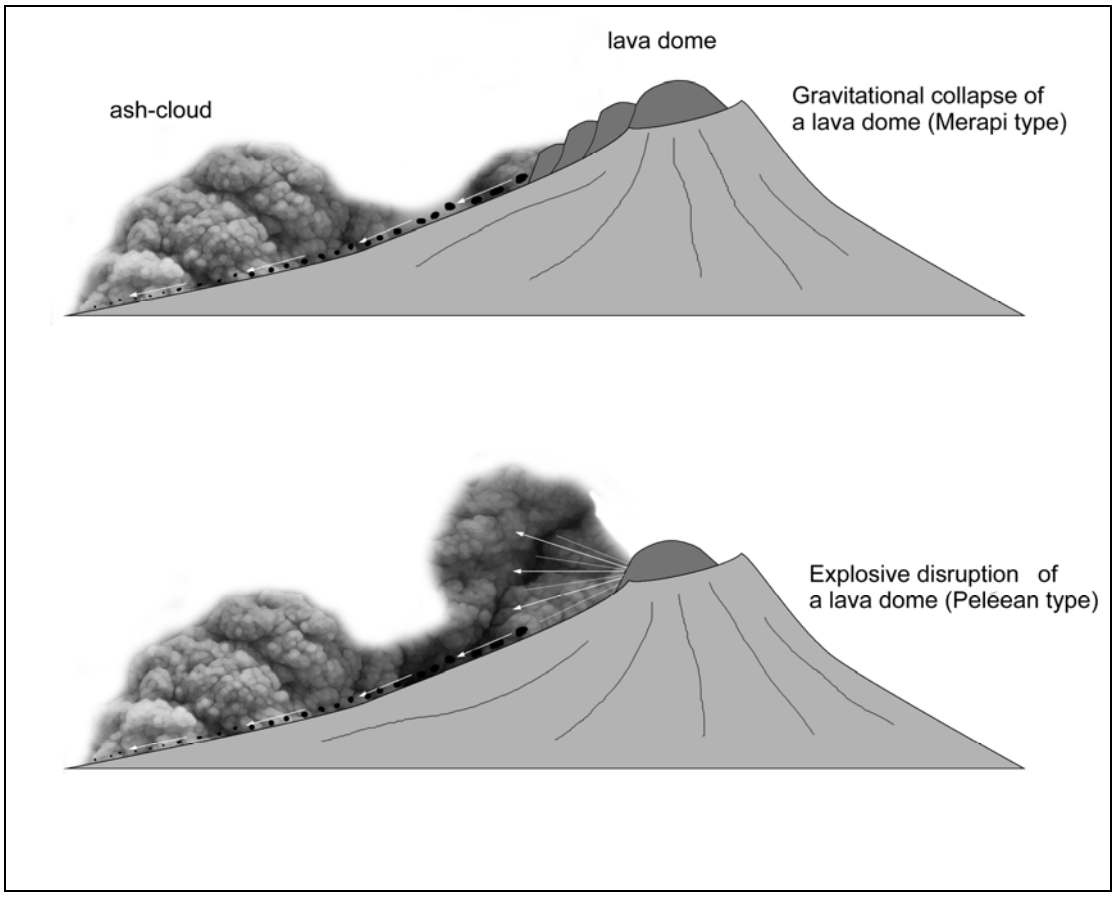

Figure 5.10: The generation of block-and -ash pyroclastic flows during the growth of silicic lava domes. The pyroclastic flow in the strict sense is a basal density current with a high concentration of rock particles, from which the overriding low-density ash-cloud is elutriated. Separation of the ash-cloud from the main body of the pyroclastic flow may result in the formation of an ash-cloud surge.

5.3.4 Hot pyroclastic surges

Hot pyroclastic surges are genetically related to pyroclastic flows, but are more dilute, less dense and turbulent, and therefore tend to be more mobile.

Pyroclastic surges occur in intimate association with pyroclastic flows, but they may also occur alone. Like pyroclastic flows they are generated during the collapse of eruption columns and also by the gravitational and explosive collapse of lava domes. In the case of the explosive destruction of lava domes they may form an integral component of laterally directed blasts (Section 5.5), although the distinction between these two phenomena is somewhat vague and arbitrary. Surges associated with pyroclastic flows tend to precede the main body of the flow in advance of the flow front and are termed **ground surges**. Additionally, **ash-cloud surges** may segregate from the overriding ash clouds which are elutriated from the denser basal part of pyroclastic flows.

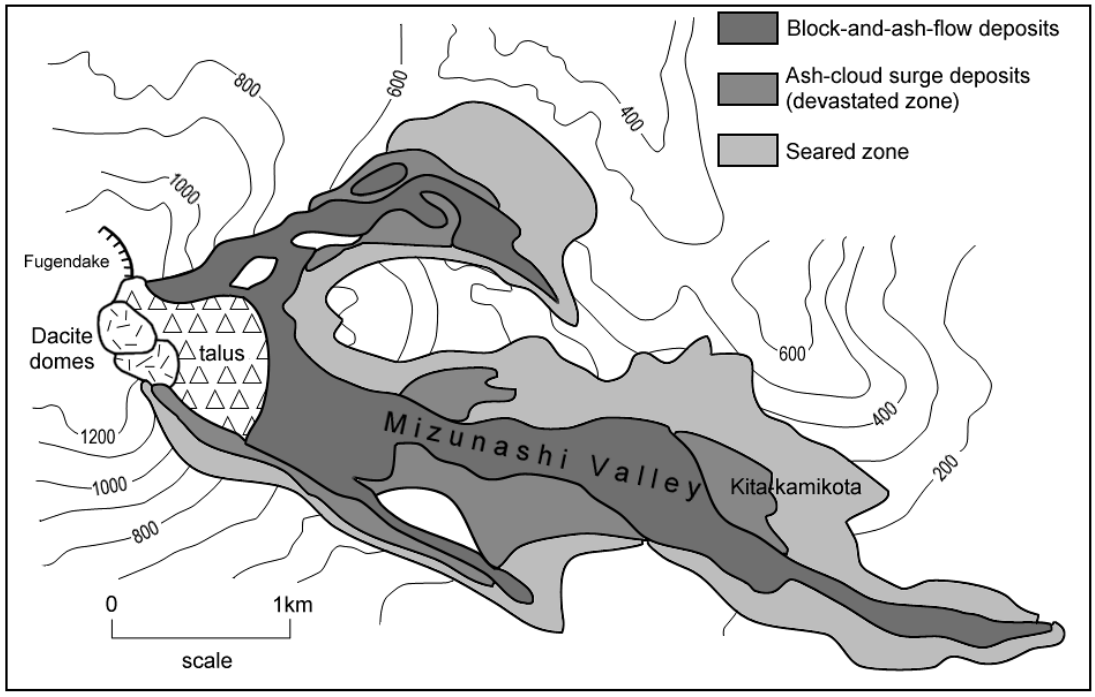

Figure 5.11: Map showing the distribution of block-and-ash flow deposits, ash-cloud surge deposits and seared zones produced by pyroclastic flows generated by the collapse of dacite domes on Mount Unzen between November 1990 and early September 1991. (After Nakada and Fuji, 1993). Note the more extensive distribution of surge deposits and searing compared with the block-and-ash deposits that are confined to the valley floors.

Although pyroclastic flows are mainly controlled by topography, the less dense surges associated with them are much more mobile and may sweep across topographical features, affecting areas high on valley sides and interfluves. When pyroclastic flows change direction due to topographic influences, such as sharp bends in valleys, the more dilute, less dense surges associated with them may become detached and continue along their original paths regardless of topography. Seared zones often border the areas affected by pyroclastic flows and are attributed to hot surges, as exemplified by the 1991 block-and-ash flows at Mt. Unzen (Nakada and Fujii, 1993), where seared zones extended for several kilometres beyond the limits of the pyroclastic flows (Figure 5.11) In such zones, vegetation is scorched and animal life rarely survives.

The most infamous disaster believed to have been caused by a surge occurred at Mont Pelée on Martinique in 1902. The volcano had been producing pyroclastic flows by the explosive collapse of an actively growing dacite dome, and during one such eruption on 8 May the town of St Pierre, situated 8 km from the summit of the volcano, was destroyed and all but two of its inhabitants of 28,000 people were killed. The exact nature of the catastrophe that befell St Pierre has been much debated. Eye-witness accounts describe a series of explosions following which the town was engulfed by a hot cloud. Fires were started and glass objects deformed plastically, testifying to the heat of the cloud, and structures were flattened or shifted by its force, but only a thin layer (<10 cm) of fine ash was deposited over the town. A widely held theory is that a block-and-ash pyroclastic flow was channelled down the valley of the Rivièr Blanche, located a few kilometres to the west of the town. From this a low-

density ash-cloud surge developed as the coarser and denser clasts segregated by gravitational settling into the basal part of the flow (Fisher *et al*., 1980). The overriding low-density ash cloud expanded and detached itself from the denser and less fluidised basal part of the flow, to produce a hot ash-cloud surge which moved across the topography at great speed to overwhelm St Pierre.

The recent activity at Montserrat provides a useful insight into the relationship between block-and-ash flows and surges produced by the collapse of lava domes. One of the main features of the eruption has been the growth of an andesitic lava dome within the summit crater of the volcano, from which numerous small to moderate size block-and-ash flows have been generated by avalanches of hot rock spalling off the unstable margins of the dome. In general surge activity does not appear to have been associated with these small-scale non-explosive pyroclastic flows. However, following a period of very rapid dome growth, a major collapse of part of the old crater wall (Galway's Wall) occurred on 26 December 1997. Initially this produced a debris avalanche composed of hydrothermally altered crater wall material, but was rapidly succeeded by a large collapse of the destabilised portion of the lava dome, which had previously been retained by the crater wall. Collapse of the dome produced pyroclastic flows and very intense and devastating pyroclastic surges which are thought to have been associated with one or more explosive blasts. This devastated a large sector on the south-west flanks of the volcano, causing extensive damage to housing by dynamic impact and heat: In many cases houses were completely removed, leaving only concrete foundation pads. A previous large-scale dome collapse in September 1997 had also produced explosive pyroclastic flows and at least one directed blast. It is generally thought that the more frequent small-scale rock falls off the margins of the dome only involve degassed and largely solidified lava, which produces non-explosive block-and-ash flows. On the other hand, when large portions of the dome have collapsed, as in September and December 1997, the very hot and gas-rich interior of the dome has been unroofed, possibly exposing the feeding conduit, resulting in sudden explosive decompression of gas and the production of explosive pyroclastic flows and surges.

The largest and most extensive pyroclastic surges are produced by the collapse of eruption columns. If the volcano itself is symmetrical and surrounded by relatively flat terrain, the surges tend to move out radially from the base of the collapsing column and flow to approximately the same distance in all directions. At asymmetrical volcanoes, or where the surrounding terrain is irregular, surges tend to be deflected and channelled by topography, and therefore flow farther in some directions than in others. Well-known examples of pyroclastic surges associated with the collapse of eruption columns are those of the 1951 eruption of Mount Lamington in Papua New Guinea, and of the 1982 eruption of El Chichón in southern Mexico, both of which resulted in major loss of life. Mount Lamington had not previously been recognised as a volcano, but after only a few days of precursor activity on 21 January 1951 it burst into a catastrophic eruption which produced an eruption column that rose to a height of 15 km. Material collapsing out of the column generated pyroclastic surges and flows which initially flowed radially away from the volcano, but were then channelled predominantly northwards by the topography, devastating an area of about 174 km^2 and killing almost 3,000 people (Taylor, 1958).

At El Chichón in southern Mexico 2,000 people were killed and nine villages destroyed.

During the main phase of the eruption, which lasted 4-5 hours, three separate pyroclastic surges were generated at the base of a major plinian eruption column. These moved out radially from the vent and the largest swept across an area of about 100 km^2. Approximately one cubic kilometre of magma was erupted, but of this only about 12% was incorporated within the surges.

5.3.5 Hazard zoning for pyroclastic flows and hot pyroclastic surges

Pyroclastic flows and surges are extremely hazardous because of their high velocities and high temperatures. Escape is virtually impossible once pyroclastic flows or surges have been initiated and therefore the only practical solution to minimise casualties is to evacuate populations from zones that are likely to be affected prior to an eruption.

Hazard zones for pyroclastic flows and surges have commonly been defined using the maximum extent of previous flows, based upon historical information or upon the recognition of older deposits. In these schemes the frequency and intensity of the hazard generally decreases away from the eruptive source, and valleys and depressions are generally more hazardous than positive topographical features. An example of such an approach to hazard zoning is that of Merapi in Indonesia, where a forbidden zone has been defined using the maximum extent of pyroclastic flows during a particularly violent eruption in 1930 which killed 1,300 people. The hazard map of Merapi (Figure 5.12) clearly reflects the tendency for pyroclastic flows to be channelled along valleys, especially in more distal areas.

An alternative approach to hazard zoning for pyroclastic flows is illustrated by the hazard zonation of Mt. Shasta (Miller, 1980). This delimited four concentric zones centred on the summit of the volcano (Figure 5.13), that were primarily defined by the percentage of ground affected by pyroclastic flows and mudflows at least once during the last 10,000 years. Zone boundaries are essentially circular but modified to take into account the effects of topography, on the assumption that certain areas of high ground are less hazardous. The outer boundary of zone 2 (20 km from the summit) is based upon the maximum extent of pyroclastic flow deposits younger than 10,000 years. Only mudflows are known to have affected the ground outside this zone, but the outer boundary of zone 3, drawn at 30 km from the summit, is based upon the hypothetical length of the largest expected pyroclastic flow. This distance was estimated using the empirical relationship between the horizontal distance (L) and vertical drop in height (H) through which previous pyroclastic flows have travelled on Mt. Shasta. The largest measured H:L (1:8.3) is for a block-and-ash flow generated by the collapse of dacite lava domes on the satellite eruptive centre of Black Butte. A hypothetical flow of similar mobility descending from the summit of the volcano could have a maximum vertical drop of 3,400 metres, and hence a theoretical length of almost 30 km (i.e. $3.4 \times 8.3 = 28.2$ km).

The relationship between vertical drop (H) and length travelled (L) has been applied to the hazard assessment of pyroclastic flows at a number of volcanoes and has also been used for predicting the lengths of other types of gravity-driven flows such as avalanches (Section 5.6). The concept is commonly referred to as the **energy line concept** and the ratio of H/L is the tangent of the slope, also known as the Heim coefficient. Sheridan and Macías (1995) used

the concept to estimate the hazard probability for gravity-driven pyroclastic flows at volcán Colima in Mexico. They assumed that all flows originated at the summit of the volcano, and on the basis of the mapped extent of flow deposits the lengths and vertical drops of past flows were measured from topographic maps, from which Heim coefficients (H/L) were calculated. The coefficients were found to cluster in two distinct modes on a histogram. One corresponding to large pumiceous flows, for which the coefficients are in the range 0.22 to 0.28, the other to small block-and-ash avalanches with coefficients ranging from 0.33 to 0.38. The distinct lack of coefficients between 0.28 and 0.33 was considered to separate large fluidised flows from less mobile hot avalanches. It was also found that the cumulative frequency distribution of the Heim coefficients for each population defined a straight line when plotted on probability paper, implying a Guassian distribution. The Heim coefficients for each urban settlement around the volcano were calculated from the difference in altitude and distance from the summit and the probability of a pyroclastic flow reaching each settlement was then estimated from the cumulative frequency distribution of the coefficients of the measured flows. Contour lines were also plotted on a map of the volcano, showing the probabilities of occurrence for each type of pyroclastic flow.

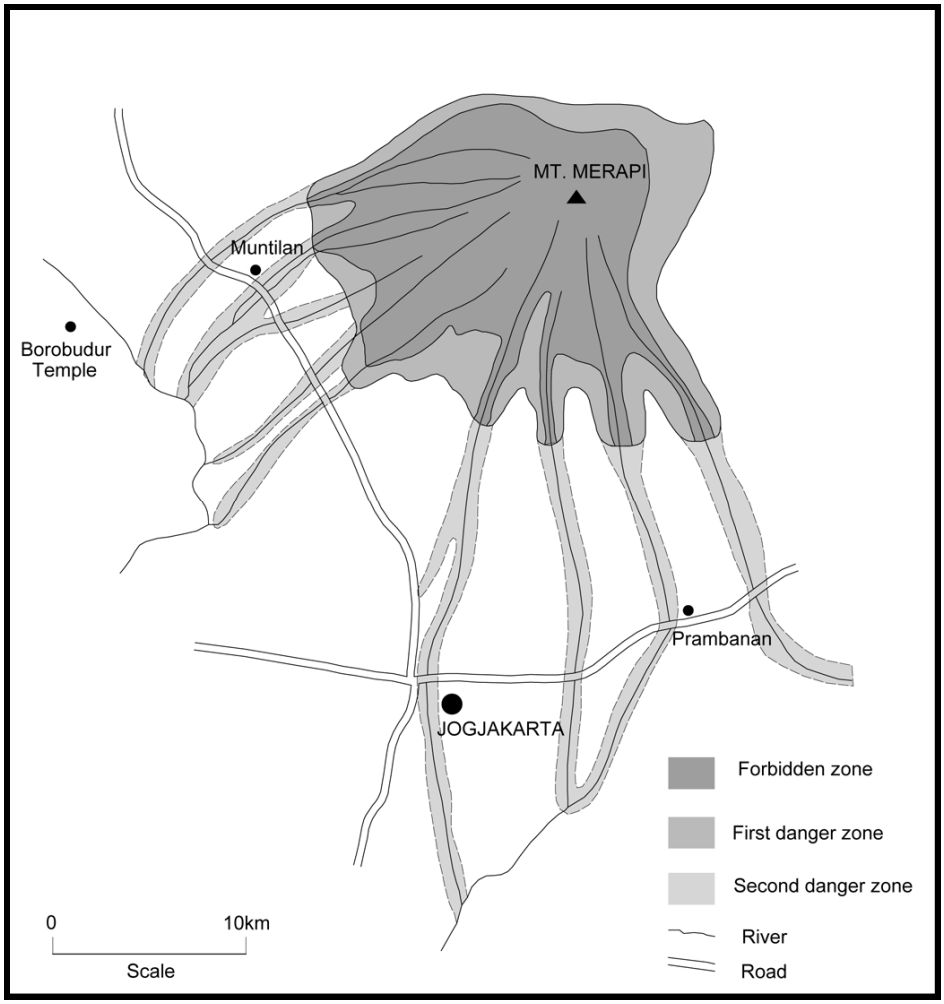

Figure 5:12: Simplified hazard zoning map of Merapi, Indonesia (from Volcanological Survey of Indonesia Report 122, 1990). The forbidden zone includes areas considered to be at risk from pyroclastic flows and surges, based on the limits of pyroclastic flows produced by a particularly violent eruption in 1930 which killed 1300 people. Note the boundaries of this zone extend down valleys, reflecting the tendency for

pyroclastic flows to be channelled by topography. The second danger zone extends for considerable distances down the valleys and delimits areas affected by lahars which are the prevalent hazard at Merapi.

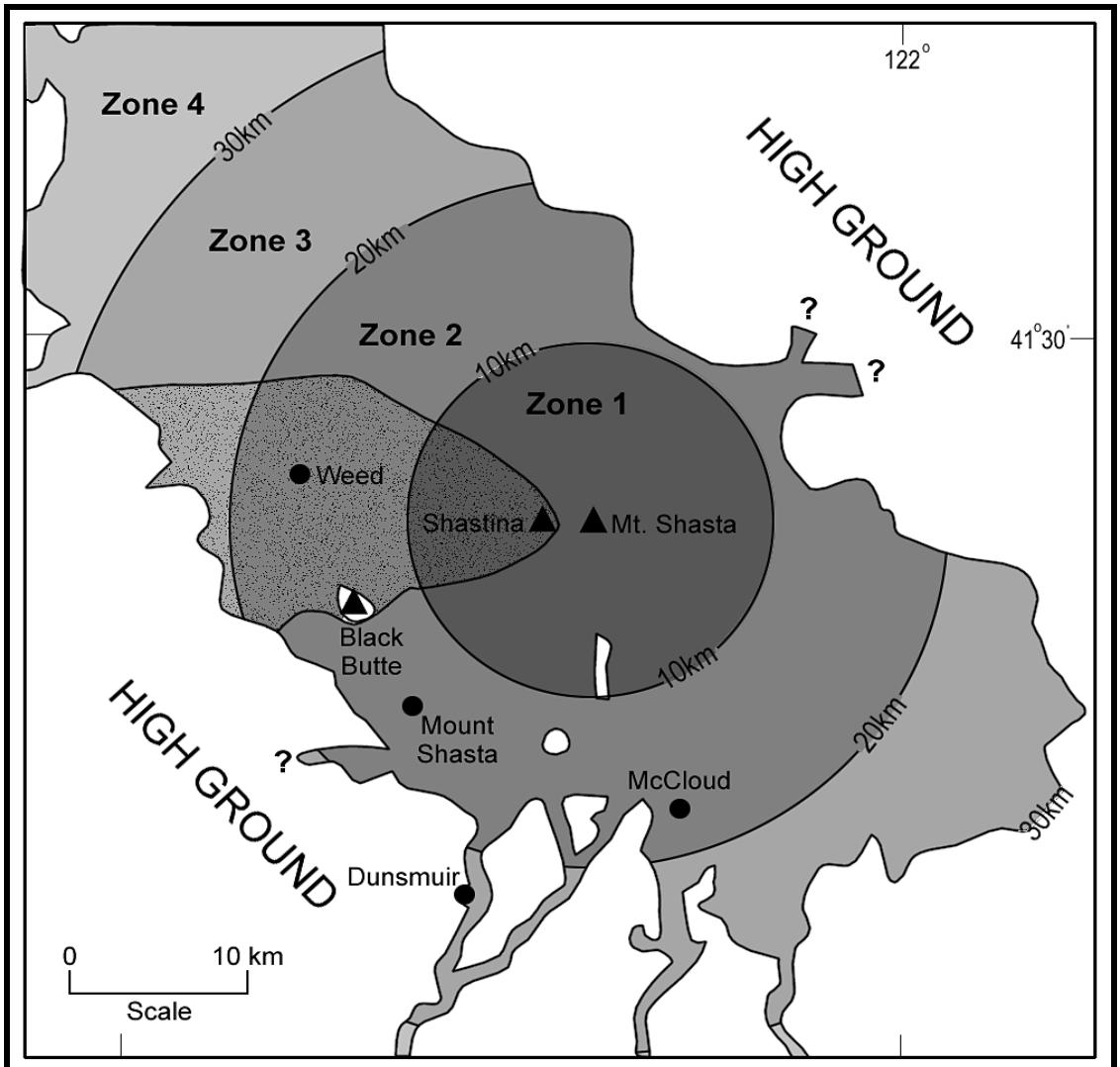

		Zone 1	Zone 2	Zone 3	Zone 4
Percentage of zone affected at least once in the last 1000 years		100	60	25	40-60? (S) <10 (NW)
Estimated future average frequency in years	Pyroclastic flows	1/800	1/1500	1/10000	0
	Lahars >10km^2	1/600	1/600	1/2000	1/5000

Figure 5.13: Map of potential hazard from pyroclastic flows and lahars at Mt. Shasta, based on events over the past 10000 years (after Miller, 1980). Unshaded areas within zones and irregular zone boundaries are related to topographically high areas that are considered to be above the effects of pyroclastic flows and lahars. The stippled area in zones 1, 2 and 3 is not likely to be directly affected by pyroclastic flows and lahars originating on the summit or the northern, eastern or southern flanks of Mt. Shasta. This area will probably be shielded from flowage hazards by the cone of Shastina. This area may however be affected by blasts and surges associated with pyroclastic flows originating near the summit of Mt. Shasta or on the northern, eastern or southern flanks. The stippled area has been affected by pyroclastic flows and lahars originating only from Shastina and Black Butte during the last 10000 years.

Although the empirical relationship between H and L provides a semi-quantitative method for predicting the length of pyroclastic flows for hazard zoning, it suffers from a number of weaknesses. One is that the method does not take into account the roughness or irregularities of topography which could affect flow paths. Another problem is that the method is not applicable for large events where pyroclastic flows are generated by large collapsing eruption columns. Such events normally have vertical drops far greater than the height of the volcano, and their mobility is also thought to be influenced by volume, a factor that is difficult to anticipate for the purpose of hazard assessment.

Hazard zoning for hot pyroclastic surges is more difficult than for pyroclastic flows, because of their greater mobility and less predictable behaviour. In addition, the deposits of ash cloud surges are thin and unlikely to be preserved or recognised in the geological record, so that evidence of previous surge activity at a particular volcano may be overlooked or no longer exist. It should therefore be generally assumed for hazard zoning purposes that areas likely to be affected by surges will be more extensive than those affected by pyroclastic flows. Thus, wider hazard zones should be delimited for surges than for pyroclastic flows, to include the sides of valleys and interfluves and to take into account the possibility of surges segregating and continuing after the main bodies of pyroclastic flows have come to rest.

Computer simulations of pyroclastic flows and surges have been used to a limited extent to assist with hazard assessment and risk management. Wadge *et al*., (1998a) simulated the paths of pyroclastic flows formed by dome collapse during the eruption of the Soufriere Hills volcano on Montserrat. The authors point out that although significant progress has been made in understanding the fundamental dynamics of pyroclastic flows, there are still many poorly understood features and there is no simple physical model that may easily be used to simulate flows and generate hazard maps. The Montserrat simulations were therefore relatively simple in concept and did not attempt to encapsulate all the physical processes of pyroclastic flows: The main purpose was to provide a quick means of simulating the runout lengths of flows for hazard mapping. For this purpose the mechanism of pyroclastic flow was split into a dense hot avalanche component and a dilute ash-cloud surge component. A simple equation of motion was used to simulate the avalanche phase of flow, which combined with a detailed digital topographic model of the volcano allowed flow paths to be computed. An inverse approach was adopted which compared simulated avalanche flow paths with the paths of actual pyroclastic flows that had occurred during the eruption, in order to constrain uncertainties in the parameters of the equation of motion for flows of various magnitudes. The resulting simulated flow path was then used to prescribe the source of fine ash material for modelling the extent of pyroclastic surges on either side of the avalanche component of the flow. The surge model assumed that material was elutriated from the avalanche component and that this advanced in a direction normal to the flow. The process of flow may simultaneously entrain air and sediment particulate material until the bulk density falls below that of the environment, at which point separation of the dilute surge cloud from the avalanche occurs. The dilute ash-cloud was modelled using the approach of Bursik and Woods (1996). Using this two step approach for modelling the avalanche and surge components it was possible to simulate with reasonable success the extent of pyroclastic flows related to reference dome collapse events that had actually occurred. The relationship between frequency and length of pyroclastic flows at the volcano during the period 1996-97 were quantified from records and this information combined with repeated simulations in a

Monte Carlo scheme to generate a probabilistic map of pyroclastic flows for the whole volcano.

Wadge *et al*. (1998b) and Hulsemann *et al.* (1998) also applied a three-dimensional hydrodynamic model to large-scale, mobile pyroclastic flows generated by eruption column collapse on Montserrat. The purpose of this was to estimate the size of eruption necessary to produce flows that would surmount the Centre Hills, which act as a barrier between the active Soufriere Hills volcano and the inhabited northern part of the island. It was concluded from the modelling of very large hypothetical eruptions, 25 to 120 times the size of a reference eruption (18 September 1996, 3×10^6 m^3), that pyroclastic flows generated by column collapse would be largely deflected out to sea by the Centre Hills. The modelling took no account of ground frictional effects nor the roughness of the topography, which in reality would inhibit the mobility of flows. The results of the modelling therefore provided a pessimistic estimate of the size of flows necessary to pose a hazard to the populated northern part of the island. This accords with the geological record, which shows no evidence that past eruptions of the Soufriere Hills volcano have produced pyroclastic flows that have crossed beyond the Centre Hills to reach the north of the island.

Dobran *et al*. (1994) also produced computer simulations of pyroclastic flows generated by column collapse for hypothetical eruptions of various sizes at Vesuvius, taking into account topography. The simulations showed many features consistent with evidence from historical eruptions at Vesuvius. It was predicted that within about 15 minutes of the initiation of medium to large-scale eruptions, complete destruction could occur within a 7 km radius (modelling was only applied to a 7 km radius), where a million people live and work. The simulations also suggested that topography would have little effect in large or medium-scale eruptions, other than to retard flow, and that only small-scale pyroclastic flows are likely to be controlled by topography.

Caution should be exercised in using the results of computer simulations for hazard zoning, since the physical processes and parameters of pyroclastic flows are not fully understood. It could be argued in the case of a well-studied volcano such as Vesuvius, that the accounts of historical eruptions and the distribution of older deposits provide a more realistic and practical basis for hazard planning than computer models: The speed of pyroclastic flows and the destruction they cause is well-known, so the results of the simulations of hypothetical eruptions at Vesuvius should therefore not be surprising. Modelling however, does have a role to play in civil protection in estimating the potential lengths of pyroclastic flows for different size eruptions. In the case of the Montserrat emergency for example, modelling provided reassuring confirmation of hazard zonation for risk management with respect to the likely size of eruptions that would be required to produce sufficiently large and energetic pyroclastic flows that could threaten the inhabited northern sector of the island.

—

5.4 Cold Pyroclastic Surges (Base Surges)

Cold pyroclastic surges, also known as **base surges**, are produced by powerful **hydrovolcanic** eruptions which occur when surface or shallow groundwater interacts with magma. They are not strictly cold, but are insufficiently hot to prevent the condensation of steam and their deposits are often wet. Turbulent debris-laden clouds are blasted radially outwards from the vent in all directions and travel at high velocities close to the surface. This typically occurs when magmas of any composition come into contact with surface water or shallow groundwater, and is common during shallow marine eruptions of emergent volcanic islands and also occurs at volcanoes with crater lakes.

Cold surges are also blasted radially outwards from the base of collapsing hydrovolcanic eruption columns, but they differ from hot surges or pyroclastic flows produced by collapsing eruption columns by containing a considerable amount of steam or condensed steam. Hot pyroclastic surges may also occur during hydrovolcanic eruptions, as for example during the formation of Unirek maars in Alaska in 1977 (Self *et al*., 1980). The ratio of water to magma mass is generally thought to be the main factor that determines the kind of surges produced by phreatomagmatic explosions, with cold surges being the product of high water to magma mass ratio.

The temperatures of cold surges vary, but the presence of water, especially near the outer limits of surges, would suggest temperatures below 100°C. Cold surges are fluidised by steam and air entrained during collapse of the eruption column. Initial velocities of between 50 km/h and 300 km/h have been inferred for surges, but they rapidly deflate and decelerate as air escapes and steam condenses, and they usually stop within less than 10km from the vent (Crandell *et al.*, 1984)

Base surges generated by eruptions on small islands or in the sea are able to move radially outwards across the surface at high speeds without being deflected by topography. Coastal settlements and shipping within range are therefore particularly exposed and vulnerable. Cold surges destroy property and vegetation in their paths by a combination of impact, severe abrasion and burial. Vegetation and structures are characteristically plastered with wet mud and ash.

The most destructive cold surges in historic times have occurred at the island volcano of Taal, situated within Lake Taal in the Philippines. Since its earliest recorded eruption in 1572 Taal has experienced 32 eruptions, four of which have caused major devastation on the volcano and shores surrounding the lake. Because of its island setting, and also the presence of a crater lake, Taal's eruptions have been predominantly phreatic or phreatomagmatic and have characteristically produced base surges. In 1911 the whole island was devastated and many settlements on the surrounding lake shores were severely affected by surges which killed 1,334 people. Powerful surges were generated at the base of a 15 km high eruption column and these swept down the flanks of the volcano and out across the surrounding lake. In 1965 a phreatomagmatic eruption blasted a large crater on the southwest shores of Taal, but fortunately due to timely evacuation loss of life was minimised to 180 people. During this event turbulent surges were again generated from the base of a 15-20 km high eruption column. These caused damage within a 5km radius of the vent and sandblasted objects up to a

distance of 8 km (Moore, 1967). Houses were destroyed and trees uprooted within a kilometer of the vent, and farther out tree trunks were severely abraded on their exposed sides but were unscathed on the reverse. Trees and other structures were plastered in thick wet mud and ash and showed no sign of charring, illustrating the relatively cool and wet nature of the surges.

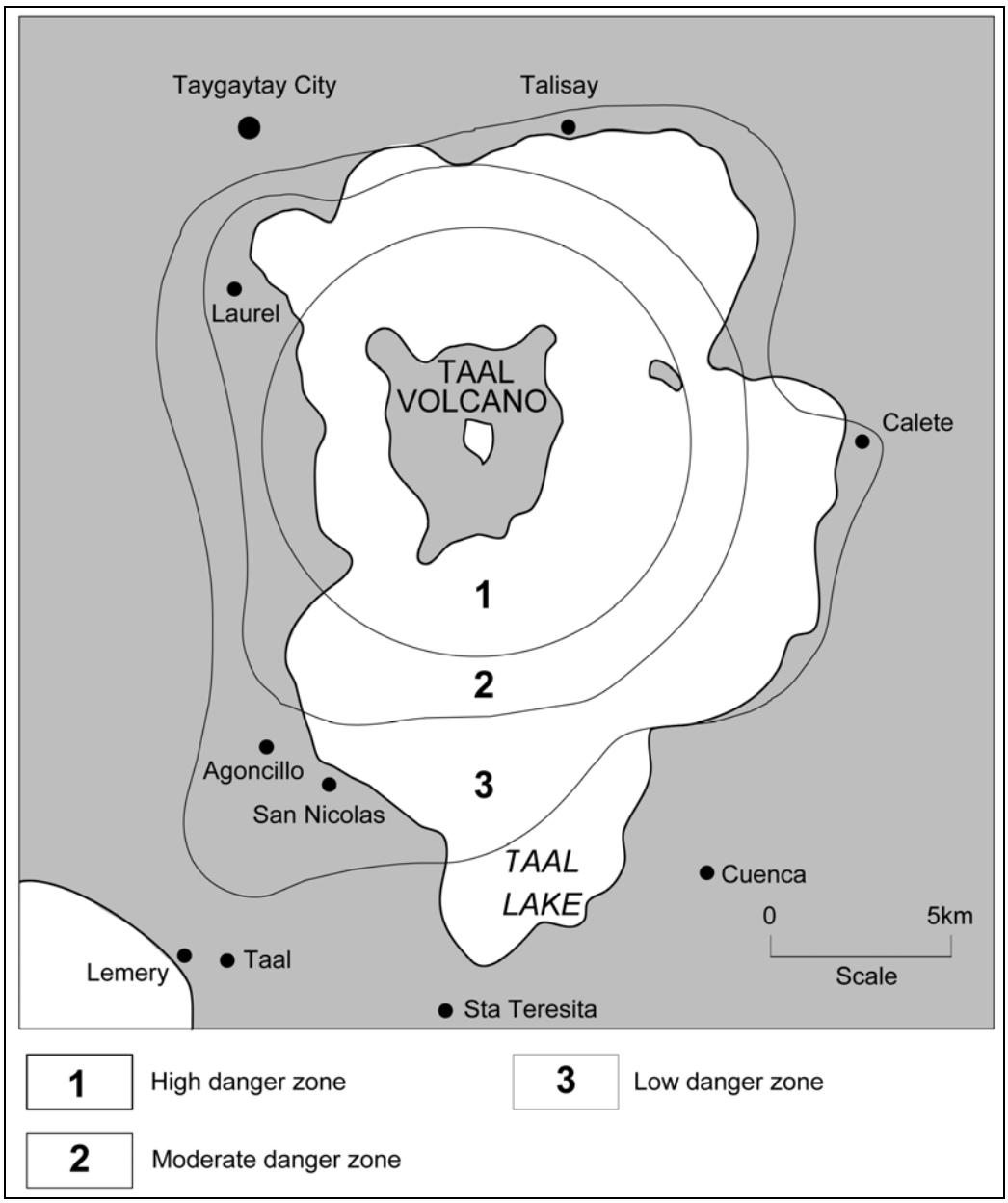

Figure 5.14: Base surge hazard map of Taal volcano, Philippines. High danger areas are likely to experience severe damage in future eruptions. Moderate danger areas are likely to experience considerable damage. Low danger areas are likely to experience the fringe effects of a base surge. (After Operation Taal, Philippine Institute of Volcanology and Seismology, undated).

—

5.4.1 Hazard zoning for cold pyroclastic surges

Cold pyroclastic surges inflict severe damage by a combination of impact and abrasion. They are a potential hazard at small island volcanoes and at emergent or near emergent submarine volcanic centres.

Coastal areas within range of base surges should be designated hazard zones, and shipping should also be excluded from areas within these zones during eruptions. Tsunamis generated by powerful phreatomagmatic eruptions should also be considered a potential hazard of shallow submarine or emergent marine volcanoes.

Hazard zones can be delimited using historical information from previous eruptions, as has been done at Lake Taal (Figure 4.14). In this example a *high danger zone* is designated with a radius of 6km from the main crater, which is essentially the limit of damage caused by base surges in the 1965 eruption. A *moderate danger zone* with a radius of 8km includes the areas affected by the 1911 and 1745 base surges; it is assumed that these areas will experience the effects of future base surges, but not so severely as the high danger zone. An outer *low danger zone* is based on those areas only affected by the 1745 base surges. It is assumed that this outer zone will only experience 'fringe effects' of base surges and the outermost limits are therefore defined by topographic barriers.

Where historical or geological information on past eruptions is not available, hazard zones for cold surges can only be defined in an arbitrary manner. Crandell *et al*. (1984) state that cold pyroclastic surges typically stop within distances of 10 km. This could be used as a general rule for the outer boundaries of hazard zones, with modifications taking local topographical barriers into consideration.

5.5 Lateral blasts

Lateral blasts are volcanic explosions which are mainly directed at a low angle over restricted sectors of a volcano's flanks and surrounding country. They occur with little or no warning and are amongst the most violent of volcanic events, destroying most things in their path by the effects of impact, abrasion, burial and heat.

Volcanic debris and heat are transported at very high velocities away from the source of the explosion by a complex combination of mechanisms, which include the ballistic ejection of rock fragments, pyroclastic flow and pyroclastic surge. Because of the complexity and uncertainty regarding transport processes Crandell and Hoblitt (1986) described lateral blasts in terms of two components without implying specific mechanisms. They used the term **blast cloud** to denote the mixture of rock fragments and gases created by an explosion, and the term **pyroclastic density flow** to refer to a mass of particulate volcanic material and gases of variable density and temperature that moves in contact with the ground mainly under the influence of gravity.

Lateral blasts may be classified into two general types, which differ in size and frequency of occurrence. These are explosions caused by the sudden release of pressurised gases from growing lava domes, and much rarer large-scale explosions caused by the sudden unloading of magmatic intrusions and hydrothermal systems within volcanoes due to structural failures of their flanks. Different hazard zoning schemes are adopted for these two types of lateral blast which take into account the differences in scale of events.

In addition to the primary hazard of lateral blasts, a number of associated secondary hazards should also be taken into account when delimiting hazard zones. These include debris avalanches, pyroclastic flows and surges, tephra-fall and lahars.

5.5.1 Lateral blasts associated with lava domes

Lateral blasts are commonly associated with the growth of silicic lava domes and may affect areas at distances of more than 10 km. They result from the sudden release of gas pressure during the collapse or partial collapse of lava domes. This may be triggered by gravitational instability of the dome or by explosive collapse, and is often associated with the generation of block-and-ash pyroclastic flows and surges (Section 5.3).

Estimates of the likely distance over which rock debris may be ballistically propelled by lateral blasts from lava domes have bearing on the delimitation of hazard zones. Unfortunately, precise details from known lateral blast eruptions are scant. Pertinent information is provided by descriptions of the 1951 eruptions of Hibok-Hibok in the Philippines (Macdonald and Alcaraz, 1956) where lateral blasts and pyroclastic flows were produced from an actively growing silicic lava dome. The maximum area of devastation produced by these blasts is not specified by Macdonald and Alcaraz, but they describe damage to coconut palms which indicates severe impact at a distance of 5 km from the dome, and it is therefore assumed that the maximum distances reached by the blasts were greater than this. Additional information may be gained from the deposits of prehistoric lateral blasts. At Mount St Helens, about 1,200 years ago lateral blasts from the Sugar Bowl dacite dome threw rock debris to distances of at least 10 km across a 30° sector of the volcano's flanks, covering an area of about 50 km^2 (Crandell and Hoblitt, 1986), whilst at Mt. Rainier, deposits interpreted as the product of lateral blasts were recognised by Mullineaux (1974) up to 12 km from the summit.

5.5.2 Hazard zoning for lateral blasts associated with lava domes

For the purpose of hazard zoning, Crandell and Hoblitt (1986) proposed that lateral blasts from active lava domes can throw rock debris at least 10km, and that if desired a safety margin of 20-50% could be added to this distance. If the general direction of a potential blast can be anticipated, as for example where a dome is actively growing on the flanks of a volcano, a hazard zone might be designated over a sector of at least 180° on the open, down-flank side of the dome. In the case of an active lava dome on or near the summit of a volcano it should be assumed that a lateral blast could occur in any direction, and therefore a circular

hazard zone of 10 km radius would seem to be appropriate, with or without an additional margin of safety. The outer boundary of such a zone could also be modified to take into account areas of positive relief which may act as a shield.

5.5.3 Large-scale lateral blasts associated with the unloading of magmatic or hydrothermal systems

The potential for large-scale lateral blasts exist when bodies of viscous, gas-rich magma are intruded at high structural levels within volcanic edifices. Under these conditions, failure of a volcano's unstable flanks can result in the sudden unloading of the magma body or a related hydrothermal system, triggering laterally directed explosions as magmatic gases and steam expand rapidly. Failure may be triggered by earthquakes or by eruptions, and is generally more likely to occur at volcanoes where the flanks have been weakened by extensive hydrothermal alteration. Lateral blasts generated in this manner are intimately associated with large-scale debris avalanches formed by flank-collapse (Section 5.6).

Examples of large-scale lateral blasts generated in this manner are the 1980 eruption of Mount St Helens and the 1956 eruption of Bezymianny in Kamchatka., both of which devastated areas of 500-600 km^2.

At Mount St Helens, a dome of dacite magma was intruded to a high level within the volcano causing the upper northern flanks to bulge outwards and upwards: The rate of deformation averaged 2 m per day for at least three weeks prior to the cataclysmic eruption, and in total the crest of the bulge rose 150 m above the pre-existing topography (Moore and Albee, 1981). Eventually, after several months of deformation and minor eruptions from the summit, a moderate size earthquake (M_s 5.1) caused the unstable bulging flank to collapse and produce a massive debris avalanche (Section 5.6). As the flank collapsed, the magma body and surrounding hydrothermal system within the volcano were unroofed and magmatic gases and steam, which had previously been confined under high pressure, were suddenly released in a huge explosion, generating a laterally directed blast (Figure 5.15).

The exact nature of the blast at Mount St Helens is uncertain, although it is generally believed that rock debris, juvenile magmatic material and hot gases moved as an inflated pyroclastic density flow, by a combination of mechanisms akin to pyroclastic surge in its more inflated parts and to pyroclastic flow within its more deflated regions. The blast travelled for distances of up to 28 km and completely devastated an area of about 550 km^2 on the northern flanks of the volcano across an arc of about 180°, but only left a relatively thin deposit, ranging in thickness from about a metre near source to less than a centimetre in peripheral areas. Hot gases produced a fringing zone of seared vegetation around the periphery of the zone of total destruction. The velocity of the blast was initially about 100 m/s (360 km/h) increasing towards an upper limit of 325 m/s (1170 km/h) as gases expanded (Kieffer, 1981), and the average velocity within the zone of devastation was about 200 km/h (55m/s). The orientation of flattened trees indicated an *inner direct blast zone* out to about 11 km, in which the blast was directed radially away from the volcano and was not deflected by topography (Kieffer, 1981). This was surrounded by an *outer channellised blast zone* in which flow was deflected by local topographic features (Figure 5.16).

At Bezymianny the large-scale directed blast was of similar nature to that at Mount St. Helens, but involved a smaller volume of ejecta and a lower proportion of juvenile magmatic material. Although it covered a more restricted arc of about 90° it travelled up to 33 km from source.

5.5.4 Hazard zoning for large-scale lateral blasts

The monitoring of seismic activity and ground deformation during the precursor stage of an eruption can provide invaluable indicators of the movement of magma within a volcano. Such indicators taken together with other structural information may be used to anticipate a laterally directed blast: Specific signs might include the swelling of a volcano's flanks or downslope movement accompanied by the development of fissures and landslip scars. At Mount St Helens, for example, the deformation of the flanks during the precursor stage led observers to anticipate a failure of the volcano's flanks at least six weeks before the cataclysmic eruption. Furthermore, the azimuth of maximum deformation of the bulging flank was within a few degrees of the axis of the lateral blast that eventually occurred.

Crandell and Hoblitt (1986) based their hazard zoning models for large-scale lateral blasts on the eruptions of Mount St Helens and Bezymianny. These large eruptions offer worst-case examples, so that hazard zones based upon them can be regarded as being conservative and therefore relatively safe. Because of the apparent rarity of eruptions of this kind Crandell and Hoblitt (1986) propose that a distinction should be made between hazard zones for long-term land-use planning purposes and those for short-term planning when an eruption is anticipated.

For short-term hazard zonation, when seismic activity is accompanied by flank deformation, they recommend delimiting a zone of potential lateral blast extending to a distance of 35 km from the site of deformation over a sector of at least 180° of arc. Although major topographic features may deflect a lateral blast, particularly near its periphery, it should be assumed that these features will not offer people protection against the effects of the ash and heat of the blast cloud. All areas within the hazard zone should be regarded as susceptible to severe damage, even though the effects will diminish with distance from the volcano. Crandell and Hoblitt also suggest that an additional zone of 10-15 km radius could be delimited on the opposite side of the volcano in case some debris is thrown in directions other that of the main blast (Figure 5.17).

For long-term planning purposes on symmetrical volcanoes, it should be assumed that large-scale lateral blasts could move outwards in any direction. In this case a circular hazard zone could be delimited with a radius of 35 km centred on the summit. Because of the apparent rarity of large-scale lateral blasts it would probably be unrealistic to impose long-term land-use restrictions over areas of several thousands of square kilometres around many volcanoes, on the remote chance that such a blast could occur in the indefinite future. Crandell and Hoblitt (1986) therefore suggest that a more practical approach might be to recognise the possibility of such an event when planning the development of areas within about 35 km of a long-dormant andesitic or dacitic stratovolcano, and to discourage the construction of certain costly or strategic installations within these areas. Public access to these zones should be restricted during or prior to an eruption if a lateral blast were to be anticipated.

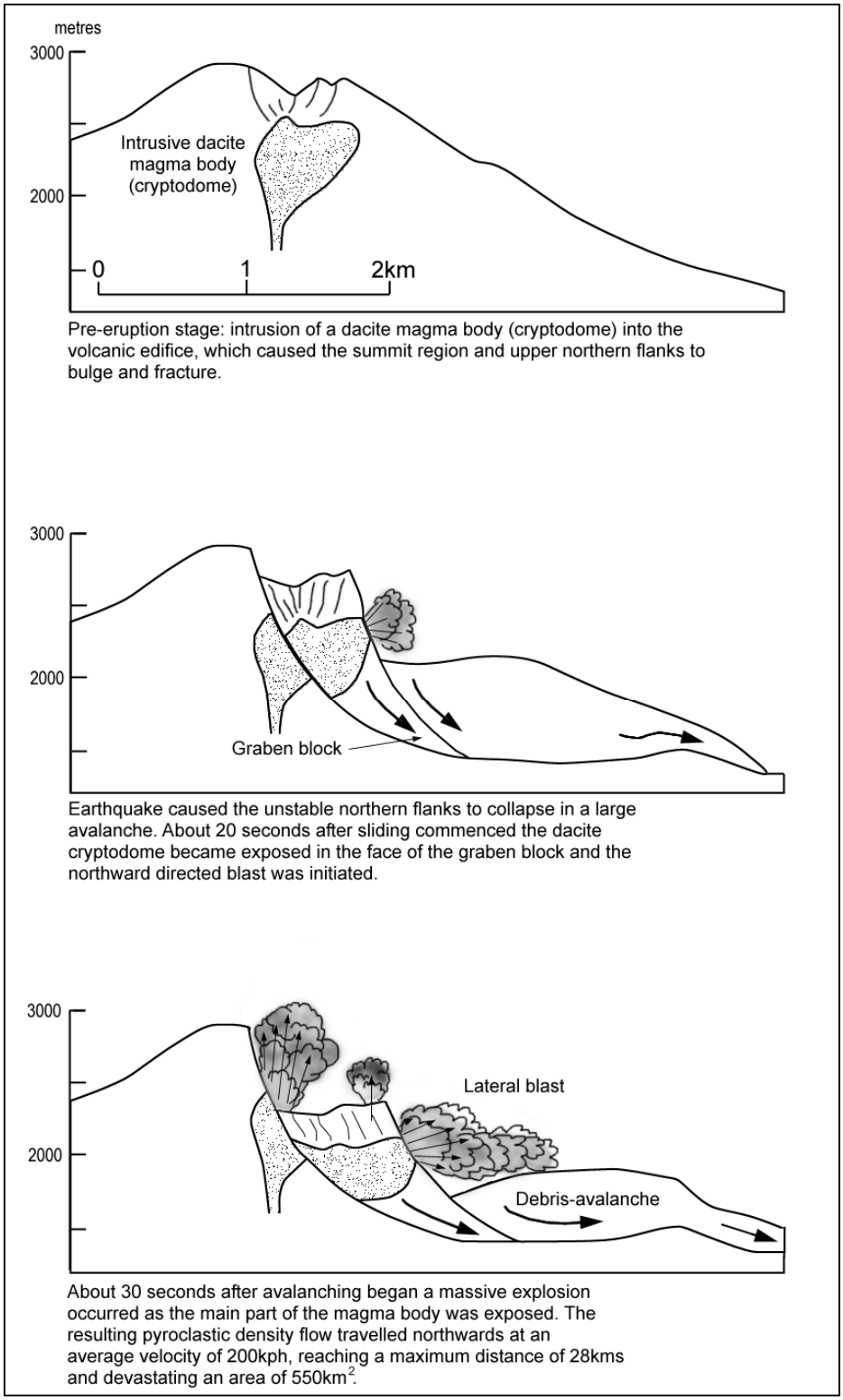

Figure 5.15: Changes in the profile of Mount St Helens during the 1980 eruption, illustrating the formation of the giant debris-avalanche and lateral blast. (After Moore and Albee, 1981).

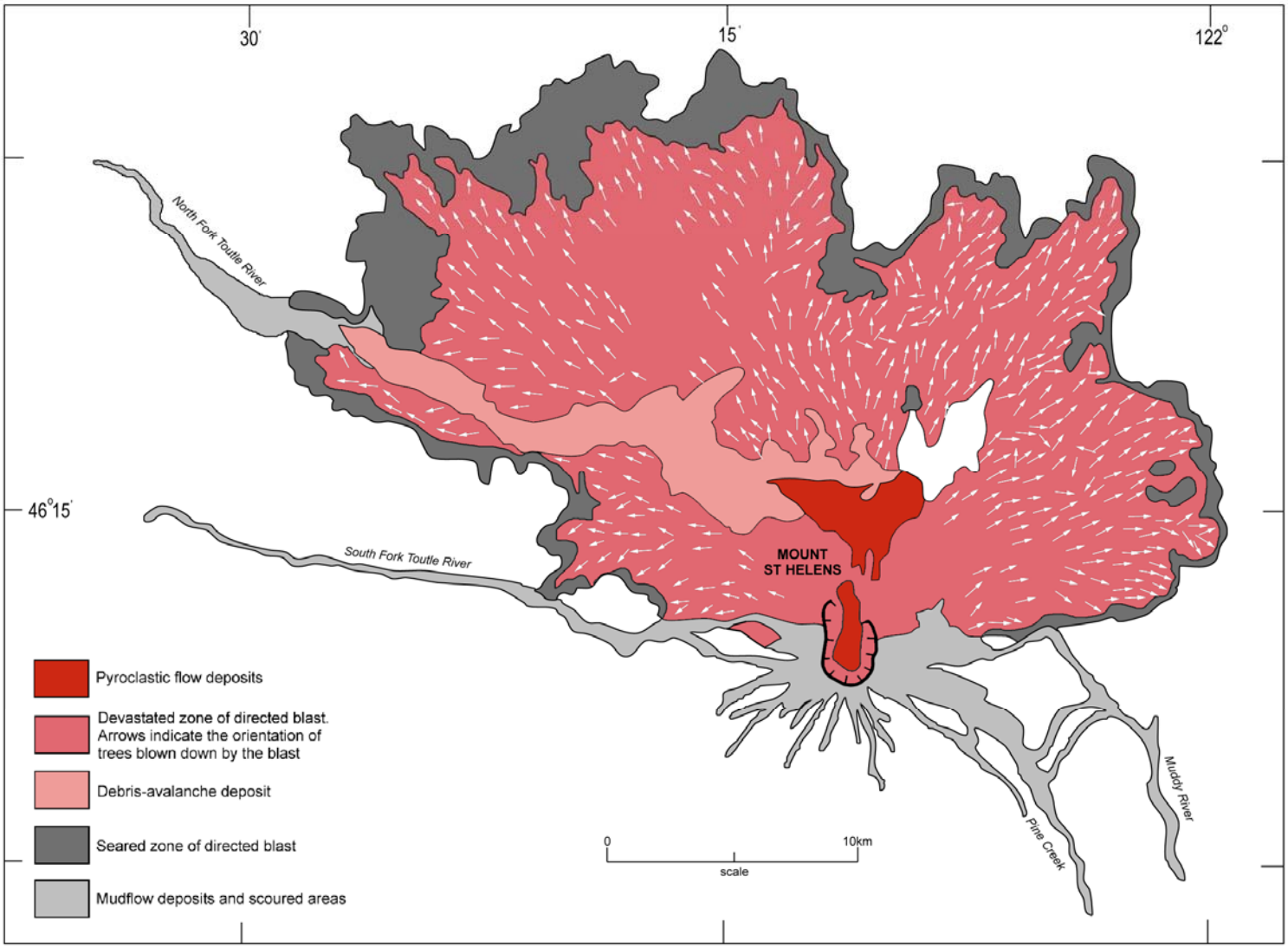

Figure 5:16: Simplified map showing the zone of devastation produced by the 1980 eruption of Mount St Helens (after Winner and Casadevall, 1981). The arrows show the orientation of trees blown over which indicate the direction of the blast. Also note the zone of searing which fringes the zone of devastation.

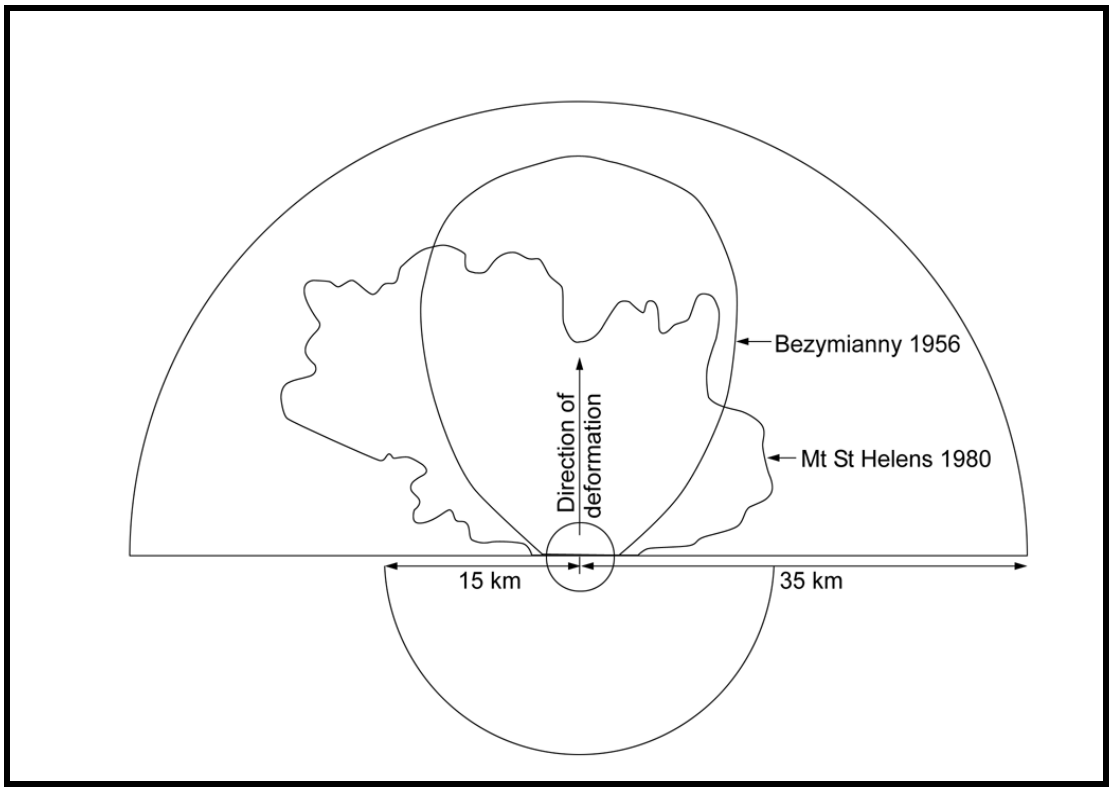

Figure 5.17: Suggested hazard zoning for short-term planning for large-scale lateral blasts, based chiefly upon the lateral blasts at Bezymianny in 1958 and Mount St Helens in 1980. The large semi-circle located at 35km from the source encloses an area principally at danger from pyroclastic density flows. The small semi-circle, located at 15km from the source, encloses a zone possibly under threat from impact from rock fragments thrown on ballistic trajectories. For long-term planning purposes, in which the direction of possible lateral blasts cannot be anticipated, a circular hazard zone of 35km radius could be centred on the volcano. (After Crandell and Hoblitt, 1986).

5.6 Debris Avalanches

Volcanic edifices are inherently unstable and under certain conditions can undergo catastrophic slope failure, producing large avalanches of rock debris which travel with great speed and mobility under the influence of gravity. These usually originate as massive rockslides which disintegrate during movement into fragments ranging in size from fine particles to blocks hundreds of metres across.

Structural failures of this kind can occur during eruptions, or without warning during periods of volcano dormancy. Because the resulting debris avalanches possess such tremendous kinetic energy they are able to move rapidly beyond the immediate environs of the volcano, causing total destruction of extensive areas. Although the mechanisms of transport are not clearly understood, large debris-avalanches are particularly mobile and are able to travel horizontal distances that are many times greater than the vertical distance through which they descend. Such avalanches are therefore often referred to as **long-runout avalanches** or **long-run landslides**.

Secondary hazards associated with the structural collapse of volcanic edifices and the formation of debris avalanches can be as destructive as the avalanches themselves and more extensive. These include large-scale lateral blasts, produced when pressurised magma bodies or hydrothermal systems become unroofed (Section 5.5.3), mudflows derived from water-saturated or ice-laden portions of debris avalanches (Section 5.7), and tsunamis generated when avalanches enter the sea (Section 5.8).

5.6.1 Features of debris avalanches

The cataclysmic eruption of Mount St. Helens in 1980 first drew attention to this kind of hazard, and subsequent studies have led to the recognition that large-scale debris avalanches have occurred at many volcanoes.

It has been estimated that major edifice failures have occurred at a rate of 4 per century over the last 500 years (Siebert, 1992). Such catastrophic events are therefore probably quite rare or unique in the life of most volcanoes and probably never occur at many volcanoes with gently sloping flanks (such as shield volcanoes). On the other hand some volcanoes may be prone to more frequent collapses, as exemplified by the extreme example of Mount St. Augustine in Alaska which on average has experienced a major collapse every 150-200 years over the past two millenia (Begét and Kienle, 1992).

The largest known prehistoric avalanche in terms of volume occurred at the ancestral volcano of Mt Shasta in the Cascade Range, USA. The deposits of this avalanche cover an area of 675 km^2 and have a volume of 45 km^3 (Crandell, 1989). The longest known debris avalanche occurred about four thousand years ago at Colima volcano in Mexico and travelled for a distance of up to 120 km covering an area of at least 2200 km^2 (Stoopes and Sheridan, 1992). Velocities in excess of 100 m/s (360 km/h) have been estimated for debris-avalanches (Siebert, 1992).

Debris avalanches form by a number of different mechanisms and vary in character. They can occur during volcanic eruptions or they may be triggered during dormant periods by other causes such as earthquakes. At one end of the spectrum debris avalanches may contain juvenile magmatic material and be hot and dry and exhibit behaviour similar to pyroclastic flows, or at the other extreme they may be cold and wet and behave in a similar manner to mudflows.

The long distances travelled by debris avalanches and the mechanisms that facilitate their mobility are not clearly understood. The mobility of hot avalanches is probably enhanced by fluidisation processes similar to those that operate in pyroclastic flows. The fact that many large avalanches show evidence of having been wet also suggests that water plays an important role in increasing mobility. High pore water pressures will reduce internal friction, and Voight *et al*. (1981) even argued that water boiled by frictional heat played an important role in fluidising the Mount St. Helens debris avalanche. There are, however, examples of large avalanches that appear to have been essentially dry. Hsu (1975) suggested that these may be self-lubricated by fluidised suspensions of dust and fine particles that reduce frictional resistance between larger blocks, whilst Melosh (1979) proposed that the dominant mechanism for sustaining motion in large avalanches could be ‘acoustic fluidization’ induced

by strong acoustic waves or vibrations.

Hydrothermal alteration also plays an important role in the formation of debris avalanches and influences their mobility and runout-lengths. Hydrothermal circulatory systems (hot water and steam) occur within all volcanoes and cause the alteration of rocks to soft clays. López and Williams (1993) drew attention to the fact that volcanic structures are weakened by this process, so much so that other triggering events such as earthquakes can produce catastrophic collapse. One of the reasons for this is that clays have high porosity but low permeability, which results in high pore-water contents. Because of high pore-water contents, clay-rich hydrothermally altered zones are more susceptible to slope failure in the first place, and once failure occurs the clay-rich rock provides a readily available and abundant source of dispersed pore-water which reduces internal friction and enhances the movement of the avalanche. There is also evidence that high proportions of hydrothermal clay can cause the transformation of some debris avalanches directly into mudflows (Vallance and Scott, 1997, see also Section 5.7.4).

5.6.2 Examples of debris avalanches

The following examples illustrate the main features and hazards of several different types of volcanogenic debris avalanches.

At Mount St. Helens in 1980 a dacite magma dome was intruded to a high level within the volcano, causing the upper northern flanks to bulge slowly outwards and upwards by up to 150 metres above the pre-existing topography. After several months of deformation and relatively minor eruptions from the summit, a magnitude 5.1 earthquake caused the unstable bulging flank to collapse. This produced a massive landslide which moved downslope at speeds of up to 80 m/s and became transformed into an enormous hot debris avalanche. Within about 10 minutes lobes of this avalanche had travelled 8 km northward and 22 km westward (see Figure 5.16, Section 5.5), choking about 60 km^2 of the North Fork Toutle River system with 2.8 km^3 of hummocky-surfaced, poorly-sorted rock debris to an average depth of 45 metres (Voight *et al*., 1981). Large mudflows were generated from the water saturated portions of the avalanche and these caused havoc for many tens of kilometres down-drainage. As the flanks of the volcano collapsed, pressurised steam and magmatic gases were released in a huge explosion, resulting in a laterally directed blast which also moved northwards eventually overtaking the avalanche (see Section 5.5.3 and Figure 5.15).

The longest known debris avalanche occurred at Colima about 4,000 years and appears to have been hot and to have contained juvenile magmatic material, suggesting that it formed during a period of volcanic activity. The presence of hot gases may have contributed to the mobility of this avalanche, in a similar manner to fluidisation in block-and-ash pyroclastic flows, thus explaining its exceptional length. It has been estimated that even at a distance of 90 km from source the avalanche had a velocity of 44 m/s (158 km/h) (Stoopes and Sheridan, 1992).

The largest known debris avalanche, which occurred at the ancestral Mount Shasta, does not appear to have been associated with contemporaneous volcanic activity (Crandell, 1989). This probably originated in a quick succession of huge landslides of water-saturated rock which evolved into a debris avalanche covering an area of 675 km^2, the fluid matrix of which drained away as major mudflows after the bulk of the deposit had come to rest.

The example of Mount Shasta illustrates an important feature, that wet avalanches have the potential to extend as mudflows far beyond the end of the debris avalanche proper, so endangering larger areas than avalanches that are not saturated. Volcanoes capped by glaciers or snowfields are more likely to produce wet avalanches because of the incorporation of snow and ice. Avalanches containing large proportions of water-saturated, clay-rich hydrothermally altered material may even transform directly into mudflows. This later point is exemplified by the enormous prehistoric Osceola mudflow of Mount Ranier (Vallance and Scott, 1997), which began as a water-saturated avalanche but within two kilometres transformed itself directly into a clay-rich cohesive mudflow which travelled for a distance of 120 km (see Section 5.7.4).

Mount Shasta is not a unique example of a volcanic edifice that has undergone structural failure in the absence of contemporaneous eruptive activity. In 1888 the northern flank of the Japanese volcano of Bandai-san collapsed during a dormant period. This appears to have been triggered by a steam explosion following a week of minor tremors. Within minutes of the explosion a debris avalanche with a volume of 1.2 km^3 had covered an area of 70 km^2 at the foot of the volcano, killing 461 people.

Elsewhere in Japan, at Mt. Unzen the 850 metre high lava dome of Mayu-yama collapsed in 1792, producing a debris avalanche with a volume of 0.48 km^3 which entered the sea and caused a catastrophic tsunami. This debris avalanche was not associated with explosive activity, but was cold and was probably triggered by an earthquake. Despite the relatively small volume of this avalanche, more than 14,500 people were killed. Ten thousand people are reported to have died when the avalanche overrode the town of Simabara and the remainder of the casualties were caused by the tsunami impacting on nearby coastal areas (Kuno, 1962).

A similar event occurred in 1888 at Ritter Island off the coast of New Britain. This was a steep-sided volcano which collapsed, apparently without any significant precursor eruptive activity, leaving only a small remnant above sea level (Cooke, 1981). Approximately 2km^3 of rock avalanched into the sea and generated a 12-15m high tsunami which devastated neighbouring coasts up to 470 km away.

Mount St. Augustine in Alaska deserves special mention because of the frequency of its large-scale collapses. This volcano has a prolific rate of silicic lava dome extrusion which causes over-steepening of its summit region culminating in periodic collapses on average every 150-200 years. Following each collapse the summit is rebuilt prior to the next edifice failure. Because St. Augustine is an island situated in an inlet, its debris avalanches have the potential to produce tsunamis, as was the case with its last summit collapse in 1883 (Kienle *et al*., 1987) (Section 5.8.1).

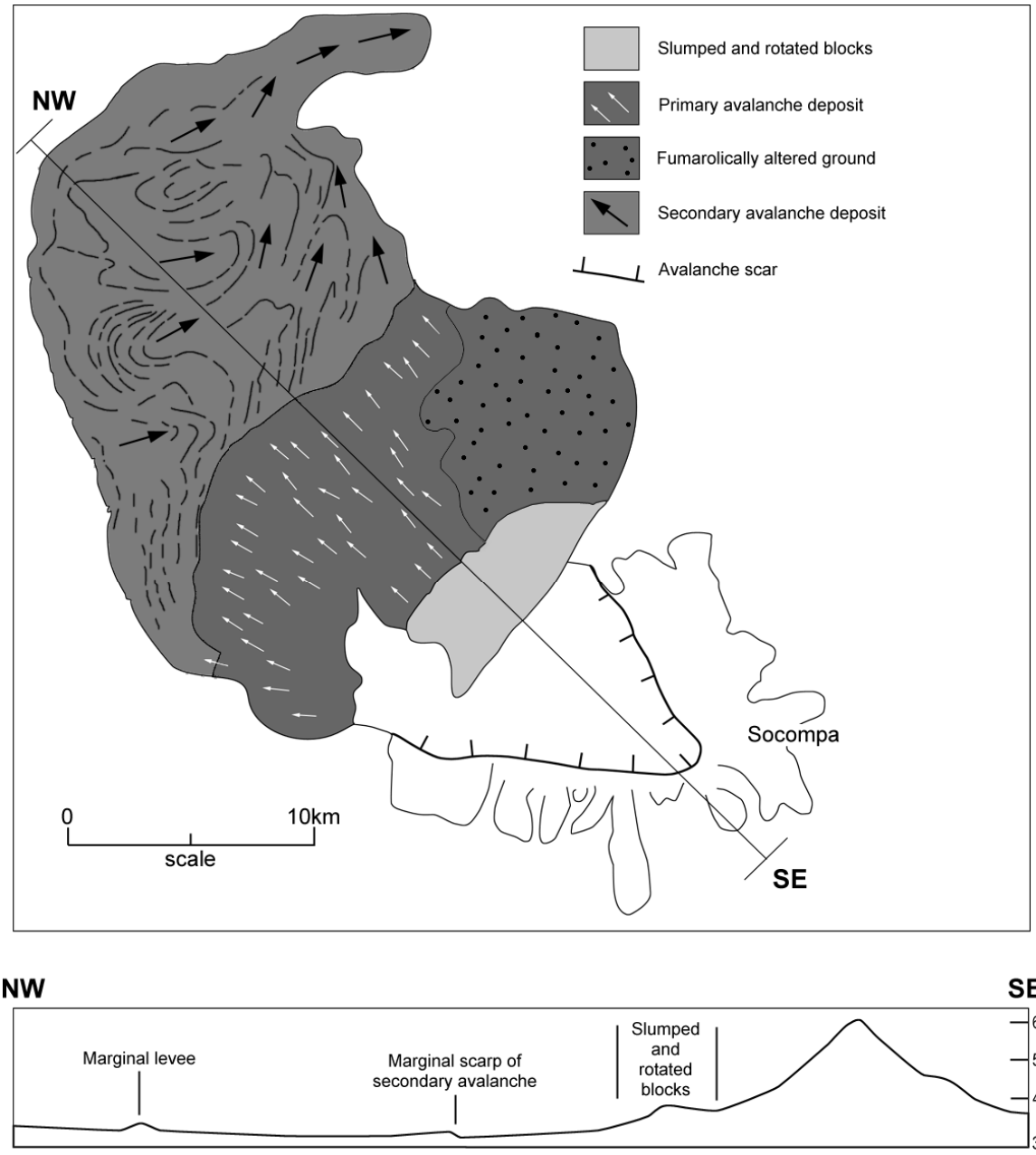

Figure 5.18: The debris-avalanche of Socompa volcano, northern Chile. The deposit covers an area of 490 km^2 and has a minimum volume of 15 km^3. Parts of the volcanic cone slumped in nearly coherent form and are now preserved as large blocks up to 400m high. The primary avalanche moved north-westward over sloping ground before coming to rest transiently, forming a prominent marginal ridge, and then slid away north-eastwards to form the secondary debris-avalanche. (After Francis et al., 1987).

5.6.3 Hazard zoning for debris avalanches

Debris avalanches are difficult to mitigate against because they can occur without warning, even on dormant volcanoes, and can completely devastate large areas. Once initiated, it is impossible to evacuate areas in the paths of debris avalanches because of the great speed with which they travel.

Debris avalanches tend to become channelled into valleys and can travel into drainage basins well beyond their source areas. Valleys draining volcanoes, and the lowland areas where these disgorge are therefore most at risk from debris avalanches.

Evidence for the occurrence and extent of previous debris avalanches serves as a guide for hazard assessment. Old debris avalanche deposits may be recognised by their distinctive hummocky surface topography which can be traced back to major amphitheatre-shaped landslide scars (backscarps) on the volcanic edifices themselves. Both the landslide scars and distinctive surface textures of avalanche deposits are commonly apparent on air photographs and satellite images, and the association of the two is diagnostic. Such features are however not ubiquitous, because wet avalanches may behave more like mudflows and produce deposits with planar surfaces which infill valleys and geomorphologically resemble alluvial deposits. The reconstruction of a volcanic edifice by subsequent activity may also mask geomorphological evidence of an earlier collapse.

The influence of regional structure on volcano stability should also be taken into account in hazard assessment, because this can control the orientation of sector collapses and hence the spatial distribution of avalanches. In Japan, for example, it has been recognised that a much higher proportion of volcanoes with strongly orientated dyke swarms have produced avalanches than volcanoes without a dominant dyke direction. This suggests that dilation orthogonal to dyke swarms is a factor that can influence the failure of volcano flanks (Siebert, 1984). Additional evidence for tectonic activity influencing sector collapse of volcanoes is also presented by Francis and Wells (1988) for the Central Andes. In this region the azimuths of sector breaches and the distribution of debris-avalanches indicate a strong tendency for collapses of volcano flanks to occur perpendicular to the regional fault trend. Volcanoes developed on sloping basements are also likely to be more prone to gravity-induced failure, especially if these contain slip planes and are faulted and tectonically unstable. Structural collapse should also be anticipated where there is evidence that magma bodies are being intruded to high levels within volcanic edifices and are actively causing flanks to bulge and fracture, as for example during the pre-cursor stage of the 1980 eruption of Mount St Helens.

It is often assumed that volcanoes showing geomorphological evidence of relatively recent edifice failures are likely to be gravitationally more stable and therefore less prone to collapse in the near future. In general such an assumption may be valid, but is not necessarily true in all cases. Conversely, well-formed, high, steep-sided volcanoes which show no signs of previous collapse are on average likely to be more unstable and therefore pose a greater hazard; especially bearing in mind that most volcanoes are likely to have been internally weakened by hydrothermal alteration.

In view of the general uncertainties in recognising volcanoes that are likely to collapse, debris avalanches should be considered a potential hazard at any high, steep-sided volcano. A practical approach to hazard zoning at such volcanoes is that based on the empirical relationship between the runout lengths (L) and the vertical distances (H) travelled by known avalanches: This relationship is referred to as the **energy line concept** and the ratio of H/L is sometimes referred to as the Heim coefficient, which is discussed in more detail in relation to hazard zoning for pyroclastic flows in Section 5.3.5.

The vertical ratio H/L has been used as an index to compare avalanche deposits and to act as a

proxy measure of their 'coefficient of friction' (F=H/L). Siebert *et al*. (1987) examined data for 40 avalanches with volumes greater than 1km^3 and found that their median length was 21km and that H/L ranged between 0.05-0.13 and averaged 0.09 (Figure 5.19). This information may be used to estimate the likely length of a debris avalanche for a given vertical distance travelled. The difference in elevation between the summit and the base of the flanks may only be taken as a minimum value of H because large avalanches typically travel beyond the base of their source volcanoes. Siebert *et al*. (1987) therefore recommended taking H as the difference in height between the summit and a point approximately 20km distant; this distance being approximately the median length (21 km) indicated by the available data for large volume debris avalanches. The runout length for hazard zoning purposes can then be estimated from L=H/F. Caution should be exercised in using this relationship, because volume may be a more dominant factor than that of vertical drop in controlling the runout lengths of the largest of debris-avalanches. Furthermore, hot avalanches may also depart from the H/L relationship and be able to travel greater distances than cold avalanches.

For hazard assessment Siebert *et al.* (1987) recommend using their lowest measured F value of 0.05 as a *worst case scenario*, although a few debris avalanches have subsequently been discovered with even lower F values. Crandell (1989) suggested that for a very conservative approach an F value of 0.05 could be used, but that for long-term planning a more pragmatic approach to hazard zoning could adopt an F value of 0.075 but also incorporate a safety factor commensurate with local conditions. Using this strategy, Crandell predicted runout lengths of debris-avalanches for Mount St Helens (Figure 5.20) and Mount Shasta (Figure 5.21) which are in good agreement with the actual extent of former avalanches. For example, at Mount St Helens, the debris-avalanche produced by the 1980 eruption travelled 29 km down the valley of the North Fork Toutle River. Taking an F value of 0.075 it was estimated that a debris-avalanche with a volume of at least 1 km^3 in that valley would have a length of 33 km, assuming pre-1980 topography.

Apart from the primary hazard, a number of secondary effects associated with debris avalanches also need to be taken into account in hazard assessments. These are to some extent dependent on local conditions. Mudflows are probably the commonest secondary hazard because wet avalanches may transform directly into mudflows or give rise to them after the primary avalanche has come to rest. Although it is generally not possible to predict whether potential avalanches will be wet or dry, it should be assumed that those forming on volcanoes covered in snow or ice will generate mudflows, which will pose an additional hazard down drainage from the limits of the primary avalanche hazard zone.

Historically, tsunamis have been the most destructive secondary hazard associated with debris avalanches. The seriousness of this is illustrated by the destruction and heavy casualties caused by the tsunami produced by the 1792 debris-avalanche at Mount Unzen. Any steep sided volcano in coastal areas should therefore be considered a potential hazard with respect to tsunamis generated by avalanches. The most hazardous areas will be those closest to the volcano in question, but even distant communities may be at risk because of the large distances travelled by tsunamis, as exemplified by the long-reaching tsunamis produced by the collapse of Ritter volcano in 1888. Given the run-out distances of the largest avalanches, even volcanoes tens of kilometres inland may have the potential to cause tsunamis in coastal areas.

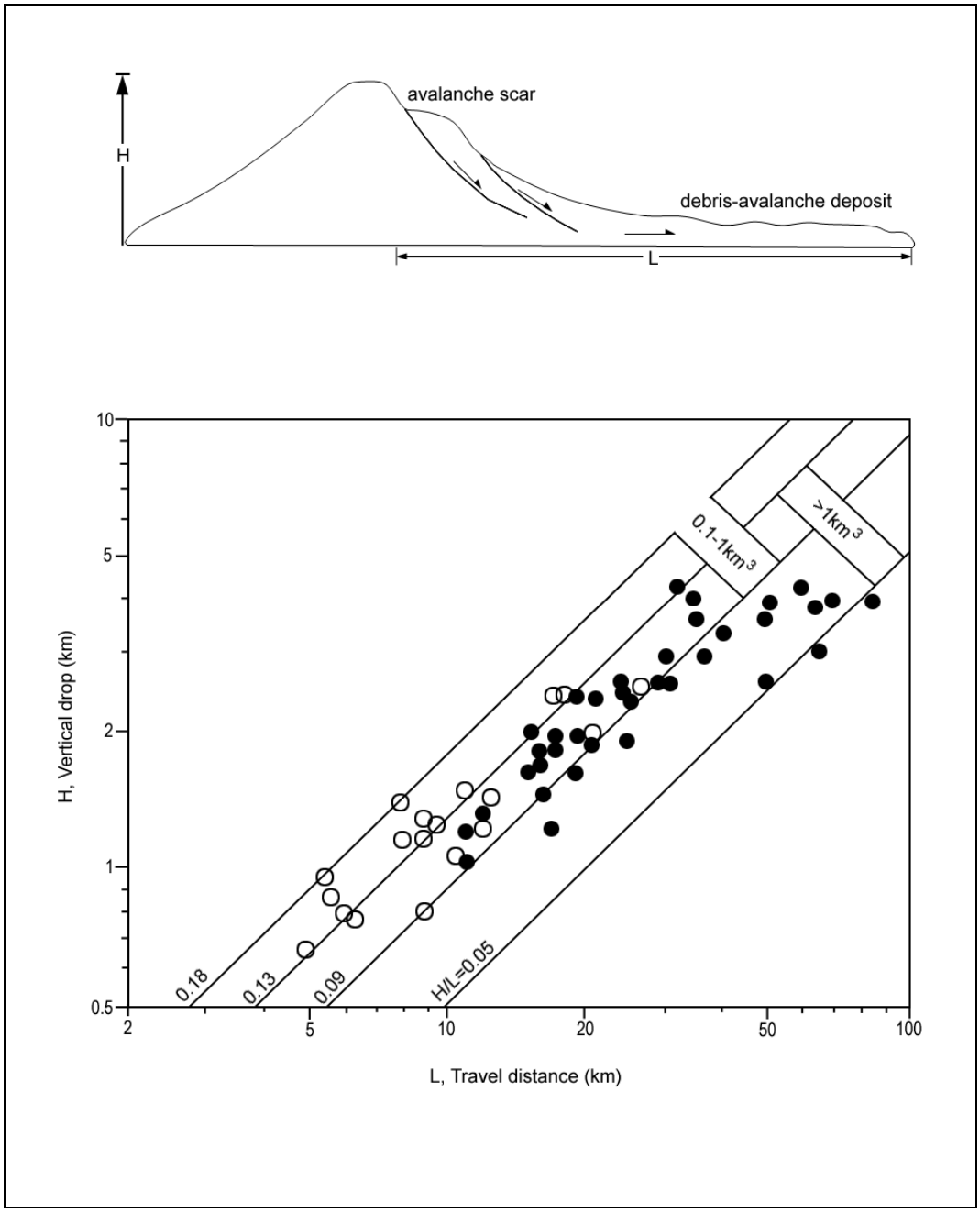

Figure 5.19: Travel distance (L) of Quaternary debris-avalanches relative to vertical drop (H) measured from top of source area (or former summit elevations, when known) to distal margin. Open circles are for deposits exceeding 1km^3. H/L ratios for volumes of 0.1-1km^3 are 0.09-0.18 (average 0.13) and for volumes exceeding 1km^3 are 0.05-0.13 (average 0.09). (After Siebert et al., 1987).

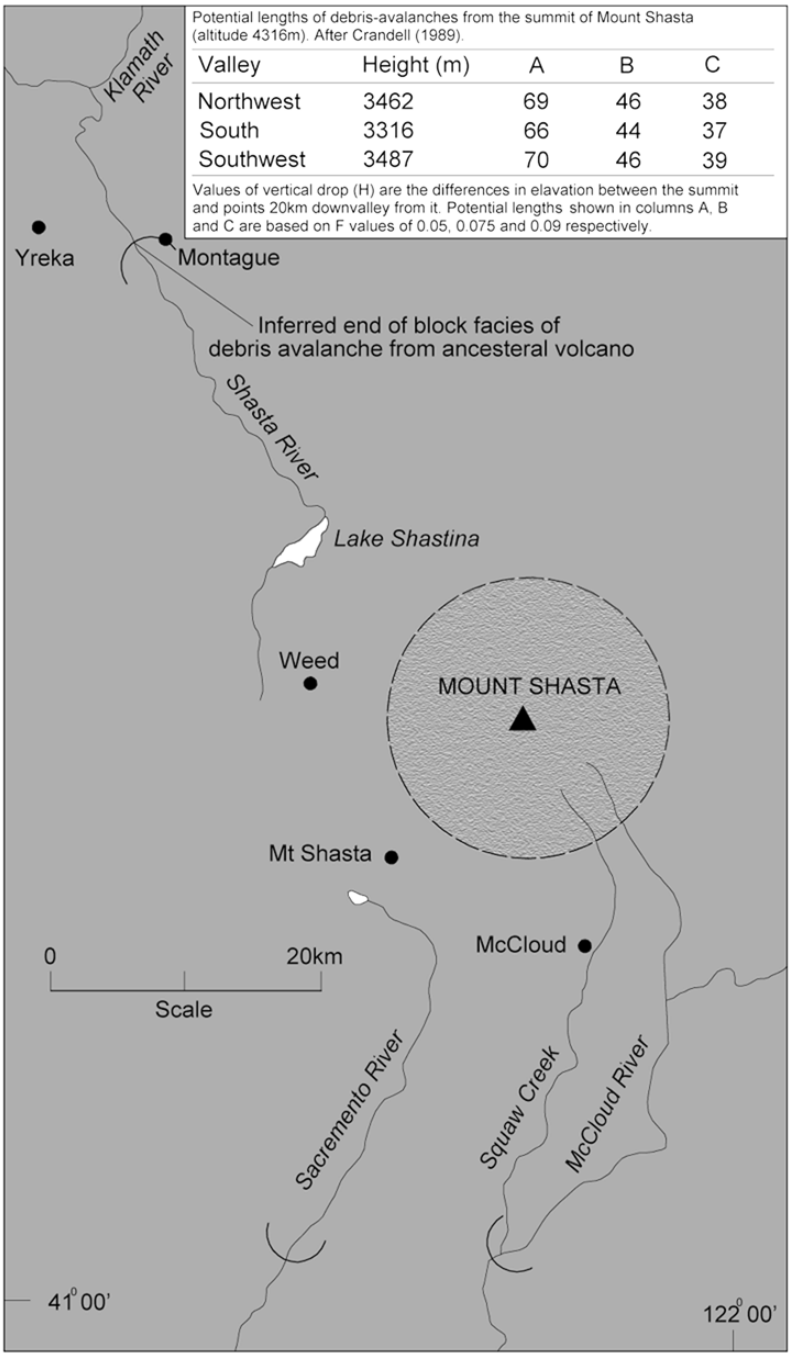

Figure 5.20: Map of Mount Shasta volcano and adjacent area. (After Crandell, 1989). Semicircles show the possible lengths of future debris-avalanches which have volumes of at least 1 km^3 in three valleys extending off the volcano. The lengths are based on differences in height between the summit and points 20km down each valley and on a height-to-length ratio of 0.075. The inferred end of the block facies of the prehistoric debris-avalanche deposit from the ancestral Mount Shasta is shown for comparison.

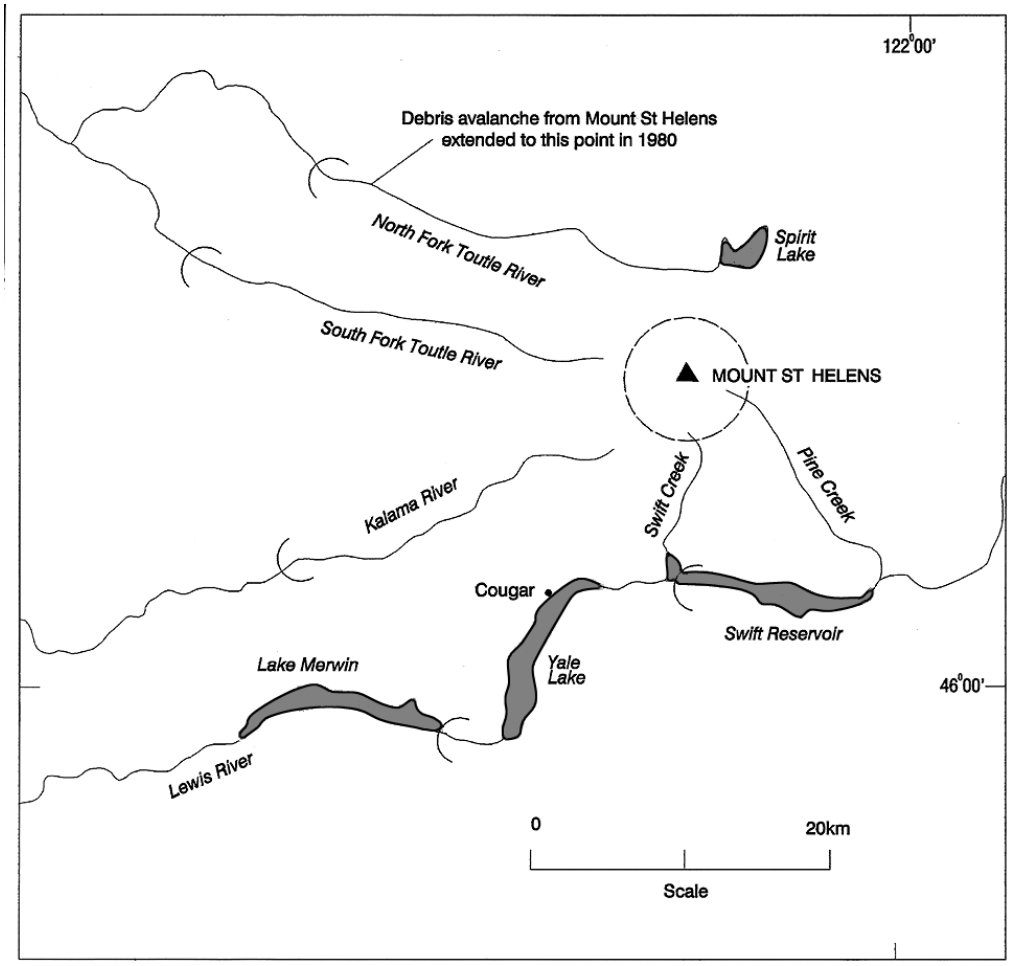

Figure 5.21: Map of pre-1980 Mount St Helens and adjacent area. Semicircles show the estimated lengths of debris-avalanches with volumes of at least 1km^3, that could have originated at the volcano before the 1980 eruption. The lengths are based on differences in height between the summit and points 20km down each valley and on a height-to-length ratio of 0.075. The end of the 1980 debris-avalanche in the North Fork Toutle River is shown for comparison. (After Crandell, 1989).

5.7 Lahars and Floods

Lahars, or **volcanic mudflows** as they are also termed, consist essentially of torrential floods or slurries of volcanic sediment and water which flow off the flanks of volcanoes, usually along pre-existing drainage courses. Settlements, agricultural developments and communications located in valleys downstream suffer in various ways from the effects of burial, erosion, flooding and destruction by physical impact.

Lahars are probably the most common of all volcanic hazards, occurring in association with all types of eruptions and also during periods of dormancy. They have been responsible for about 15% of deaths attributable to volcanic activity since 1600, although the proportion of fatalities increased during the 20th century to around 47%. One of the worst volcanic disasters of historic times was caused by a lahar which killed 23,000 people during the 1985 eruption of a Nevado del Ruiz in Colombia.

5.7.1 General characteristics of lahars

Lahars vary in nature and origin. They may be hot or cold and they show a range of physical characteristics which are largely dependent on the amount of sediment they carry in proportion to their water content. **Viscous mudflows** or **debris-flows** may contain more than 60% by volume of sediment (80% by weight) and have the consistency of wet concrete. Flows with higher water contents, but still with high sediment loads typically between 20 and 60% by volume, resemble torrential floods of particularly muddy water and are termed **hyperconcentrated flows**. The proportion of sediment to water is governed by a complex interplay of factors which include the source of the water, the rate and duration of flow, the quantity and grainsize characteristics of the mobilised sediment, and the morphology and gradient of drainage channels.

Vallance and Scott (1997) defined debris flows as having more than 60% sediment by volume, and they further distinguished between cohesive and non-cohesive debris flows on the basis of clay content, with cohesive flows having ratios of clay to total clay, silt and sand of 0.05 or greater. In their view, non-cohesive flows commonly begin as water floods which transform into dilute (non-cohesive) mudflows by the erosion and incorporation of sediment, whereas cohesive flows typically begin as water-saturated avalanches which transform into debris flows that remain as debris flows until termination. Vallance and Scott suggested that the water-saturated debris avalanches which give rise to cohesive debris flows contain a high proportion of clay-rich hydrothermally altered rock.

Lahars exhibit complex flow behaviour, changing in character from debris flow to hyperconcentrated flow and *vice versa*. Debris-flows are non-Newtonian fluids which in general move as a coherent mass in a laminar fashion, whereas hyperconcentrated flows are more fluid and turbulent.

The bulk density of cohesive lahars is sufficiently high that they are capable of carrying boulders and vehicles in suspension, and can even move large man-made constructions such as houses or bridges. Cohesive lahars tend to deposit their sediment and raise the beds of drainage channels, particularly in the lower reaches of drainage systems where gradients are less steep. This increases the likelihood of subsequent lahars or floods overspilling channel margins and inundating adjacent land. As a result, river channels may shift their courses significantly. During their passage, lahars commonly show alternating changes in consistency and velocity due to variations in valley morphology and to additional inflows of water or pulses of lahar joining from tributary valleys. Velocities typically range from less than 10 km/h up to a few tens of kilometres per hour, but on steep slopes can be much higher: For example, during the 1980 eruption of Mount St Helens some mudflows on steep slopes are estimated to have had speeds exceeding 40 m/s (145 km/h) (Janda, 1981).

Lahars form by a number of different processes, which include:

- Mobilisation of pyroclastic deposits by rain
- Melting of snow or ice during eruptions
- Derivation from water-saturated debris avalanches
- Explosions within crater lakes
- Pyroclastic flows entering rivers

5.7.2 Mobilisation of pyroclastic material by rain

During and in the aftermath of eruptions, unconsolidated volcanic deposits such as ash or pumice on the flanks of volcanoes are readily mobilised into lahars by rainfall. This is particularly prevalent on steep-sided volcanoes in tropical regions subject to torrential rainfall. The problem is aggravated in tropical climates because an impervious weathered capping often forms on the surface of ash deposits, which reduces rainfall infiltration and results in a concomitant increase in surface run-off and flooding. Run-off is also enhanced when vegetation has been killed or stripped of foliage due to tephra falls. Major pyroclastic eruptions are also often accompanied by torrential rainfall and electrical storms which can cause mudflows simultaneously with the deposition of pyroclastic material.

Rainfall-generated lahars usually begin as strongly erosive hyperconcentrated flows which are channelled along incised headwater valleys and gorges draining volcano flanks. During their passage they incorporate increasing proportions of sediment by erosion and through this 'bulking-out' process can evolve into more viscous sediment-rich flows. Lahars generated in this manner are probably the most common type of lahar and are a persistent hazard at many volcanoes.

Mount Pinatubo provides a well-studied example of the hazard posed by lahars produced by the mobilisation of pyroclastic deposits. Its eruption in 1991 produced a large volume of ash and pumice, variously estimated to have been between 4 and 8 km^3, which mantled the flanks of the volcano and choked valleys. The eruption coincided with torrential rainfall caused by a passing typhoon, which mobilised large amounts of the tephra in numerous hot lahars during and in the aftermath of the eruption. Most of the tephra remained on the volcano and subsequent typhoons and rainstorms continued to produce large and destructive lahars for a number of years, many of which were hot.

Studies at Pinatubo indicate that tephra was remobilised by a number of mechanisms (Rodolfo *et al.*, 1996). Hot lahars were triggered by rainfall with threshold values of 0.3 to 0.4 mm per minute sustained over periods longer than 30 minutes. Others were generated as a result of mass failure, induced by steam explosions, of partially water-saturated unconsolidated tephra blocking headwater channels in pyroclastic fans. The initial lahars usually contained 20-60% sediment and moved downstream as turbulent hyperconcentrated flows, but when rainfall and flow-rates were particularly high, sufficient sediment could be incorporated to produce debris-flows. Hot lahars displayed transitional flow characteristics, starting as turbulent hyperconcentrated flows which transformed during peak discharges into debris-flows with smooth slurry-like surfaces, before reverting once more to turbulent

hyperconcentrated flows in the waning stages. Interaction of principle lahar channels and contributing tributaries with variable discharges, including tributaries not draining areas with tephra, resulted in multiple peak discharges and complex flow behaviour. The average temperature of hot lahars in 1992 was slightly above 45°C, but some were as hot as 70°C, whilst the earliest flows in 1991 may have been even hotter (Rodolfo *et al.*, 1996).

The velocities with which the lahars move is dependent upon stream gradient. Speeds of 7-10 km/h were typically recorded on the gently sloping lower flanks of Pinatubo, but in headwater regions they were considerably faster. Punongbayan *et al*. (1992) also reported that for a given gradient the more viscous mudflows tended to move more quickly than hyperconcentrated flows because they expend less energy in turbulence and tended to flow more smoothly in relatively straight lines. This, however, contrasts with observations following the 1980 eruption at Mount St Helens, where more dilute water-rich lahars had significantly higher average velocities than viscous sediment-rich lahars (Cummans, 1981). In the lower reaches of the Pinatubo drainage systems the lahars deposited much of their sediment and continued as floods of muddy water. Deposition in these areas raised the beds of drainage channels causing later flows to spill sideways and inundate large tracts of land. In this way river courses were diverted and large areas of agricultural land and many settlements buried.

Studies have been undertaken at a number of volcanoes in order to quantify the factors that influence the initiation of rain-generated mudflows from poorly consolidated pyroclastic deposits. Such information may be used to predict the threshold conditions necessary for the formation of lahars in a given area, and therefore have application in hazard forecasting.

The most important of these factors are:

- Intensity and duration of rainfall
- Angle and length of slope
- Volume of pyroclastic material on the surface

Research in Japan, based on empirical and experimental data from Mount Usu and Unzen (Bryant, 1992; Yanagi *et al.*, 1992) indicate that lahar occurrence criteria can be expressed by the following relationship:

$$R_{lhr} = ((Dk)/L)\tan\theta$$

Where:

R_{lhr} = hourly rainfall rate (cm/sec)
D = depth of ash deposit (cm)
k = coefficient of permeability (cm/sec)
L = length of slope (cm)
θ = angle of slope (degrees)

This relationship has been employed by the present project in the case study of volcán Irazú

(Young *et al.* 1998) to estimate the amount of rainfall required to trigger lahars from unconsolidated pyroclastic deposits on the upper flanks of the volcano. For slopes with angles of around 35° and lengths of between 300 and 800 metres, and coefficients of permeability between 0.5 to 5 cm/sec, it was estimated that rainfall exceeding 10 mm/h could trigger lahars at Irazú for ash layers ranging between 20 and 50 cm in thickness. Because of uncertainties, estimates of this type should only be used as indicators rather than exact predictors. In the Irazú study for example, a table was compiled for various hourly rainfall rates and ash thickness, and the probability of lahars was expressed in relative terms as presented in Table 5.1.

Precipitation rate (mm/hour)	Probability of lahar Ash layer c. 20cm	Probability of lahar Ash layer c. 50cm
<10	Possible	Unlikely
10 – 30	Likely	Possible
31 – 50	Very likely	Likely
>50	Extremely likely	Very likely

Table 5.1: Rainfall intensity and likelihood of lahar occurrence at Irazú (Young *et al.*, 1998)

5.7.3 Lahars formed by the melting of snow and ice

Some of the largest and most destructive lahars and floods have been produced by eruptions on volcanoes that have substantial snow and ice caps. Even relatively small eruptions at such volcanoes have the ability to produce catastrophic lahars.

Major and Newhall (1989) reviewed the information on lahars and floods caused by eruptions on snow and ice covered volcanoes during historical times. Most of these volcanoes occur at latitudes higher than 35°, although at lower latitudes the hazard is also prevalent on volcanoes that generally exceed 4,000 m in height.

Major and Newhall identified five main eruptive mechanisms that can melt snow and ice caps, but not all of these produce sufficient meltwater to generate lahars. These mechanisms are:

- Deposition of tephra fall
- Surface melting by lava flows
- Ejection of water by eruptions through crater lakes
- Basal melting of ice and snow by subglacial eruptions or geothermal activity
- Scouring and melting by pyroclastic flows, surges and blasts

Tephra falls alter the ablation rate of snow and ice, and when hot have been known to produce minor amounts of meltwater, but of insufficient volume to cause lahars.

Lavas flowing over ice and snow do not generally cause sufficiently rapid melting to form large lahars and floods, because heat transfer by conduction is slow, and meltwater that is produced tends to be converted to steam. Small lahars are known to have been produced by the eruption of lavas onto snow and ice at Llaima and Villarrica volcanoes in southern Chile. Large lahars have also occurred at these volcanoes (Young, 1998), but are caused by subglacial melting of ice by lava and the ponding of meltwater, which eventually bursts out (see jökulhaups below).

Explosions in crater lakes can eject water onto snow and ice, causing melting and the production of lahars. In historic times four episodes of crater-lake explosions have produced lahars on Ruapehu volcano in New Zealand, the largest and most recent events having occurred during the 1995-96 eruption. Two of these eruptions occurred in summer time when snow and ice cover was limited, but even during the winter event of 1969 the main source of water appears to have been from the lake itself and not from the melting of snow and ice. Lahars produced by crater lake explosions in 1995 were reported to contain very little liquid water, but to have consisted of between 70% and 90% by mass of entrained snow and ice particles. These deposits froze almost immediately, corroborating the view that explosive expulsion of the crater lake water does not cause significant melting of snow and ice.

Heating at the base of ice sheets or snowpacks by lavas or geothermal systems produces meltwater, the ponding of which can lead to sudden outbursts. The majority of glacier outbursts of this kind in historic times have occurred in Iceland where they are known as **jökulhaups**. Most have produced large floods of water and ice, although during the subglacial eruption at Katla in 1918 two catastrophic sediment-rich mudflows covered an area of about 400 km^2. These had discharge rates of 10^5-10^6 m^3/s and contained more than 80% sediment and carried enormous amounts of ice. The most recent Icelandic jökulhaups occurred during the Gjálp eruption beneath the ice cap of Vatnajökull in 1996. It has been calculated that 3 km^3 of ice was melted during the 13 days of the eruption and a further 1.2 km^3 during the following three months (Gudmundsson *et al.*, 1997). During the first four days of the eruption an average of between 0.4 - 0.6 km^3 of ice was melted per day.

Floods and lahars produced in the same manner as jökulhaups, but on a smaller scale, can also occur under certain circumstances at stratovolcanoes, as exemplified by Villarrica in southern Chile (Young, 1998, and Section 6.3 of this report). Here ponding of sub-glacial lavas within the ice-filled summit caldera causes significant melting, which from time to time results in sudden breaches of the ice and the formation of destructive lahars which are a persistent hazard to the surrounding area.

The most common and hazardous lahars produced from snow and ice are those generated by pyroclastic flows and surges. This is because pyroclastic flows and surges have the ability to scour the surface and turbulently entrain and mix large amounts of snow and ice with hot pyroclastic material, promoting very efficient melting and the liberation of large volumes of water with sufficient rapidity to trigger lahars. Fracturing of the ice by precursor seismic and explosive activity greatly increases the efficiency of the mixing and melting process, and the

size of the ice cap is also an important influence, with larger surface areas having greater potential for melting.

Because pyroclastic flows and surges are able to promote rapid melting of snow and ice, even relatively small eruptions on the summits of snow-clad volcanoes can generate large lahars which have catastrophic effects on relatively distant settlements down-drainage. This important point is all too poignantly illustrated by the 1985 eruption of Nevado del Ruiz in Colombia. During this relatively small eruption (VEI3) pyroclastic flows and surges scoured and melted 5-15% of the volcano's ice cap: The process of mixing and heat transfer was also probably enhanced by fracturing of the ice cap by precursor seismic shaking (Pierson *et al*., 1985). The meltwaters together with pyroclastic material and avalanches of snow, slush and ice were rapidly channelled into narrow headwater valleys where tremendous floods scoured loose sediment and soil and developed into catastrophic (non-cohesive) lahars. Approximately 50 km to the east of the summit of the volcano the lahars disgorged from the mouth of the canyon of the Rio Lagunillas (Figure 5.22) and engulfed the city of Armero, killing about 23,000 of its 29,000 inhabitants. The lahars arrived in pulses. The first and largest took approximately one and a half hours to reach Armero, travelling at an average velocity of 38 km/h, and issued from the mouth of the Lagunillas canyon at a rate of about 27,000 m^3/s, producing a wave nearly 40 m high. A second large pulse arrived 15 minutes later, followed by six smaller pulses over the following hour and ten minutes. The 1985 lahars at Nevado del Ruiz were not a unique event. The tragedy was that Armero was located on a debris fan at the mouth of the canyon and was known to have been overrun by destructive lahars during eruptions of the volcano in 1595 and 1845.

It has been estimated that at Nevado del Ruiz 5×10^6 m^3 of magma ejected as pyroclastic flows produced about 2×10^7 m^3 of meltwater, which generated 9×10^7 m^3 of lahar slurry. Melting took place predominantly at the surface of the ice cap over an area of about 10 km^2. Pierson *et al*. (1990) concluded from this fact that the surface area of an ice cap is more important than its volume when considering the magnitude and hazard of potential lahars. Additional lessons from the Nevado del Ruiz catastrophe are that lahars can increase in volume significantly during flowage by the entrainment of water and eroded sediment, and that confined valleys can maintain high velocities over long distances and produce catastrophic impacts at considerable distances downstream from an eruption.

Cotapaxi is another very high Andean volcano situated almost on the equator, where catastrophic lahars produced by the melting of snow and ice have been a common feature during historical and prehistorical times (Mothes, 1992). During the last eruption of Cotopaxi in 1877 a relatively small scoriaceous pyroclastic flows melted snow and ice on the summit and produced devastating lahars which caused loss of life at considerable distances from the volcano.

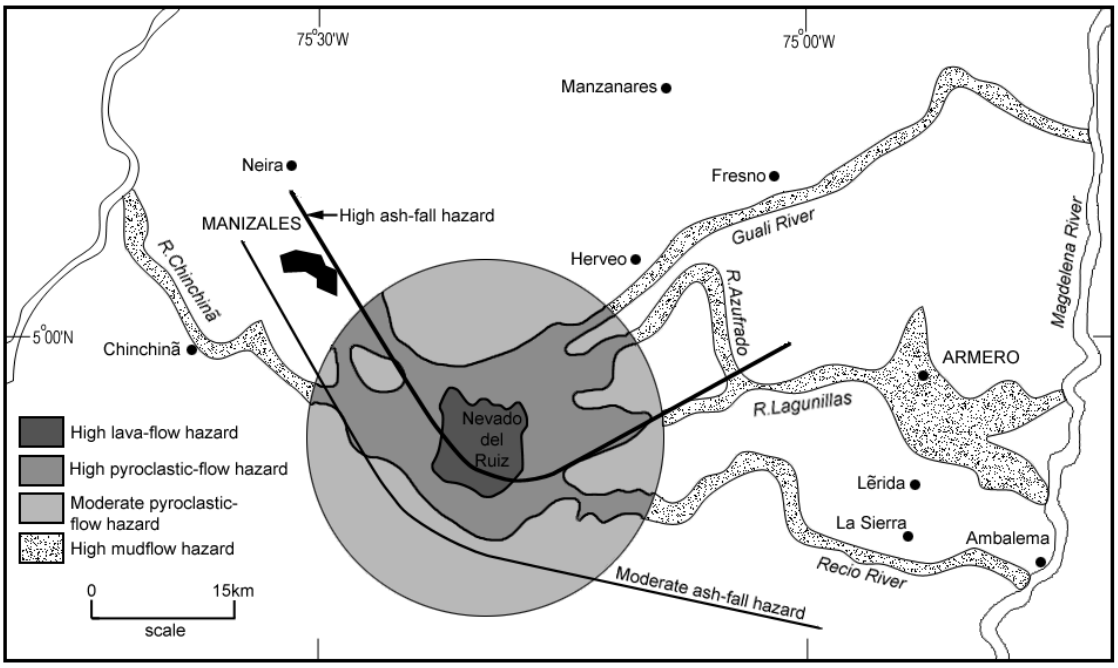

Figure 5.22: Simplified volcanic hazard map of Nevado del Ruiz, Colombia. (After Parra and Cepeda, 1990, Figure 3). During the eruption of 13 November 1985, mudflows travelled down the Chinchiná, Guali, Azufrado and Lagunillas rivers and were confined to the areas previously designated as high mudflow hazard zones. Lahars were disgorged from the mouth of the Lagunillas gorge where they spread laterally and engulfed the town of Armero.

Although the historic mudflows of Cotopaxi may have been large and destructive, they pale into insignificance in terms of size when compared with a prehistoric flow which occurred approximately 4,500 years ago (Mothes *et al.*, 1998). During this event a small sector collapse occurred on the north and northeast flanks of Cotopaxi and was followed by the eruption of a rhyolitic pyroclastic flow of moderate size which melted part of the volcano's ice cap and transformed very rapidly into an enormous mudflow (the Chillos Valley Lahar). The mudflows were channelled along valleys, travelling 326 km to the northwest before entering the Pacific Ocean, and more than 130 km eastwards into the Amazon Basin. The ash-flows are estimated to have had a volume of about 2.5 km^3 and were transformed into mudflows with an estimated water content of 30% and a volume of about 3.8 km^3, which is 40 times greater than the volume of the catastrophic 1985 flows of Nevado del Ruiz (0.09 km^3). The deposits of the mudflows cover an area of 440 km^2 and have an average thickness of 2 m. Along the main valleys the flows reached widths of up to 11 km and depths ranging from tens of metres up to 200 m where they became constricted and ponded. The mudflows do not appear to have picked up much extraneous sediment during flow, and their deposits are very similar in composition to those of the parental ash-flow. The very rapid transformation of the pyroclastic flow into the mudflow took place over a distance of only a few kilometres, and is believed to have been influenced by the precursor sector collapse, which probably thoroughly fragmented the ice cap, so promoting efficient mixing and melting of the ice within the pyroclastic flow that followed.

—

5.7.4 Lahars derived from water-saturated debris avalanches

As described in section 5.6, lahars are a common secondary hazard associated with debris avalanches. These may be generated in a number of ways.

When wet or water-saturated debris avalanches come to rest, large amounts of the water may drain away rapidly as mudflows, extending the hazard far beyond the limits of the avalanche.

Water saturated debris avalanches may also evolve directly into mudflows. The enormous Osceola mudflow of Mount Ranier illustrates this point (Vallance and Scott, 1997). Approximately 5,600 years ago a debris avalanche occurred on the flanks of Mount Ranier during the course of a summit phreatomagmatic eruption. The avalanche had a volume of 3.8 km^3 and was composed of water-saturated, clay-rich hydrothermally altered and weakened rock which transformed completely into a clay-rich cohesive debris flow within 2 km of the source. This filled valleys to depths of a 100 m and flowed north and west for 120 km, covering 200 km^2 of the Puget Sound lowland. The flow is estimated to have had a peak discharge rate of 2.5×10^6 m^3/s and a velocity of 19m/s at a distance of 40-50 km downstream. Another giant lahar, the Paradise mudflow, flowed down the south side of the volcano and was probably genetically related to it.

Vallance and Scott (1997) reviewed the information on cohesive debris flows and suggested that the amount of hydrothermally altered clay-rich rock in the pre-avalanche mass determines whether a debris avalanche transforms into a cohesive debris flow or remains largely as an unsaturated debris avalanche. The clay-rich material is thought to provide a ready and abundant source of dispersed water necessary for the transformation of debris avalanches into debris flows.

5.7.5 Lahars originating in crater lakes

The explosive expulsion of water from summit crater lakes can generate very destructive lahars, sometimes without warning. This, however, only occurs at a relatively small number of volcanoes, but is nevertheless a serious hazard where populations exist.

Kelud volcano in eastern Java has a deep crater lake which has repeatedly been the source of devastating lahars. In historic times these have mostly occurred when water in the lake has been blown out during eruptions, although one major lahar is also known to have been generated when a large volume of water spilled through a breach formed in the lowest point of the crater rim during a period of heavy rainfall. The area most prone to lahars occurs on the southwest flanks, adjacent to the lowest part of the crater rim, where in 1919 one explosive eruption produced a lahar that covered an area of 130 km^3, damaging or destroying more than 100 villages and killing 5,110 people. The lahars of this disaster are estimated to have travelled at an average speed of 64 km/h. After this particular disaster a series of tunnels were constructed to partly drain the lake. This has proved to have been largely effective in reducing the hazard.

Ruapehu in New Zealand is another volcano were explosive expulsion of water from a summit crater lake has been a persistent hazard. One such explosion in 1953 generated a mudflow which destroyed a railway bridge on the lower flanks of the volcano just as a train was passing, causing the deaths of 151 people.

5.7.6 Hazard zoning and mitigation for lahars

Although lahars are probably the most common of all volcanic hazards, there is much that can be done to mitigate against their effects. This is because the generation of lahars can be anticipated with reasonable confidence once an eruption is underway and certain pre-requisite conditions are met, and because potential flow courses can be predicted accurately.

Mitigation against the effects of lahars may be achieved by three broad groups of measures, which are:

- Hazard ***zoning*** and long term land-use planning
- Warning systems
- Engineering measures

As a first step to hazard assessment the deposits of previous lahars should be identified and mapped. Although laharic deposits are fairly distinctive, their absence or apparent absence does not necessarily mean that the threat of lahars does not exist; in particular, hyperconcentrated flows or floods produced by eruptions on snow and ice-capped volcanoes can be strongly erosive and leave no significant deposits within the immediate environs. Historical or local information should therefore be sought in helping to establish the extent and frequency of previous lahars.

As a conservative approach to hazard assessment, all valleys draining volcanoes should be considered at risk from lahars. Valleys in proximal areas close to volcanoes are also likely to be subject to a range of gravity controlled hazards such as pyroclastic flows and lava flows in addition to mudflows and floods. It is therefore probably more practical in proximal areas to delimit zones of combined flowage hazards. This approach has been adopted for several volcanic hazard maps produced by the United States Geological Survey. At Mount St Helens for example, Crandell and Mullineaux (1978) delimited a flowage-hazard zone covering the volcano and immediately surrounding area that could be affected by future pyroclastic flows, lava flows, mudflows and floods. Farther from the volcano additional hazard zones were delimited along the main drainage courses for mudflows and floods (Figure 5.23). The hazard zones have gradational boundaries and are based on the extent of flowage hazards during the last 4,500 years. Estimated probabilities of future flowage hazards are given for each zone, based upon the past frequency of such events. The interval of 4,500 years was chosen because of the large number and variety of eruptions that have occurred during that period. At Mount Shasta, zones have been delimited in a similar manner for the combined flowage-hazard of mudflows and pyroclastic flows (Figure 5.13).

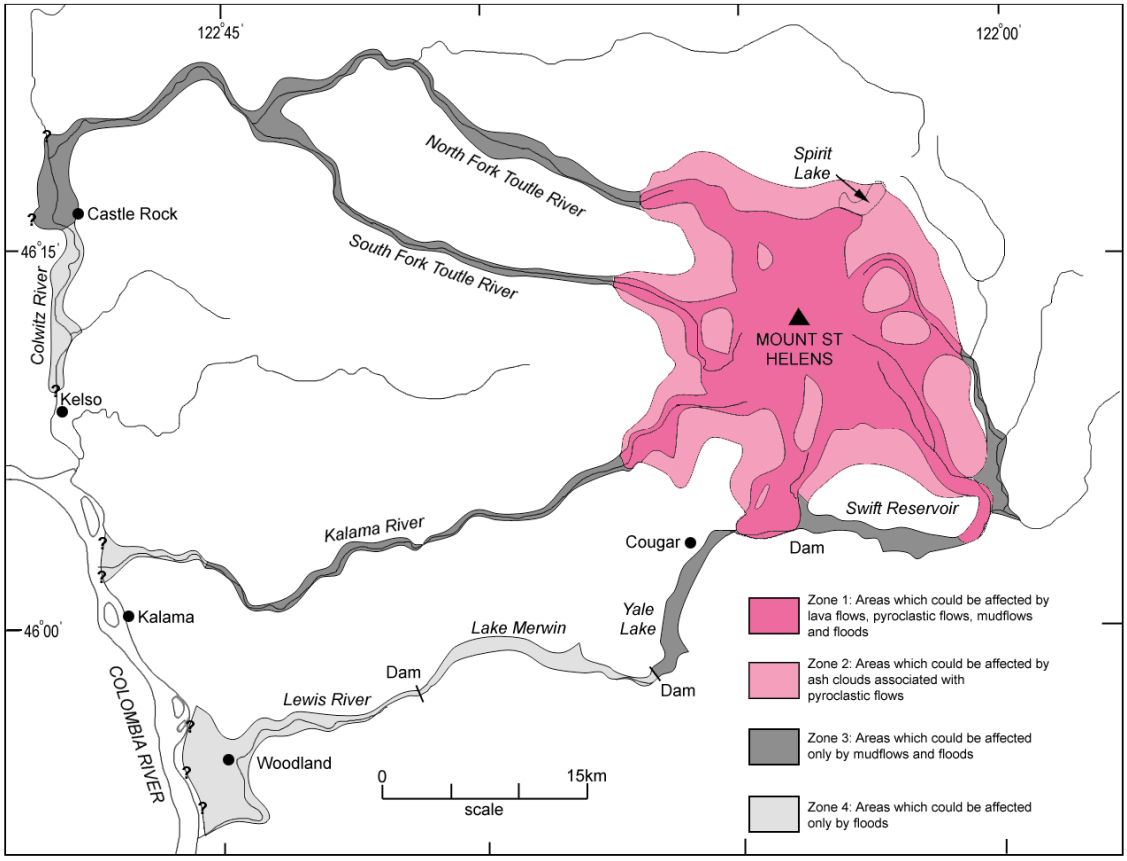

Figure 5.23: Simplified map of potential hazards at Mount St Helens (after Crandell and Mullineaux, 1978). Zone 1 delimits an area of combined flowage hazards which include mudflows and floods in addition to pyroclastic flows and lava flows. Zone boundaries were based on the extent of lava flows, pyroclastic flows, mudflows and floods during the last 4500 years. The 4500 year interval was chosen because of the large number and variety of eruptions that occurred during that time. Boundaries between zones are gradational. The area of the volcano covered by Zone 1 has experienced flowage hazards at an average rate of one per century. The inferred average frequency of mudflows in Zone 2 ranges from at least one per 500 years at the up-valley end to at least one per 3000 years at the down-valley end.

Although valleys in volcanic areas are at risk from lahars, they commonly offer the most suitable ground for settlement and agricultural development within an otherwise difficult terrain. Therefore, even though areas prone to be affected by lahars can be delimited relatively precisely, it may be difficult to enforce hazard ***zoning*** in land-use planning. Accepting this conflict of interest, wherever possible the construction of buildings or the development of communities should be undertaken away from river channels on relatively high ground, such as valley sides or river terraces. Strategic facilities or sensitive developments such as hospitals, schools, airstrips and communications installations should not be constructed in high risk areas, and wherever possible existing facilities should be relocated. Development should not be allowed in confined valleys nor near the mouths of such valleys where they disgorge in piedmont areas.

Although lahars move quickly it is often possible to provide warnings and evacuate populations to higher ground to avoid casualties. There are a number of ways in which warnings can be provided. Lahars might reasonably be expected during the course of

eruptions on ice and snow-capped volcanoes, or during periods of heavy rainfall contemporaneous with or following pyroclastic eruptions. Under these circumstances communities considered to be under threat should be put on alert or evacuated. Radio-telemetred rain gauges can provide information on the amount and rate of rainfall occurring on the flanks of volcanoes, and can be used to trigger warnings once empirically pre-determined local threshold conditions have been exceeded. Observation posts situated in headwater regions can provide warnings of lahars to communities down drainage. Warnings can also be provided by telemetered sensors positioned strategically within the drainage network upstream from communities. These usually work on the principle of trip wires strung across drainage channels. Lahars also produce characteristic seismic signals which can be detected on volcanoes which have seismic monitoring networks.

The control of lahars by engineering structures has proved to be successful in some regions. Such structures include embankments or dikes, diversion dams and storage reservoirs. These constructions are expensive and are generally not affordable in developing countries, or may only be justifiable where risks are high. In the longer term, however, engineering measures can aggravate the problem by causing the accumulation of sediment, which may eventually be remobilised when structures fail, to produce destructive lahars.

5.8 Tsunamis

Tsunamis are very large sea waves produced by the displacement of water caused by the sudden movement of the sea floor during submarine earthquakes or submarine landslides, or as a result of volcanic activity. Although only about 5% of historic tsunamis have been of volcanic origin, those that have occurred have been very destructive and are estimated to have caused 20-25% of deaths related to volcanic activity since 1000 AD (Latter, 1981).

The velocity of tsunamis increases with water depth according to the relationship:

$$c=(gH)^{1/2}$$

Where:

c = velocity
g = acceleration due to gravity
H = water depth

Consequently in deep ocean waters the velocities of tsunamis commonly reach 700-800 km/h. Here they have very large wavelengths, ranging from tens to hundreds of kilometres, but their amplitudes or heights are very low, being typically about a metre or less. Because of their very large wavelengths and small amplitudes, tsunamis are not obviously apparent in the open ocean, although they may be detected as abnormal tidal fluctuations on tidal gauges. On entering shallow coastal waters tsunamis rapidly decelerate and at the same time dramatically increase in amplitude and decrease in wavelength. As a result they may appear almost suddenly in coastal areas, growing rapidly in height to several tens of metres, and travel inland causing considerable destruction and casualties.

—

5.8.1 Tsunamis related to volcanic activity

Tsunamis are known to have been caused by a number of different volcanic mechanisms which are summarised in a review by Latter (1981). Of these, the commonest and most destructive volcanogenic tsunamis result from the displacement of water by volcanic avalanches entering the sea. Catastrophic subsidence of submarine or island volcanoes is also an important mechanism, and shock waves caused by explosions are also known to have generated destructive tsunamis.

The most destructive volcanogenic tsunamis in historic times were associated with the 1883 eruption of the island volcano of Krakatau situated in the Sunda Straits of Indonesia. The first tsunami caused by the eruption was followed over a period of 24 hours by a series of waves of gradually diminishing height, 14 of which occurred at almost regular intervals of about 2 hours. These reached heights of more than 15 m in coastal areas around the Sunda Straits (Wharton, 1888) and are estimated to have killed more than 34,000 people in Java and Sumatra, with casualties occurring up to 120 km from the volcano. In terms of fatalities, this represents the second most catastrophic volcanic disaster of historic times and serves to illustrate the seriousness of the hazard posed by volcanogenic tsunamis to coastal communities. Debate has surrounded the origin of the Krakatau tsunamis. Latter (1981) concluded that they were caused by several different mechanisms, including the impact of pyroclastic flows and rockfalls on the sea, the impact of atmospheric shockwaves, and the displacement of water as a result of subsidence. Yokoyama (1981) concluded that the main tsunami was caused by the sudden upheaval of seawater due to a violent explosion: Calculations by Yokoyama suggest that the seawater in the area of Krakatau was elevated by 30-40 metres by the explosion. Numerical modelling by Normandhoy and Satake (1995) suggested that each of the three mechanisms of collapse, pyroclastic flow impact and submarine explosion, could have displaced sufficient water to generate the tsunamis, but that the explosion model provides the best comparison with the observed waveforms and wave heights of the largest tsunami. Francis (1985) also reasoned that whilst pyroclastic flows may have caused a number of small tsunami, the most plausible mechanism for the large destructive tsunamis was a major submarine collapse of the volcanic edifice associated with a large explosion, in many ways akin to the debris avalanche and associated lateral blast of the 1981 eruption of Mount St Helens (see Figure 5.15.). The irregular topography of the sea floor to the north of Krakatau is strongly suggestive of the existence of a slumped mass, and supports the collapse hypothesis (Francis, 1985; Francis and Self, 1983).

Some of the most destructive tsunamis are generated by large-scale debris-avalanches entering the sea. At Mount Unzen in Japan in 1792 the collapse of an old inactive lava dome produced a debris-avalanche which overrode the town of Shimabara, killing 10,000 people, and entered the sea. The ensuing tsunami caused widespread destruction in nearby coastal areas, killing an additional 4,300 people (Kuno, 1962). This avalanche was not associated with an eruption and occurred without warning.

A similar event also occurred in 1888 at Ritter Island off the coast of New Britain. This was a steep-sided volcano which collapsed, apparently without any significant precursor eruptive activity (Cooke, 1981). Approximately 2 km^3 of rock avalanched into the sea, leaving only a small remnant above sea level, and this generated a 12-15 m high tsunami which devastated neighbouring coasts up to 470 km away.

Mount St Augustine is an island volcano situated in the Cook Inlet of Alaska, and has been the source of frequent debris-avalanches in historic times that have caused tsunamis (see Section 5.6.2). Here catastrophic collapses of the steep summit region have occurred cyclically with a periodicity of 150-200 years. In 1883 the collapse of a small lava dome produced a debris-avalanche which entered the sea and caused a tsunami (Kienle *et al*., 1987). Four waves were recorded within Cook Inlet travelling at 30 mph (50 km/h) and rising 20 feet (6 m) above normal levels. Fortunately this occurred at low tide and although houses were deluged and fishing boats carried off, damage was relatively minor.

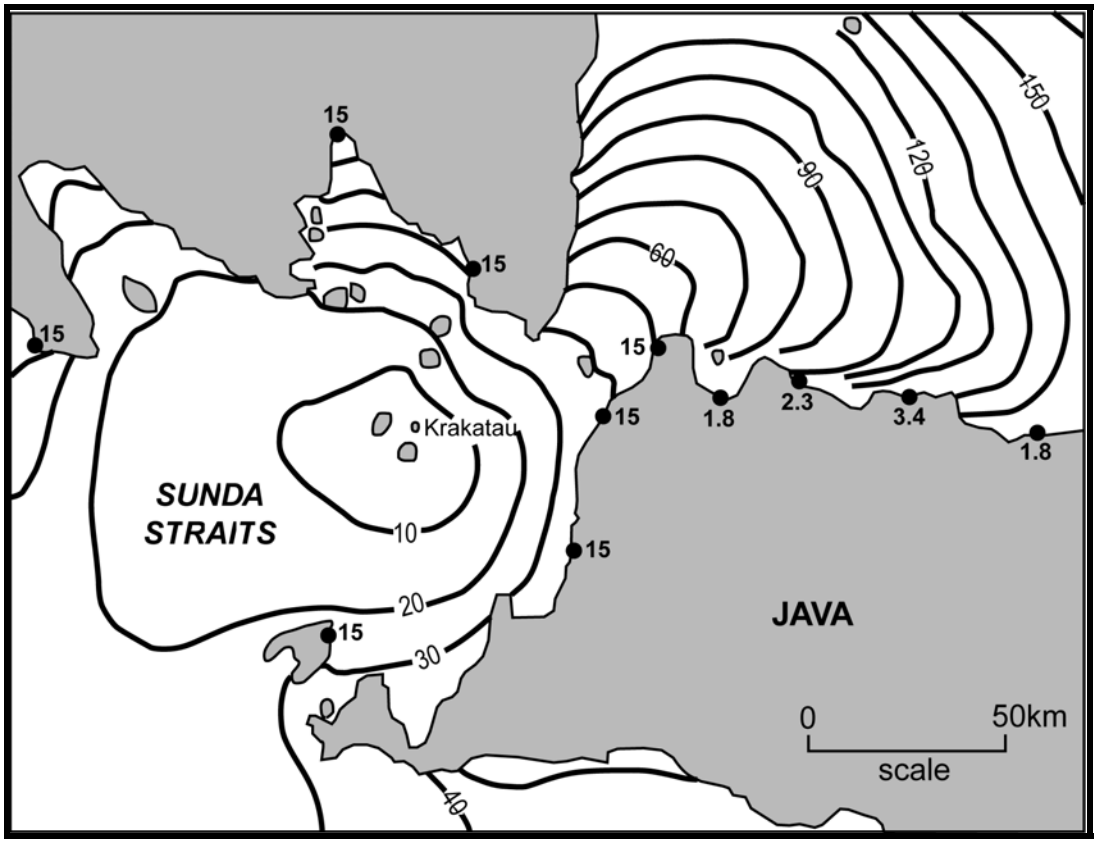

Figure 5.24: Refraction diagram of tsunami caused by the 1883 eruption of Krakatau showing travel time in minutes and wave heights at coastal locations in metres. (After Yokoyama, 1981 with information on wave height from Wharton, 1888).

Latter (1981) cited the 1871 tsunami at the Indonesian volcano of Ruang as an example produced by the impact of pyroclastic flows on the sea. This was based on the description of Neumann van Padang (1959) of a destructive and fatal tsunami, locally up to 25 metres high, which was reported to have been produced by a pyroclastic flow generated by the collapse of an active summit lava dome. However, the original description of Neumann van Padang suggests that the triggering event may have been more akin to a debris avalanche produced by the collapse of a large portion of the dome, rather than by a pyroclastic flow entering the sea. A rapid displacement of substantial volumes of water is necessary for the generation of tsunamis. Whilst debris avalanches generated by the wholesale collapse of domes can produce

such displacements and are known to have generated tsunamis, small to moderate size block-and-ash flows may not generally have sufficient volume nor enter the sea over a broad front with sufficient rapidity to displace enough water by sudden impact. This point is supported by evidence from the recent eruptions of Montserrat, where numerous block-and-ash pyroclastic flows produced by the piecemeal collapse of the dome have entered the sea without generating tsunamis. On the other hand, a small tsunami was produced when part of a debris avalanche reached the sea during a major collapse of the dome in December 1997 (Calder *et al*., 1998). Large pyroclastic flows entering the sea over a broad front may however be capable of generating tsunami, as proposed for example in the case of Krakatau (see above).

5.8.2 Hazard zoning and mitigation of volcanogenic tsunamis

Significant tsunami hazards exist near many coastal volcanoes in the circum-Pacific region, the West Indies and the Mediterranean.

Although this section is primarily concerned with volcanogenic tsunamis, further insight into the hazard may be gained by considering information on tsunamis generated by earthquakes, which are much more common and for which mitigation procedures have been established. Warning systems exist for earthquake-related tsunamis in the Pacific region and are actuated when large earthquakes (M_s 7.0) occur in known tsunamigenic regions. A Pacific-wide system issues warnings within about an hour of a seismic event, which allowing for the great velocity of tsunamis can provide effective warnings to areas that are more than 750 km from source. Some regional systems have also been established and are effective in providing warnings for areas within 100-750 km of the source.

Lander and Lockridge (1986) found that for earthquake generated tsunamis, 99% of all tsunami-related fatalities occur within 400 km of the epicentre. In deep ocean areas this is equivalent to a time scale of about 30 minutes from the time of generation, although arrival in shallower waters would take longer. This indicates that coastal communities under threat need to be evacuated extremely quickly once a warning has been issued. It is crucially important therefore to have clear and well-rehearsed civil defense plans, with well-defined evacuation routes that are known to the communities at risk. An example of a tsunami hazard zone map with evacuation routes is shown in Figure 5.25.

The problem with volcanogenic tsunamis is that, unlike earthquake-generated tsunamis, routine warning systems do not exist. Therefore, in the normal course of events, once a volcanogenic tsunami has been generated it is unlikely that nearby, low-lying coastal communities will have sufficient time to be effectively evacuated. This point is illustrated by the most destructive tsunami produced by the 1883 eruption of Krakataua, which reached mainland coasts around the Sunda Straits within 20 to 50 minutes (Figure 5.24).

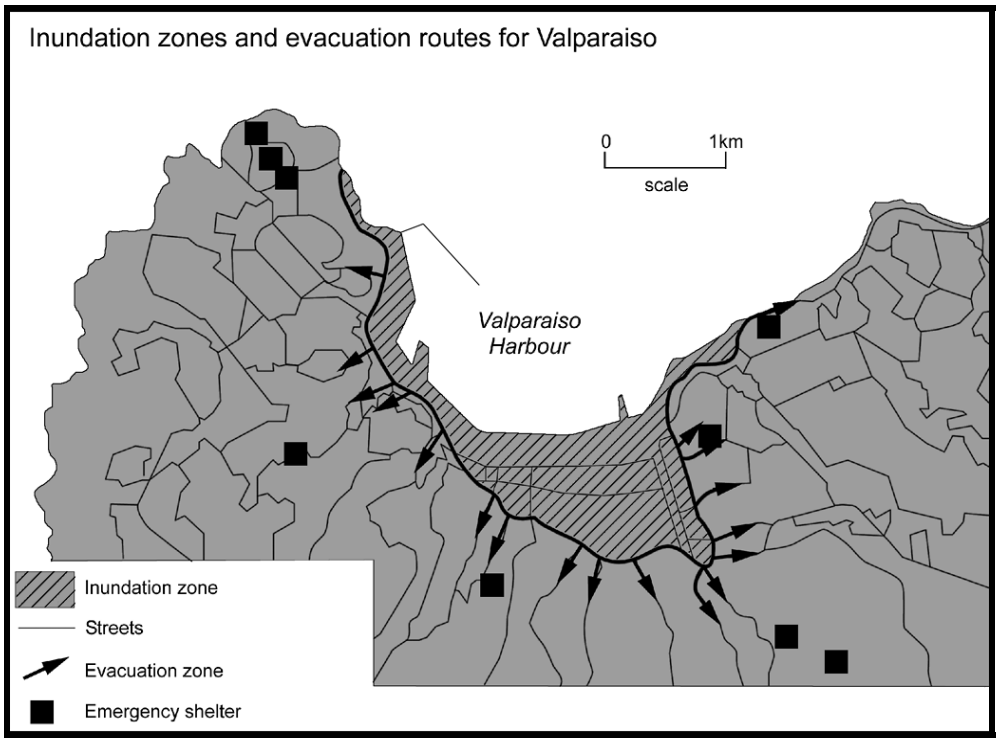

Figure 5.25: An example of a tsunami hazard zone map for Valparaiso, Chile. The inundation zone was estimated from numerical simulations. (After Bernard et al., 1988).

Because of their depth dependence, tsunamis may affect parts of the same coast differently according to local variations in bathymetry, and in the configuration of headlands and embayments. The state of the tide may also affect their impact. Tsunamis are commonly preceded by a lowering of the water level, often lower than the lowest tides. This is followed by a series of large waves, with successive waves separated by periods of a few minutes up to several hours. The first wave is often smaller than successive ones. The abnormal lowering of water levels, or the arrival of a first wave may provide a warning to coastal populations. In the event of such a warning, people in low-lying coastal areas should immediately move to higher ground and boats at sea should also head immediately for deeper water.

Despite the difficulty of providing adequate warnings because of the rapid onslaught of volcanogenic tsunamis, several measures may be taken to mitigate the effects of the hazard in the longer term. In areas where the potential hazard of tsunamis from nearby volcanoes exists, long term planning measures should be taken to ensure that, where possible, emergency services and installations of a strategic nature should not be developed in low lying coastal areas that could be inundated. In the event of eruptions at nearby coastal or island volcanoes, communities in low-lying coastal areas should be placed on alert and preferably evacuated to higher ground as a precautionary measure.

As a first step to hazard assessment, those volcanoes that could potentially trigger tsunamis should be identified. Any steep-sided volcano in coastal areas has the potential to collapse and produce debris-avalanches which may in turn generate tsunamis. Coastal or island volcanoes with actively growing and unstable lava domes should also be considered hazardous in this respect. Furthermore, debris avalanches at volcanoes in restricted waters,

such as inlets, are more likely to generate tsunamis than at volcanoes in the open ocean. It is important in such cases to assess slope stability, particularly where fumarolic activity is advanced and the edifice weakened and possibly more prone to collapse. Volcanoes that pose a risk should be closely monitored. This should involve seismic monitoring, which can provide warning of pending eruptions and possibly of movement along potential planes of failure, and the monitoring of ground deformation by a range of precise surveying techniques. The appearance and propagation of fissures may provide the most obvious and clearest evidence of slope instability.

Historical information provides a means of identifying areas at risk from inundation by tsunamis. However, due to the short history of many coastal communities, the lack of accurate records, and the general rarity of tsunamis in a given area, historical information of this nature tends to be uncommon.

Where historical information does not exist, but tsunamis are perceived to be a potential hazard, hydrodynamic modelling techniques which take local bathymetry into account can be applied to tsunami propagation and provide useful information on the likely run-up effects for hazard planning purposes. This approach has been used extensively for estimating zones of inundation for earthquake generated tsunamis on selected coastal sites, and has been applied to a minor extent to the hazard of volcanogenic tsunamis.

An example of numerical modelling of volcanogenic tsunamis is provided by the simulations undertaken by Keinle *et al*. (1987) for tsunamis generated by debris avalanches caused by the structural collapse of the summit region of Mount St Augustine volcano. This volcano has an oversteepened form and a history of repeated edifice collapse, and is known to have produced a tsunami in 1883. Concern was therefore heightened during an eruption cycle in 1986 that the volcano could collapse once again and generate tsunamis of potential danger to nearby coastal areas. Although the exact run-up effects of tsunamis depend upon local bathymetry, observations of the 1883 tsunami indicate that run-ups of 5 metres or more could be expected and that certain low-lying coastal communities would be particularly vulnerable during such an event. Given the high velocity with which tsunamis travel in deep water, the nearest coastal settlements could only expect a warning of about an hour.

In anticipation of a debris-avalanche at Mount St. Augustine, Kienle *et al*. (1987) applied numerical modelling techniques to try to simulate the tsunamis produced by the 1883 debris-avalanche, which was travelling at about 50 m/s when it entered the sea. This yielded a forecast of potential wave height and travel time based upon local bathymetry. The results of the modelling were in imperfect but plausible agreement with actual observations of the 1883 tsunami, but were nevertheless useful for emergency planning during the 1986 eruption.

5.9 Volcanic Gases

All volcanic activity, whether latent or otherwise, is accompanied by gas emission. The gases consist mainly of water vapour and carbon dioxide (CO_2), which are usually accompanied by minor amounts of toxic gases including sulphur dioxide (SO_2), hydrogen sulphide (H_2S), carbonyl sulphide (COS), the hydrogen halides (HCl, HF) and carbon monoxide (CO). In addition, much smaller quantities of gases including hydrogen (H_2), ammonia (NH_3),

hydrocarbons (e.g. CH_4), rare gases (He, Ar) and volatile metallic elements such as mercury and selenium may be present. The atmospheric gases, principally nitrogen and oxygen, are also incorporated into volcanic gases. The radioactive gas radon (Rn) is also found in volcanic gases and can be a hazard in some areas that are subject to long-term fumarolic activity.

Gases are dissolved in magmas and are readily liberated during periods of increased volcanic activity, when internal magmatic pressures are reduced as magmas rise. Gases dissolved in magmatic fluids generally only range between 0.5% and 5% by weight (Greenland, 1987), but are a major driving force in explosive eruptions. Large-scale gas emissions accompanying explosive activity can cause death or injurious effects, due either to toxicity or asphyxiation through displacement of oxygen.

All volcanoes continue to degas during dormant periods. This is generally not a problem because fluxes are low and the gases are readily diluted and dispersed into the atmosphere. However, some volcanoes produce considerable amounts of gas and have permanent or semi-permanent plumes. Although gases are only present in fatal concentrations at or close to their source, the dispersal of plumes downwind can result in detrimental long-term effects to the health of people, livestock, vegetation and crops over significant areas.

It is generally accepted that monitoring changes in gas composition on a routine basis can be used to predict the onset of renewed volcanic activity. During a series of eruptions at Mt Etna in Sicily in 1977, it was shown that daily emissions of sulphur dioxide rose from 1,000 to 10,000 tonnes some 48 hours prior to each eruption (Pendick, 1995). The continuous monitoring of low temperature fumarole gases has also been used to detect increased gas emission prior to an eruption at Kilauea on Hawaii (McGee *et al*., 1987). Gas monitoring will not be discussed further, but for a brief resumé of the subject the reader is referred to Sutton *et al*. (1992; 1993).

5.9.1 Volcanic gases and their properties

Some gases, especially the rare gases, originate from deep within the earth, and are released from magmas in varying quantities depending on the current state of the volcanic activity. It is the major gas constituents that are emitted constantly from volcanoes, no volcanoes being known that only emit the minor components such as H_2, He or NH_3. Gases given off by magmas react with the rocks through which they pass. They also cool down as they migrate towards the surface and the more soluble species, such as SO_2, HCl and HF tend to dissolve in groundwaters. This can have the effect of enriching residual gases in the less reactive and flammable components CO, COS, H_2 and CH_4, which may then spontaneously ignite on contact with the air, as is occasionally seen during fumarolic activity.

Next to water vapour, carbon dioxide is the second most prevalent volcanic gas. It is colourless and odorless, and although non-toxic, it is heavier than air and can collect in depressions or confined spaces where it can cause asphyxiation of people or animals due to displacement of air and lack of oxygen.

Carbon monoxide is a colourless unstable gas, has no smell, is very flammable and acutely toxic. It is a strong reducing agent which burns in oxygen to produce CO_2, and reacts with both the halogens and sulphur to form additional toxic compounds such as phosgene and carbonyl sulphide. CO is toxic to both animals and plants.

Depending on the state of the volcanic activity, sulphur may occur as either native sulphur, sulphur dioxide or hydrogen sulphide, although the oxidation state is determined by the subsurface geology and chemistry, and also by the temperature and flow-rate of the gas emissions. Specific reactions are temperature dependent, sulphur dioxide being more stable at higher temperatures whilst the formation of hydrogen sulphide is favoured at lower temperatures. Typical chemical reactions that involve sulphur modification at various temperatures, and commonly cited in the literature (e.g. Giggenbach, 1987, Rowe *et al*., 1991) are as follows:

$$SO_2 + 2H_2S \leftrightarrow 3S + H_2O$$
$$4S + 4H_2O \leftrightarrow 3H_2S + H_2SO_4$$
$$SO_2 + 3H_2 \leftrightarrow H_2S + 2H_2O$$
$$3CO_2 + H_2S \leftrightarrow 3CO + SO_2 + H_2O$$

The two principal sulphur-bearing gases present in volcanic plumes are sulphur dioxide and hydrogen sulphide. Sulphur dioxide is a colourless gas, heavier than air, non-flammable and relatively stable. It is very irritating to the eyes, throat and nose (olfactory threshold 3 ppm), and a concentration of 20 ppm causes coughing. It is very toxic to vegetation, especially in combination with other acid gases.

Hydrogen sulphide is a colourless gas which is heavier than air and smells like rotten eggs. Concentrations as low as 150 ppm induce a loss of smell. It is flammable, forms explosive mixtures with air between 4% and 45% by volume, and is toxic to plants and animals at low concentrations.

Hydrogen chloride is a colourless gas which is very soluble in water, with which it readily combines to form hydrochloric acid. In gaseous form the acid irritates the mucous membranes, and concentrations as low as 5 ppm induce coughing after a short exposure time. It is toxic to vegetation due to the lowering of pH. It occurs in significant concentrations around some actively degassing crater lakes, and can cause local problems where lavas flowing into the ocean react at high temperature with sea water.

Hydrogen fluoride is also colourless, very soluble in water, and is a component of many acid gas plumes. The vapour of HF irritates the mucous membranes and the respiratory tract, and low concentrations produce burns in humans that only become apparent hours after exposure. Contamination of vegetation by fluorine compounds causes fluorosis in grazing livestock

—

5.9.2 Examples of disasters attributable to volcanic gases

Several disasters have been attributable to the catastrophic release of carbon dioxide. Such incidents can occur during volcanic eruptions and during periods of dormancy.

A number of people were killed in 1979 on the Dieng Plateau in Central Java, when a phreatic eruption from Sinilar crater released a mixture of gases. The eruption lasted 24 hours and resulted in the deaths of 142 persons who were being evacuated along a nearby jungle track. It was said at the time that a mixture of HCN (hydrogen cyanide) and COS was responsible for the deaths, but it was subsequently concluded that asphyxiation by CO_2 was the most probable cause (Le Guern *et al*., 1982). The CO_2 is believed to have overwhelmed the villagers as they tried to escape from the eruption. At Tangkubanprahu volcano near Bandung in western Java, children have sometimes been asphyxiated by CO_2 streams flowing down the mountainside (Le Guern *et al*., 1982).

At the crater of Lake Monoun in Cameroon, 37 people died under similar circumstances in 1984, but the mechanism of gas release was different. An earthquake triggered a landslide into the lake, which disturbed a delicately balanced density stratification, resulting in convective overturn and the rapid exsolution of CO_2 from super-saturated waters deep within the lake. Effervescence and large-scale ebullition of the escaping gas at the surface of the lake produced a dense cloud of gas which drifted eastwards into the depression of the nearby Pangke river valley, where it overwhelmed and killed people walking along a road. Death appears to have been caused by asphyxiation, but the appearance of lesions and apparent skin burns on the bodies of the victims suggesting that other gases may also have been present (Sigurdsson *et al*., 1987). The high CO_2 concentration was attributed to long-term volcanic exhalations from vents within the crater, which lead to a gradual build-up of HCO_3^- in the bottom waters of the lake.

A more serious release of carbon dioxide is believed to have occurred in a similar manner at the crater of Lake Nyos in Cameroon in August 1986, when at least 1,700 people and numerous cattle were killed within an area approximately 20 km long and 15 km wide. This is by far the largest known gas-related disaster and it occurred in a region that had not been widely recognised as being volcanic. Survivors reported that there was a smell of 'rotten eggs' immediately before they lost consciousness, but subsequent medical examinations appeared to rule out the possibility that hydrogen sulphide had contributed to the loss of life (Baxter *et al*., 1989). The following month scientists attempted to collect water samples from deep within the lake, but the water was so highly charged with CO_2 that sampling vessels exploded as they were brought to the surface. It is now thought that, as at Lake Monoun, the density stratification of the lake was disturbed, resulting in deep water which was highly charged with CO_2 rising rapidly to the surface. As the water started to degas the convective flow within the lake was self-perpetuated, releasing large volumes of gas to the surrounding area in a very short space of time (Freeth, 1992).

—

5.9.3 Secondary gas hazards during eruptions

Large quantities of gas are rapidly released during pyroclastic activity. This can be a serious hazard close to source, although people are not normally found in proximity to vents under such perilous circumstances. However, gases continue to be released from pyroclastic deposits after deposition, and these can be a threat to life. Buildings that are heavily inundated by tephra should only be entered with caution, because under these conditions the build-up of toxic gases or CO_2 within has been known to cause fatalities.

An extreme example of secondary hazard caused by volcanic gases was associated with the 1783 fissure eruption of Laki in Iceland. Large quantities of sulphur gases released by the eruption gave rise to widespread acid rain over northwest Europe, and in Iceland most crops were destroyed and grazing stunted, resulting in the death of 79% of the country's sheep and 50% of its cattle and a famine which killed 24% of the population (Thorarinsson, 1969).

5.9.4 Gas hazards associated with resident gas plumes and long-term degassing during dormant periods

Volcanic gases continue to be released from fumaroles and springs during periods of quiescence or dormancy, and they also diffuse directly through the ground on the flanks of volcanoes (e.g. Allard *et al*., 1989).

On the volcanic island of Vulcano, Italy, diffusing gases from fumaroles, soils and well waters contain up to 100% carbon dioxide (Baubron *et al*., 1990; 1991). These heavier-than-air gases are able to seep into poorly-ventilated areas such as basements, where they displace oxygen, leading to the formation of discrete pools of gas with attendant dangers for people and animals unaware of the potential hazard. The problem of CO_2 ponding and asphyxiation is also prevalent in craters and calderas, especially those with vigorous fumarolic activity. This point is exemplified by the deaths by asphyxiation of several volcanologists during a routine monitoring visit to the crater of the Ecuadorian volcano Guagua Pichincha in 1993.

Problems also exist with the acidic gases such as SO_2 and the halogen acids. These gases may occur in lethal concentrations around source vents, but on moving away they are rendered less harmful by dilution with the air. They are also very soluble in water and therefore contribute to acid rain. Although high concentrations of acid gases only occur at source, persistent low concentrations of these gases can have serious long-term environmental effects on large areas downwind. Resident gas plumes occur at many volcanoes, and the potential for acid deposition at these centres is therefore great. At Poás volcano in Costa Rica for example, periodic increases in fumarolic activity result in the transport of gases laden with ash to the immediate environment. For much of the time a crater lake exists at Poás and this tends to dissolve a large proportion of the acidic gases. Periodically, however, the lake dries out through evaporation, and with the removal of the natural 'scrubber' the output of gases to the atmosphere increases dramatically. The gases impact on downwind areas, particularly during the dry season, affecting the health of the local population and livestock, and causing visible foliar damage to crops, especially coffee plantations. During the most recent crisis in 1994, local sources reported losses of up to 80% of the coffee crop. This problem was not especially apparent prior to about 1989 when the lake was up to 50 m deep, and acted as a sink for the

volcanic gases. However, lower than usual rainfall combined with a change in magmatic activity caused the lake to disappear (Brown *et al*., 1989). It is also probable that rainfall has a scrubbing effect on the acid gases, which may partly explain why the problem to the surrounding area increases during the dry season.

5.9.5 Gas hazard zoning

The risk imposed by exposure to volcanic gases depends upon the nature and concentration of the gas or gases involved. The hazard may be one of asphyxiation or poisoning, or secondary effects such as corrosion when acid gases are involved.

Exposure to localised pockets of gas in badly-ventilated locations and buildings can cause asphyxiation. This is a problem with background degassing during periods of inactivity as well as during eruptions. Care should therefore be exercised near known dangerous areas or when entering calderas and craters, to ensure that there is sufficient air movement to prevent build-up of levels of toxic gases. This advice can equally be applied to other low-lying areas in close proximity to active vents, especially valleys downwind or at the bottom of steep slopes, which might be potentially at risk from the release of large volumes of gas.

Gas hazard zonation maps are uncommon. Examples are presented for Dieng and for Poás in figures 5.26 and 5.27. At Dieng, where CO_2 (a heavy gas) is the danger, hazard zones are based upon the location of known gas vents and areas of low topography. At Poás, where there is a long-term regional problem due to a resident gas plume, zones have simply been delimited upon effects, such as corrosion, irritation to eyes, respiratory problems and smell.

A recent example of a gas hazard assessment is that undertaken at Furnas on the Azores island of São Miguel (Baxter *et al.*,1999). The settlement of Furnas is situated within a caldera which is the site of fumarolic activity and pervasive soil degassing of a number of gas species, of which carbon dioxide and radon are of principal concern with respect to health. Concentrations of CO_2 and Rn were measured in soil gases at 550 sites within and around the settlement, and the data was used to prepare a contoured map showing the distribution of CO_2 concentrations within the soil. Concentrations of CO_2 was also monitored within 25 residential houses. The concentrations found within the houses were related to the soil gas map. Thus for example, zones with >50% CO_2 in soil were found to contain houses in which concentrations were >15% at ground level, which is considered to be lethal, and in which all spaces below ground level were considered to accumulate lethal concentrations within a few hours: This zone (i.e.>50% soil CO_2) was therefore designated an area with high risk of asphyxiation. A total of five categories of risk or hazard within residential houses were related in this way to the contoured soil CO_2 map, and are summarised in Table 5.2.

Information on health and damage to crops is difficult to quantify on a regional basis, and hazard maps based on these parameters are therefore likely to be subjective. A more systematic approach would be to monitor the ambient concentrations of one or more gases in the region surrounding a volcano, using a grid of sampling points over a prolonged period. Varying levels of hazard, in terms of effects on health or crop damage, may then be related to known gas concentrations at well-studied localities, and zone boundaries then interpolated on the basis of appropriately selected threshold concentration values.

It is difficult to apply a systematic approach to gas hazard ***zoning*** for areas prone to sudden large-scale disasters, such as that of Dieng or Lake Nyos. This is because of the infrequent or freak nature of these events, in which little or no reliable information remains on the nature and concentration of the gases. Under these circumstances the best approach is probably to base hazard zones upon the distribution of casualties (both human and animal) resulting from past disasters, and also take cognizance of topography and prevailing winds in relation to gas sources for refining the positions of zone boundaries.

Soil CO_2 concentration	**Hazard zones**
>50%	**High risk of asphyxia** Lethal concentrations of CO_2 (>15%) found at ground level in houses. All spaces below ground will accumulate lethal concentrations within a few hours.
<50% - >25%	**Moderate risk of asphyxia** Concentrations up to 1% CO_2 commonly measured at bed level in houses. Spaces below ground will accumulate lethal concentrations.
<25% - >5%	**Low risk of asphyxia** Some evidence of CO_2 contamination at bed level in houses. Lethal concentrations can be reached in non-ventilated spaces below ground.
<5% - >1.5%	**No risk of asphyxia** Weak soil degassing. No dangerous concentrations of CO_2 in houses or spaces below ground.
>1.5%	**No hazard at any time** CO_2 concentrations are those of non-volcanic areas.

Table 5.2: Hazard zones for CO_2 degassing at Furnas (after Baxter *et al.*,1999).

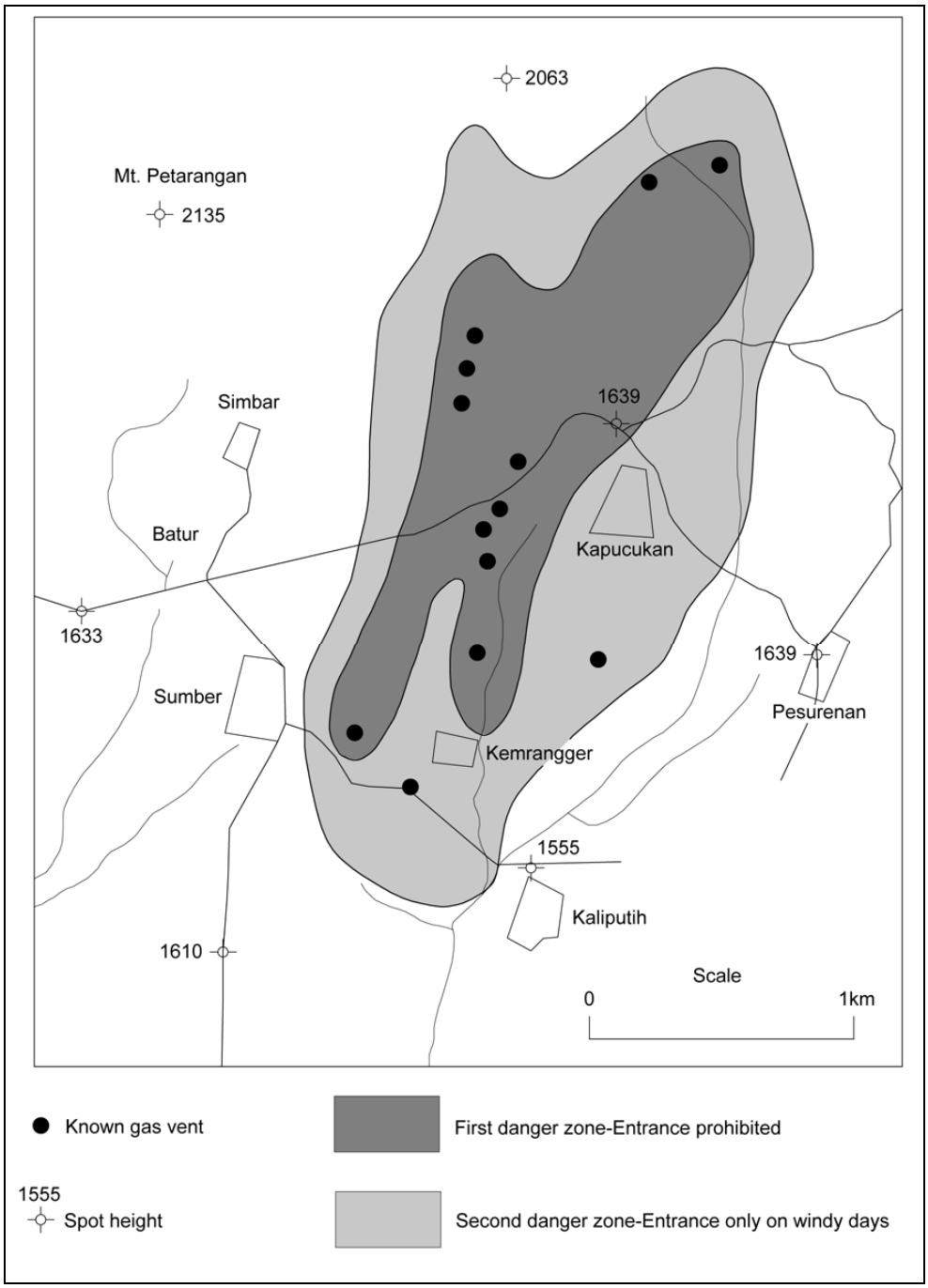

Figure 5.26: Simplified gas-hazard map of the Dieng Plateau, Java. Volcanological Survey of Indonesia. (Modified after Kusumadinata in Crandell et al., 1984, page 59). The map is based on known sites of gas emission and on topography. The hazard area is topographically highest at the northern end and extends downslope along two broad valleys.

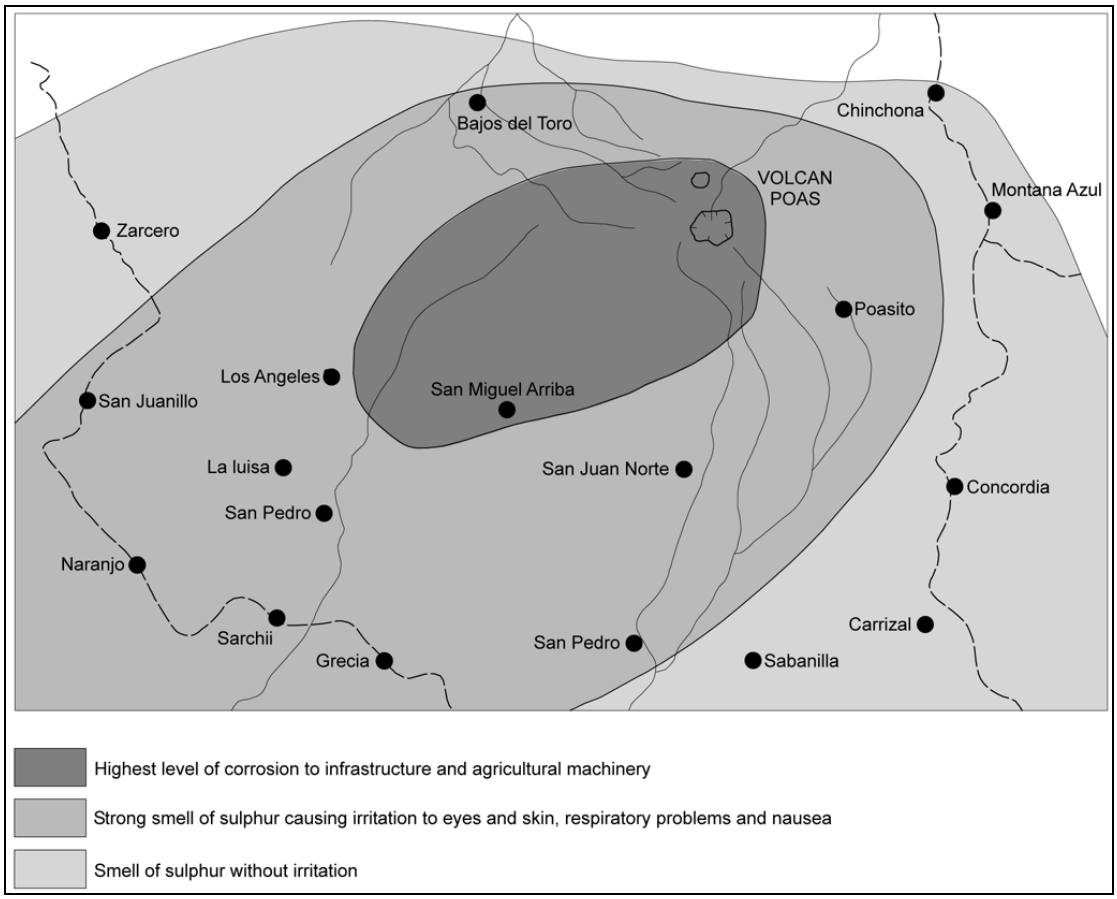

Figure 5.27: Simplified map showing the effects of gas on the country surrounding Poas Volcano, Costa Rica. (After Barquero and Fernandez, 1990).

5.10 Volcanic Earthquakes

Volcanic earthquakes are associated with most eruptions. On the one hand precursor seismic activity can give warning of an impending eruption, allowing disaster preparedness plans to be put into action, so reducing loss of life and damage. On the other they can cause damage to buildings and trigger landslides and avalanches, which may lead to casualties.

In most cases volcanic earthquakes are of small magnitude and only felt close to the source volcano, although there have been examples of notably large events. For example, the formation of the Katmai caldera in 1912 was associated with a series of moderate to strong earthquakes (Hildreth, 1991). Felt seismicity was reported for at least 5 days prior to the eruption and earthquakes continued to be felt at a village 60 km from the volcano for 50 of the following 70 days. A major earthquake (M_S 6.5) is believed to have coincided with the first main pulse of caldera formation, and over the following two days there were at least 25 more quakes with magnitudes ranging from M_S 5.1 to 7.0 (Abe, 1991; Hildreth, *op. cit.*). A large earthquake of magnitude 7 also occurred on the rim of the Aira Caldera during the 1914 eruption of Sakurajima, and some remarkably strong earthquakes of magnitude 7 and greater have also occurred during periods of unrest at a number of other large calderas (Newhall and Dzurisin, 1988).

Most volcanic earthquakes are small and do not have the shock characteristics of tectonic earthquakes, but consist of tremors with less potential to do damage. Nevertheless, because of their very shallow foci they can shake the ground strongly near to source, although their strength attenuates quickly with distance.

Volcanic earthquakes can be caused by various mechanisms (Schick, 1981) which include:

- Large scale mass-movement, such as caldera collapse and dome collapse
- Magma movement and associated fracturing
- Gas explosions

In addition, volcanoes are located in geologically active areas which are affected by tectonic earthquakes also.

5.10.1 Types of volcanic earthquakes

Volcanic earthquakes are generally classified into two broad types. **Volcano-tectonic** earthquakes are produced by fracturing of solid (brittle) rock induced by changes in stresses due to the injection or withdrawal of magma, and they are recorded as high-frequency features on seismographs. **Long period** earthquakes are generally believed to be produced by the movement of pressurised gases and magma through constricted pathways, and are recorded as low-frequency features on seismographs. In addition, two other terms are commonly used to describe volcanic earthquakes. **Volcanic tremor**, also known as **harmonic tremor**, is a continuous release of seismic energy (of long period type) produced by sustained magma movement, and commonly occurs during eruptions and in the precursor phase to eruptions. It differs from the sharp shocks associated with volcano-tectonic events, consisting of earthquakes that are closely spaced so as to be indistinguishable from one another. **Hybrid earthquakes** are characterised by seismic signals containing long and short frequencies and occur at shallow depths, usually of less than 2 km. They are believed to result from fracturing under high gas pressures, and are usually associated with the rise of magma.

5.10.2 Magnitude and intensity

The **magnitude** of an earthquake is a measure of the total energy released and is measured by a number of scales, of which the Richter scale is probably the most widely known. This is based on the logarithm of the amplitude of recorded seismic waves and is expressed in whole numbers and decimals: Thus a quake of 6.5 would be 10 times more energetic than a quake of 5.5. The scale has no upper limit, although the largest earthquakes recorded have had magnitudes of about 8.8 to 8.9.

The **intensity** of an earthquake is different to magnitude, and is a measure of the amount of ground shaking at a particular site. It is determined from reports on how people felt or experienced the earthquake and on damage to structures. The most commonly used intensity scale is the Modified Mercalli Intensity Scale. For a given earthquake with a given

magnitude, the intensity will vary with distance from the epicentre. Based upon information provided by a large number of people it is possible to map isoseismal lines which delimit zones of intensity. Such a map of Modified Mercalli seismic intensity was produced by Pomonis *et al*. (1999) for the 1630 eruption of Furnas volcano in the Azores. As summarised in section 4.4, this was used together with vulnerability information to assess the risk related to building damage and human casualties that could be expected as a result of seismic activity during a future eruption of similar size at Furnas.

SCALE	DESCRPTION
I	Not felt except by a very few under especially favourable circumstances
II	Felt only by a few persons at rest, especially on upper floors of buildings. Delicately suspended objects may swing
III	Felt quite noticeably by persons indoors, especially on upper floors of buildings. Many people do not recognise it as an earthquake. Standing motor cars may rock slightly. Vibration similar to the passing of a truck. Duration estimated
IV	Felt indoors by many, outdoors by few during the day. At night, some awakened. Dishes, windows, doors disturbed; walls make cracking sound. Sensation like heavy truck striking building. Standing motor cars rocked noticeably
V	Felt by nearly everyone; many awakened. Some dishes, windows broken. unstable objects overturned. Pendulum clocks may stop
VI	Felt by all; many frightened. Some heavy furniture moved; a few instances of fallen plaster. Damage slight
VII	Damage negligible in building of good design and construction; slight to moderate in well-built ordinary structures; considerable damage in poorly built or badly designed structures; some chimneys broken. Noticed by persons driving motor cars
VIII	Damage slight in specially designed structures; considerable in ordinary substantial buildings with partial collapse. Damage great in poorly built structures. Fall of chimneys, factory stacks, columns, monuments, walls. Heavy furniture overturned
IX	Damage considerable in specially designed structures; well-designed frame structures thrown out of plumb. Damage great in substantial buildings, with partial collapse. Buildings shifted off foundations
X	Some well-built wooden structures destroyed; most masonry and frame structures destroyed with foundations. Rails bent.
XI	Few, if any (masonry) structures remain standing. Bridges destroyed. Rails bent greatly
XII	Damage total. Lines of sight and level distorted. Objects thrown into the air

Table 5.3: The Modified Mercalli scale

6 PROJECT CASE STUDIES

6.1 Introduction

Three case studies were undertaken as part of the project, each developing different aspects of volcanic hazard mapping and risk assessment. Two projects in Chile and one in Costa Rica are summarised below, along with an example of rapid and vital take-up of project findings in the ongoing volcanic crisis on Montserrat.

The hazard assessment of Nevados de Chillán was the main case study of the project, and undertook thorough assessments of the volcanic geology, geography and volcanic history which were integrated into the hazard assessment. The volcano had not previously been studied in detail and proved to be a large and complex structure, with a history extending back more than 100,000 years and much activity within the past 10,000 years. The volcanic geology is reported in Dixon *et al.* (1995), with supporting geochemical and petrological work reported in Murphy (1995a; 1995b). The geography of the region surrounding the volcano was described by Chávez (1995) and the recorded volcanic history by Petit-Breuilh (1995). A summary report and hazard assessment is presented in Gilbert *et al.* (1998).

The Villarrica case study concentrated on developing a methodology for rapid volcanic hazard mapping utilising satellite and aerial photography and limited field work. It also explored ways of presenting volcanic hazard maps through the utilisation of Geographical Information Systems. This work is reported in Young (1998).

The Irazú case study involved a multi-disciplinary approach which addressed some of the peripheral issues of volcanic hazard and risk assessment. This work is reported in Young *et al.* (1998). It involved assessment of volcanic hazards, the impact of the main hazard types on the built environment, the impact of ash on health and the environment, and the economic consequences of the last eruption in 1963-65.

The final part of this section is devoted to the volcanic crisis on Montserrat, where some of the methodologies and expertise developed during this project have been tested and proven useful in the most direct application possible.

6.2 Volcán Nevados de Chillán, Chile

6.2.1 Objectives of the case study

The Nevados de Chillán sub-project investigated the volcanic geology, geography, volcanic history and hazards of an active volcano in southern central Chile.

The approach used to assess the volcanic hazards can be regarded as a conventional one based upon relatively detailed geological mapping undertaken over two field seasons. However, attempts were made to streamline operations through the use of remotely-sensed imagery (satellite and aerial photography) for assistance in mapping. Additional information was compiled on the geography of the area and on the recorded eruptive history of the volcano in order to take initial steps towards risk analysis.

Figure 6.1: Location of Nevados de Chillán and Villarrica volcanoes

6.2.2 General background on the volcano

Nevados de Chillán is a major active volcanic complex located in a populated part of the Andes in southern Central Chile at approximately 36º 50'S, 71º 25'W between volcán Nevado de Longaví in the north and volcán Antuco in the south (Figure 6.1). It comprises two edifices which cover an area of approximately 150 km^2. These are the Cerro Blanco Complex (3212 m.) in the north and the Las Termas Complex (3185 m.) in the south. Cerro Blanco has several small glaciers and a permanent snow cap, whereas the Las Termas Complex only has extensive snow covering in Winter and Spring. Both complexes have several volcanic cones and may be envisaged as mutually independent centres which have the potential for simultaneous eruption. Numerous vents have been active over the last 60,000 years and the volcano has experienced a number of glaciations. The last eruption occurred at the Las Termas Complex in 1987.

Volcán Nevados de Chillán is located within the Pinto borough of the Ñuble county in the Bíobío region (VIII region) of Chile, approximately 80 km southeast of the city of Chillán which has a population of 134,000. Pinto is the most important borough for tourism and an increasing number of people visit the volcano each year for skiing, hot spring bathing, horse riding and many other outdoor recreations. Rapidly increasing investment is taking place on and around the volcano in support of the tourism, with little regard for the volcanic hazards of the area. The main population centres are to the west of the volcano within the Central Valley, where the principal north-south communication routes also lie.

6.2.3 Work undertaken and methodology

Traditional methods of reconnaissance mapping were utilised for in order to fully assess the geology of the volcanic complex as a basis for hazard assessment. A map was produced at 1:50,000-scale from analysis of aerial photographs and satellite imagery, combined with data derived from the sparse literature available. This map acted as the starting point for a first field season of reconnaissance mapping and sampling of the entire volcanic edifice.

Sample analysis using conventional petrological and geochemical techniques was undertaken (Murphy, 1995a) in order to characterise lithological units and to assist with the correlation of these. Carbon samples were also dated by radiometric techniques to evaluate the chronology and frequency of eruptions during the Holocene and late-Pleistocene. A few rock samples were also dated using Ar/Ar methods as part of a related research programme. Simultaneous with sample analysis and re-drafting of the initial reconnaissance geological map, a study of the historically recorded volcanic activity of Nevados de Chillán was also undertaken by Petit-Breuilh (1995) and the geography of the region was documented by Chávez (1995).

The second field season focused on areas that had not been covered during the first year and on problems identified during the petrological and geochemical work. This fieldwork was aided by helicopter which provided easy and rapid access to the more inaccessible parts of the volcano. Greater focus was also given to assessment of volcanic hazards, in particular in the characterisation of Holocene pyroclastic flow and airfall tephra units. Some additional samples were collected for petrological and geochemical work and for radiometric dating.

Following further petrological and geochemical analysis (Murphy 1995b) and radiometric dating of samples collected during the second field season, a final geological map and report on the geology of the volcano was produced (Dixon *et al.*, 1995). This together with the information on historically recorded activity and the geography of the region acted as a basis for the hazard assessment undertaken as the final part of the case study (Gilbert *et al.*, 1998).

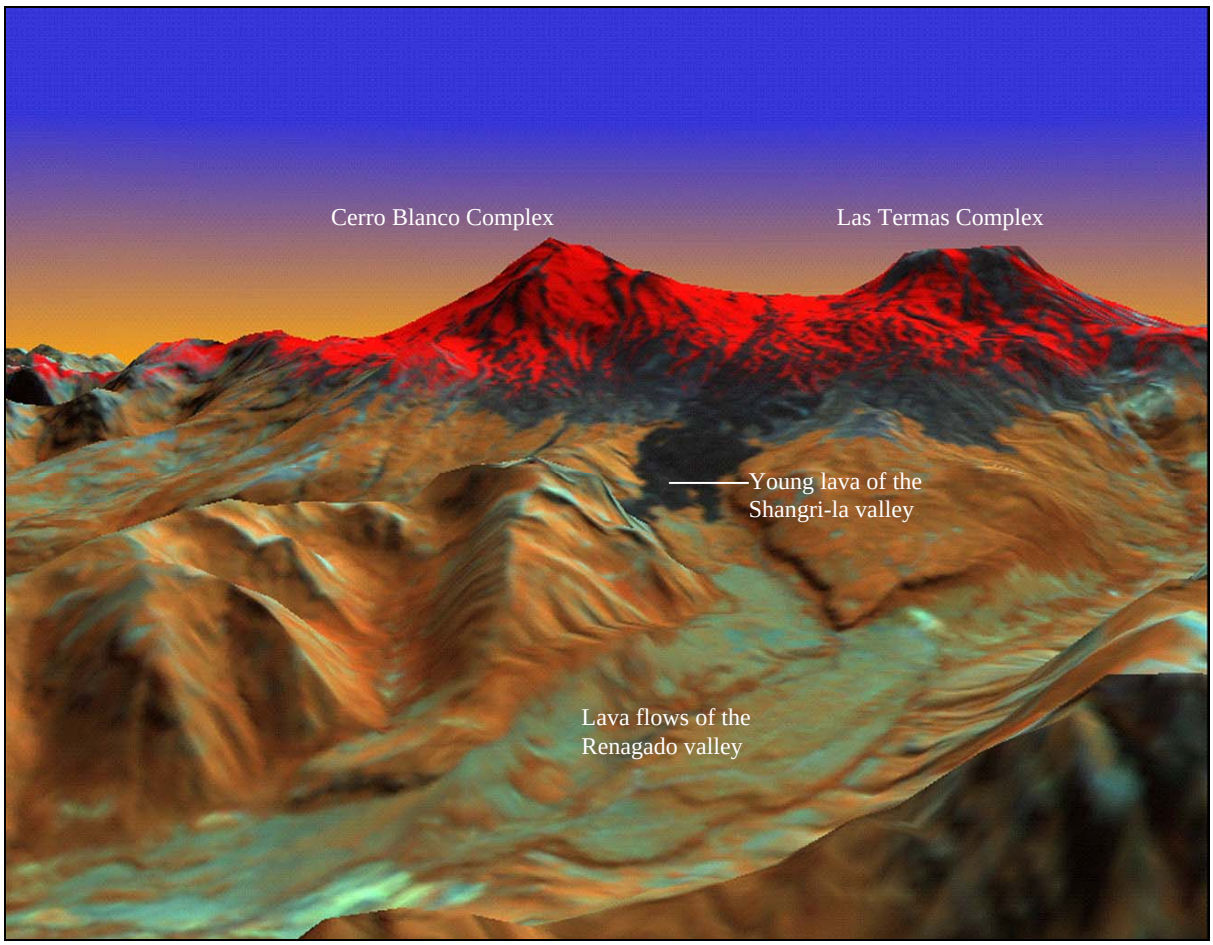

Figure 6.2: Landsat TM false colour image of Nevados de Chillán draped over a digital terrain model. Viewed from the west. Snow in red and young lavas in dark grey to black. This method of presentation allows the volcano to be viewed from any perspective in real time on a computer.

6.2.4 Hazard assessment and hazard maps

Nevados de Chillán is a large, complex stratovolcano which currently comprises two separate eruptive centres which have been characterised by different styles of activity due to different magma chemistry. The historical record and Holocene geological record suggest that very large-scale, caldera-forming activity has not taken place at the volcano in the past 10,000 years or more. However, such activity did occur during the late-Pleistocene history of the volcano and cannot be ruled out entirely in the future: Areas in the Central Valley of Chile, including the city of Chillán, could be threatened by such activity.

The tourism and skiing infrastructure on the Las Termas complex of the volcano and the population living in the surrounding valleys are at risk from smaller but more frequent eruptions, such as have occurred many times during Holocene and historical times.

Lahars are the greatest hazard at this snow and ice-covered volcano. Eruptions could be most dangerous with respect to lahars during the late spring (November), when snow melt-waters are at their highest levels, or during mid-Winter (July) when precipitation is highest. Eruption of pyroclastic flows onto the upper flanks of the volcano can lead to very rapid melting and generation of floods. These can entrain unconsolidated morainic and pyroclastic debris on the upper flanks and so increase their bulk considerably. Once within the drainage channels on the lower flanks, bulking-up can continue through incorporation of fluvial and laharic deposits.

All of the valleys around the volcano are at risk from lahars. Eruptions at the Cerro Blanco complex in the north could produce lahars in the Ñuble river which eventually flows into the Central Valley immediately north of Chillán city. The town of San Fabián, 35 km from the volcano, is the community most at risk from such an event. Eruptions at the Las Termas complex in the south could lead to lahar generation in the Chillán, Renegado or Diguillín river valleys, all of which hold significant population centres as well as being the location of all the tourist infrastructure in the area. Proposed dam construction for hydro-electric power production in the Diguillín valley is also within the hazard zone for lahars. There is danger to people high on the volcano, either skiing or climbing, from sudden-onset lahars generated by even minor volcanic activity, especially at the Las Termas complex.

The hazard of pyroclastic flows at the volcano is considered to be small except in the areas within a few kilometres of the summits. The style of activity deduced from the historical record is not one that includes generation of large pyroclastic flows. However, vulcanian eruptions and emplacement of lava flows and domes can generate small flows which would be a danger to the area of most tourist activity; namely the ski-lift and ski slopes on the upper flanks and the Termas de Chillán area itself. Furthermore, even relatively small pyroclastic flows could produce rapid melting of the summit snow and ice and generate lahars and floods.

The Holocene record contains evidence for several pyroclastic flow deposits in the valleys leading from the volcano, although none have been found more than 15 km from the summit area. However, evidence for very large-volume ignimbrites probably related to caldera collapse has been found in the late Pleistocene record. Thus, although dangers from pyroclastic flows during normal eruptive activity at the volcano are small except in the proximal areas, large eruptions on the 500 to 1,000-year time scale would threaten population centres farther afield.

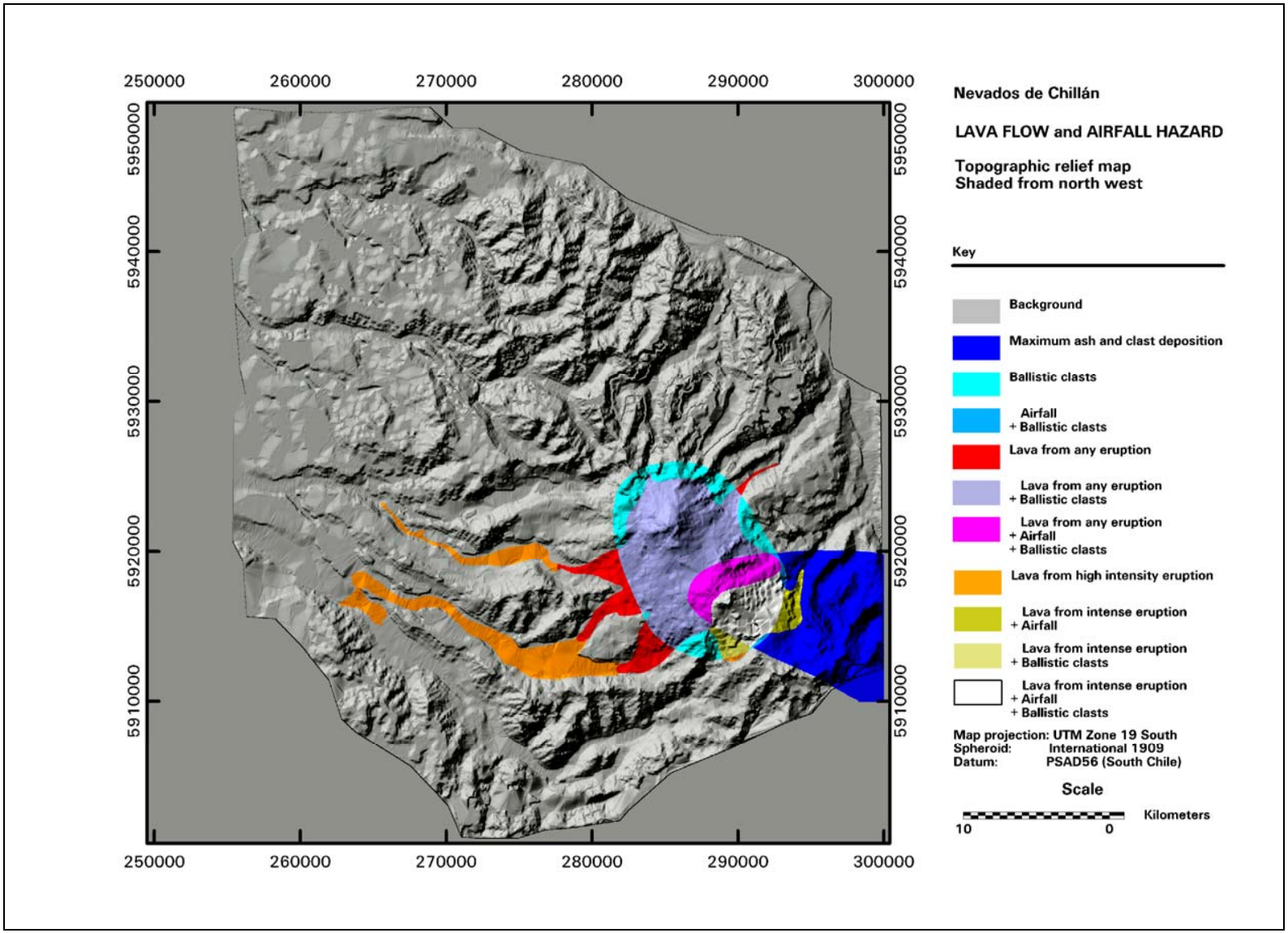

Figure 6.3: Example of a hazard zone map Nevados de Chillán for lavas and airfall presented on a shaded relief map

Thick deposits of Holocene airfall tephra occur on the eastern (down-wind) flanks of the volcano and have been produced by vulcanian and strombolian activity. Given the relatively limited distribution of airborne tephra from such activity and the remote and unpopulated nature of this side of the volcano, the direct hazard to population or infrastructure is considered to be minimal. However, ballistic bombs do present a hazard. Accepting that bombs are commonly ejected to distances of up to 5 km and occasionally farther (Section 5.2.2), then, in the case of Nevados de Chillán this could pose a hazard to the tourist infrastructure, particularly the ski industry on the western flanks of the Las Termas complex. Larger eruptions could produce high volcanic plumes which again would be unlikely to impact severely on populated areas but could, cause problems to air traffic.

Lava flows are the most common eruption product on the volcano. Although these constitute a hazard in themselves, lava flows tend to be slow-moving and are unlikely to pose a risk to life, even in proximal areas. However, much of the ski lift infrastructure is at high risk of destruction from lava flows. Old flows have flowed for up to 35 km in the Renegado valley to the west of the volcano, so that infrastructure in valleys even considerable distances from the volcano could be threatened. Lahars could also be generated during emplacement of lava flows onto the summit snow and ice fields, although as described in section 5.7.3 lahars produced by this mechanism are not usually large.

Finally, landslides and debris avalanches present a significant volcanic hazard at Nevados de Chillán. Although no large debris avalanche deposits have been found, there have been landslides in the hydrothermally altered areas above Termas de Chillán on numerous occasions in the recent past, with the last occurrence in 1990 destroying considerable tourist infrastructure. There has been rapid development within the hazardous area since that time, so that a similar event in the future would carry a far higher risk than previously.

6.2.5 Conclusions

Traditional, though reconnaissance geological mapping methods were used to obtain detailed volcanological information about this large and little-known volcano in the Chilean Andes. When combined with studies of geography and volcanic history, a thorough assessment of volcanic hazards could be made. This type of study is necessary on large, inaccessible volcanoes where little is known about the volcanic geology and where historic eruptions may not be representative of larger less frequent types of events.

The rapid tourist development on the volcano, especially in the Termas de Chillán area, is being undertaken with little regard to potential volcanic hazards. These areas are at high risk during future activity at the volcano, which was in fact erupting for over half of the 20th century. There is no monitoring of the volcano so that no early warning can be provided to those at most risk closest to the summit area in the event of a rapid renewal of activity. Population centres and roads farther from the volcano are also at some risk from lahar activity during any eruption and from pyroclastic flows if particularly energetic eruptions occur. The probability of very large caldera-forming eruptions which could threaten large population centres in the Central Valley is very low.

6.3 Volcán Villarrica, Chile

6.3.1 Objectives of case study

The main objective of the Villarrica case study was to investigate the potential for undertaking volcanic hazard mapping using low-cost and rapid reconnaissance methods based upon remote-sensing techniques augmented by a limited amount of fieldwork. In addition the case study was used to develop methods for the compilation of hazard map information using a Geographical Information System (GIS) and for its presentation using 3D imagery and other techniques.

6.3.2 Background information on the volcano

Volcán Villarrica is situated in south-central Chile at approximately 39.5°S, 72°W, in the western foothills of the Andes (Figure 6.1).

The volcano is a composite stratocone of basaltic-andesite composition which has a snow and ice-covered summit at an altitude of 2,840 m. It lies at the western end of the Lanín-Villarrica volcanic lineament which runs orthogonal to the main crest of the Andean volcanic arc in this region. Historic activity has been dominated by lava flows, small strombolian explosive events and common lahar activity. The post-glacial geological record, however, shows evidence of numerous violent explosive eruptions which have generated pyroclastic flows on the flanks of the volcano and have resulted in two caldera collapse events. Extensive tephra fall layers are not present, although thick proximal deposits are found to the southeast in the dominant downwind direction.

The main towns within the environs of the volcano are Villarrica, which is located 30 km to the west-northwest, and Pucón which is situated 16 km to the north of the summit. A number of smaller but rapidly growing towns are situated at the base of the volcano along the shores of several of the large lakes. Tourism and skiing are the main businesses in the region and economic growth and associated development is rapid. A population of over 45,000 is at risk from the volcano, with an additional 65,000 visitors in the region at the peak of the tourist season.

6.3.3 Work undertaken and methodology

Initial office-based studies included processing and analysis of Landsat imagery of the volcano and surrounding area in combination with detailed aerial photograph interpretation at a scale of 1:60,000. Literature searches on the general nature of volcanism in the area and on the reported volcanic history were also undertaken in order to provide an initial background to the hazard mapping.

A brief period of fieldwork lasting about 2 weeks was undertaken. This was partly planned using aerial photographs and satellite images and focussed on the examination of drainage channels because they offer good sections through the deposits and also act as the main hazard pathways from the upper flanks of the volcano to the inhabited areas. Fieldwork

mainly involved the logging of sections through pyroclastic and laharic deposits within all of the main drainages around the volcano, but also included a visit to the summit and a reconnaissance flight over the volcano in a light aircraft. Samples of charcoal for radiocarbon dating were also collected where possible.

Hazard maps were drawn using the field data in combination with the preliminary office-based assessment, and the main hazards were reported.

Some of the information that would normally have been collected in such a study as this was already available from previous investigations. For example, radiocarbon dating was not undertaken; instead, dates obtained by previous workers from known sections were utilised. Similarly, a study of historically recorded volcanic activity had already been undertaken for the volcano, and this information was therefore utilised rather than a separate study being carried out. Care was taken not to utilise this or other previously obtained information relevant to the hazard assessment before it would normally have been available in such a study. Furthermore, the detailed geological and hazard assessment work which had been undertaken by previous researchers was not available in the UK and was only collected from Chile for comparative purposes after completion of the main part of the project, so that it did not influence the course of the project.

Additional methods were employed using the hazard information in a GIS to combine different hazard layers and assist with the visualisation and presentation of the data. Preliminary investigations were also carried out in order to demonstrate the use of the hazard maps for the rapid assessment of risk within a GIS framework.

6.3.4 Hazard assessment and hazard maps of volcán Villarrica

The detailed historical information and geological data obtained during the project were used to construct several scenarios for typical eruptions of different size and frequency, which acted as the basis for the hazard assessment. Zones likely to be affected in each of the eruption scenarios were delineated partly on the basis of those areas affected by previous eruptions at Villarrica and partly on empirical evidence from other volcanoes of similar type elsewhere. The time scales used for these scenarios were for guidance only and were order-of-magnitude estimates: There is considerable variation in the frequency of all scales of volcanic activity.

A typical 10-year eruption at volcán Villarrica is characterised by strombolian activity confined to the summit area, with the generation of lava flows and lahars on one of more flanks of the volcano. Lava flows may or may not descend to the lower flanks, and lahars will usually be confined to previously-established drainage channels. Minor scoria may be produced on the summit area and ash may be blown several tens of kilometres downwind. Such activity is due to the periodic rise of the magma column in the conduit, and formation of a lava lake in the summit crater which normally precedes eruption. Insufficient seismological evidence is available to deduce likely pre-cursor earthquake activity, but some change in style of seismicity is likely before such eruptions, although it might only precede it by hours. Eruptions of this nature occur most often during the spring months (October to December) due to depressurisation of the system during snow-melting. This is a common occurrence at

other Andean volcanoes but is best documented at Villarrica. Large regional earthquakes may also prompt such activity.

Areas at direct risk during 10-year eruptions are confined to the near-summit area (the ski-resort and lift system) and infrastructure within the main drainage channels. This includes access roads to the National Park, which are busy in summer and winter, and small amounts of established housing on the lower flanks of the volcano, especially along the lake shores of Villarrica and Calafquén. New development along the access road to the National Park and in Coñaripe is also impinging upon areas of high hazard during 10-year eruptions.

A typical 100-year eruption might comprise more violent strombolian and sub-plinian explosive activity at the summit or at a flank vent (either new or previously established), with high rates of lava production, voluminous lahar generation and possibly small pyroclastic flows close to the vent. Ash and scoria would also be produced. Lava flows would almost certainly occur in more than one drainage and are likely to reach one or other of the lake-shores. Lahars might be generated directly by the rapid effusion of lava, or by fire fountaining or eruption of pyroclastic flows onto the snow-field. Most likely, however, is the generation and ponding of sub-glacial meltwater within the upper old caldera, due to melting caused by high heat flow or the subglacial extrusion of lava, which on bursting out could form large, debris-rich floods similar to those produced during sub-glacial eruptions in Iceland (see Section 5.7.3).

Areas threatened by such 100-year activity are considerably larger than for the 10-year eruption scenario, and impacts are likely to be much more severe. The upper flanks of the volcano would almost certainly be severely affected, and emplacement of pyroclastic flows could be very rapid and devastating. Lava flows would probably have less impact than the lahars which would inevitably be generated by such an eruption. Ash and scoria would not normally cause major concern, although anomalous wind directions might lead to considerable tephra deposition on nearby towns such as Pucón. The main impact would be from lahars. These would not necessarily be confined to channels either high on the volcano or on the lower flanks. Any infrastructure within channels even on the lakeside would be at great risk, and major changes in stream courses could occur, giving rise to impact over very much wider areas, especially in broad valleys such as the Voipir to the west. Lahars would likely be generated in many of the drainages around the volcano and would have great power even at considerable distances (>15 km) from the summit.

The development of a small to moderate 10-year type eruption into a large 100-year eruption scenario might be subtle, and there is likely to be little precursor evidence that would indicate the scale of eruption that might occur: Precursor activity is likely to be indiscernible from that of previous smaller eruptions, when gauged against the limited baseline data currently available.

A typical scenario for a 1,000-year eruption is more difficult to construct because there is no recorded history for such an event. However, the nature of the deposits from these events and a comparison with activity at other volcanoes makes reconstruction of such an eruption scenario possible. Generation of relatively dilute, low aspect-ratio pyroclastic flows from a collapsed eruption column is the likely style of a typical 1,000-year eruption at Villarrica. Such processes are not well-documented in the worldwide historical record, but recent

examples at El Chichón in1982 (Sigurdsson *et al.*, 1984) and Mt Pinatubo in 1991 (Hoblitt *et al.*, 1996) serve as model events. In such a scenario, generation of lava flows would be insignificant in terms of hazard. There is little evidence for widespread Plinian-type airfall tephra deposits around volcán Villarrica, and thus tephra would also be a relatively minor hazard. Pyroclastic flows from such explosive eruptions would be emplaced very rapidly on all flanks of the volcano and would devastate everything in their paths. Evidence from Villarrica indicates that such pyroclastic flows have travelled several tens of kilometres during past eruptions. They would thus threaten all of the communities around the base of the volcano and some even farther afield. Rapid melting of the snow and ice cap by such pyroclastic flows would also produce large and destructive lahars. Caldera formation is possible during an eruption of this magnitude, and in such an event the associated pyroclastic flows could be even more violent and travel longer distances.

It is almost impossible to know what precursor activity might be expected prior to a 1,000-year type event. However, it is likely that some precursor signs would be given, possibly in the form of 10- or 100-year type events. The difficulty is predicting when or if a 10-year event might develop into a 100- or 1,000-year event. Only detailed long-term monitoring of seismicity, gas and rock geochemistry and volcano-deformation could provide such information.

A number of secondary hazards are possible as a consequence of volcanic eruptions at Villarrica. Tsunami could possibly occur on lagos Villarrica and Calafquén should large-volume lahars or pyroclastic flows suddenly enter the lake, although such sudden impacts are unlikely. Other secondary hazards may include gases, which are a hazard in the summit area at all times, and structural damage due to earthquake shaking during and prior to major eruptions. Ash hazards to aircraft in the area are minor but would become important during vigorous phases of a 100-year eruption or a 1,000-year event.

Several additional volcanic hazards should be mentioned, although there is no evidence for such phenomena at Villarrica. Sector collapse generating debris avalanches and lateral blasts is increasingly recognised at volcanoes around the world, with the Andean volcanoes especially prone to such hazards. Although no evidence has been recognised for sector collapse at Villarrica, the western flank of the volcano is steep and could, under certain eruption scenarios, be prone to collapse. Volcanic hazards related to lava dome growth are well-documented; such a style of activity is not known at Villarrica and is unlikely to occur in the future, but cannot be totally discounted.

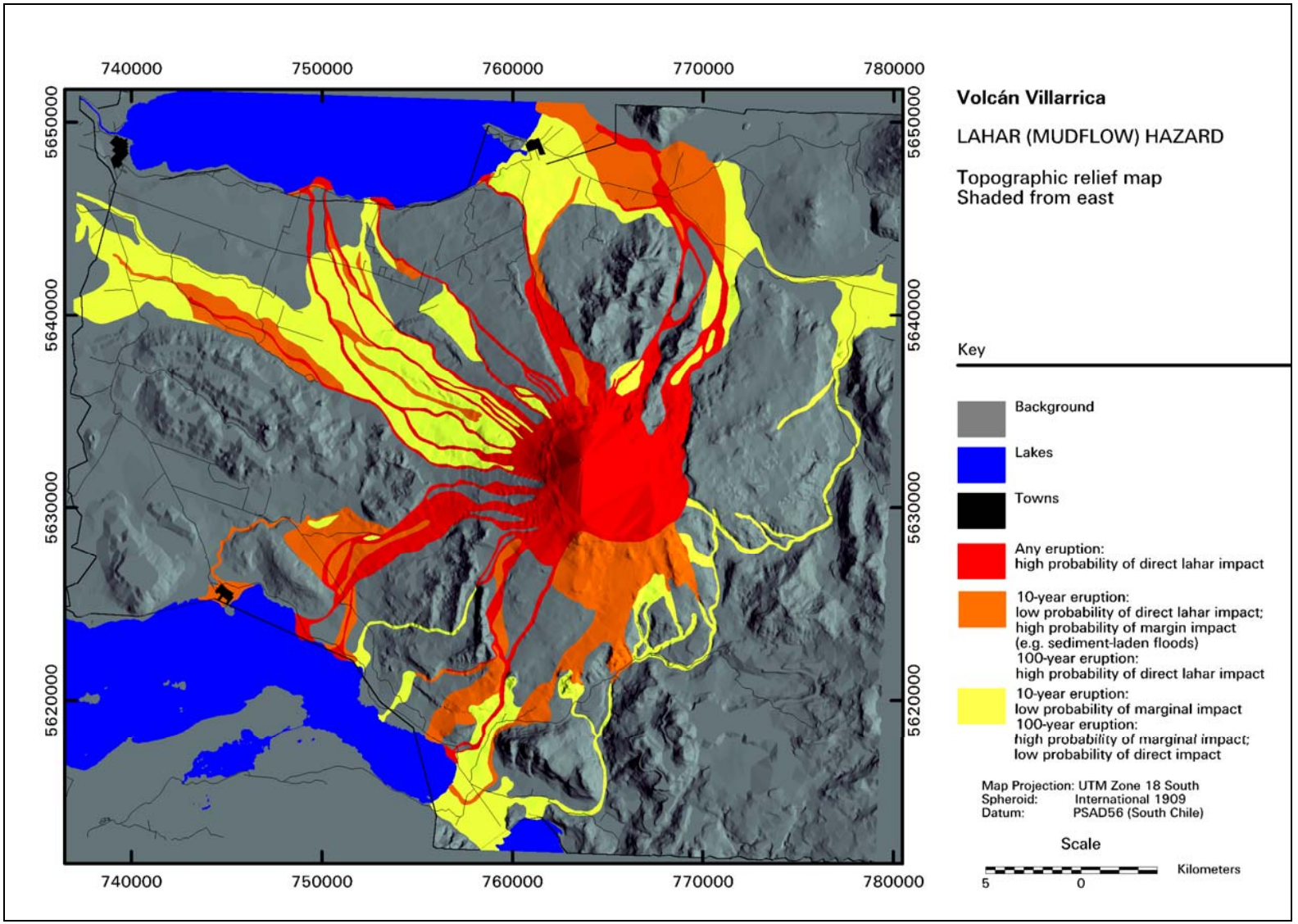

Figure 6.4: Example of a hazard zone map of volcán Villarrica showing the hazard of lahars draped over a shaded relief map

Using the described eruption scenarios as a basis, hazard maps were drawn for the four main hazard types of lahars, pyroclastic flows, lava flows and airfall tephra. These indicate the areas likely to be affected for different scales of event, which are in turn related to probability of occurrence. Preliminary work has been undertaken within a GIS framework, to combine these hazard maps into single, derived hazard maps aimed at specific users. Examples of these maps are presented in Young (1998) and one is given as Figure 6.4. Some work is also presented by Young (*op. cit.*) on rapid, semi-quantitative risk assessment for bridge crossings around volcán Villarrica; such information is easily transferable into the GIS framework and could be upgraded in future.

6.3.5 Comparison of the rapid hazard assessment of Villarrica with an earlier detailed assessment

The results of the rapid hazard assessment undertaken by this project on Villarrica have been compared with hazard maps of the volcano that were previously prepared from the results of a much more detailed study of the volcano undertaken over a period of many years by Chilean workers. This has allowed the benefits of rapid hazard mapping over conventional volcano research to be assessed.

The most obvious benefits are that the rapid techniques are considerably less expensive and can be completed in a fraction of the time needed for a conventional hazard assessment based upon detailed geological fieldwork.

The level of detail of hazard mapping is only slightly compromised in the rapid assessment, and basic information relevant to development planning and disaster preparedness is certainly sufficiently accurate to be worthwhile, even if only as a preliminary measure. The difficulty in assessing larger, less frequent events in a volcano's geological history has been identified as a potential weakness with rapid hazard mapping techniques, when compared with more detailed assessments. However, this was not considered a particular problem in the study of volcán Villarrica due to the high frequency of eruptions and excellent preservation of deposits.

6.3.6 Conclusions

Volcán Villarrica provided an excellent example for developing rapid mapping techniques, and the hazard assessment produced by the case study in a very short period of time compares favourably with an earlier assessment based on many years of more detailed studies of the volcano.

The good accessibility of the volcano and its relatively simple structure made hazard mapping straightforward. The high level of activity recorded in historical archives and indicated within the well-preserved and easily interpreted post-glacial deposits, means that the hazard assessments for the 10-, 100- and 1,000-year eruption scenarios are based upon reliable evidence. In the case of volcán Villarrica, this well-preserved or written record includes events of a scale rarely seen in such short time intervals at other volcanoes, and this has enabled the frequency of even large events to be reasonably well-constrained. In this respect

the volcán Villarrica study has probably been unusual, because at many volcanoes evidence for such large infrequent events is usually found only far back in geological history, and its recognition usually requires detailed studies, often involving expensive and time-consuming petrological, geochemical and radiometric dating programmes.

This sub-project has been most effective in demonstrating the possibilities of low-cost, rapid volcano hazard mapping in developing countries with high numbers of potentially active volcanoes. It is encouraging to report that a similar project farther north in the Chilean Andes (Naranjo *et al.*, 1998) has utilised these techniques for rapid volcanic hazard mapping, with equal success. Improvements in the presentation of hazard information using GIS have also been investigated during the Villarrica sub-project and further work in this area would be very beneficial in terms of improving disaster reduction capability.

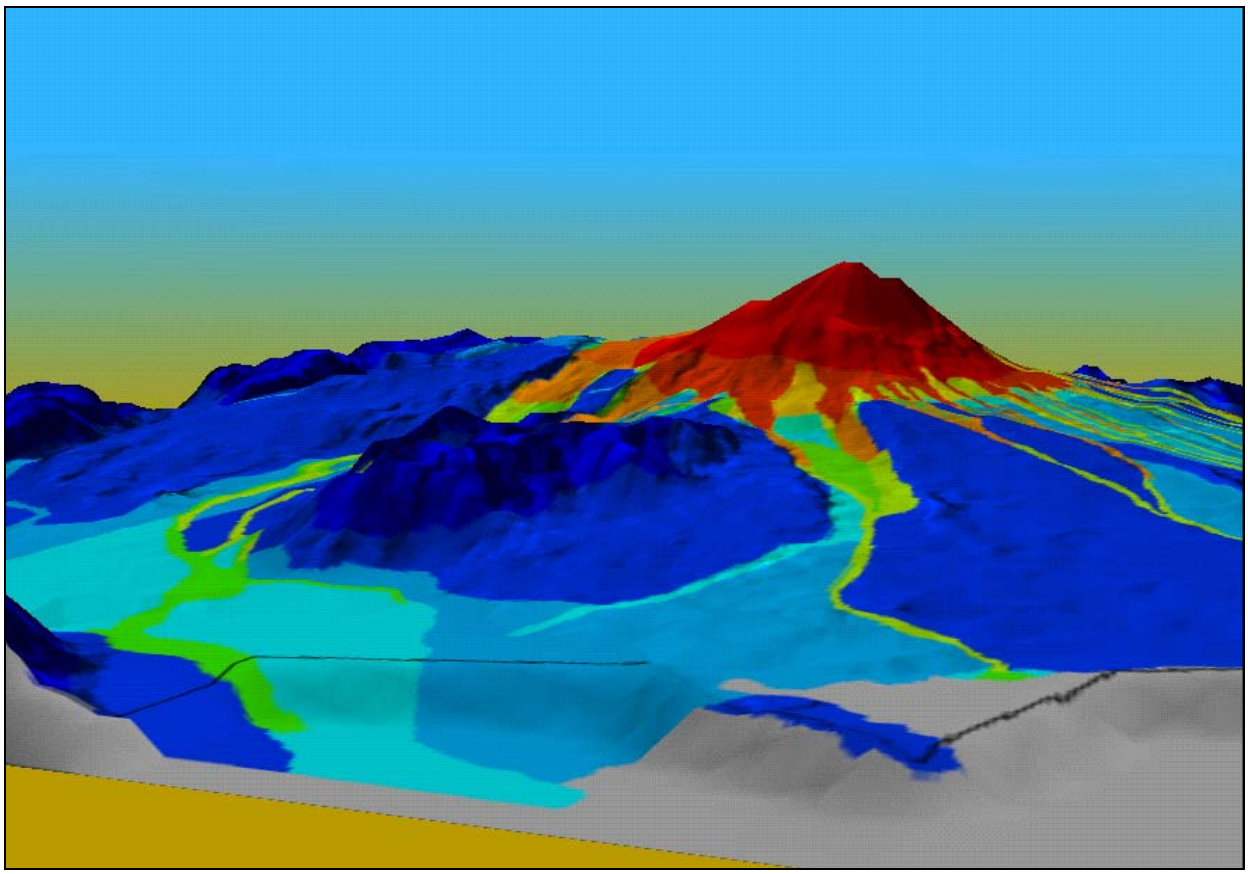

Figure 6.5: Example of a digital terrain model of volcán Villarrica draped with hazard zones. The terrane model may be viewed from any perspective and provides a very powerful method of presenting hazard map information in a more easily visualised form.

6.4 Volcán Irazú, Costa Rica

6.4.1 Objectives of case study

Volcán Irazú is situated in central Costa Rica, close to the capital of San José and other important population centres, all of which lie within 50 km of the summit.

When the volcano erupted over a two year period between 1963 and 1965, the impact was felt throughout Costa Rica. Although the eruptions were not particularly large nor violent and loss of life was relatively small, some of the impacts were significant.

The aim of the case study was to investigate specific aspects of the 1963-65 eruptions in terms of volcanic hazards and risks, and to assess the progress that has subsequently been made in terms of risk reduction and civil protection measures in preparation for a similar eruption, which could be expected within the next few decades.

Four specific aspects of hazard and risk assessment were investigated. These were the rapid mapping of hazards, with particular emphasis on the modelling of ash fallout; the assessment of building vulnerability and consequent risk posed by airfall and lahar-generating eruptions; the assessment of impacts on health of volcanic ash; and investigation of the economic consequences of the 1963-65 eruptions and how the economy might be protected against the detrimental impact of future eruptions.

6.4.2 Background information on the volcano

Irazú lies at the southeastern end of the Cordillera Central in the heart of Costa Rica. It is the highest volcano in Central America, rising to 3,432 m above mean sea level. The Valle Central extends westwards from the volcano with the capital, San José, just 26 km from the summit. The Valle Central contains a high proportion of the country's population as well as being the most densely cultivated area. The second city of Cartago lies 15 km south of the summit.

Irazú is a basaltic andesite shield volcano with a recorded history of numerous eruptions similar in nature to those of 1963-65 phase of activity. The geological record contains abundant evidence for the long-lived nature of the volcanic centre, the activity of which appears to have been broadly similar during the past 10,000 years to that described in the historical record. Eruptions of a phreatic or phreatomagmatic nature are common, producing ash columns in semi-continuous eruptive episodes which last for days to years. Ash is usually distributed to the west by prevailing winds and, even in very small amounts, is toxic to some plants and an irritant to humans. Close to the volcano, thick ash deposition and ballistic bombs can cause building damage and be hazardous to humans. The remobilisation of ash deposits on the flanks of the volcano can lead to the generation of lahars, which were the main hazardous phenomena encountered during the 1963-65 eruptions. Other less frequent volcanic hazards include pyroclastic flows on the upper flanks of the volcano, lava flow emplacement at the summit or on the flanks, and landslides or debris avalanches which may occur during particularly violent eruptions or can be triggered by large earthquakes.

6.4.3 Work undertaken and methodology

The case study of Irazú comprised four semi-independent components, each of which investigated one particular aspect of the hazards and risk posed by the volcano. A field visit was made by four of the five project team members in April 1995 for field work and data collection; the remainder of the work was undertaken in the UK, with input from collaborative partners in Costa Rica.

Volcanic hazard assessment was partly undertaken using the rapid mapping methodologies developed in the other case studies of the project. Special emphasis was given to mapping and modelling of ash hazards using techniques based upon ongoing research work being undertaken at Bristol University.

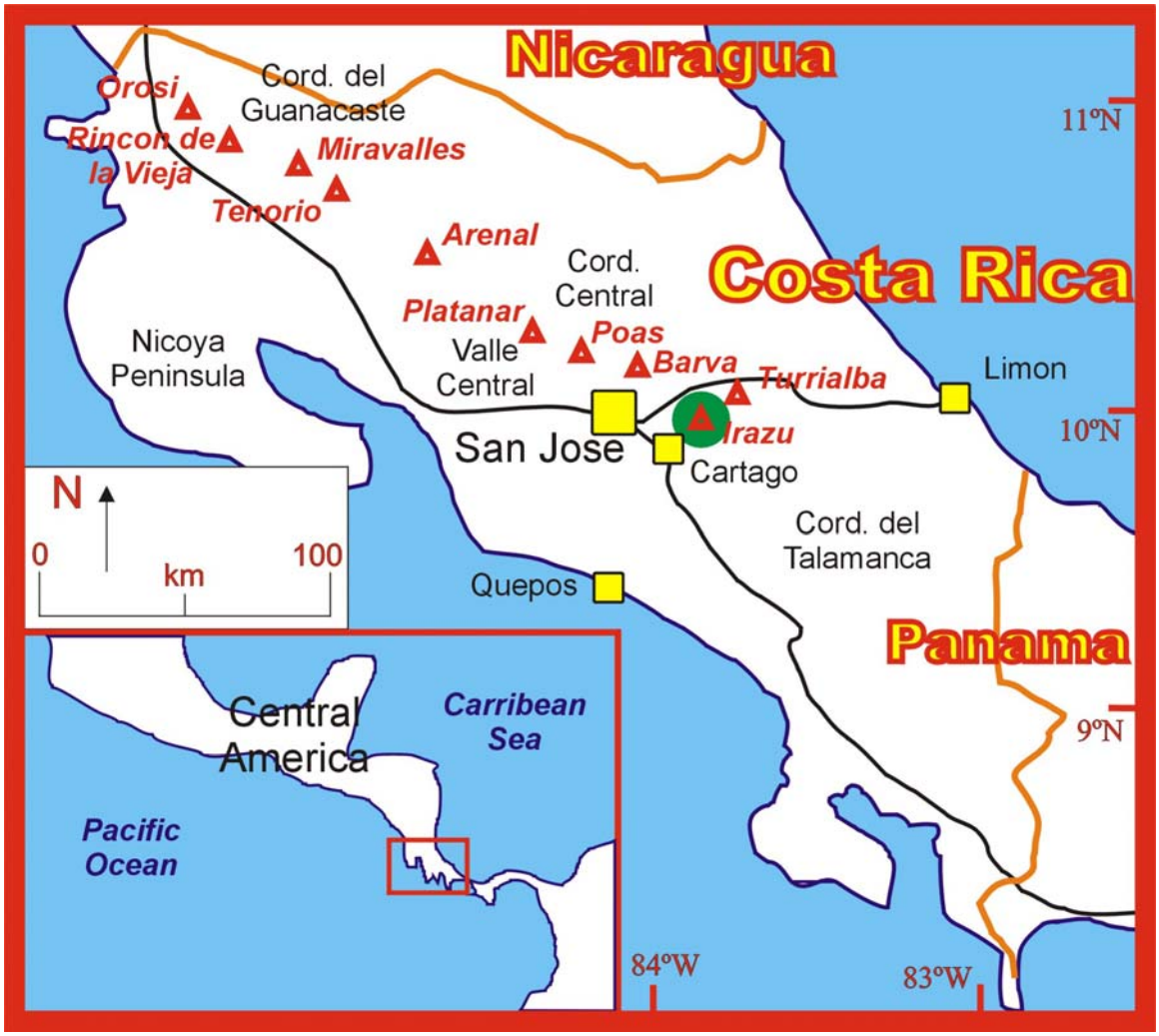

Figure 6.6: Location of volcán Irazú

Investigations of the vulnerability of the built environment concentrated on the effects of ash loading and lahar impact on buildings. Data was collected on building type and design in villages around the volcano and also on the general spatial distribution of housing, industry and communications and emergency infrastructure. Data from ash fallout modelling and hazard mapping was then utilised in order to consider the risk of building damage and failure from eruptions similar to that of 1963-65. Mitigation of the risks to the built environment are discussed in the context of the findings.

The impact of the 1963-65 eruptions on the population and environment was investigated using health and other data from the period, including information on ash particle size and chemical composition. Although credible scientific and health data were sparse for the eruptions, some assessment of the general impact was possible.

The fourth component of the case study was into the economic consequences of the 1963-65 eruption. Most economic data utilised was available in the UK, although some comes from Costa Rican sources. Various methods of looking at the economic consequences of the eruption were utilised. Assessment of the current economy in the light of the findings of the remainder of the study enabled some conclusions to be drawn concerning the likely impact of a similar eruption at the present time, and also propose some remedial measures which might be taken to better protect the economy from impact.

The different elements of this case study were drawn together in the context of community preparedness for another eruption at Irazú. Whilst they concentrate on this particular volcano, each of them is applicable to many other volcanoes, especially those which have long-lasting, ash generating eruptive style. Some of the subjects investigated in this case study would not normally be addressed in a conventional volcanic hazard assessment, but are important in progressing towards risk assessment and in highlighting the many-faceted nature of volcanic hazards to different end-users.

6.4.4 Hazard assessment and ash fallout modelling

A rapid hazard assessment of Irazú was undertaken in order to provide future activity scenarios for the other aspects of the project. Special attention was paid to the ash and lahar deposits around the volcano and to aspects of these phenomena in historical accounts, as these represent the most important volcanic hazards at Irazú.

Two generalised volcanic hazard maps were prepared for the region, although more detailed maps of specific areas under threat from lahars would be beneficial for community-level planning.

Ash deposits occur mainly to the west, and details of this distribution were examined using a modelling approach (see below). Lahars occur on the western and southern flanks of the volcano and are usually, though not exclusively, associated with periods of rapid ash deposition and heavy rain. The main threat is to parts of the town of Cartago: Part of the town was destroyed by lahars in December 1963 with the loss of 20 or so lives and considerable damage to property. The whole town is built upon a debris fan derived from the upper flanks of the volcano, probably over the past few thousand years. Since the 1963-65 eruptions,

development has taken place in areas of high hazard with respect to lahars, despite the efforts of the Costa Rican authorities to provide planning and development guidelines using a geographical information system within the National Emergency Office.

Fieldwork revealed that other volcanic hazards are relevant to Irazú. Landslides are common on the upper flanks, and are caused by a variety of mechanisms not necessarily associated with an eruption, although it is clear that ash loading on already unstable slopes can induce landsliding. Another potential hazard is seismic (shaking) damage from volcano-related earthquakes associated with the onset or continuation of volcanic activity. The historical record and more recent seismic records indicate that large earthquakes occur beneath the volcano, both associated with volcanic activity and independent of it.

Pyroclastic flows, lava flows and sector collapse are less likely hazards at Irazú, but nevertheless have potentially devastating consequences.

Pyroclastic flows have been confined to within 10 km of the vent and are not particularly voluminous. However, they appear to be generated during eruptions which are in other respects very similar to those documented in history: It may therefore be impossible to forecast whether or not pyroclastic activity will occur during any particular eruption.

Lava flows represent a hazard to infrastructure, but in the case of Irazú the hazard is difficult to define as lava flows can be extruded from either the summit area or from the flanks of the volcano.

Evidence for catastrophic sector collapse at Irazú is ambiguous, but coarse debris avalanche deposits are widespread on at least the southern flank of the volcano. Such an event in the future cannot therefore be ruled out.

Modelling of ash dispersal was undertaken in order to understand the behaviour of ash falling out of eruption columns in cross-winds, and also as a first step towards development of real-time ash fallout prediction models which could assist in mitigating the impact of ash fall. Existing models of eruption columns and their behaviour in winds were developed to involve sedimentation of ash from such plumes. Data on wind speed and eruption column height during the 1963-65 eruption at Irazú were then used to simulate ash fallout out and compare it with known results. Initial indications were that the modelling was in good agreement with information collected at the time of the eruptions on ash thickness and rates of accumulation.

More thorough testing of the models with Irazú data was not possible as the ash fall information collected during the 1963-65 eruptions was not sufficiently accurate. Wind speed and direction also plays an important role, and records from the mid-60s were again poor. The models do not take into account the possibility of ballistic impacts within a few kilometres of the vent and therefore do not address all of the hazards associated with tephra fall.

Modelling of ash dispersal continues, and it is envisaged that a real-time ash prediction tool will be available in future. This would require input of wind and other meteorological data and eruption column height for a specific event, and would calculate and map fallout thickness and rate. Such information would be available in a few minutes once an eruption

column had been produced, and therefore mitigation measures could be taken prior to ash starting to fall.

6.4.5 Vulnerability of buildings related to lahar and airfall hazards

The two main volcanic hazards for Irazú are lahars and airfall tephra, which have significant effects on the built environment. Lahars have a much smaller area of impact, but their destructive power is generally much greater than for airfall tephra.

Lahars generated during the 1963-65 eruptions did considerable damage to infrastructure, especially in late-1963. The Reventado drainage on the southern flank of the volcano is the most hazardous channel. The squatter settlement of Diques, home to about 1,500 people, has been built within the protective dikes constructed in early 1964 following the loss of 20 people and numerous buildings in late–1963. Other areas of Cartago are at lesser risk, as are areas around Tres Ríos. Transport infrastructure is at risk in a number of drainages, with numerous bridges being damaged by lahars during the 1963-65 eruptions. Also at some risk is the El Alto oil terminal, the main oil distribution point for Costa Rica.

A number of parameters can be used to estimate the likelihood of lahar generation. Rainfall intensity and runoff potential are important in controlling the rate and volume of water entering the drainage systems. Mean annual rainfall at Irazú is between 1,500 and 2,500 mm, with 75% falling in the wet season between mid-April and mid-November, a significant proportion of which falls during severe storms. Runoff depends largely on vegetation and soil cover; runoff greater than 95% (of precipitation) was reported for Irazú (Waldron, 1967) due to an impermeable crust formed chemically on ash deposits of greater than 20 cm thickness. Once water enters a drainage, the discharge and flooding potential become important. Use of experimental and empirical data suggests that lahars can be generated at Irazú at precipitation rates of about 10 mm/h with ash cover of 20 cm. At rates of greater than 50 mm/hour, probability is extremely high for lahar generation (See Table 5.1).

The destruction potential of lahars is greater than that of normal floods due to their higher specific gravity and potential for impact by large objects within the flow. Impact pressures of the order of 80 to 180 kPa are estimated for typical lahars on the lower flanks of Irazú. Such pressures are capable of destroying most buildings. Other effects such as inundation by water, solidification of lahars and duration of lahar impacts also assist in destruction of buildings.

Building lahar-resistant structures is prohibitively expensive except in exceptional circumstances. Lahar warning is possible by monitoring rainfall and river levels on the upper flanks of the volcano: This could give sufficient warning for evacuation of population from lahar-prone areas. Lahar control structures have been successfully utilised elsewhere in the world (especially Japan), but must be carefully planned and are expensive. Two main methods can be employed; watershed and drainage protection (e.g. reforestation, stabilisation of slopes, river dredging) and dike or check-dam construction.

Airfall tephra impact on buildings has been documented from a number of eruptions, but few quantitative assessments have been made. Over 400 buildings were destroyed by airfall tephra during the 1963-65 eruption of Irazú, and of these, all 250 that were situated within 5 km of the summit to the west-southwest were destroyed. A further 626 building suffered repairable damage. The population in areas affected during the 1963-65 eruptions has almost trebled since that time, and therefore the impact from a similar eruption in the future would be much more severe.

A building vulnerability survey was undertaken in the village of Llano Grande to investigate the potential impact of airfall tephra. Building use, structural type, wall material, roof cover and condition, roof pitch and window shutters were all rapidly documented. Engineering evaluation of the most common roof types in terms of collapse potential from ash loading was then undertaken. This revealed that roof purlins were the most likely structural element to fail, and tephra depths of 40 to 80 cm could lead to roof collapse. It was estimated that certain roof joints might fail at slightly lower ash loading thicknesses. Failure of the typical galvanised iron roof sheets could also occur at lower tephra thicknesses due largely to corrosion by the acidic ash.

6.4.6 Health and environmental impacts of ash eruptions

Ashfalls during the 1963-65 eruptions of Irazú had a substantial impact on human health, crops and vegetation. Most of the harmful effects were due to a high proportion of ash particles less than 10 microns in diameter, the fine size range being due at least in part to the eruptive processes in the crater which had a milling effect on lithic and juvenile ejecta. In addition, acids were readily adsorbed on to the fine ash surfaces, a process which was enhanced when ash clouds were emitted immediately following eruptions of acid steam clouds and the two mixed together. Acidity was associated mainly with sulphate and sulphuric acid soluble residues. The additional irritancy of the ash increased the potential of the particles to cause conjunctivitis, nose and throat irritation and bronchitic symptoms. From studies of other volcanoes, it is now known that the ash would have been capable of exacerbating symptoms in patients with asthma and chronic lung disease. Furthermore, the latest research on urban air pollution links daily hospital admissions and deaths in the general population with exposure to particles of the size and concentrations measured in San José during the eruptions. The absence of epidemiological studies and a programme of air monitoring in San José during the 1963-65 eruptions limits a full understanding of the impact on health at the time.

The acidic ash also caused pronounced damage to the flowers and leaves of susceptible plant species, especially if the ash fell at night or early morning when the foliage was damp with dew. The acid solution was found to spread over the whole of the leaf surface and then result in leaf-burn when it dried out during the day. Plants most at risk were tomato, potato, imperial grass, tobacco, onion, citrus fruits and the coffee flower. Livestock were affected by being unable to find forage because grazing areas were covered in ash, the ingestion of which led to diarrhoea in cattle. Imperial grass which they normally ate was destroyed, and farmers had to resort to washing giganti grass as the animals would not eat it with the ash coating. Herds had to be moved down to the plain. In future eruptions of this type the fresh-cut flower industry, which has only recently developed in the Central Valley area, is also likely to be

affected. Measures which might be expected to protect horticulture, for example green houses and plastic coverings, may not be fully effective because of the fine nature of the ash, which would also be capable of infiltrating buildings and machinery.

A reawakening of activity at volcán Irazú should be regarded as a public health emergency. Although the eruptive behaviour may not follow the same patterns as shown in 1963-65, urgent investigations will be needed on the ash to determine its characteristics and potential toxicity. Epidemiological monitoring of the respiratory health of the population of the San José area will be needed and the necessary information systems should be established well in advance of a future crisis. Air pollution monitoring in the populated areas should be extended to include fixed sites and studies of schools and occupational activities. Some of this work is already being undertaken in San José to investigate urban air pollution in general (e.g., from traffic emissions) and this should be strengthened given the potential hazards of the volcanoes overlooking the Central Valley area. Attention should also be given during future ashfalls from Irazú to relocate susceptible individuals and their families, such as children suffering from severe asthma and patients with chronic cardio-respiratory diseases.

6.4.7 Economic impact of volcanic activity

One aspect of volcanic eruptions which has received little attention is that of the economic consequences. The Irazú eruption had been used as an example of the economic impact of long-lived, low intensity eruptions, but no systematic assessment had been undertaken and no efforts had been made to apply an eruptive and economic impact model to the modern economy of Costa Rica, which is of greater value to risk assessment and disaster planning.

Despite the scarcity of economic data for the 1963-65 period, macro-economic impact was successfully elucidated. Micro-economic impact at a household level is much more difficult to assess, and insufficient data was available to do this successfully. Gross Domestic Product (GDP) for Costa Rica for the period 1961-70 averaged 6.1 %. Both 1963 and 1964 showed below average GDP growth, at 4.8 % and 4.1 % respectively. The construction industry was particularly hard-hit in 1964 due to eruption–related uncertainty, but general investment in the economy was boosted by the creation of the Central American Common Market in 1964. Economic impact was offset by high world prices for the country's primary exports. There is some evidence to suggest that uncertainty over the potential destructive capability of the eruption impacted significantly on long-term investment in the country.

Continued growth of the economy and migration of people into potentially hazardous areas of Irazú has considerably changed the manner in which future eruptions would impact upon the economy. At the micro-economic level, economic improvement is not mirrored by poverty reduction, and those most vulnerable to natural disasters have increased in numbers since 1965.

Gradual diversification of agriculture since the last eruption means that the direct impacts of future ashfall are likely to be reduced, although increasing dependence of the macro-economy on electrical power and communications infrastructure means that impacts at some key locations could be very damaging (e.g. El Alto oil terminal, Cachi hydroelectric plant, road and rail bridges, and the telecommunications infrastructure on the summit of the volcano).

Tourism is a major growth area in the economy, and the disruption of air travel as well as lack of confidence in safety could severely impact on this sector during a future eruption.

Despite the wide range of potential impacts, it is not thought that another eruption of Irazú, if similar to that in 1963-65, would on its own severely impact on the Costa Rican economy. However, coincidence of an eruption with other downward economic trends could lead to a domino effect in the economy. Mitigating against such situations can be effective, and continued economic diversity, disaster planning and more effective development of the insurance sector could all assist in reducing the impact of future eruptions on the economy.

6.4.8 Conclusions

The Irazú sub-project investigated a number of issues in volcano hazard and risk assessment, most of which are not taken into account during normal hazard assessment projects. Many of the findings in the areas of health, economic and physical impact are widely applicable to other volcanoes, but baseline data are still sparse, and more work is required to fully understand and successfully model such impacts.

The 1963-65 eruptions proved an interesting case study and many recommendations were made that would minimise the adverse impact of future eruptions at the volcano. These recommendations mainly involve preparedness at a community level through emergency planning, the enforcement of building regulations and the integration of monitoring and warning systems.

6.5 Montserrat, West Indies

6.5.1 Background to the study

The British Dependent Territorial Island of Montserrat became an active test-bed for volcanic hazard management on 18 July 1995 when the Soufriere Hills volcano erupted. A number of the key workers in this project became involved in the management of the Montserrat crisis, and many of the techniques and issues addressed during the project proved to be useful and relevant.

The volcanic eruption on Montserrat came as a surprise, but it should not have: Hazard assessment undertaken in 1986 highlighted the vulnerability of the capital town, Plymouth, and also stated that the mid-1990s would be a time when an eruption was quite likely, based upon periodic volcano-seismic activity throughout the previous 100 years (Wadge and Isaacs, 1987; 1988). Furthermore, pre-cursor seismicity from late 1992 to 1994 provided further short-term warning. Despite these clear forewarnings no volcano-related emergency plans were formulated, and development continued apace in Plymouth with the construction of key infrastructure within a few kilometres of the volcano.

After 4 months of phreatic eruptions, a lava dome began to be extruded in the summit crater of the volcano in November 1995 and continued to grow until March 1998. The generation of pyroclastic flows from dome collapse and, from September 1996, of explosive activity, led to

the evacuation of two thirds of Montserrat and the departure of 75 % of the population from the island. From early in 1998 until late in 1999 the existing dome was partially destroyed by piecemeal avalanches, which generated pyroclastic flows, and by less frequent large-scale collapses. In November 1999 a new dome began to grow rapidly.

Much of the island's key infrastructure became inaccessible in early to mid-1997, and most of the important facilities were destroyed by subsequent volcanic activity. These include the port and associated facilities, new and old hospitals, the power station, the main industrial area, government headquarters (including the parliament building and law courts), numerous houses and shops and the island's airport.

The steady increase in the violence of the eruption and the area affected by it, has meant that hazard and risk assessment has been an ongoing process, based upon intensive volcano monitoring by the Montserrat Volcano Observatory. The desire of the population to remain on Montserrat as long as it was safe to do so has severely tested the scientific understanding of volcanic activity on Montserrat and the extent to which hazard and risk assessments can be used to manage such crises.

6.5.2 Hazard and risk assessments on Montserrat

Informal hazard assessments were undertaken on Montserrat during the early days of the eruption. The absence of any historical activity and the poor understanding of the volcano once in eruption meant that these early assessments had to be relatively generalised. Once work had been undertaken on the volcanic history of the island and monitoring information became available to build a better understanding of the activity, more detailed hazard assessments were undertaken. These were converted to risk assessments at a very basic level by inclusion of such factors as ease of evacuation.

A significant upsurge in activity in the summer of 1997 and the need for evacuation from a larger area than before led to requests for a formal hazard and risk assessment to be undertaken. The hazard assessment included very detailed scientific consideration of possible eruptive scenarios, based upon the wide range of monitoring and research data gained during the eruption. Such intimate knowledge of the activity enabled future eruptive scenarios to be proposed and probabilities of occurrence to be estimated.

Population vulnerability was assessed through knowledge of population distribution and studies of building vulnerability (using methods developed on the Irazú case study of this project) and possible injury and mortality rates for different hazardous phenomena (also based on work undertaken during this project). The problem of toxic fine ash on Montserrat has been an important issue with respect to health, and expertise developed during the Irazú sub-project proved to be very useful in assessing the extent of the problem and monitoring and mitigating against it.

A series of formal risk assessments have been undertaken approximately every 6 months. These utilise a process of expert elicitation to estimate the probabilities of the occurrence of various hazardous volcanic phenomena, which are then converted into impacts through application of models and volcanological experience. Due to the high uncertainties in many

parameters, Monte Carlo simulation has been used to obtain statistically valid societal risk levels for various population distributions and also individual risk levels. The results of these formal hazard and risk assessments provide information very pertinent to the management of the crisis and have proved most useful to decision makers. Details of these assessments are described in a series of open reports produced by the Montserrat Volcano Observatory (e.g. MVO,1997; 1998a; 1998b).

6.5.3 Conclusions

The Montserrat eruption has provided an intense test bed for a number of aspects of volcano hazard and risk assessment addressed in this project. Experience gained through the project has been applied to the Montserrat crisis, leading to successful hazard and risk assessment and provision of pertinent and timely advice to management authorities. The lack of action on early hazard reports highlights the problem of communication between scientists and planners, as discussed earlier in this report (Section 3.4.1).

7. CONCLUSIONS

Natural disasters in developing countries seriously disrupt development plans, causing burdensome economic setbacks by diverting precious resources into relief and reconstruction, which would otherwise be destined for development. Additionally, income from production and export declines because of the disruption caused by disasters, and this can be severe in nations with small, poorly diversified economies.

Because disasters are inextricably linked to human and economic development, the most efficient way to prevent them or reduce their impact is to take natural hazards into routine consideration when formulating development plans. Disaster reduction measures embodied within a development project from the outset will undoubtedly be less expensive and will be more effective than the introduction of such measures at a later stage, when hazardous areas may have already been developed and vested interests render compliance with disaster prevention difficult, if not impossible. An integrated approach to hazard management and development planning will also result in more realistic cost-benefit analyses of potential development projects, by taking into account the estimated costs and benefits of hazard reduction measures.

It is estimated that more than 500 million people are at risk from the hazards posed by volcanoes, a large proportion of whom live in the developing world. The potential therefore exists for major loss of life and damage to property in a number of regions, especially where large urban areas occur in proximity to dangerous volcanoes. As population pressures intensify, hazardous areas are likely to become increasingly developed, so raising the level of risk.

In the case of major eruptions, such as that of Mount Pinatubo in 1991, losses to property, infrastructure and economic activity can run into billions of dollars, but even relatively minor and benign activity, such as that at Irazú in the early 1960s can have adverse impacts through the disruption of economic activity, lack of investor confidence, and harm to the health of humans, animals and crops.

Although numerous volcanoes pose a high level of risk in many developing countries, relatively few have been the subject of hazard assessments. One of the main objectives of the current project has therefore been the development and evaluation of rapid and cost-effective methods for volcanic hazard mapping in developing countries.

The volcanic hazard mapping case studies of the Chilean volcanoes of Nevados de Chillán and Villarrica, described in Section 6, allow the merits of rapid mapping techniques to be compared with more conventional methods. Nevados de Chillán had not previously been studied and was assessed using a conventional approach by a team of specialists over a period of several years, supported by extensive petrological and geochemical laboratory studies and a radiometric dating programme. In contrast, the assessment of Villarrica concentrated on developing a methodology for rapid hazard mapping based upon the interpretation of satellite images, aerial photographs and a few weeks of field work undertaken by a single geologist. A very detailed but little known hazard assessment of Villarrica, produced over a period of

many years by several Chilean geologists, was made available on completion of the project's case study. This allowed a direct comparison of rapid versus conventional hazard assessments to be made on the same volcano.

The Villarrica study effectively demonstrated the possibilities of low-cost, rapid volcanic hazard mapping in developing countries where high numbers of potentially active volcanoes occur. The level of detail of hazard mapping is only slightly compromised using these methods compared with conventional assessments, and is certainly sufficiently accurate and informative to be fit for the purpose of development planning and disaster preparedness. It is encouraging to report that a similar project farther north in the Chilean Andes (Naranjo *et al.*, 1998) has utilised these techniques successfully for rapid volcanic hazard mapping, and that the methodology is currently being taken forward in a rapid assessment of Tristan da Cunha.

The most obvious benefits of such rapid volcanic hazard assessments are that they are considerably less expensive and can be completed in a fraction of the time needed for conventional assessments based upon detailed geological fieldwork.

The difficulty of identifying larger, less frequent events in a volcano's geological history is a potential weakness of rapid hazard mapping techniques when compared with more detailed conventional assessments. However, this shortcoming can be reduced to some extent by making inferences from similar volcanoes elsewhere whose eruption histories are better known. Thus for example, the hazard of flank collapse and debris avalanche (which is generally rare) should be considered a possibility at any high, steep-sided volcano, even if previous events of this type have not been recognised in the volcano's history.

During the course of hazard assessment, it is important to ascertain the age of key eruptive events in the evolution of the volcano in question, on the assumption that future activity is likely to be of similar style and frequency as past activity. Without information on the frequency of hazardous events it is not possible to utilise hazard map information in the downstream activity of risk assessment. Wherever possible therefore, radiometric dating should therefore be undertaken during the course of rapid hazard assessments, in order to gain an idea of the ages of past events, even though such techniques are relatively expensive and the analysis of samples in the laboratory is a lengthy process which can introduce delays in completion of the overall hazard assessment. The analysis of local archival material should also be carried out during rapid hazard assessments, as this can be effective in revealing the style and frequency of historical activity, as demonstrated for example by the Nevados de Chillán case study.

The interpretation of aerial photographs has an important part to play in rapid volcanic hazard assessments. In the case study of Nevados de Chillán a detailed photo-geological map was prepared prior to fieldwork, and this successfully identified most of the main structural features of the volcano and served as an invaluable basis for planning fieldwork and focusing attention on key localities for detailed examination, so saving valuable time during the field assessment. Satellite images seldom provide the level of geological information that can be obtained from aerial photographs, although they may afford good overviews of volcanoes and their environs, outlining the main hazard pathways and elements of infrastructure, as illustrated for example by the satellite image of Figure 2.1.

Digital cartographic techniques and geographical information systems have greatly increased the efficiency of data analysis and presentation of volcanic hazard information. Such techniques undoubtedly speed up the overall process of hazard assessment, facilitate the presentation of hazard information in different forms and allow it to be readily integrated and analysed with other information.

Hazard maps should be used as a basis for land-use planning in volcanic areas, with the objective of regulating the development of hazardous zones and reducing the level of risk posed by future eruptions. In addition to land use planning, the information provided by hazard maps is needed for the formulation of civil defence plans. Volcanic hazard maps should therefore not be considered as an end product in their own right, but should be viewed as a component or tool within the broader process of risk reduction. Consequently it is important that hazard maps contain relevant information presented in a form that can be understood by civil authorities and decision makers involved with the downstream activities of planning and risk reduction.

Experience from past volcanic crises has shown that problems exist in the uptake and utilisation of volcanic hazard information by civil authorities responsible for risk reduction and planning, due allegedly to failures in communication with geoscientists. There is undoubtedly some truth in this, although the issue is complicated and the reasons for failure are manifold. For example, political indecision, misjudgement and bureaucratic short-sightedness appear to have been crucial factors in precipitating several of the worst volcanic disasters of the 20 century, rather than a lack of clear volcanological information.

Complacency in acting upon hazard information also plays a part, given that in most volcanic areas people hardly ever experience the adverse effects of an eruption in their lifetimes, whilst the largest and most destructive eruptions are rare events. The problem is summarised by Voight (1990) as one in which the volcanologist has to state the probabilistic chance of error in the forecasting and delineation of hazards, but at the same time has to be sufficiently specific to encourage the authorities to take action, and the public to respond. Unfortunately, because of the nature of volcanoes, which in general appear to be dormant for prolonged periods, a window of opportunity for meaningful communication opens infrequently between volcanologists who foresee disaster on a crude probabilistic scale, and authorities that have to make pragmatic decisions. As a result authorities may choose not to implement risk-reduction policies under dormant volcanic conditions, and may only be galvanized into action when confronted with a volcanic event which is perceived to be dangerous.

Another impediment to the communication of volcanic hazard information appears to be that civil authorities and other decision makers have difficulties in understanding volcanic hazard maps. This issue is more complicated than appears at first sight and is not simply due to the specialised nature of such maps, although this is a contributing factor, but may also be due to the fact that many of those involved in the downstream processes of risk reduction are not generally conversant with using maps, and therefore have difficulties in understanding spatial information presented in this form. Volcanic hazard zone maps therefore need to be clear and simple, and alternative methods of presentation should be considered which make the hazard information easier to visualise. Such methods include the presentation of hazard zones draped over three dimensional terrain models, shaded relief maps or oblique aerial photographs, as

has been demonstrated to good effect in the case studies of this project (e.g. Figures 6.4 and 6.5).

In order to overcome the impediments to the uptake of volcanic hazard maps and ensure they are used effectively, closer co-operation and mutual understanding is essential between planners, politicians and volcanologists. Planners should be involved with all stages of hazard and risk assessment and should instigate and take the co-ordinating role in the overall process. By doing so, they are likely to become more conversant with the nature of the hazards, and the resultant maps will be better tailored to their requirements. Ideally, hazard assessments should be carried out at the request and under the direction of planners or national emergency bodies, so that a sense of ownership of the resultant hazard maps is engendered.

Probably the most effective means of communicating the potential impact of volcanic hazards to planners and decision makers is to take hazard assessments a stage further and incorporate the information within risk maps. Although very few volcanic risk assessments have been undertaken, they offer distinct advantages over hazard maps, by providing more meaningful and tangible indications of the economic losses and casualties that may arise as a consequence of volcanic activity. Such risk assessments require that volcanic hazard maps contain information on the probability or frequency of eruptions, which again underlines the necessity of obtaining historical information and radiometric ages of past activity as part of the hazard assessment process. They also require information on the vulnerability of people, buildings and economic activity, with respect to the hazards in question.

Whilst the project has demonstrated that the methods exist for producing effective and cost-beneficial hazard and risk assessments by rapid methods, the problem remains of convincing civil authorities that such assessments are necessary in the first place, bearing in mind the reluctance to implement risk-reduction policies under dormant volcanic conditions, which are the norm at most volcanoes.

8. REFERENCES

ABE, K. 1992. Seismicity of the great eruption of Mount Katmai, Alaska, in 1912. *Bulletin of the Seismological Society of America.* Vol. 82, 175 – 191.

ADB. 1991a. *Disaster mitigation in Asia and the Pacific*. (Manila: Asian Development Bank).

ADB. 1991b. *Report of the Task Force on the damage caused by the eruption of Mt. Pinatubo and proposed rehabilitation/restoration measures.* Agricultural Department, August 1991. (Manila: Asian Development Bank).

ALLARD, P, BAUBRON, J C, CARBONELLE, J, DAJLEVIC, D, LEBRONEC, J, ROBE, M C, and ZETTWOOG, P. 1989. Diffuse soil degassing from volcanoes; Geochemical and volcanological implications [Abstract]. IAVCEI General Assembly, Santa Fe, 1989. *New Mexico Bureau of Mines and Mineral Resources Bulletin*, No. 131, 3.

ARAMAKI, S. 1976. The 1783 activity of Asama volcano, Part 1. *Japanese Journal of Geology and Geography*, Vol. 27, 189-229.

ARMIENTI, P, MACEDONIO, G, and PARESCHI, M T. 1988. Numerical model for simulation of tephra transport and deposition: Applications to May 18, 1980, Mount St. Helens eruption. *Journal of Geophysical Research*, Vol. 93, B6, 6463-6476.

BARBERI, F, MACEDONIO, G, PARESCHI, M T, and SANTACROCE, R. 1990. Mapping the tephra fallout risk: an example from Vesuvius, Italy. *Nature*, Vol. 344, 142-144.

BARQUERO, J, and FERNANDEZ, E. 1990. Erupciones de gases y sus consecuencias en el Volcan Poás, Costa Rica. *Boletin de Vulcanologia Universidad Nacional, Costa Rica*, No. 21, 13-18. [In Spanish.]

BAUBRON, J C, ALLARD, P, and TOUTAIN, J P. 1990. Diffuse volcanic emissions of carbon dioxide from Vulcano Island, Italy. *Nature*, Vol. 344, 51-53.

BAUBRON, J C, ALLARD, P, SABROUX, J C, TEDESCO, D, and TOUTAIN, J P. 1991. Soil gas emanations as precursory indicators of volcanic eruptions. *Journal of the Geological Society*, Vol. 148, 571-576.

BAXTER, P J, and KAPILA, M. 1989. Acute health impact of the gas release at Lake Nyos, Cameroon, 1986. *Journal of Volcanology and Geothermal Research*, Vol. 39, 265-275.

BAXTER, P J, BAUBRON, J-C, and COUTINHO, R. 1999. Health hazards and disaster potential of ground gas emissions at Furnas volcano, São Miguel, Azores. *Journal of Volcanology and Geothermal Research*, Vol. 92, 95-106.

Baxter, P J, Bonadonna, C, Dupree, R, Hards, V L, Kohn, S C, Murphy, M D, Nichols, A, Nicholson, R A, Norton, G, Searl, A, Sparks, R S J, AND Vickers, B P. 1999. CRISTOBALITE IN VOLCANIC ASH OF THE SOUFRIERE HILLS VOLCANO, MONTSERRAT, BRITISH WEST INDIES. *SCIENCE*, VOL. 283, 1142-1145.

BEGÉT, J E, and KIENLE, J. 1992. Cyclic formation of debris avalanches at Mount St. Augustine volcano. *Nature*, Vol. 356, 701-704.

BERNARD, E N, BEHN, R R, HEBENSTREIT, G T, GONZALEZ, F I, KRUMPE, P, LANDER, J F, LORCA, E, MCMANAMON, P M, and MILBURN, H B. 1988. On mitigating rapid onset disasters: Project THRUST (Tsunami hazards reduction utilizing systems technology). *Eos*, Vol. 69, 649-661.

BLONG, R J. 1981a. Some effects of tephra falls on buildings. 405-420 in *Tephra Studies*. SELF, S, and SPARKS, R S J (editors). Proceedings NATO Advanced Studies Institute, Series C, Vol. 75, Laugarvatn and Reykjavik, 1980. (Dordrecht: D. Reidel).

BLONG, R J. 1981b. Tephra fallout from Karkar volcano: a first approximation. 85-93 *in* Cooke-Ravian volume of volcanological papers. JOHNSON, R W (editor). *Geological Survey of Papua New Guinea Memoir*, No. 10.

BLONG, R J. 1984. *Volcanic Hazards. A sourcebook on the effects of eruptions*. (Sydney: Academic Press).

BOUTROS-GHALI, B. 1994. The United Nations mobilize people around the world to reduce the impact of natural disasters. *Stop Disasters*, No. 17, 3-4.

BROWN, G C, RYMER, H, DOWDEN, J, KAPADIA, P, STEVENSON, D, BARQUERO, J, and MORALES, L D. 1989. Energy budget analysis for Poás crater lake: implications for predicting volcanic activity. *Nature*, Vol. 339, 370-373.

BRYANT, R. 1992. *Natural Hazards.* Cambridge University Press.

BURSIK, M I. and WOODS, A W. 1996. The dynamics and thermodynamics of large ash flows. *Bulletin of Volcanology*, Vol. 58, 175-193.

CAREY, S, and SIGURDSSON, H. 1986. The 1982 eruption of El Chichon volcano, Mexico (2): Observations and numerical modelling of tephra-fall distribution. *Bulletin of Volcanology*, Vol. 48, 127-141.

CALDER, E S, YOUNG, S. SPARKS, R S J. and MVO staff. 1998. *Montserrat Volcano Observatory, Special Report 06*, The Boxing day collapse, 1998.

CAREY, S, and SPARKS, R S J. 1986. Quantitative models of the fallout and dispersal of tephra from volcanic eruption columns. *Bulletin of Volcanology*, Vol. 48, 3-15.

CASADEVALL, T J. 1994a. Introduction. In: Volcanic ash and aviation safety. Proceedings of the first international symposium on volcanic ash and aviation safety. CASADEVALL, T J (editor). *United States Geological Survey Bulletin*, No. 2047.

CASADEVALL, T J (editor). 1994b. Volcanic ash and aviation safety. Proceedings of the first international symposium on volcanic ash and aviation safety. *United States Geological Survey Bulletin*, No. 2047.

CHAVEZ, R. 1995. Geography report Nevados de Chillán volcanic hazards project. *British Geological Survey Technical Report* WC/95/83R.

COBURN, A W, SPENCE, R J S, and POMONIS, A. 1992. Factors determining human casualty levels in earthquakes: mortality prediction in building collapse. *Proceedings of the 10th World Conference on Earthquake Engineering, Madrid, July 1992.* Balkema, Rotterdam. 5989-5994.

COLE, P.D., CALDER, E.S., DRUITT, T.H., HOBLITT, R., ROBERTSON, R., SPARKES, and R.S.J. YOUNG, S.R. 1998. Pyroclastic flows generated by gravitational instability of the 1996-1997 lava dome of Soufrière Hills Volcano, Montserrat. *Geophysical Research Letters,* Vol. 25, No. 18, 3425-3428.

COOKE, R J S. 1981. Eruptive history of the volcano of Ritter Island. 115-123 *in* Cooke-Ravian volume of volcanological papers. JOHNSON, R W (editor). *Geological Survey of Papua New Guinea Memoir*, No. 10.

CRANDELL, D R. 1983. Potential hazards from future volcanic eruptions on the island of Maui, Hawaii. *United States Geological Survey Miscellaneous Geologic Investigations,* Map I-1442.

CRANDELL, D R. 1989. Gigantic debris avalanche of Pleistocene age from ancestral Mount Shasta Volcano, California, and debris-avalanche hazard zonation. *United States Geological Survey Bulletin*, No. 1861.

CRANDELL, D R, and HOBLITT, R P. 1986. Lateral blasts at Mount St Helens and hazard zonation. *Bulletin of Volcanology*, Vol. 48, 27-37.

CRANDELL, D R, and MULLINEAUX, D R. 1978. Potential hazards from future eruptions of Mount St Helens volcano, Washington. *United States Geological Survey Bulletin*, No. 1383-C.

CRANDELL, D R, BOOTH, B, KUSUMADINATA, K, WALKER, G P L, and WESTERCAMP, D. 1984. *Source-book for volcanic-hazards*. (Paris: UNESCO).

CUMMANS, J. 1981. Chronology of mudflows in the South Fork and North Fork Toutle River following the May 18 eruption. 479-486 *in* The 1980 eruptions of Mount St. Helens, Washington. LIPMAN, P W, and MULLINEAUX, D R (editors). *United States Geological Survey Professional Paper,* No. 1250.

DAVIS, I. 1994. Assessing community vulnerability. 11-13 in *Medicine in the International Decade for Natural Disaster Reduction (IDNDR): Research, preparedness and response for sudden impact disasters in the 1990's*. Workshop Proceedings, 19 April 1993. (London: The Royal Academy of Engineering).

DAVIS, I, SANDERSON, D, PARKER, D and STACK, J. 1998. The dissemination of warnings. 5.1 – 5.64. In: Forecasts and warnings. Lee B, and Davis, I. (Editors). Thomas Telford, London.

DECKER, R, and DECKER, B. 1981. *Volcanoes*. Freeman, San Francisco. 244pp.

DIXON, H J, SPARKS, R S J, CHAVEZ, R, NARANJO, J A, DUNKLEY, P N, YOUNG, S R, and GILBERT, J S. 1995. The geology of Nevados de Chillán volcano, Chile. *British Geological Survey Technical Report* WC/95/84R.

DOBRAN, F, NERI, A, and TODESCO, M. 1994. Assessing the pyroclastic flow hazard at Vesuvius. *Nature*, Vol. 367, 551-554.

EQE INTERNATIONAL. 1995. The January, 1995 Kobe Earthquake: Economic Impact. *http://www.eqe.com/publications/kobe/economic.htm*

EWART, J W, and SWANSON, D A. 1992. Monitoring volcanoes: Techniques and strategies used by staff of the Cascades Volcano Observatory, 1980-90. *United States Geological Survey Bulletin*, No. 1966.

EWART, J W, and SWANSON, D A. 1993. Vigilando volcanes: Técnicas y estrategias empleadas por el personal del Observatorio Vulcanológico Cascades, 1980-90. *United States Geological Survey Bulletin*, No. 1966. [In Spanish.]

FISHER, R V, SMITH, A L, and ROOBOL, M J. 1980. Destruction of St. Pierre, Martinique, by ash-cloud surges, May 8 and 20, 1902. *Geology*, Vol. 8, 472-476.

FRANCIS, P W. 1985. The origin of the 1883 Krakatau tsunamis. *Journal of Volcanology anf Geothermal Research.* Vol. 25, 349-363.

FRANCIS, P W, GARDEWEG, M, RAMIREZ, C F, and ROTHERY, D A. 1985. Catastrophic debris avalanche deposit of Socompa volcano, northern Chile. *Geology*, Vol. 13, 600-603.

FRANCIS, P W, and SELF, S. 1983. The eruption of Krakatau. *Scientific American.* Vol. 249, 172-187.

FRANCIS, P W, and WELLS, G L. 1988. Landsat thematic mapper observations of debris avalanche deposits in the Central Andes. *Bulletin of Volcanology*, Vol. 50, 258-278.

FREETH, S. 1992. The deadly cloud hanging over Cameroon. *New Scientist*, Vol. 135, No. 1834, 23-27.

GIGGENBACH, W F. 1987. Redox processes governing the chemistry of fumarole gas discharges from White Island, New Zealand. *Applied Geochemistry*, Vol. 2, 143-161.

GILBERT, J S, SPARKS, R S J, and YOUNG, S R. 1998. Volcanic Hazards at Volcán Nevados de Chillán, Chile. *British Geological Survey Technical Report* WC/98/14R.

GREENLAND, L P. 1987. Hawaiian eruptive gases. 759-770 *in* Volcanism in Hawaii. DECKER, R W, WRIGHT, T L, and STAUFFER, P H (editors). *United States Geological Survey Professional Paper*, No. 1350.

GUDMUNDSSON, T. M., SIGMUNDSSON, F. and BJÖRNSSON, H. 1997. Ice-volcano interaction of the 1996 Gjálp subglacial eruption, Vatnajökull, Iceland. *Nature*, Vol. 389, 954-957.

HELIKER, C C. 1990. Volcanic and seismic hazards on the island of Hawaii. *United States Geological Survey General Interest Publication.*

HILDRETH, W. 1991. The timing of caldera collapse at Mount Katmai in response to magma withdrawal toward Novarupta. *Geophysical Research Letters*. Vol. 18, 1541-1544.

HOBLITT, R P, WOLFE, E W, SCOTT, W E, COUCHMAN, M R, PALLISTER, J S, and JAVIER D. 1996. The preclimactic eruptions of Mt Pinatubo, June 1991. 457-511 in *Fire and Mud, Eruptions and Lahars of Mt Pinatubo, Philippines*. NEWHALL, C G and PUNONGBAYAN R S (editors). (Quezon City, Philippines: Phivolcs/University of Washington Press).

HÜLSEMAN, F, WADGE, G and WOODS, A W. 1998. Large pyroclastic flows over the Centre Hills, Montserrat. *http://www.nerc-essc.ac.uk/~gw/home.html.*

HSU, K J. 1975. Catastrophic debris streams (sturzstroms) generated by rockfalls. *Geological Society of America Bulletin*, Vol. 86, 129-140.

HURST, A W. 1994. ASHFALL - A computer programme for estimating volcanic ash fallout. *Institute of Geological and Nuclear Sciences Science Report*, 94/23. New Zealand.

IDNDR. 1999. El Niño/La Niña some impact figures. *http:/www.idndr.org/nino/impactfig.htm*.

JANDA, R J, SCOTT, K M, NOLAN, K M, and MARTINSON, H A. 1981. Lahar movement, effects and deposits. 461-478. *in* The 1980 eruptions of Mount St. Helens, Washington. LIPMAN, P W, and MULLINEAUX, D R (editors). *United States Geological Survey Professional Paper*, No. 1250.

KIEFFER, S W. 1981. Fluid dynamics of the May 18 blast at Mount St. Helens. 379-400 *in* The 1980 eruptions of Mount St. Helens, Washington. LIPMAN, P W, and MULLINEAUX, D R (editors). *United States Geological Survey Professional Paper,* No. 1250.

KIENLE, J, KOWALIK, Z, and MURTY, T S. 1987. Tsunamis generated by eruptions from Mount St. Augustine volcano, Alaska. *Science*, Vol. 236, 1442-1447.

KUNO, H. 1962. *Catalogue of the active volcanoes of the world including solfatara fields*. Part 11: Japan, Taiwan and Marianas. (Rome: International Association of Volcanology).

LANDER, J F, and LOCKRIDGE, P A. 1986. Uses of a tsunami data base for research and operations [Abstract]. *Eos*, Vol. 67, 1003.

LATTER, J H. 1981. Tsunamis of volcanogenic origin: Summary of causes, with particular reference to Krakatoa, 1883. *Bulletin Volcanologique*, Vol. 44, 467-490.

LATTER, J H. 1989. Preface. v-viii *in* Volcanic Hazards - assessment and monitoring. LATTER, J H (editor). *IAVCEI Proceedings in Volcanology*, No. 1. (Berlin: Springer-Verlag).

LE GUERN, F, TAZIEFF, H, and FAIVRE-PIERRET, R. 1982. An example of health hazard: people killed by gas during a phreatic eruption: Dieng Plateau (Java, Indonesia), February 20th 1979. *Bulletin Volcanologique*, Vol. 45, 153-156.

MACDONALD, G A, and ALCARAZ, A. 1956. Nuée ardentes of the 1948-1953 eruption of Hibok-Hibok. *Bulletin Volcanologique*, Vol.18, 169-178.

MACEDONIO, G, PARESCHI, M T, and SANTACROCE, R. 1988. A numerical simulation of the plinian fall phase of 79 A.D. eruption of Vesuvius. *Journal of Geophysical Research*, Vol. 93, B12, 14817-14827.

MACEDONIO, G, PARESCHI, M T, and SANTACROCE, R. 1990. Renewal of explosive activity at Vesuvius: models for expected tephra fallout. *Journal of Volcanology and Geothermal Research*, Vol. 40, 327-342.

MAJOR, J, and NEWHALL, C G. 1989. Snow and ice perturbation during historical volcanic eruptions and the formation of lahars and floods. *Bulletin of Volcanology*, Vol. 52, 1-27.

MCGEE, K A, SUTTON, A J, and SATO, M. 1987. Use of satellite telemetry for monitoring active volcanoes, with a case study of a gas-emission event at Kilauea volcano, December 1982. 821-825 *in* Volcanism in Hawaii. DECKER, R W, WRIGHT, T L, and STAUFFER, P H (editors). *United States Geological Survey Professional Paper*, No. 1350.

MCGUIRE, W J, KILBURN C, and MURRAY, J B. 1995. *Monitoring Active Volcanoes: Strategies, procedures and techniques*. (London: UCL Press).

MCKEE, C O, JOHNSON, R W, LOWENSTEIN, P L, RILEY, S J, BLONG, R J, SAINT OURS, P DE, and TALAI, B. 1985. Rabaul caldera Papua New Guinea: Volcanic hazards, surveillance, and eruption contingency planning. *Journal of Volcanology and Geothermal Research*, Vol. 23, 195-237.

MELOSH, H J. 1979. Acoustic fluidization: a new geologic process? *Journal of Geophysical Research*, Vol. 83, B13, 7513-7520.

MERCADO, R A., LACSAMANA, J B T. and PINEDA, G L. Socioeconomic impacts of the Mount Pinatubo eruption. 1063 – 1070. In: *Fire and Mud, Eruptions and Lahars of Mt Pinatubo, Philippines*. NEWHALL, C G and PUNONGBAYAN R S (editors). (Quezon City, Philippines: Phivolcs/University of Washington Press).

MILLER, C D. 1980. Potential hazards from future eruptions in the vicinity of Mount Shasta volcano, Northern California. *United States Geological Survey Bulletin*, No. 1503.

MILLER, T.P. and CHOUET, B.A. 1994, The 1989-1990 eruptions of Redoubt Volcano, Alaska: *Journal of Volcanology and Geothermal Research*, Special Issue, v. 62, no. 1-4, 520 pp.

MONTSERRAT VOLCANO OBSERVATORY. 1997. Assessment of the status of the Soufriere Hills Volcano, Montserrat and its hazards. 15 pages, 5 appendices.

MONTSERRAT VOLCANO OBSERVATORY. 1998a. Preliminary assessment of volcanic risk on Montserrat, January 1998. 16 pages, 9 appendices.

MONTSERRAT VOLCANO OBSERVATORY. 1998b. Scientific and hazard assessment of volcanic risk of the Soufriere Hills volcano Montserrat, July 1998.

MOORE, J G. 1967. Base surge in recent volcanic eruptions. *Bulletin Volcanologique*, Vol. 30, 337-363.

MOORE, J G, and ALBEE, W C. 1981. Topographic and structural changes, March-July 1980-photogrammetric data. 123-134 *in* The 1980 eruptions of Mount St. Helens, Washington. LIPMAN, P W, and MULLINEAUX, D R (editors). *United States Geological Survey Professional Paper*, No. 1250.

MOORE, J G, and MELSON, W G. 1969. Nuée ardentes of the 1968 eruption of Mayon Volcano, Philippines. *Bulletin Volcanologique*, Vol. 33, 600-620.

MORENO, H. 1993. Volcán Villarrica: geología y evaluación del riesgo volcánico, Regiones IX y X, 39°25'S. *Report of the Servicio Nacional de Geología y Minería*. [In Spanish].

MOTHES, P A. 1992. Lahars of Cotapaxi Volcano, Ecuador: hazard and risk evaluation. 53-63 in *Geohazards - Natural and man-made*. MCCALL, G J H, LAMMING, D J C, and SCOTT, S C (editors). (London: Chapman and Hall).

MOTHES, P.A., HALL, M.L. and JANDA, R. J. 1998. The enormous Chillos Valley Lahar: an ash-flow-generated debris flow from Cotopaxi Volcano, Ecuador. *Bulletin of Volcanology*, Vol. 59, 233-244.

MULLINEAUX, D R. 1974. Pumice and other pyroclastic deposits in Mount Ranier National Park, Washington. U*nited States Geological Survey Bulletin*, No. 1326.

MURPHY, M D. 1995a. The petrology and geochemistry of Nevados de Chillán Volcano, Chile. *British Geological Survey Technical Report* WC/95/6R.

MURPHY, M D. 1995b. The petrology and geochemistry of Nevados de Chillán Volcano, Chile, Second Report. *British Geological Survey Technical Report* WC/95/85R.

NAKADA, S, and FUJII, T. 1993. Preliminary report on the activity at Unzen volcano (Japan), November 1990 - November 1991: Dacite lava domes and pyroclastic flows. *Journal of Volcanology and Geothermal Research*, Vol. 54, 319-333.

NARANJO, J A, YOUNG, S R and POLANCO, E. 1998. Rapid volcanic hazard mapping in the Bíobío drainage basin, south-central Chile (abs). *Proceedings of the International Conference on Modern Preparation and Response Systems for Earthquake, Tsunami and Volcanic Hazards*, Santiago, Chile, April 1998.

NATIONAL SCIENCE AND TECHNOLOGY COUNCIL. 1996. Natural disaster reduction: A plan for the Nation. Report of the Subcommittee on Natural Disaster Reduction of the Committee on the Environment and Natural Resources. *www.usgs.gov/sndr/report/index.html*.

NEUMANN VAN PADANG, M. 1959. Changes in the top of Mount Ruang (Indonesia). *Geologie en Mijnbouw*, Vol. 21, 113-118.

NEWHALL, C G, AND DZURISIN, D. 1988. *Historical unrest at large calderas of the world*. United States Geological Survey Bulletin, 1855, Vol.1.

NEWHALL, C G, and SELF, S. 1982. The Volcanic Explosivity Index (VEI): an estimate of explosive magnitude for historical volcanism. *Journal of Geophysical Research*, Vol. 87, 1231-1238.

NOMANBHOY, N and SATAKE, K. 1995. Generation mechanism of tsunami from the 1883 Krakatau eruption. *Geophysical Research Letters.* Vol. 22, 4, 509-512.

OPERATION TAAL. Philippine Institute of Volcanology and Seismology.

PARRA, E, and CEPEDA, H. 1990. Volcanic hazard maps of the Nevado del Ruiz volcano, Colombia. *Journal of Volcanology and Geothermal Research*, Vol. 42, 117-127.

PENDICK, D. 1995. And here is the eruption forecast. New Scientist, Vol. 145, No. 1959, 26-29.

PERRY, R W, and HIROSE, H. 1991. *Volcano management in the United States and Japan.* (Greenwich: JAI Press).

PRESS, F. 1993. The need for action. 2-4 *in* Disaster Reduction. *UNESCO Environmental and Development Briefs,* No.5. (Paris: UNESCO).

PETIT-BREUILH, M-E. 1995. The volcanic history of Nevados de Chillán volcano, Chile. *British Geological Survey Technical Report* WC/95/86R.

POMONIS, A, SPENCE, R, and BAXTER, P J. 1999. Risk assessment of residential buildings for an eruption of Furnas Volcano, São Miguel, the Azores. *Journal of Volcanology and Geothermal Research*, Vol. 92, 107-131.

PUNONGBAYAN, R S, UMBAL, J, TORRES, R, DAAG, A S, SOLIDUM, R, DELOS-REYES, P, and RODOLFO, K S. 1992. A technical primer on Pinatubo lahars. *Philippine Institute of Volcanology and Seismology*, unnumbered report.

RODOLFO, K S. UMBAL, J V, ALONSO, R A, REMOTIGUE, C T, PALADIO-MELOSANTOS, M L, SALVADOR, J H G, EVANGALISTA, D, and MILLER, Y. 1996. Two years of lahars on the western flank of Mount Pinatubo: Iniation, flow processes, deposits and attendant geomorphic and hydraulic changes. In: *Fire and Mud, Eruptions and Lahars of Mt Pinatubo, Philippines*. NEWHALL, C G and PUNONGBAYAN R S (editors). (Quezon City, Philippines: Phivolcs/University of Washington Press).

ROWE, G L, BRANTLEY, S L, FERNANDEZ, M, FERNANDEZ, J F, BORGIA, A, and BARQUERO, J. 1992. Fluid-volcano interaction in an active stratovolcano: the crater lake system of Poás Volcano, Costa Rica. *Journal of Volcanology and Geothermal Research*, Vol. 49, 23-51.

SARNA-WOJCICKI, A M, SHIPLEY, S, WAITT, R B JR., DZURISIN, D, and WOOD, S H. 1981. Areal distribution, thickness, mass, volume, and grain size of air-fall ash from the six major eruptions of 1980. 577-600 *in* The 1980 eruptions of Mount St. Helens, Washington. LIPMAN, P W, and MULLINEAUX, D R (editors). *United States Geological Survey Professional Paper*, No. 1250.

SCADONE, R., ARGANESE, G. and GALDI, F. 1993. The evaluation of volcanic risk in the Vesuvian area. *Journal of Volcanology and Geothermal Research*, Vol. 58, 263-271.

SCHICK, R. 1981. Source mechanism of volcanic earthquakes. *Bulletin Volcanologique.* 44, 491-497.

SELF, S, KIENLE, J, and HUOT, J P. 1980. Unirek maars, Alaska, II. Deposits and formation of the 1977 craters. *Journal of Volcanology and Geothermal Research*, Vol. 7, 39-65.

SHERIDAN, M F and MACIAS, L J. 1995. Estimation of risk probability for gravity-driven pyroclastic flows at volcan Colima, Mexico. *Journal of Volcanology and Geothermal Research*. Vol. 66, 251-256.

SIEBERT, L. 1984. Large volcanic debris avalanches: characteristics of source areas, deposits and associated eruptions. *Journal of Volcanology and Geothermal Research*, Vol. 22, 163-197.

SIEBERT, L. 1992. Threats from debris avalanches. *Nature*, Vol. 356, 658-659.

SIEBERT, L, GLICKEN, H, and UI, T. 1987. Volcanic hazards from Bezymianny - and Bandai-type eruptions. *Bulletin of Volcanology*, Vol. 49, 435-459.

SIGURDSSON, H. 1982. Volcanic pollution and climate: The 1783 Laki eruption. *Eos*, Vol. 63, 601-602.

SIGURDSSON, H, CAREY, S N, and ESPINDOLA, J M. 1984. The 1982 eruptions of El Chichón volcano, Mexico: Stratigraphy of pyroclastic flow deposits. *Journal of Volcanology and Geothermal Research*, Vol. 23, 11-37.

SIGURDSSON, H, DEVINE, J D, TCHOUA, F M, PRESSER, T S, PRINGLE, M K W, and EVANS, W C. 1987. Origin of the lethal gas burst from Lake Monoun, Cameroon. *Journal of Volcanology and Geothermal Research*, Vol. 31, 1-16.

SIMKIN, T. 1994. Volcanoes: their occurrence and geography. 75-78 *in* Volcanic ash and aviation safety. Proceedings of the first international symposium on volcanic ash and aviation safety. CASADEVALL, T J (editor). *United States Geological Survey Bulletin*, No. 2047.

SIMKIN, T, and SIEBERT, L. 1984. Explosive eruptions in space and time: durations, intervals, and a comparison of the World's active volcanic belts. 110-121 in *Explosive volcanism: Inception, evolution and hazards*. (Washington: National Academy Press).

SIMKIN, T, and SIEBERT, L. 1994. Volcanoes of the World. Second Edition. A regional directory, gazetteer, and chronology of volcanism during the last 10,000 years. (Tuscon, Arizona: Geoscience Press).

SPARKS, R S J. 1986. The dimensions and dynamics of volcanic eruption columns. *Bulletin of Volcanology*, Vol. 48, 3-15.

SPARKS, R S J, and WILSON, L. 1976. A model for the formation of ignimbrite by gravitational collapse. *Journal of the Geological Society*, Vol. 132, 441-451.

STEPHENSON, P J, and GRIFFIN, T J. 1976. Some long basaltic lava flows in North Queensland. 41-51 in *Volcanism in Australasia*. JOHNSON, R W (editor). (Amsterdam: Elsevier).

STOOPES, G R, and SHERIDAN, M F. 1992. Giant debris avalanches from the Colima Volcanic Complex, Mexico: implications for long-runout landslides (>100 km) and hazard assessment. *Geology*, Vol. 20, 299-302.

SUTTON, J A, MCGEE, K A, CASADEVALL, T J, and STOKES, B J. 1992. Fundamental volcanic-gas-study techniques: an integrated approach to monitoring. 181-188 *in* Monitoring volcanoes: Techniques and strategies used by staff of the Cascades Volcano Observatory, 1980-90. EWART, J W, and SWANSON, D A (editors). *United States Geological Survey Bulletin*, No. 1966.

SUTTON, J A, MCGEE, K A, CASADEVALL, T J, and STOKES, B J. 1993. Técnicas fundamentales para el estudio de gases volcánicos: Un acercamiento integral a la vigilancia. 195-202 in Vigilando volcanes: Técnicas y estrategias empleadas por el personal del Observatorio Vulcanológico Cascades, 1980-90. EWART, J W, and SWANSON, D A (editors). *United States Geological Survey Bulletin*, No. 1966. [In Spanish.]

TANGUY, J-C, RIBIERE, CH, SCARTH, A, and TJETJEP, W S. 1998. Victims from volcanic eruptions. *Bulletin of Volcanology*. Vol. 60, 137-144.

TAYLOR, G A. 1958. The 1951 eruption of Mount Lamington, Papua. *Australian Bureau of Mineral Resources, Geology and Geophysics Bulletin*, No. 38.

THORARINSSON, S. 1969. The Lakagígar eruption of 1783. *Bulletin Volcanologique*, Vol. 33, 910-927.

THORARINSSON, S, and SIGVALDASON, G E. 1970. The Hekla eruption of 1970. *Bulletin Volcanologique*, Vol. 36, 269-288.

TILL, A B, YOUNT, E M, and RIEHLE, J R. 1993. Redoubt volcano, Southern Alaska: A hazard assessment based on eruptive activity through 1968. *United States Geological Survey Bulletin*, No. 1996.

TILLING, R. I. 1989. Editor, *Short Course in Geology: Volume 1. Volcanic Hazards.* American Geophysical Union, Washington, DC. 123 pp.

TILLING, R I, and LIPMAN, P W. 1993. Lessons in reducing volcano risk. *Nature*, Vol. 364, 277-280.

TUCK, B. H. and HUSKEY, L. and TALBOT, L. 1992, The economic consequences of the 1989-90 Mt. Redoubt eruptions: University of Alaska, Anchorage, Institute of Social and Economic Research. Unpublished report prepared for the United States Geological Survey Alaska Volcano Observatory. 39p

TUCK, B. H. and HUSKEY, L. 1994. Economic disruptions by Redoubt Volcano: Assessment methodology and anecdotal empirical evidence, in Casadevall, T.J., ed., Volcanic ash and aviation safety-Proceedings of the First International Symposium on Volcanic Ash and Aviation Safety: *United States Geological Survey Bulletin* 2047, p. 137-140.

TSUYA, H. 1955. On the 1707 eruption of Volcano Fuji. *Earthquake Research Institute Bulletin*, Vol.33, 341-383.

UNDRO. 1990. *Mitigating natural disasters: phenomena, effects and options. A manual for policy makers and planners*. UNDRO manual E.90.III.M.1. (Geneva: UNDRO).

UNESCO. 1993. Disaster Reduction. *Environmental and Development Briefs*, No. 5. (Paris: UNESCO).

VALLANCE, J. W. and SCOTT, K. M. 1997. The Osceola Mudflow of Mount Ranier: Sedimentology and hazard implications of a huge clay-rich debris flow. *Bulletin of the Geological Society of America*, Vol. 109, 143-163.

VOIGHT, B. 1990. The 1985 Nevado del Ruiz volcano catastrophe: anatomy and retrospection. *Journal of Volcanology and Geothermal Research*, Vol. 44, 349-386.

VOIGHT, B, GLICKEN, H, JANDA, R J, and DOUGLAS, P M. 1981. Catastrophic rockslide avalanche of May 18. 347-377 *in* The 1980 eruptions of Mount St. Helens, Washington.

LIPMAN, P W, and MULLINEAUX, D R (editors). *United States Geological Survey Professional Paper*, No. 1250.

VOLCANOLOGY SURVEY OF INDONESIA. 1990. Merapi Volcano. Monitoring - Forcasting - Mitigation. *Report*, No. 122.

WALKER, G P L. 1973. Lengths of lava flows. *Philosophical Transactions of the Royal Society of London*, Vol. A274, 107-118.

WADGE, G, and ISAACS, M C. 1987. *Volcanic hazards from Soufriere Hills volcano, Montserrat, West Indies.* Report to the Government of Montserrat and the Pan Caribbean Disaster Preparedness and Prevention Project.

WADGE, G, and ISAACS, M C. 1988. Mapping the volcanic hazards from Soufriere Hills volcano, Montserrat, West Indies using an image processor. *Journal Geological Society of London*, Vol. 145, 541-51.

WADGE, G, JACKSON, P, BOWER, S M, WOODS, A W and CALDER, E. 1998a. Computer simulations of pyroclastic flows from dome collapse. *Geophysical Research Letters*, Vol. 25, No. 19, 3677-3680.

WADGE, G, WOODS, A W, JACKSON, P, BOWER, S M, WILLIAMS, C, and HÜLSEMANN, F. 1998b. A hazard evaluation system for Montserrat. 3.1 – 3.32 In: Forecasts and warnings. Lee B, and Davis, I. (Editors). Thomas Telford, London.

WALKER, G P L, HEMING, R F, SPROD, T J, and WALKER, H R. 1981. Latest major eruptions of Rabaul volcano. 181-193 *in* Cooke-Ravian volume of volcanological papers. JOHNSON, R W (editor). *Geological Survey of Papua New Guinea Memoir*, No. 10.

WHARTON, W J L. 1888. On the seismic sea waves caused by the eruption of Krakatoa, August 26th and 27th, 1883. *in* The eruption of Krakatoa and subsquent phenomena. SYMONS, G J (editor). *Report of the Krakatoa Committee of the Royal Society*. (London: Trübner).

WILSON, C J N. 1985. The Taupo eruption, New Zealand II. The Taupo ignimbrite. *Philosophical Transactions of the Royal Society of London*, Vol. A314, 229-310.

WINNER, W E, and CASADEVALL, T J. 1981. Fir leaves as thermometers during the May 18 eruption. 315-320 *in* The 1980 eruptions of Mount St. Helens, Washington. LIPMAN, P W, and MULLINEAUX, D R (editors). *United States Geological Survey Professional Paper*, No. 1250.

WRIGHT, T L, and PIERSON, T C. 1992. Living with volcanoes. *United States Geological Survey Circular*, No. 1073.

YANAGI, T., OKADA, H. and OHATA, H. (editors). 1992. *Unzen Volcano: The 1990-1992 Eruption.* (Tokyo: Nishinippon and Kyushu University Press).

YOKOYAMA, I. 1981. A geophysical interpretation of the 1883 Krakatau eruption. *Journal of Volcanology and Geothermal Research*, Vol. 9, 359-378.

YOUNG, S R. 1998. Rapid volcanic hazard assessment at Volcán Villarrica, south-central Chile. *British Geological Survey Technical Report* WC/98/15R.

YOUNG, S R, BAXTER, P J, POMONIS, A, ERNST, G J, and BENSON, C. 1998. Volcanic hazards and community preparedness at Volcán Irazú, Costa Rica. *British Geological Survey Technical Report* WC/98/16R.

ZEN, M T, and HADIKUSOMO, D. 1964. Preliminary report on the 1963 eruption of Mt. Agung in Bali (Indonesia). *Bulletin Volcanologique*, Vol. 127, 269-299.